THE UNIVERSITY *of* EDINBURGH

UNIVERSITY of EDINBURGH

Analysis of Integrated Gasification Combined Cycle Power Plants and Process Integration with Pre-combustion Carbon Capture

by

Zoe Kapetaki

A Thesis Submitted for the

Degree of Doctor of Philosophy

of the University of Edinburgh

Declaration

I, Zoe Kapetaki, declare that this thesis titled, "**Analysis of Integrated Gasification Combined Cycle Power Plants and Process Integration with Pre-combustion Carbon Capture"** and the work presented in it are my own. I confirm that:

- The thesis has been composed by me.
- The work is my own.
- This work has not been submitted for any other degree or professional qualification except as specified.
- This work was done wholly or mainly while in candidature for a research degree at this University.
- Where I have consulted the published work of others, this is always clearly attributed.
- Where I have quoted from the work of others, the source is always given.

Signed:

Date: 13/03/2015

Lay Summary

Globally, electricity and heat generation sectors rely heavily on coal. Global consumption of fossil fuels continues to increase, leading to increased CO_2 emissions. As demand growth is expected to be particularly increased in developing countries, it is expected that by 2035, fossil fuels will account for 75% to accommodate the global energy demand. In World Energy Outlook 2013, the International Energy Agency (IEA) estimated that energy related CO_2 emissions will rise by 20% to 2035. Under this estimation, the average temperature increase to be expected is well above the internationally agreed 2°C target.

This work presents results obtained by examining the effective use of abundant resources by power plants for electricity production in an environmentally friendly manner. Undertaken in the University of Edinburgh, Scotland by Zoe Kapetaki under the supervision of Professor Stefano Brandani and Dr Hyunwoong Ahn, this work was funded within the Innovative Gas Separations for Carbon Capture project (IGSCC EPSRC – EP/G062129/1).

In particular, this work investigated Integrated Gasification Combined Cycle (IGCC) power plants for power generation. These plants have been reported by industry and the research community to be attractive not only as an option to potentially reduced CO_2 emissions, but also in terms of technical performance and cost.

Under this context, we examined different configurations of IGCC plants and developed automated tools to represent both conventional and plants with carbon capture, i.e. the process of capturing CO_2 produced by the power plant. To achieve this, we examined state-of-the-art processes, but also novel configurations. We found that IGCC performance can be improved with the novel processes and approaches we propose.

The tools developed and presented in this thesis can be helpful for engineers to overcome data barriers and lack of detailed approaches regarding clean energy production. Finally, we hope that this thesis can be a useful guide for stakeholders and decision makers to reaching essential and accurate conclusions with regards to energy and environmental issues.

Abstract

Integrated Gasification Combined Cycle (IGCC) power plants have been considered as one of the best options for energy production in an environmental friendly manner. IGCC power plants are demonstrating better results, both in terms of plant performance and economics, when compared to a Pulverised Coal (PC) power plant with CO_2 capture. The additional components required for an IGCC power plant when it is desired to operate in CO_2 capture mode, give research potential with respect to an improved IGCC power plant performance. The IGCC power plant design framework studied and developed was based in DOE/NETL report and is presented. The conventional and CO_2 capture IGCC power plants have been benchmarked in rigorous process flow diagrams developed using the commercial software Honeywell UniSim Design R400. As an essential part of the Innovative Gas Separations for Carbon Capture project (IGSCC EPSRC – EP/G062129/1) predictive simulation tools were produced to investigate the IGCC performance. The case studies considered include different gasification options for non-capture and carbon capture IGCCs, with a two stage Selexol process for the CO_2 capture cases. Particular effort has been made to produce an accurate simulation component to describe the behaviour of the syngas in the Selexol solvent. The two stage Selexol configuration was investigated in detail and novel schemes are presented. No similar approaches have been reported in the literature, in terms of the proposed configuration and the capture efficiency. Moreover, innovative CO_2 capture schemes incorporating combined units of physical absorption and membranes have been examined with respect to the power plant's performance. In this thesis, contrary to other studies, all simulations cases have been conducted in unified flow diagrams. The results presented include overall investigations and can be a helpful tool for engineers and stakeholders in the decision making process.

Ithaca, Konstantinos Kavafis (1863-1933)

As you set out for Ithaca, wish the voyage is a long one,

full of adventure, full of discovery.

Laistrygonians and Cyclops,

angry Poseidon – don't be afraid of them:

you'll never find things like that on your way,

as long as you keep your thoughts raised high,

as long as a rare excitement stirs your spirit and your body.

Laistrygonians and Cyclops,

angry Poseidon – you won't encounter them

unless you bring them along inside your soul,

unless your soul sets them up in front of you.

Keep Ithaca always in your mind.

Arriving there is what you are destined for.

But do not hurry the journey at all.

Better if it lasts for years,

so you are old by the time you reach the island,

wealthy with all you have gained on the way.

Do not expect Ithaca to make you rich.

Ithaca gave you the marvellous journey.

Without her you would not have set out.

She has nothing left to give you now.

And if you find her poor, Ithaca won't have deceived you.

Wise as you will have become, so full of experience,

you will have understood by then what these Ithacas mean.

Acknowledgements

First and foremost I would like to thank the Engineering and Physical Sciences Research Council for the funding of the Innovative Gas Separations for Carbon Capture project (IGSCC EPSRC–EP/G062129/1), under which the work presented in this thesis was undertaken.

I would, moreover like to thank Professor Claire Adjiman and Dr Maria-Chiara Ferrari for the comments and recommendations provided on my viva voce examination.

A special thanks to my PhD supervisors Professor Stefano Brandani and Dr Hyungwoong Ahn for their invaluable inputs throughout my studies.

I would like to thank the group of Carbon Capture and Storage at the University of Edinburgh and the people in the Institute of Materials and Processes, for their encouraging words and their kindness. They made Edinburgh home for me.

Many thanks to the people I met at the University of Fortaleza, Brazil for their exceptional hospitality and warmth that reminded me who I truly am.

There are no words to express how grateful I feel for the continuous love and support of everlasting friends and the ones I made while undertaking my PhD studies, Alex, Ana, Chiara, Daniel, Davide, Dursun, Elisavet, Elli, Enzo, Evi, Hatice, Iliana, Jovana, Katerina, Maria, Meropi, Peyman and Simone. Thank you very much.

I wish to thank my family for their unconditional love and endless support throughout these years. I would like to especially thank my parents George and Dimitra. Without their efforts and sacrifices I would have never fulfilled my dreams.

Finally, I would like to thank George for his love, understanding and tireless support. These past years, as much exciting, have been challenging and demanding, and he has always been next to me during good and bad times. Thank you very much.

This thesis is dedicated to the memory of my grandparents Athanasios Kapetakis and Athanasia Kapetaki

List of publications/presentations

Kapetaki, Z., Brandani, P. Brandani S., Ahn, H. "Process Simulation of a Dual-Stage Selexol Process for 95% Carbon Capture Rate at an Integrated Gasification Combined Cycle Power plant". International Journal of Greenhouse Gases. Submitted on 11/2014.

Kapetaki, Z., Ahn, H., Brandani S. "Detailed Process Simulation of Pre-combustion IGCC Plants Using Coal-slurry and Dry Coal Gasifiers". Energy Procedia Volume 37, 2013, Pages 2196–2203.

11/2014 AIChE 2014, "Process Design of a Coal-Based Hydrogen Plant with CO_2 Capture and Its Improvement". Hyungwoong Ahn, Mauro Luberti, Zoe Kapetaki, Daniel Friedrich, Dursun Can Ozcan, Xiao Luo, Pietro Brandani and Stefano Brandani. Atlanta, US.

11/2013 AIChE 2013, "Process Configuration Studies of Conventional Pre- and Post-Combustion Carbon Capture for Power Plants". Hyungwoong Ahn, Zoe Kapetaki, Pietro Brandani, Mauro Luberti and Stefano Brandani, San Francisco, US.

11/2013 CIEM, "IGCC potential and performance as an option for clean energy production". Zoe Kapetaki, Davide Bocciardo, Maria-Chiara Ferrari, Hyungwoong Ahn and Stefano Brandani, Bucharest, Romania.

04/2013 IChemE Separation Technologies for CO_2 Capture, "Process Configuration Studies of Conventional Pre- and Post-Combustion Carbon Capture for Power Plants", Zoe Kapetaki, Hyungwoong Ahn and Stefano Brandani, Edinburgh, UK.

11/2012 GHGT-11, "Detailed process simulation of pre-combustion IGCC plants using coal-slurry and dry coal gasifiers". Zoe Kapetaki, Hyungwoong Ahn and Stefano Brandani, Kyoto, Japan.

09/2012 Euromembranes 2012, "Performance of hybrid membrane-solvent configuration for Pre–combustion Carbon capture in IGCC power plants". Zoe Kapetaki, Davide Bocciardo, Maria-Chiara Ferrari, Hyungwoong Ahn and Stefano Brandani, London, UK.

List of contents

List of Tables

List of Figures

List of abbreviations

AGR, Acid gas removal

ASU, Air separation unit

COE, Cost of electricity

COS, Carbonyl sulfide

CT, Combustion turbine

CW, Cold water

DOE, Department of Energy

E-Gas™, ConocoPhillips gasifier technology

EP ASU, Elevated pressure air separation unit

EPRI, Electric Power Research Institute

EU, European Union

FG, Flue gas

FGD, Flue gas desulfurization

GEE, GE Energy

GT, Gas turbine

HHV, Higher heating value

HP, High pressure

HRSG, Heat recovery steam generator

IGCC, Integrated gasification combined cycle

IP, Intermediate pressure

LCOE, Levelized cost of electricity

LHV, Lower heating value

LP, Low pressure

Chapter 1 MDEA, Methyldiethanolamine

MEA, Monoethanolamine

N/A, Not applicable

NETL, National Energy Technology Laboratory

NGCC, Natural gas combined cycle

NOx, Oxides of nitrogen

PC, Pulverized coal

PSA Pressure Swing Adsorption

SGS, Sour gas shift

SOx Oxides of sulphur

TCR, Total capital requirement

TGTU, Tail gas treating unit

V-L, Vapour Liquid

Chapter 1 General introduction

1.1 Fossil fuels and global CO_2 emissions

The use of coal increased rapidly mainly due to the industrial revolution and has continued to grow since, only with some occasional temporary decreases. Coal was the dominant fuel during the 19th century and the first half of the 20th century (Encyclopaedia of Energy 2004). The development that has occurred during the years in all societies is directly linked to the growth of the coal industry. Technological advancements closely associated with the use of coal have clearly influenced the definition given nowadays to a developed society. For over a century, coal was the major energy source for the world and remains the largest and most readily available energy source (Encyclopedia of Energy 2004). According to **Figure 1-1**, its use is predicted to continue, which means that coal will continue to play an important role in the energy production for the following years.

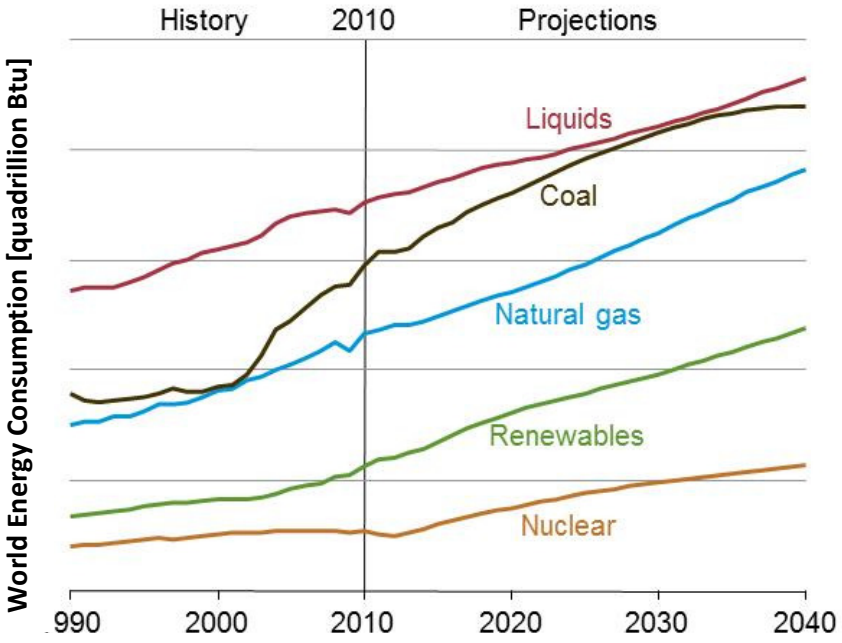

Figure 1-1: World energy consumption by fuel type, 1990-2040 (quadrillion Btu) (DOE/EIA 0484(2012))

Inevitably, however, the use of coal leads to unavoidable CO_2 production. From **Figure 1-2**, it can be seen that in 2010, 43% of CO_2 emissions from fuel combustion were produced from coal, 36% from oil and 20% from gas (DOE/EIA 0484 (2012)).

Additionally, the growing energy demand of the developing countries, where energy intensive industrial production is growing rapidly, is mostly driven by coal. The World Energy Outlook (WEO 2012) projects that emissions from coal will grow to 15.3 $GtCO_2$ in 2035. It has been reported that CO_2 atmospheric concentration has increased from a pre-industrial level of 200ppm and is expected to reach 550ppm by 2050 even if the emission levels are stable for the next four decades (Kumar 2013). Adopting the use of more efficient plants and end-use technologies as well as increased use of renewables and nuclear energy could lead to a decrease in coal consumption. In combination with carbon capture and storage (CCS) technologies a reduction of CO_2 emissions to 5.6 Gt by 2035 could be achieved. However, the intensified use of coal would substantially increase CO_2 emissions unless there is a very widespread deployment of CCS (WEO 2012).

As illustrated in **Figure 1-3**, the sectors that contributed the most to the global CO_2 emissions are: electricity and heat generation which accounted for 41% of global emissions in 2010, and transport where 22% were produced (DOE/EIA 0484 (2012)). Regarding world energy sources consumption and future predictions, several scenarios have been developed by different institutions based on different perspectives and techniques (Coates 2002; Schiffer 2008; BP 2011).

Globally, electricity and heat generation sectors rely heavily on coal. By 2035, the WEO 2012 projected that demand for electricity would be more than 70% higher than current demand. Therefore, the future development of the CO_2 emissions intensity of this sector would depend strongly on the fuels used to generate electricity and on the share of fossil-fuel plants equipped with CCS.

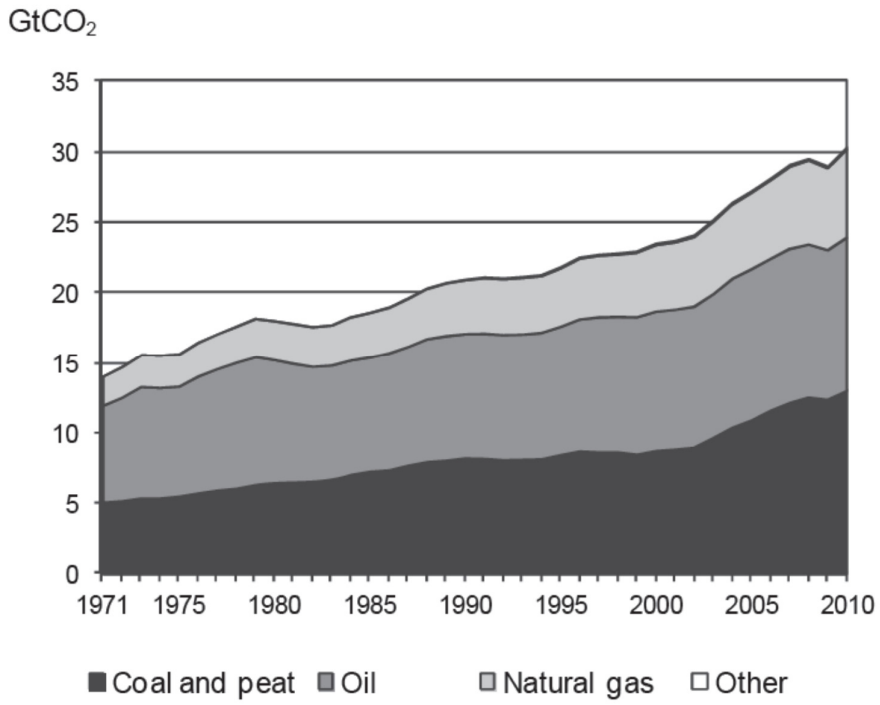

Figure 1-2: Global CO_2 emission (%) by fuel in 2010 (DOE/EIA 0484 (2012))

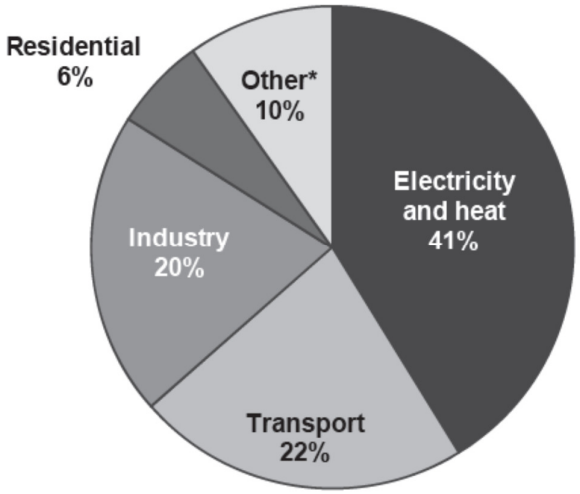

Figure 1-3: Global CO_2 emission by sector in 2010 (DOE/EIA 0484 (2012))

Developing methods for reducing emissions from coal fired power plants is one of the major research interests of our time, and therefore the focus of this thesis is to study

an efficient way of reducing CO_2 emission from coal fired power plants by carbon capture.

1.2 What is Carbon Capture?

Horn and Steinberg (1982) and Hendriks et al. (1989) were among the first to discuss the application of certain technologies to mitigate climate change, focusing initially on electricity generation.

Since the early 1990's when Carbon Capture and Storage (CCS) started receiving a significant share as a viable option to tackle climate change, several definitions have been used to describe what CCS really is. One of the most traditional is probably the one reported in the IPCC Special report for Carbon Dioxide Capture and Storage:

"Carbon dioxide (CO_2) capture and storage (CCS) is a process consisting of the separation of CO_2 from industrial and energy-related sources, transport to a storage location and long-term isolation from the atmosphere. This report considers CCS as an option in the portfolio of mitigation actions for stabilization of atmospheric greenhouse gas concentrations." (IPCC 2005)

Currently, several technologies can be applied to implement CCS operation in power plants and they will be elaborated in the next paragraph of this chapter.

1.2.1 CO_2 capture methods

There are four basic methods for capturing CO_2 from use of fossil fuels:

• Post-combustion capture

• Oxy-fuel combustion capture

• Pre-combustion capture

• Capture from industrial process streams

These systems are shown in simplified form in **Figure 1-4**.

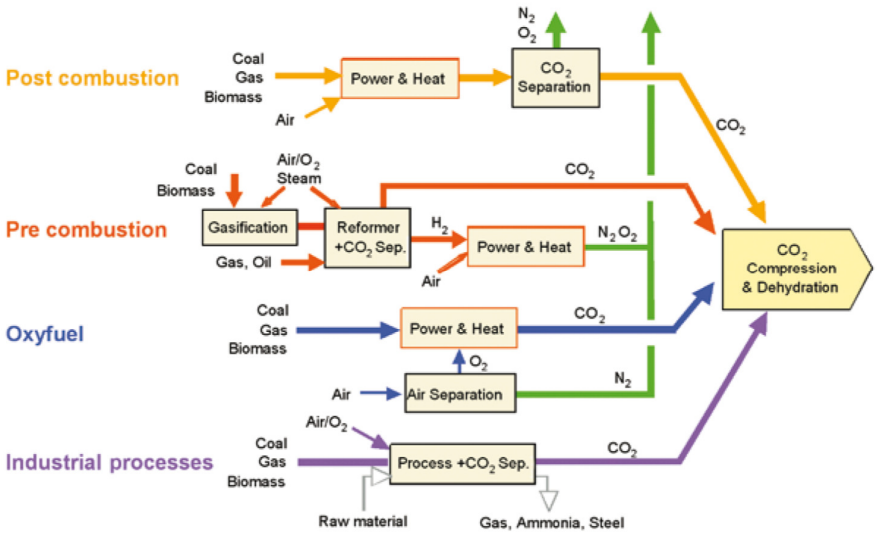

Figure 1-4: CO_2 capture methods (IPCC 2005)

Post-combustion capture

The capture of CO_2 from flue gases produced by combustion of carbonaceous fuels, such as fossil fuels and biomass with air is referred to as post-combustion capture. Instead of being discharged directly to the atmosphere, flue gas is passed through a post-combustion capture unit which separates most of the CO_2 usually by means of contact with chemical solvents represented by monoethanolamine (MEA). The CO_2 captured is compressed for its subsequent use in Enhanced Oil Recovery (EOR) or CO_2 storage, and the remaining flue gas is discharged to the atmosphere.

Several modifications to the amine capture process have been proposed over the years, as discussed by Zhao et al. (2013), Abu-Zahra et al. (2013) and more recently by Ju and Kocaoglu (2014) and references therein. Ahn et al. proposed innovative modifications of the traditional scheme, reporting improved performances for such schemes (Ahn et al. 2013).

Oxy-fuel combustion capture

In oxy-fuel combustion, nearly pure oxygen is used for combustion instead of air, resulting in a flue gas that is composed of mainly CO_2 and H_2O as was recently reported in a review by Leunga et al. (2014). If the fuel is burnt in pure oxygen, the flame temperature is excessively high, but CO_2 and/or H_2O-rich flue gas can be recycled to the combustor to moderate this (Takami et al. 2009). Oxygen is usually

produced conventionally by low temperature (cryogenic) air separation unit and several novel techniques to supply oxygen to the fuel are being developed, such as Ion Transport Membranes (ITM), Chemical Looping Combustion (CLC), and Chemical Looping Oxygen Uncoupling (CLOU).

Pre-combustion capture

Pre-combustion capture involves reacting a fuel with oxygen or air and steam to give mainly a 'synthesis gas (syngas)' or 'fuel gas' composed of carbon monoxide and hydrogen. The carbon monoxide reacts with steam in the shift reactor which is a catalytic reactor, to give CO_2 and more hydrogen. CO_2 is then separated, usually by a physical or chemical absorption process, resulting in a hydrogen-rich fuel. CO_2 product from pre-combustion physical solvent scrubbing processes typically contains about 1-2% H_2 and CO and traces of H_2S and other sulphur compounds (European CCS Project Network, 2012).

The potential use of pre-combustion capture technologies is not limited to the coal-driven IGCC but includes a number of chemical plants utilising syngas to produce hydrogen, synthetic natural gas, fuels or chemicals (Knoef 2005).

Capture from industrial process streams

CO_2 has been separated from industrial process streams for 80 years (Kohl 1997), although most of the CO_2 that is captured is vented to the atmosphere because there is no incentive or requirement to store it. Current examples of CO_2 capture from process streams are purification of natural gas and production of hydrogen-containing synthesis gas for the manufacture of ammonia, alcohols and synthetic liquid fuels. Most of the techniques being employed for CO_2 capture in the above-mentioned examples are also similar to those used in pre-combustion capture. On the other hand, significant amounts of CO_2 are being produced by operating refining and petrochemical plants, cement plants, iron and steel plants, and fermentation processes for food and drink production. The CO_2 generated from these sources could be captured using techniques that are common to post-combustion capture and oxy-fuel combustion capture.

1.2.2 CO_2 capture technologies

There are various CO_2 capture technologies proposed for IGCC power plants (Wall 2007; Figueroa et al. 2008). A very generic scheme describing the trends that categorised in terms of separation technologies are presented in **Table 1-1**.

Table 1-1: Pre combustion capture methods

Capture Technology	Description
Solvents	Physical/Chemical
Membranes	Polymeric, Ceramic, Metallic
Sorbents	Zeolites, Activated Carbon, Alumina, CaO, MgO
Cryogenic	Liquid CO_2 products

Solvents

Usually, conventional IGCC power plants are equipped with a H_2S removal unit using solvents to recover H_2S from the syngas due to strict sulphur emission regulation. For H_2S capture from the syngas, syngas is fed to an absorber where the H_2S is selectively absorbed into the solvent liquid by counter-current contact. The one-stage absorption unit for H_2S removal can be modified to a dual-stage absorption unit for recovering a very high purity CO_2 from the syngas as well as removing H_2S by making use of the difference of selectivity of solvents toward H_2S and CO_2. The H_2S free stream passes through a second absorber where CO_2 is captured. Several configurations have been proposed for this process and they are discussed in detail later in this thesis.

Physical solvents

Several physical solvents such as Dimethyl Ether of Polyethylene Glycol (DEPG or Selexol™ or Coastal AGR®), N-Methyl-2-Pyrrolidone (NMP or Purisol®), Methanol (Rectisol®), Propylene Carbonate (Fluor Solvent™), and others have been developed

over the years, to serve as acid gas removal options in gasification plants utilizing coal as well as natural gas (Kohl A. 1997).

According to the DOE/NETL report (NETL 2007), there are well over thirty acid gas removal processes in common commercial use throughout the oil, chemical, and natural gas industries using physical solvents. The partial pressure of the acid gas in gasification plants is sufficiently high to justify the use of physical solvents.

In general, the partial pressure of CO_2 in the feed gas is probably the determining factor for the choice of the solvent to be used in the capture process. At low CO_2 partial pressures, there is no practical benefit of using physical solvents since the CO_2 loading is relatively low compared to those of chemical solvents. However, the CO_2 loading of physical solvents increase steadily with the increase of the CO_2 partial pressure while those of chemical solvents reaches a maximum at a certain pressure and cannot be enhanced by increasing the pressure further. Therefore, the physical solvents can exhibit a higher CO_2 loading in the range of relatively high CO_2 partial pressure than the chemical solvents as shown in **Figure 1-5**.

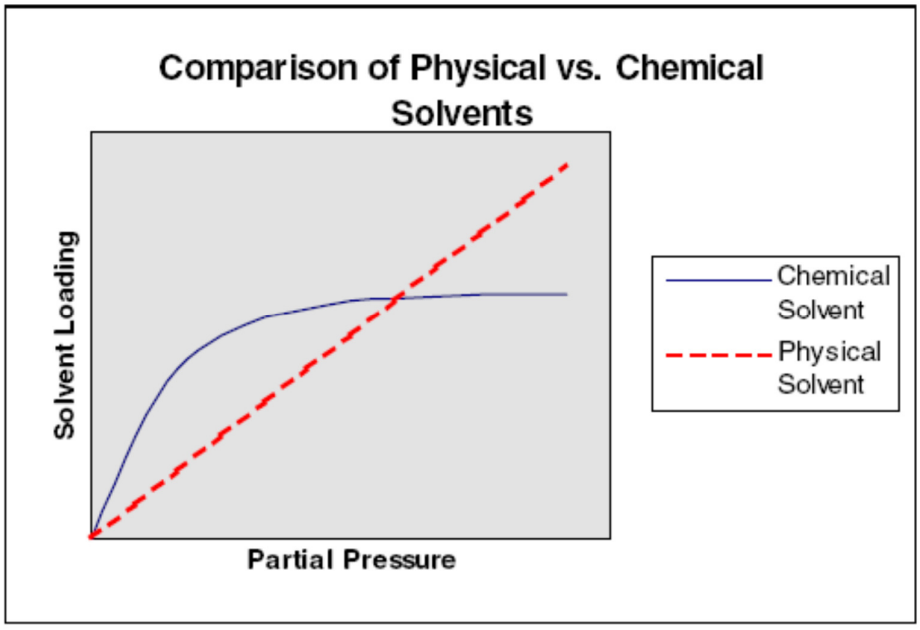

Figure 1-5: Solvent loading versus partial pressure for physical and chemical solvents (Sciamanna and Lynn 1988)

In physical absorption, the solvent capacity or loading which initially follows Henry's law, assumes an almost liner dependence on the gas partial pressure. In chemical

absorption, the solvent loading is described by a non-linear dependence and is higher at low partial pressures. At the concentrations approaching the saturation loading of the solvent, chemical absorption increases sharply. After this point, even large increases in the partial pressure, result in a very small increase in the solvent loading. This behaviour is caused by the gas absorption in the aqueous component of the solvent used in the process (Kohl and Nielsen, 1997). Chemical solvent processes are usually used for CO_2 partial pressures below around 15 bar (Puigjaner, 2011). The properties of some physical solvents are presented in **Table 1-2**.

Table 1-2: Properties of some physical solvents (Newman 1985)

Solvent	**DEPG**	**PC**	**NMP**	**MeOH**
Process	Selexol or Coastal AGR	Fluor	Purisol	Rectisol
Viscosity at 25ºC (cP)	5.8	3.0	1.65	0.6
Specific gravity (kg/m^3)	1,030	1,195	1,027	785
Molecular weight	280	102	99	32
Vapour pressure at 25ºC (mm Hg)	0.00073	0.08500	0.40000	125
Freezing point (ºC)	–28	–48	–24	–92
Boiling point (ºC)	275	240	202	65

Chemical solvents

Chemical solvents, such as amines, are generally more suitable for carbon capture from the streams having relatively low CO_2 partial pressures. In a conventional amine unit, the chemical solvent reacts exothermically with the acid gas constituents to form a weak chemical bond that can be broken, releasing the acid gas and regenerating the solvent for reuse (NETL 2007).

Although, primary and secondary amines can be used for gasification plants as an acid gas removal method, Methyl Diethanol Amine (MDEA), which is a tertiary amine, has been reported since the early ‘80s to demonstrate superior ability towards selective

absorption of H_2S over CO_2 (Jou et al. 1982). This is an important characteristic, given that in carbon capture mode, it is usually aimed to simultaneously separate both gases. The process typically consists of an absorber and a stripper, as shown in **Figure 1-6**.

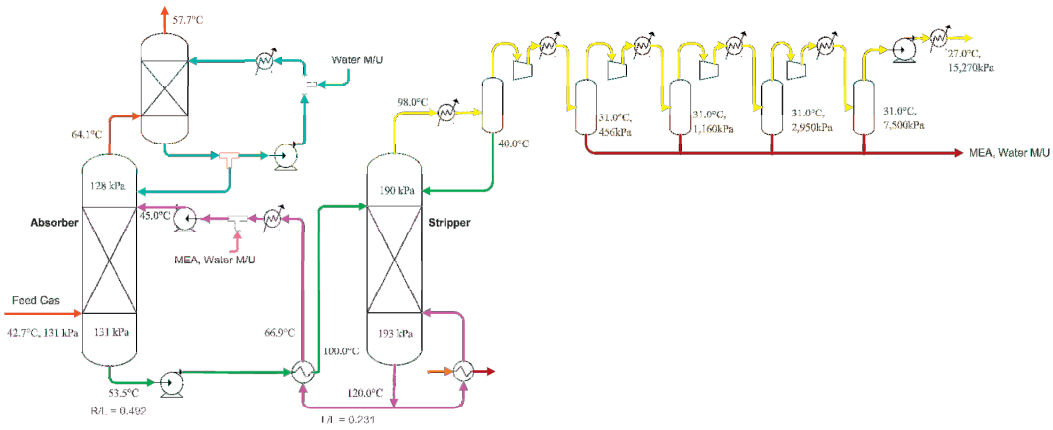

Figure 1-6: Schematic of a conventional process using chemical solvent (Ahn et al. 2013)

The gas stream contacts the aqueous chemical solvent in the absorber where the acid gas is removed. The acid gas is then stripped off the solvents in the stripper and the regenerated solvent after being cooled and pumped to the absorber pressure is recycled back to the process.

Mixed solvents

Mixed solvents are a mixture of chemical and physical solvents, which combines the properties of both components. The idea behind the development of mixed solvents is to augment the capability of the chemical solvent offering high CO_2 selectivity and loading in order to improve the performance of the physical solvent having the lower energy consumption. Among the commercialised mixed solvents such as Sulfinol, Flexsorb PS, Ucarsol LE etc. it has been reported that Sulfinol has been the most conventional solvent for acid gas removal from the syngas in industry (Kohl 1997). Sulfinol is an aqueous solution of Sulfolane which is a physical solvent, and either DiIsoPropanolAmine (DIPA) or MDEA which are the chemical solvents. Depending on the composition of the solvent, Sulfinol can be characterised as Sulfinol D (when the chemical solvent is DIPA) or Sulfinol M (when the chemical solvent is MDEA). Sulfinol D is used preferentially when the objective is the total removal of the acid

gases while Sulfinol M is beneficial when the objective is to remove H_2S selectively over CO_2 (Nasir 1990).

Membranes

When membranes are used as a CO_2 capture method, the objective is to utilise the materials' property for selective permeation of the species contained in the gas passing through them. As this separation is driven by the partial pressure difference across the membrane, high pressure syngas streams originated from coal gasification at IGCC power plants can be decarbonised by making use of membrane capture units. Several membrane materials have been reported in the literature and references therein for CO_2 capture processes (Krishnan et al. 2009; Franz and Scherer 2010; Scholes et al. 2010; Merkel et al. 2012). The target however, regardless the approach, is to achieve the production of a stream with high CO_2 concentration for storage.

1.3 Integrated Gasification Combined Cycle (IGCC) power plants overview

A typical IGCC plant incorporates a gas turbine and a steam cycle for power generation. Coal is fed to the gasifier along with the required O_2 for the gasification. An Elevated Pressure Air Separation Unit (EP ASU) plant produces sufficient amount of O_2 needed for gasification. The hot raw syngas exiting the gasifier is cooled down for gas clean-up, including removal of slag particles and different trace elements, sulphur and if relevant CO_2 capture. In case of CO_2 capture, a shift reaction step where CO and H_2O exothermically react to CO_2 and H_2 is necessary to achieve acceptable CO_2 capture ratios. Sulphur (as H_2S) and CO_2 are removed by physical absorption, with the state-of-the-art being the Selexol process. The remaining gas mixture is the fed to the combustor. The fuel is preheated and diluted with nitrogen from the ASU before the combustion. The product gas is then sent to the gas turbine. The heat recovery steam generator (HRSG) utilizes the gas turbine exhaust heat to produce steam at different pressure levels which is fed to the steam turbine. The exhaust gas after passing the HRSG leaves the plant's stack at approximately 393K (120°C). A simplified schematic of a typical IGCC plant is presented in **Figure 1-7**. Blocks in dashed lines are incorporated in carbon capture mode.

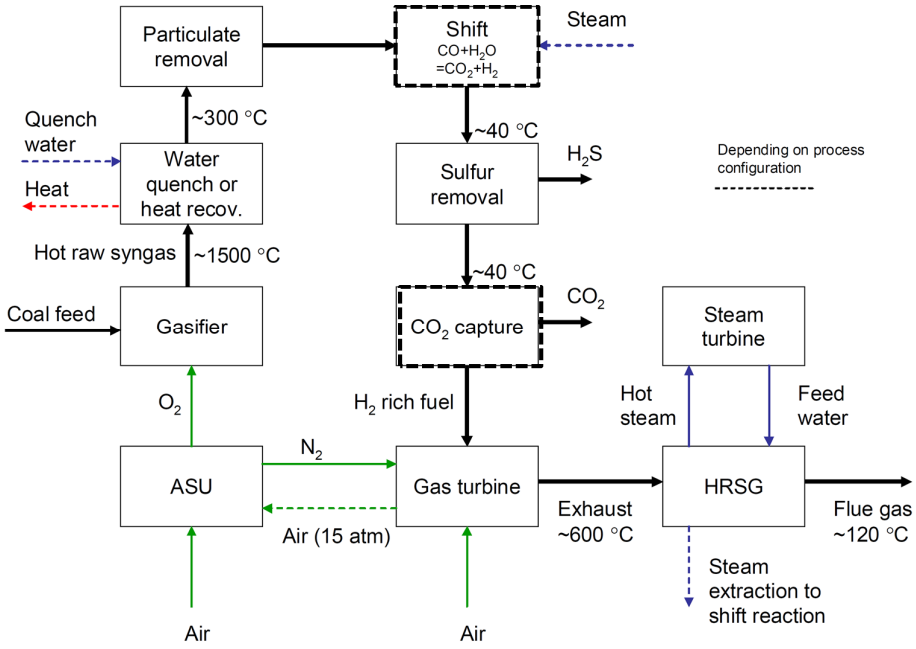

Figure 1-7: IGCC process schematic (Maurstad et al. 2006)

Perez-Fortes et al. (2009) and Maurstad (2005), listed a number of advantages and disadvantages associated with IGCC power plants.

Advantages

- IGCC power plants demonstrate competitive net plant efficiency (Higher Heating Value, HHV) compared to Pulverised Coal (PC)-boiler power plants in a non-capture mode and significantly higher overall net plant efficiency when the plant operates with a CO_2 capture unit.
- Thanks to the presence of the impurities in the syngas at high partial pressures, they can be removed more effectively than in a conventional coal flue gas cleaning system. The IGCC process can reduce emissions by fuel gas clean up, instead of flue gas clean up.
- IGCC technology leads to lower emissions of SOx, NOx and particulate matter compared to PC boiler power plants. More particularly, during gasification, most of the elemental nitrogen in the coal is remains in the product stream as harmless nitrogen gas (N_2). Sulphur is mostly converted to hydrogen sulphide (H_2S) which is further treated to be converted finally to elemental sulphur.

- Ideally, all solids are converted into gas, but any mineral material (ashes and other inert species) is transformed into slag which can be used in construction and building applications.
- Cogeneration or coproduction in gasification adds another advantage to IGCC plants, as there is the ability for a gasification plant to vary the downstream processing of the produced syngas depending on market conditions. Cogeneration can also be viewed from a process standpoint as a means for optimising usage of the fuel(s) at a gasification facility.

Disadvantages

- The release of NOx depends mainly on the gas to electricity conversion stage and consequently gas cleaning to a high standard before the combustion stage is not the optimal approach.
- To achieve high environmental standards, a large economic investment in the operation and maintenance of the gas cleaning system is necessary. For instance, the costs of IGCC plants are between 10 and 20% higher than a natural gas fired combined cycle plant (Ansolabehere 2007; Katzer 2008).
- Plant reliability is a problem due to long construction periods and few real experiences.

The obvious advantage of IGCC power plants over PC-boiler power plants in terms of net plant efficiencies when implementing carbon capture is taken into account is illustrated in **Table 1-3**.

Table 1-3: Net plant efficiencies (HHV) for Pulverised Coal (PC) Rankine cycle plants and Integrated Gasification Combined Cycle with entrained flow gasifiers for non-capture and carbon capture modes (NETL 2007)

Power plant type	Mode	Net plant efficiency (HHV), %
Subcritical PC	Non-capture	36.8
	Carbon capture	24.9
Supercritical PC	Non-capture	39.1
	Carbon capture	27.2
NGCC case	Non-capture	50.8
	Carbon capture	43.7
GEE IGCC	Non-capture	38.2
	Carbon capture	32.5
Shell Global Solutions IGCC	Non-capture	41.1
	Carbon capture	32.0
ConocoPhilips IGCC	Non-capture	39.3
	Carbon capture	31.7

IGCC can also be a cost effective option for plant operation in a carbon capture mode. Hoffman and Szklo (Hoffmann and Szklo 2011) reviewed the studies performed for PC boiler and IGCC power plants in terms of the costs associated with them.

They reported three criteria to evaluate the plants studied: the total capital requirement (TCR), the levelised cost of electricity (LCOE) and the cost of CO_2 avoided. It is

obvious from the following Figures, that most studies have demonstrated that IGCC power plants, regardless of the year that they were undertaken and the assumptions that they were based on, would be more economical than the PC boiler power plants when CO_2 capture units are integrated.

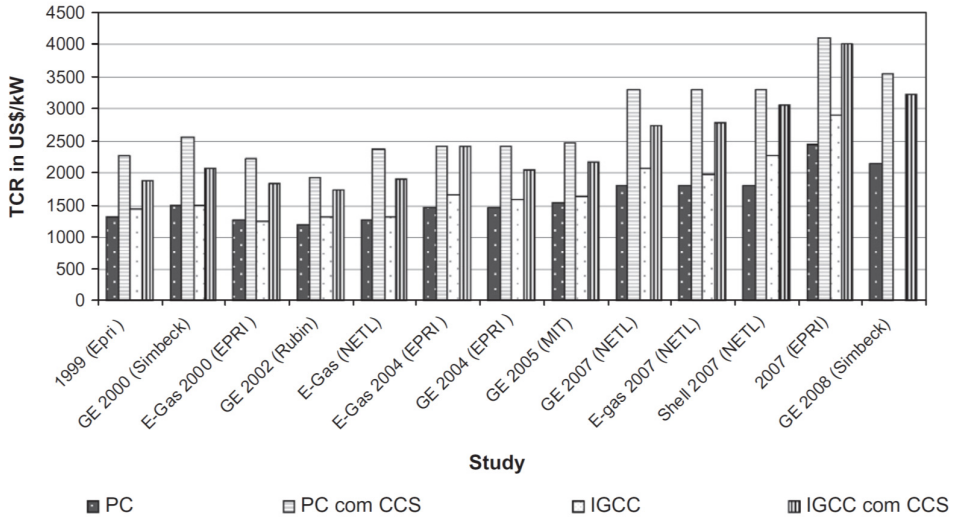

Figure 1-8: TCRs of PC and IGCC power plants (Hoffman and Szklo 2011)

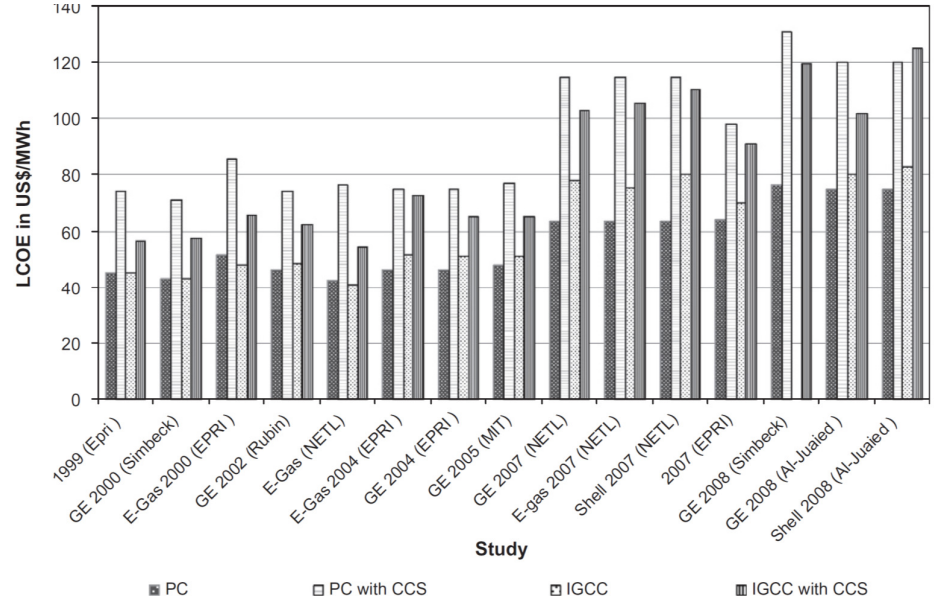

Figure 1-9: LCOE of PC and IGCC power plants (Hoffmann and Szklo 2011)

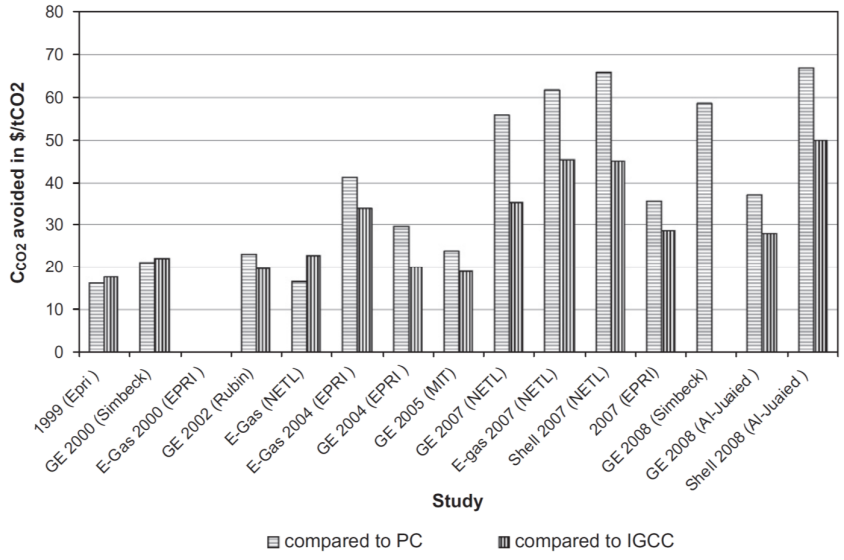

Figure 1-10: Cost of CO_2 avoided for PC and IGCC power plants (Hoffmann and Szklo 2011)

1.4 IGCC power plants literature review

IGCC power plants have attracted the research interest of the scientific community since the 1990s. A significant body of literature exists, examining different aspects of the IGCC plant characteristics. **Table 1-4** presents the studies that are most relevant to the work presented in this thesis, published through the years, discussing IGCC power plants with physical absorption for carbon capture. None of the studies combines the simulation and evaluation of the IGCC plant to the extent conducted and presented in this thesis. While studies reported by Foster Wheeler (2003), Kanniche et al. (2007), Huang et al. (2008), Battacharrya et al. (2010) examine different gasifiers (i.e. GEE, formerly known as GE and Texaco, and Shell), similarly to this study, there are significant differences in either scale or AGR/CO_2 capture units, CO_2 capture rates or simulation methodology. The differences observed with the studies reported in the literature, i.e. the type of the gasifier incorporated, the plant scale, the unit assumed for AGR/CO_2 capture unit, the CO_2 capture rate targeted or achieved, together with the energy penalty resulted in the process and the simulation methodology adopted in the studies are presented in the following table.

Table 1-4: Bibliographic studies of IGCC power plants with physical absorption forCO_2 capture

Study	Gasifier	Scale (MW_e)	AGR/CO_2 capture unit	CO_2 Capture (%)	Energy Penalty (%)	Simulation methodology
Doctor et al. (1996)	KRW	318-445	Glycol, Methanol	90	3.2-8.9	Not Specified
Chiesa and Consonni (1999)	Texaco	350-400	Selexol	90	5-7 (LHV)	Not Specified
Haslbeck et al. (2002)	Destec and Shell	400	Selexol	87	6.6-7.3	Not Specified
Parsons (Haslbeck 2002)	Conoco Philips E-gas	424.5	MDEA/ Selexol	90	6.1	Not Specified
O'Keefe et al. (2002)	Texaco	900	Selexol	75	2	Not Specified

Table 1 – 4 (Continued): Bibliographic studies of IGCC power plants with physical absorption for CO_2 capture

Study	Gasifier	Scale (MW_e)	AGR/CO_2 capture unit	CO_2 Capture (%)	Energy Penalty (%)	Simulation methodology
Foster Wheeler (2003)	Shell and Texaco	750	MDEA/ Selexol	85	5.1- 12.5-	Not Specified
Maustard et al. (2006)	GE and Shell	343-421	Selexol	90	5 and 10	Aspen Plus and GTPro
Huang et al. (2008)	GE and Shell	478-523	Selexol		8.5-11	Eclipse
Battacharrya et al. (2010)	GEE	533-576	Selexol	>90	5.7	Aspen Plus
Kanniche et al. (2010)	Shell and GE	320 and 1200	MDEA, Methanol, Selexol	85	8-9	Not Specified
Kreutz et al. (2010)	Shell	320	Selexol	93	11.1	Aspen Plus

Table 1 – 4 (Continued): Bibliographic studies of IGCC power plants with physical absorption for CO_2 capture

Study	Gasifier	Scale (MW_e)	AGR/CO_2 capture unit	CO_2 Capture (%)	Energy Penalty (%)	Simulation methodology
Field and Brasington (2011)	GEE	550	Selexol	90	-	Aspen Plus
ZEP (2011)	Entrained pressurised	900	Rectisol/ Selexol	90	8	Not Specified
Cormos (2012)	Shell and Siemens	400-500	Selexol	90	9.5 and 7.1	ChemCAD and Thermoflex
Padurean et al. (2012)		425-450	Selexol	70, 80, 90		Aspen Plus
Mansouri Majoumerd et al. (2014)	Shell	404-467	Selexol	93	10	Enssim, ASPEN Plus and IPSEpro

1.5 Objectives and structure of this thesis

Since climate change is a recognised challenge the world is facing today and coal is playing and will continue to play an important role in energy production globally, the development of efficient CO_2 capture technologies is urgently required in order to effectively meet the targets set for the CO_2 emissions reduction.

IGCC power plants with pre combustion carbon capture can be an attractive option for achieving this goal, since it has been reported to be efficient and economical. Physical absorption has been attracting research interest for many decades as an effective technology initially for acid gas removal, but also for the recovery of CO_2 at a high purity for subsequent CO_2 storage or EOR. However, moving towards very high recoveries (CO_2>90%), while maintaining very high purities (CO_2>95%), accurate process simulations are essential. Moreover, running CO_2 capture processes gives rise to an additional energy penalty at the power plants Therefore, it is necessary to develop new and more efficient carbon capture process configurations to minimise the energy penalty involved. The development of automated tools that represent realistically the overall operation of IGCC power plant is essential to evaluate quickly and accurately the performance of the power plant.

In this thesis the current state of IGCC power plants has been identified and automated tools consisting of rigorous and detailed process flow diagrams that can deliver a benchmark for evaluation at the first instance have been developed.

The detailed representation with process simulation of an IGCC power plant is not trivial. Such elaborate process flow diagrams have been however developed and are presented in this thesis. In fact, more than three hundred unit operations are involved in the complete and continuous process flow diagrams developed, depending on the case examined. The models assumed in the simulation cases and the simulation environments uses are presented in Appendix A. Process flow diagrams and operating conditions are reported for corresponding areas of IGCC in the relevant sections.

Each unit of the power plant has to be modelled and the results have to be validated for both non-capture and carbon capture plant operation. Process simulators provide

several options for modelling the unit operations involved, depending on the type and characteristics of each process. Physical absorption occurring in the CO_2 capture processes adopted for IGCC power plant is described by Henry's Law which is well established. However, when it is required to construct process simulations for a physical solvent process, the key to a correct implementation of the separation, is to establish the validity of the VLE relationships. Chemical absorption, can be modelled by using predefined packages available in commercial simulators (e.g. Amines Pkg in Honeywell UniSim Design R400). However, appropriate calibration of the existing software packages is necessary, for the final simulation to predict the behaviour of the acid/shifted gas in the physical solvent, accurately. Henry's law equation parameters, regressed from experimental data, had to be embedded in the simulator to form a reliable component within the overall IGCC simulation. This provided accurate VLE equilibrium calculations and therefore allowed further the thorough evaluation of the performance of process.

The major criteria for determining the optimal process configuration are estimating the energy consumptions at the H_2S removal and CO_2 capture units and evaluating the effect of various specifications imposed on the acid gas removal units on the energy penalty at the power plant. To implement this study, it is necessary to develop a unified process flow diagram where all units composing an IGCC power plant are interconnected so that the behaviour and performance of each unit can be examined and interpreted in the context of overall process operation. In this thesis, IGCC power plant cases with and without carbon capture have been considered. Due to particular focus on the gasifier section and carbon capture processes, specific Chapters have been dedicated to these sections.

In Chapter 2 the gasification technologies adopted in IGCC power plants are presented and discussed. Different gasifiers are incorporated in the power plant and the effect of the type of gasifier in the power plant performance is examined and the results are presented.

A detailed approach of the power plant parts process simulation is presented in Chapter 3. In this Chapter the processes upstream carbon capture processes are presented. Although included in the overall IGCC process flow diagrams produced with Honeywell UniSim Design R400, particular focus has been given individually to syngas scrubber, syngas cooling and sour stripper sections. Simulations of these sections have been additionally conducted with ProMax and the results have been compared with the ones produced by Honeywell UniSim Design R400 and the reference report (NETL 2007). Inaccuracies identified within the reference study are highlighted and improved schemes are suggested for the processes discussed in this Chapter.

In Chapter 4, the CO_2 capture technologies are discussed in detail. Theoretical background describing physical absorption of the gases in the solvent used is provided. The methodology taken for the simulation approach is presented. The process configuration schemes examined are discussed and evaluated.

The alternative configurations that can be used for CO_2 capture in IGCC power plants is the focus of Chapter 5. AGR unit combinations with hydrogen selective polymeric and metallic membranes modules have been examined. Contrary to other studies in this study, promising materials, already developed even if at experimental level have been used for the simulations.

A detailed comparison of the proposed configurations with the state-of-the-art technology is conducted and presented. Amongst the cases investigated, the IGCC power plant with single stage Selexol and a metallic membrane module for H_2S and CO_2 capture respectively, demonstrated the best performance in terms of net power plant efficiency, in both “sweet” and “sour” AGR removal.

In Chapter 6, the major units downstream carbon capture processes within an IGCC power plant are presented. Similar to the approach taken for units upstream carbon capture process, detailed representation with process simulations have been produced for these parts, namely sulphur recovery plant and combined cycle. Along with UniSim Honeywell simulation, BR&E ProMax has been used for the sulphur recovery plants.

Chapter 7 discusses the carbon capture unit effects on IGCC power plants. All the units affected are presented and the energy penalty related to the CO_2 capture technology implementation is discussed and presented.

Figure 1-11 and **Figure 1-12** give a visual guidance within the IGCC block flow diagram as per the power plant sections discussed in each of the Chapters of this thesis. Dashed lines represent the units incorparated when in carbon capture mode.

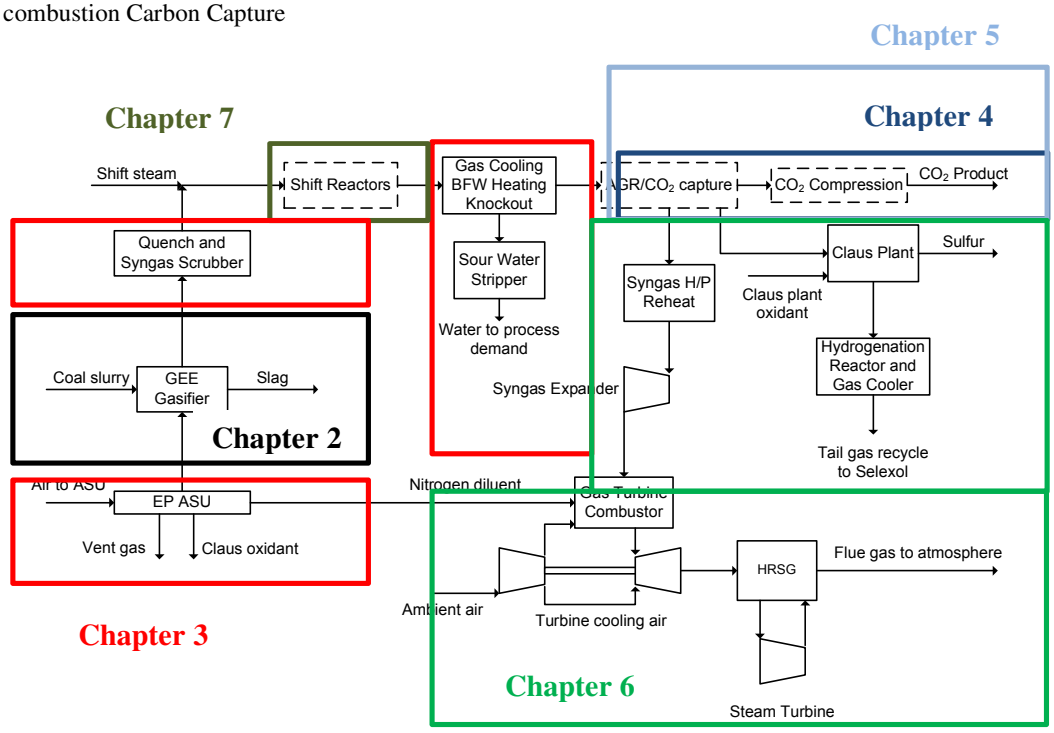

Figure 1-11: GEE IGCC block flow diagram and corresponding Chapters on units presented and discussed

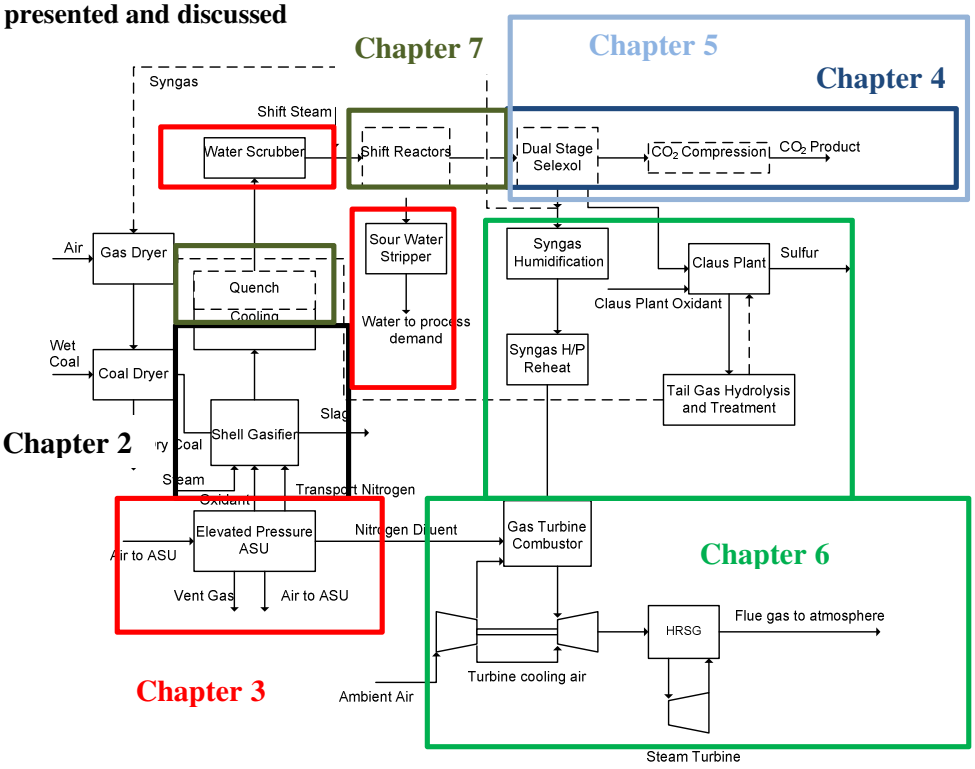

Figure 1-12: Shell IGCC block flow diagram and corresponding Chapters on units presented and discussed

Chapter 2 Gasification technology in IGCC power plants

2.1 Introduction

In the mid-2000s, there were 160 gasification plants operating, with about 35 in planning (Minchener 2005), with the products including electricity, ammonia, chemicals, methanol and hydrogen. For power generation, initial projects were mainly based on coal feed but recently refinery waste has also been considered as an alternative feed (Wall 2007). For power generation, gasification technologies can be classified into entrained flow, fluidised bed and moving bed gasifiers with respect to solid fluid dynamics, oxygen and air blown with respect to its oxidants, and dry or wet slurry fed with respect to the phase of the coal feed (Collot 2002).

The gasifier is the "heart" of the IGCC power plant. It is the part of the plant where coal is converted at high temperature and pressure into synthesis gas (syngas). Maurstad et al. (Maurstad) investigated the effect of the quality of the coal used, as well as the type of the gasifier, on the performance of IGCC power plants, such as net power efficiency as well as the CO_2 emission per unit of electricity produced. They concluded that slurry feed IGCCs are less efficient and have lower net power output for low rank coals. This was explained by the fact that the less energy dense slurry fuel demands that more of the coal's energy is converted to heat instead of syngas and increases the auxiliary power consumption. They calculated a drop of approximately 5% in thermal efficiency (HHV) for this gasification option when in carbon capture mode. In contrast, dry feed IGCCs were reported to be little affected by coal type in terms of thermal efficiency and power output. The corresponding drop in thermal efficiency calculated for this gasification option when in carbon capture mode was approximately 10%.

Carbon conversion by gasification is an important indicator in evaluating the performance of different gasifiers. In this study, for coal slurry-fed GEE gasifiers, the carbon conversion occurring was determined as 98%, while in dry coal-fed Shell gasifiers, the carbon conversion was 99.4% (NETL 2007).

IGCC power plants show a variation in energy penalty depending on different types of gasifier. Conventional IGCC power plants with slurry coal-fed GEE gasifiers typically present the net plant efficiency on the HHV basis of about 38%. In the case of IGCC with carbon capture, this efficiency is subjected to a decrease of approximately 6%. An IGCC process with a Shell gasifier fed by dry coal has 42% net plant efficiency (HHV) without carbon capture but it ends up with 31% net plant efficiency when integrated with a two-stage Selexol process for carbon capture (NETL 2007). While in this Chapter different IGCC gasification options are presented, the effect of carbon capture within the gasification section will be further discussed in Chapter 4.

2.2 Coal and gasification

2.2.1 What is Coal?

Many definitions have been developed through the years to describe what coal really is. According to the World Coal Association (2009), Coal is a combustible, sedimentary, organic rock, which is composed mainly of carbon, hydrogen and oxygen. It is formed from vegetation, which has been consolidated between other rock strata and altered by the combined effects of pressure and heat over millions of years to form coal seams.

The energy that is extracted from coal is in fact the solar energy which is stored in plants through the process of photosynthesis. This energy is usually released as the plants decay after dying. However, if the conditions are favourable to coal formation, the decaying process can be interrupted. If this is the case, the stored solar energy instead of being released, is “locked” into the coal.

The formation of coal is an extremely long process that requires millions of years to complete. The length of the coal formation, along with temperature and pressure, are generally the parameters that determine the quality of the coal deposits. The initial transformation of the peat is towards lignite or “brown coal”. The continuing effects of temperature and pressure over the years and subsequently the chemical and physical changes occurring, are subjecting the lignite into transforming to the range of coals known as “sub-bituminous”. The next step in this process is for the sub-bituminous

coal to transform to harder and blacker kind of coal, which is called “bituminous” or “hard coals”. The final step of the coal formation process is the formation of anthracite. **Figure 2-1** illustrates the carbon, moisture and energy content of each coal range along with the reserves world distribution and uses of each kind of coal.

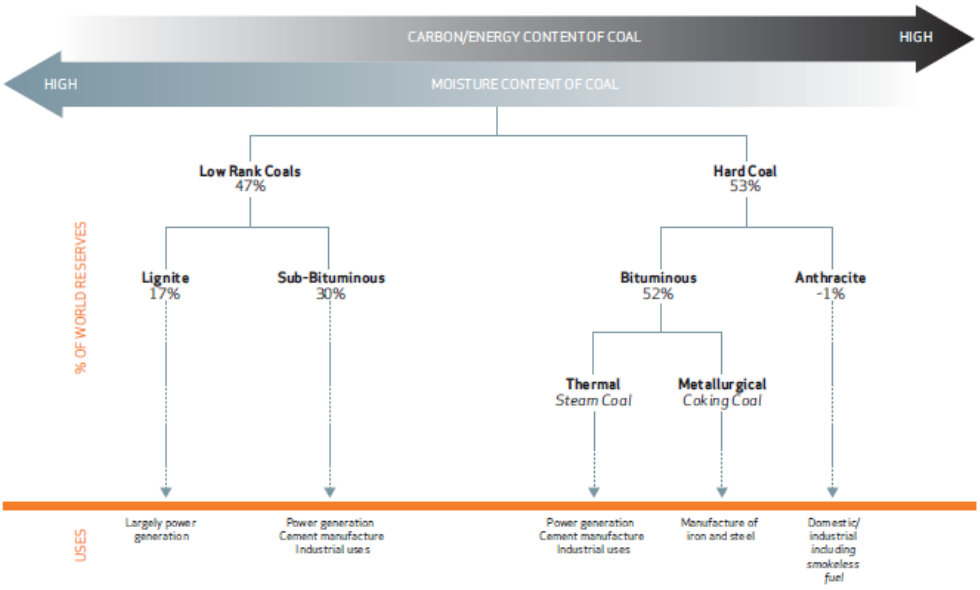

Figure 2-1: Types of Coal (The Coal resource 2009)

2.2.2 Gasification

Gasification is a technological process that uses heat, pressure, and steam to convert any carbonaceous (carbon-based) raw material into synthesis gas (Syngas). Syngas is composed primarily of CO and H_2 but it also contains CO_2, H_2O, H_2S and smaller amounts of N_2 and NH_3. There are a variety of uses for syngas as it can be seen in **Figure 2-2**. Syngas can be used to produce electricity, ultrapure hydrogen after the shift reaction, transportation fuels or chemical products like ammonia.

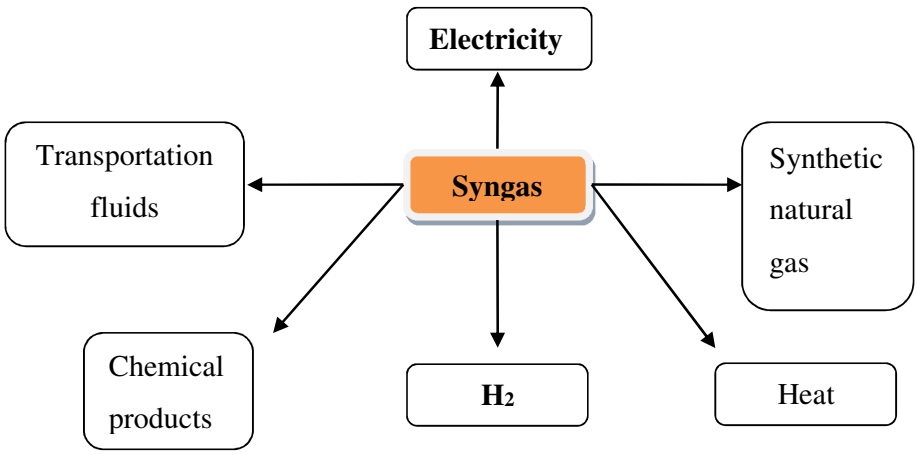

Figure 2-2: Uses of Syngas

As with any technology, widespread market penetration of gasification relies on economic conditions and enabling infrastructures that allow it to be competitive with other alternatives. For gasification, the largest potential market is electricity generation from coal, where Integrated Gasification Combined Cycle (IGCC) power plants are being proposed with increasing frequency (Puigjaner 2011).

Gasification reactions and thermodynamics

The gasification process takes place at temperatures in the range of 1,073 to 2,073 K (800°C to 1800°C). The exact temperature depends on the characteristics of the feed such as the softening and melting temperatures of the ash. Pyrolysis or devolatilisation followed by gasification of the remaining char are the predominant phenomena occurring, and are common for the full range of feeds. Over the whole temperature range described above, the reaction rates are sufficiently high to make it possible to assume that modelling on the basis of the thermodynamic equilibrium of chemical reactions can generate results that approximate the performances observed actually in most commercial gasification reactors (Higman 2003).

The principle chemical reactions occurring during the gasification process involve combustion of carbon, CO and H_2 to form CO_2 and H_2O. Carbon is also reacting with CO_2 to form CO by reverse Boudouard reactions. Gasification reaction by steam, the methane/steam reforming reaction and hydrogasification reaction also occur but have not been included in the reaction set of the gasifiers for this study.

The operation temperatures of coal gasifiers are generally so high that formulation of C2+ hydrocarbons including tar, can be suppressed (Higman 2003).

The temperature dependency of the equilibrium constants can be derived from fundamental data but are usually expressed with the general correlation of the type:

$$\ln K_{p,T} = \ln K_{p,T_o} + f(T) \tag{2-1}$$

T is the absolute temperature in Kelvin. Assuming that the reactions have reached equilibrium the concentrations of the components in the syngas can be determined.

2.3 Gasification technologies

For the gasification processes several types of reactors have been used. These reactors can be generally classified into one of the following three categories: moving bed, fluidised bed, and entrained flow. Some characteristics of the aforementioned gasifiers are summarized in **Table 2-1**.

Moving-bed gasifiers utilise lump coal as feed. Coal feed moves slowly down the bed under the effect of gravity and gasification occurs with the oxidant flowing counter-currently. The oxygen requirements in this gasifier are generally low but the syngas produced contains products resulting from the coal pyrolysis. The temperature of the produced syngas in this gasifier is generally low.

Heat and mass transfer is promoted in fluidized bed gasifiers due to the improved mixing between coal and oxidant inside the reactor. Contrary to entrained-flow gasifier, carbon conversion is limited in fluidized-bed gasifiers as a certain amount of the fuel that has only partially reacted is inevitably removed with the ash.

Table 2-1: Categories of gasification processes (Simbeck 1993)

	Moving-Bed	**Fluid-Bed**	**Entrained flow**
Typical process	Lurgi, BGL	Winkler, HTW, CFB, KRW, U-Gas	Shell, GEE, E-Gas, GSP, KT
Feed rank	Any/High	Low/Any	Any
Outlet gas temperature	425-650°C	900-1050°C	1200-1600°C
Oxidant demand	Low	Moderate	High
Steam demand	High/Low	Moderate	Low

It is very common for fluidized bed gasifiers to operate at temperatures below the softening point of the ash, since ash slagging will disturb the fluidization of the bed (Higman 2003). The size of the particles in the feed is a significant factor affecting the operation of the fluidized bed gasifiers. Fluid-bed gasifiers can generally operate with low-rank coals and biomass.

In the entrained-flow gasifiers the feed and the oxidant flow concurrently along the reactor. They can operate with slurry or dry coal feed. The feed is ground to a size of 100 μm or less to promote mass transfer and allow transport in the gas (Higman 2003). Entrained-flow gasifiers operate in high temperatures to ensure good carbon conversion. The high temperature interlinked with these gasifiers however, creates a high oxygen demand for this type of process. Entrained flow gasifiers can operate with any type of coal, however if there is high moisture or ash content in the coal used, inevitably the oxygen requirements of the gasification process increase. Both gasification technologies examined herein belong to the entrained flow category.

2.4 General Electric Energy (GEE) gasifier

This gasifier was firstly developed during the 1940's at the Texaco's Montebello laboratories in California. In the 1950's the Texaco gasifier was used at the Olin Mathieson Chemical Plant, West Virginia, for ammonia production (NETL 2007). Since then, pilot plants have been built to test different coals and optimise the process operating conditions. The first commercial Texaco coal gasification plant started up in 1983. Regarding the electricity generation industry the Cool Water plant was the first coal gasification project. This plant operated for five years and is considered the first successful IGCC project in terms of operability, availability, and environmental performance (NETL 2007). The experience gained by this commercial operation gives a clear advantage to the GEE gasifier in terms of operability and commercial availability, and has led to the construction of several power plants, demonstrating the use of the GEE gasifier in IGCC power plants. It has been reported that GEE gasifiers have limited refractory life and that as they are operating with a slurry feed system, they are limited to handle low rank coals compared to moving-bed, fluidised-bed and dry feed gasifiers.

GEE offers three design configurations (Rington and Schmoe 2005):

• **Quench**: In this configuration, the hot syngas exiting the gasifier passes through a pool of water to quench the temperature to less than 260°C before entering the syngas scrubber. It is the simplest and lowest capital cost design, but also the least efficient.

• **Radiant Only**: In this configuration, the hot syngas exiting the gasifier passes through a radiant syngas cooler where it is cooled from about 1,586K or 1316°C to 1,089K or 816°C, then through a water quench where the syngas is further cooled to about 477K or 204°C prior to entering the syngas scrubber. Relative to the quench configuration, the radiant only design offers increased output, higher efficiency, improved reliability/availability, and results in the lowest cost of electricity. This configuration was chosen by GEE and Bechtel for the design of their reference plant.

• **Radiant-Convective**: In this configuration, the hot syngas exiting the gasifier passes through a radiant syngas cooler where it is cooled from about 1,589K (1,316°C) to 1,033K (760°C), then passes over a pool of water where particulate is removed but the syngas is not quenched, then through a convective syngas cooler where the syngas is further cooled to about 644K (371°C) prior to entering additional heat exchangers or the scrubber. This configuration has the highest overall efficiency, but at the expense of highest capital cost.

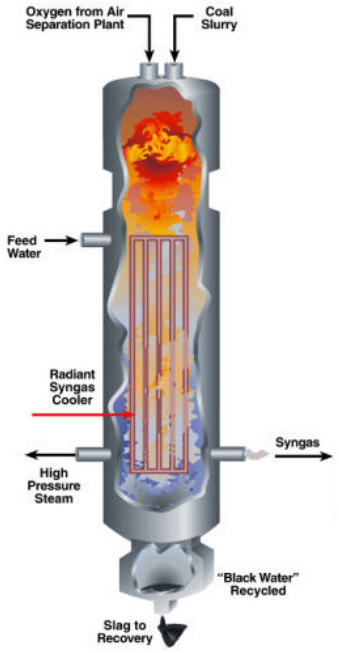

Figure 2-3: General Electric Energy gasifier (NETL 2007)

2.5 Shell gasifier

The development of the Shell gasifier begun in the early 1950's for partial oxidation of oil and gas. However, it was not until 1972 that Shell Internationale Petroleum Maatschappij B.V., begun to work on coal gasification. Several pilot plants have been built and demonstration projects have led to useful experience and conclusions with regards to the quality of the coal used for the gasification as well as extensive environmental monitoring of different Acid Gas Removal (AGR) technologies.

Currently the Nuon power plant at Buggenum, in the Netherland, uses Shell technology for IGCC coal gasification (NETL 2007).

Shell gasifiers can operate with a wide variety of dry coals ranging from anthracite to brown coal so they are regarded as having less limitation with respect to coal quality than GEE gasifiers.

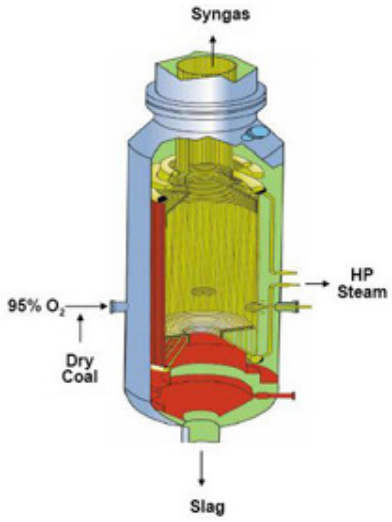

Figure 2-4: Shell gasifier (NETL 2007)

2.6 Simulation approach

The gasification process is simulated using the commercial software Honeywell UniSim Design R400. Illinois No.6 bituminous coal is fed to the gasifier with the properties as shown in **Table 2-2**. The selection of feed coal was primarily driven to have a direct comparison of the results produced herein and the results as presented in the reference report (NETL 2007).

Table 2-2: Illinois No. 6 analysis (NETL 2007)

Proximate Analysis	**w/w (%)**	**w/w (%) Dry**	**Ultimate Analysis**	**w/w (%)**	**w/w (%) Dry**
H_2O	11.12	0.00	H_2O	11.12	0.00
Ash	9.70	10.91	C	63.75	71.72
Volatile Matter	34.99	39.37	H	4.50	5.06
C	44.19	49.47	N	1.25	1.41
Total	100.00	100.00	Cl	0.29	0.33
S	2.51	2.82	S	2.51	2.82
HHV, kJ/kg	**27,113**	**30,506**	Ash	9.70	10.91
LHV, kJ/kg	**26,151**	**29,544**	O	6.88	7.75
			Total	100	100

The oxygen required for the gasification consists of 95% oxygen, 1.4% nitrogen and 3.6% argon, and is provided by the Elevated Pressure Air Separation Unit (EP ASU). The GEE gasifier operates at 1,589K or 1,316 °C and 5,617 kPa, while the Shell gasifier operates at 1,891K or 1,618 °C and 4,031 kPa. Both gasifiers were modelled as "Conversion" reactors in Honeywell UniSim Design R400 with the Peng-Robinson EOS to account for non-ideality resulting from the high pressures of the gasifiers. It was assumed that the following reactions take place in the gasifiers:

$$2C + O_2 \leftrightarrow 2CO \quad (2\text{-}2)$$

$$C + O_2 \leftrightarrow CO_2 \quad (2\text{-}3)$$

$$H_2 + \frac{1}{2}O_2 \leftrightarrow H_2O \quad (2\text{-}4)$$

$$N_2 + 3H_2 \leftrightarrow 2NH_3 \quad (2\text{-}5)$$

$$C + H_2 \leftrightarrow CH_4 \quad (2\text{-}6)$$

$$S + H_2 \leftrightarrow H_2S \quad (2\text{-}7)$$

$$Cl_2 + H_2 \leftrightarrow 2HCl \quad (2\text{-}8)$$

$$2C + 2S + O_2 \leftrightarrow 2COS \quad (2\text{-}9)$$

The conversion rate of each reaction was carefully estimated to reproduce the composition of the syngas at the outlet of the gasifier as reported by the DOE NETL (2007). The results obtained with the estimated conversions were then checked back against the data as reported from DOE NETL for the gasifiers' outlet stream to verify the validation of the calculated conversions. The conversions occurring in the GEE and Shell gasifiers are shown in **Table 2-3**.

Table 2-3: Conversion rates in GEE and Shell gasifiers

Reaction	Base component	GEE (%)	Shell (%)
(2-2)	Carbon	67.94	95.64
(2-3)	Carbon	29.82	3.53
(2-4)	Water	48.32	59.20
(2-5)	Nitrogen	9.73	2.80
(2-6)	Carbon	0.20	0.07
(2-7)	Sulphur	97.50	92.06
(2-8)	Chlorine	100.00	100.00
(2-9)	Carbon	0.04	0.12
Total Carbon conversion:		98.00	99.36

Based on the conversion rates shown in **Table 2-3**, the syngas composition estimated for the two gasifiers are shown in **Table 2-4.**

At this point it should be clarified that the heating values are reported on a higher heating value (HHV) basis.

The carbon conversion is defined as:

$$Carbon\ conversion\ (\%) = \left[1 - \left(\frac{Carbon\ \ in\ slag}{Carbon\ \ in\ \ feed}\right)\right] x100 \qquad (2\text{-}10)$$

As shown in **Table 2-3**, the total carbon conversion for GEE gasifier is estimated to be 98.0%, while for the Shell gasifier the total carbon conversion is 99.4% approximately.

The results obtained for the GEE and Shell IGCC power plants without carbon capture are presented in **Tables 2-4** and **2-5** for the gas stream exiting the gasifier prior to entering the syngas scrubber.

Table 2-4: Validation of the simulation approach with DOE NETL data (NETL 2007) for GEE and Shell IGCCs without carbon capture

	GEE		Shell	
	Simulation	**DOE NETL**	**Simulation**	**DOE NETL**
Ar	0.0079	0.0079	0.0097	0.0097
CH_4	0.0010	0.0010	0.0004	0.0004
CO	0.3442	0.3442	0.5720	0.5717
CO_2	0.1511	0.1511	0.0211	0.0211
COS	0.0002	0.0002	0.0007	0.0007
H_2	0.3348	0.3348	0.2900	0.2901
H_2O	0.1429	0.1429	0.0364	0.0364
H_2S	0.0073	0.0073	0.0081	0.0081
N_2	0.0079	0.0089	0.0574	0.0585
NH_3	0.0017	0.0017	0.0033	0.0033
O_2	0.0003	0.0000	0.0000	0.0000
SO_2	0.0000	0.0000	0.0000	0.0000
F, kg/s	131.87	131.90	195.05	195.09
(lb/h)	1,046,639	1,046,880	1,548,048	1,548,350
T, K	866	866	1,164	1,164
(°F)	(1,100)	(1,100)	(1,635)	(1,635)
P, 10^5 Pa	55.14	55.14	42.38	42.38
(psia)	(799.7)	(799.7)	(614.7)	(614.7)

Table 2-5: Validation of the simulation approach with DOE NETL data (NETL 2007) for GEE and Shell IGCCs with carbon capture

	GEE		Shell	
	Simulation	**DOE NETL**	**Simulation**	**DOE NETL**
Ar	0.0079	0.0079	0.0097	0.0097
CH_4	0.0010	0.0010	0.0004	0.0004
CO	0.3439	0.3442	0.5720	0.5716
CO_2	0.1510	0.1511	0.0211	0.0211
COS	0.0002	0.0002	0.0007	0.0007
H_2	0.3343	0.3349	0.2900	0.2901
H_2O	0.1428	0.1429	0.0364	0.0364
H_2S	0.0073	0.0073	0.0081	0.0081
N_2	0.0089	0.0089	0.0574	0.0585
NH_3	0.0019	0.0017	0.0033	0.0033
O_2	0.0000	0.0000	0.0000	0.0000
SO_2	0.0000	0.0000	0.0000	0.0000
F, kg/s	135.04	134.80	109.07	109.11
(lb/h)	(1,071,733)	(1,069,860)	(865,655)	(865,967)
T, K	866	866	1,697	1,697
(°F)	(1,100)	(1,100)	(2,595)	(2,595)
P, 10^5 Pa	55.14	55.14	41.69	41.69
(psia)	(799.7)	(799.7)	(604.7)	(604.7)

Selection of gasification pressure and temperature

It is generally considered advantageous for gasification to occur under pressure. The reasons for this are potential savings in compression energy and reduction of equipment size (Higman 2003). It is therefore sensible to select the gasification pressure according to the requirements of the process and equipment upstream or downstream of the gasifier. Since the advanced F-class gas turbine selected for the cases investigated requires a pressure of approximately 32 bar, the gasifier pressure should be chosen to be sufficiently higher than 32 bar taking into account pressure losses at the units located between the gasifier and the gas turbine. The minimum operating temperature is generally set on the basis of the ash properties. Since the gasification processes are assumed to operate at approximately 55 and 42 bar for the GEE and Shell gasifier cases, the operating temperatures selected are 1,573K (1,300°C) and 1,700K (or 1,427°C) respectively, so that the syngas produced contains low methane concentration.

Although GEE offers three design configurations (Rigdon 2005) gasifier chosen in this study is the so-called “Radiant Only”. In this configuration, the gasifier is equipped with a radiant syngas cooler for producing additional High Pressure (HP) steam by cooling down the hot syngas stream. While in the conventional IGCC case, the gas leaving the scrubber is sent to a COS hydrolysis reactor for COS removal, the syngas does not have to be sent to a COS removal unit in the carbon capture case since the COS can be removed in the Water Gas Shift Reactors (WGSR) as shown in the following Figures.

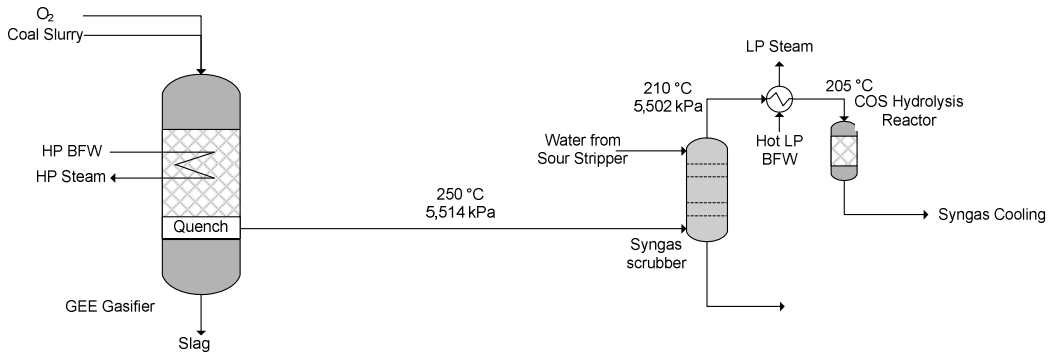

Figure 2-5: GEE Gasifier, syngas scrubber and COS hydrolysis reactor for non-capture mode (Kapetaki et al. 2013)

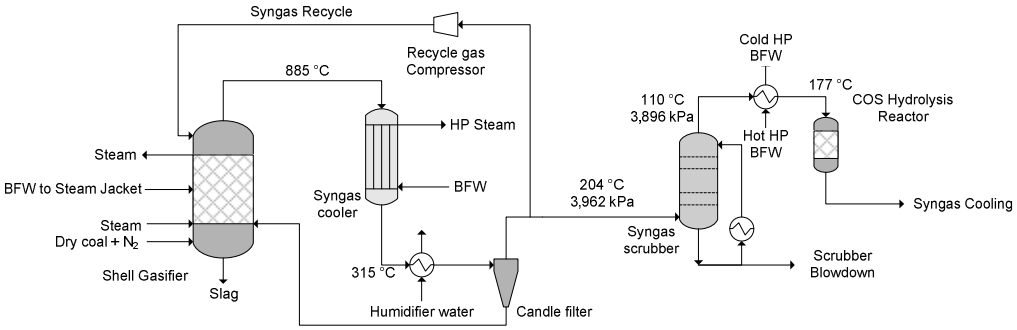

Figure 2-6: Shell Gasifier, syngas scrubber and COS hydrolysis reactor for non-capture mode (Kapetaki et al. 2013)

2.7 Points of discussion

The main difference in IGCC power plants with GEE and Shell gasifiers arises from the fact that they operate with different coal feeds. GEE gasifiers are coal slurry gasifiers, while Shell gasifiers are fed with dry coal. This fact, together with the different operating conditions for each gasifier and the different conversion rates, results in different compositions in the syngas produced, as well as different carbon loss in the slag.

98.0% of the feed carbon is converted to the syngas in the GEE gasifier resulting in, a H_2/CO fraction of 0.97. On the other hand, the corresponding conversion for the Shell gasifier is 99.4% resulting in a H_2/CO fraction of 0.51. This difference significantly affects the two cases in carbon capture mode, as for GEE gasifiers, the water gas shift

reaction can start immediately. This is not the case for Shell IGCC, as the gasification product has to be saturated with water prior to entering the water gas shift reactors.

The coal feed for each case of IGCC power plant examined is reported in **Table 2-2**. This feed corresponds to a thermal input which is determined by the gas turbine incorporated in the power plant. Consequently, the oxygen demand for the gasifier is determined in accordance with the gasifier conversion and the Gas Turbine (GT) electrical output.

In the DOE NETL report it has been assumed that the GT consists of two identical F-Class GE turbines. This assumption was adopted herein as well, and fuel specifications as reported in (Erickson 2003; GEI-41040G 2002). As shown in **Table 2-6**, the thermal input, i.e. the coal feed in the gasifier, is increased in the carbon capture cases to maintain the electrical GT output identically for all the cases. Different gasification options in IGCC cases will produce gasification streams of different mass densities which obviously affects the turbine mechanical efficiency and electrical output. Shell gasifiers produce an output stream with lower mass density than the density of the stream produced by GEE gasifiers. It is therefore expected that the mechanical efficiency of the Shell IGCC GT will be higher. However, while acknowledging this effect, for all cases investigated it was assumed a GT electrical output of 464 MW_e.

Table 2-6: Coal feed in GEE and Shell gasifiers for non-capture modes

	GEE	**Shell**
H_2O	255,589	20,982
C	312,120	288,550
H	22,020	20,368
N	6,136	5,658
Cl	1,436	1,312
S	12,272	11,360
Ash	47,476	43,901
O	33,727	31,140
Mass density, kg/m^3	8.616	6.158
Total solids, kg/s	54.83	50.69
(lb/h)	(435,187)	(402,289)
Thermal input, kW_t HHV	1,674,044	1,547,493
Oxygen feed, kg/s	51.64	44.12
(lb/h)	(409,853)	(350,168)

It should be highlighted that discrepancies have been found within the reference report in the non-carbon capture GEE and Shell IGCCs for the composition of the gasification product stream in nitrogen and oxygen. Particularly for nitrogen, the discrepancy is nearly 13% between the simulation result and the reference for the GEE IGCC. This inaccuracy arises from the mass balance around the GEE gasifier for the non-capture case which is not closing as presented in DOE NETL report. The same applies to non-capture Shell IGCC, even if to a lesser extent. Particularly for nitrogen, the discrepancy

is nearly 2% between the simulation result and the reference. Moreover, results in the reference report present remaining oxygen in the gasification product of the non-capture GEE IGCC case (0.3%). It is therefore probable that there are inaccuracies in the estimations of the reaction stoichiometry in this gasifier. No discrepancies have been found regarding oxygen in Shell cases.

2.8 Summary and conclusions

The Shell IGCC demonstrates a far better plant efficiency than the GEE IGCC in case of the non-capture case due to its higher efficiency in the conversion of coal to gas. However, the syngas of the Shell IGCC using dry coal has lower water content than that of the GEE IGCC using coal slurry, results in a drop in net plant efficiency of 10% for the carbon capture Shell IGCC case. To avoid this drastic plant efficiency drop, it is worth considering how to improve the carbon capture rate in the AGR unit without significant increase in its power consumption in order to compensate the energy penalty related to the syngas quench and the shift conversion which occurs in the carbon capture Shell IGCC, for achieving 90% carbon capture rate overall.

Four simulation cases for GEE and Shell IGCCs without and with carbon capture have been constructed based on the DOE NETL report. The simulation cases with different gasifier in carbon capture mode will be presented in detail in Chapter 4. Discrepancies have been however identified and presented. Therefore, the approach adopted herein suggests an improved design for the GEE and Shell gasifiers compared to the reference study, for all the IGCC cases examined.

Chapter 3 IGCC approach and simulation of major units upstream carbon capture processes

3.1 Introduction

A complete and fully functional representation of the overall IGCC power plant operation is essential for a comprehensive overview of the power plant. For this purpose, process flow diagrams including all the unit operations were developed for IGCC power plants. The simulation cases consist of continuous processes that represent the IGCC power plant operation. Particular attention has been paid to each one of the processes, as a part of the overall operation and performance. Due to the importance and the particular focus on carbon capture processes, there are dedicated Chapters for these sections (Chapters 4 and 5). The approach adopted for units upstream carbon capture process, i.e. EP ASU and syngas clean-up are presented in this Chapter.

3.2 Air Separation Unit (ASU) and surroundings

Smith and Klosek (2001) reported a detailed review of ASUs. Elevated Pressure Air Separation Unit (EP ASU) in particular, is the unit providing oxygen of 95 % purity to the gasifier, so that the gasification reactions occur. The operating pressures of the "Elevated" pressure air separation scheme are approximately twice as high as the pressures of traditional plants. In this scheme, the main air compressor discharge pressure is set at 1.3 MPa (190 psia) compared to a traditional ASU plant operating pressure of about 0.7 MPa (105 psia) (NETL 2007). For IGCC designs the elevated pressure ASU process minimizes power consumption and decreases the size of some of the equipment (NETL 2007), therefore being advantageous over the traditional schemes.

ASU operation and energy consumption strongly depend on whether it is integrated with the gas turbine or not. In the case of air integration, the ASU operates with pressures determined by the gas turbine's air compressor discharge. The integration between the ASU and the gas turbine is usually performed by extracting some, or all,

of the ASU's requirement for air from the compressor feeding air to the combustor. Air extraction is in some cases essential to maintain stable compressor or turbine operation to compensate for increased fuel flow rates. In other cases, the air extracted can be compensated by injecting the available nitrogen produced from the ASU (Kelhofer et al. 2009).

However, the compressed air originated by extracting the air from the gas turbine is usually very hot (672K-727K or 399-454°C) and has to be cooled before the air integration with the ASU occurs. The heat of compression of the extracted air can be recovered by a gas/gas heat exchanger, by transferring this heat to the nitrogen stream which is injected into the gas turbine.

Air integration is reasonable for the non-carbon capture cases. In the carbon capture cases, once the syngas is diluted to meet the target heating value, all of the available combustion air is required to maintain mass flow through the turbine and hence maintain power output.

3.2.1 EP ASU process

The air separation unit is designed to produce 95 % pure oxygen which is then directed to the gasifier. Nitrogen which is also recovered from the ASU after being compressed is used in the gas turbine combustor to provide the required dilution.

A general schematic of the ASU is illustrated in **Figure 3-1**.

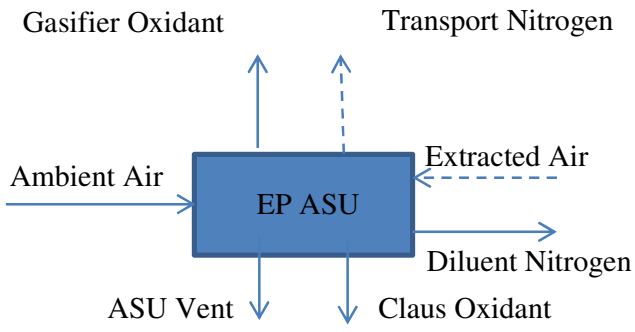

Figure 3-1: ASU simplified schematic

Depending whether a non-capture or carbon capture case are considered, the air feed to the ASU is supplied either by extracting some air from the compressor of the gas turbine with the remaining air required provided from the ASU's Main Air Compressor (MAC) or solely by the MAC. It was assumed that the particulates contained in the ambient air are removed by a suction filter prior to entering the MAC, so that erosion and fouling are avoided. The filtered air is compressed in four stages in the MAC, implementing intercooling between each stage. It has also been assumed that water, carbon dioxide, and saturated hydrocarbons contained in the air are removed with the use of adsorption beds, while any adsorbent fines that may remain in the air are removed by a dust filter.

The general scheme of the EP ASU adopted herein was based in the configurations proposed in the literature (Jones et al. 2011) and was modified accordingly to accommodate the overall IGCC requirements in oxygen and nitrogen. Since no air integration was performed in the carbon capture cases, the ambient air required for the EP ASU operation in these cases is fed solely to the MAC. The compressed air passes through the main heat exchanger, where liquefied and refrigerated air is produced.

The air feeds are cooled to cryogenic temperatures against returning product oxygen and nitrogen streams in plate-and-fin heat exchangers. The large air stream fed is liquefied against the liquid oxygen produced before it is fed to the distillation columns.

Oxygen and nitrogen are produced by the two distillation columns of the process. The oxygen product is withdrawn from the distillation columns as a liquid and is pressurized by a cryogenic pump.

The pressurized liquid oxygen is then vaporized against the high-pressure air feed before being warmed to ambient temperature. The gaseous oxygen exits the unit and is fed to the centrifugal compressor with intercooling between each stage of compression. The compressed oxygen is then fed to the gasification unit.

Nitrogen is produced in the ASU at two pressure levels. Low-pressure nitrogen is split into two streams. The majority of the low-pressure nitrogen is compressed and fed to

the gas turbine as diluent nitrogen. The high-pressure nitrogen stream, also produced from the ASU, is further compressed and it is also directed to the gas turbine.

The DOE/NETL report (2007) failed to represent in detail the ASU process flow diagram. Inconsistencies where also discovered in terms of overall mass balances around the unit as demonstrated in **Table 3-1** and **Table 3-2**[1,2]. The oxygen balance for example is negative in both non capture and carbon capture GEE cases. On the contrary, in both Shell cases, oxygen and nitrogen are reported to be remaining, while there is negative balance for argon.

[1] Imperial units are also provided within tables to enable direct comparisons with results as presented in reference study (DOE NETL 2007).

[2] The mass balance calculations where conducted from data as reported in Appendix A for all cases.

Table 3-1: EP ASU mass balances verification for GEE simulation cases and reference (DOE 2007)

	GEE					
	Non capture			Carbon capture		
kg/s (lb/h)	Total Mass In	Total Mass Out	**Balance**	Total Mass In	Total Mass Out	**Balance**
Ar	2.99	2.97	+0.20	3.04	3.02	+0.02
	(23,754.53)	(23,536.25)	(+218.28)	(24,158.22)	(24,006.47)	(+151.75)
N_2	172.33	171.46	+0.87	175.19	174.31	+0.88
	(1,367,695.93)	(1,360,786.54)	(+6,909.39)	(1,390,398.77)	(1,383,437.91)	(+6,960.86)
O_2	52.97	53.03	–0.05	53.85	53.9	–0.05
	(420,424.68)	(420,859.06)	(–434.38)	(427,363.70)	(427,793.62)	(–429.92)

Table 3-2: EP ASU mass balances verification for Shell simulation cases and reference (DOE 2007)

	Shell					
	Non capture			Carbon capture		
kg/s (lb/h)	Total Mass In	Total Mass Out	**Balance**	Total Mass In	Total Mass Out	**Balance**
Ar	2.55	2.74	–0.19	2.67	2.86	0.19
	(20,264.35)	(21,715.60)	(–1,451.25)	(21,175.39)	(22,691.02)	(994.88)
N_2	147.01	146.31	0.70	153.62	152.96	0.66
	(1,166,744.78)	(1,161,181.16)	(5,031.62)	(1,219,198.78)	(1,213,977.73)	(5,221.05)
O_2	45.19	45.07	0.12	2.67	2.86	–0.19
	(358,653.04)	(357,718.50)	(934.54)	(21,175.39)	(22,691.02)	(–1,515.64)

While the ASU was simulated in detail, it should be noted that these simulation cases serve solely as a benchmark. Further work is required and recommended to achieve an optimised configuration in terms of design, operation and energy requirements.

3.2.2 EP ASU simulation

The EP ASU was simulated using the commercial software Honeywell UniSim R400 adopting the Peng-Robinson equation of state to describe the thermodynamic regime of the process.

The oxygen and nitrogen produced are sufficient to accommodate the requirements of the gasifier for oxygen for both GEE and Shell gasification technologies, oxygen requirements at the Claus plant, and the combustor injection with nitrogen.

Nitrogen is produced from both High Pressure (HP) and Low Pressure (LP) columns. Oxygen is obtained from the LP columns and then is heated in the main heat exchanger.

Air is fed to the compressor and after is liquefied. The liquid air being refrigerated at 122K (–151°C) is fed to the HP absorber in two separate air inlets. The operating pressure in HP column is 12.55 bar, and produces at the top high purity nitrogen (>99%). The HP column nitrogen product is split and a portion is used as a reflux to the column so that the targeted nitrogen purity can be obtained. The rest of the high purity nitrogen product is sent to the LP column along with the oxygen rich bottom stream. LP absorber operates at 4 bar.

It has been assumed that air is cooled and fed to an adsorbent-based pre-purifier system. The adsorbent removes water, carbon dioxide, and saturated hydrocarbons in the air. Any adsorbent fines that may be present are assumed to be removed from the air by a dust filter. The inlets stream for the air and extracted air feeds are given in Tables below (**Table 3-3** and **Table 3-4**) while the resulting oxygen and nitrogen product streams are given in **Table 3-5** and **Table 3-6**. The schematics describing the simulation cases of the IGCC EP ASU process are shown in **Figure 3-2** to **Figure 3-5**.

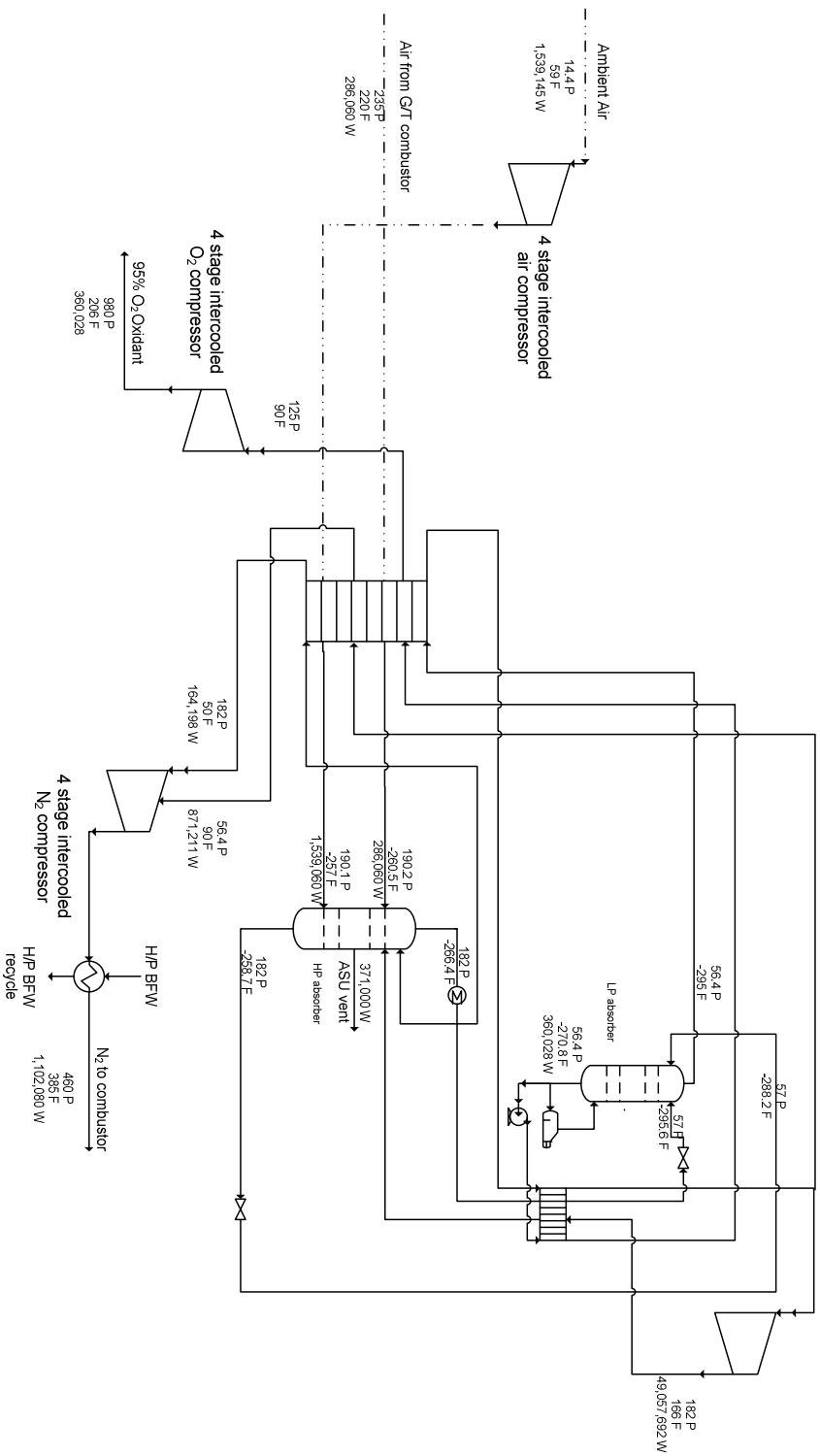

Figure 3-2: GEE IGCC EP ASU schematic in non-capture mode

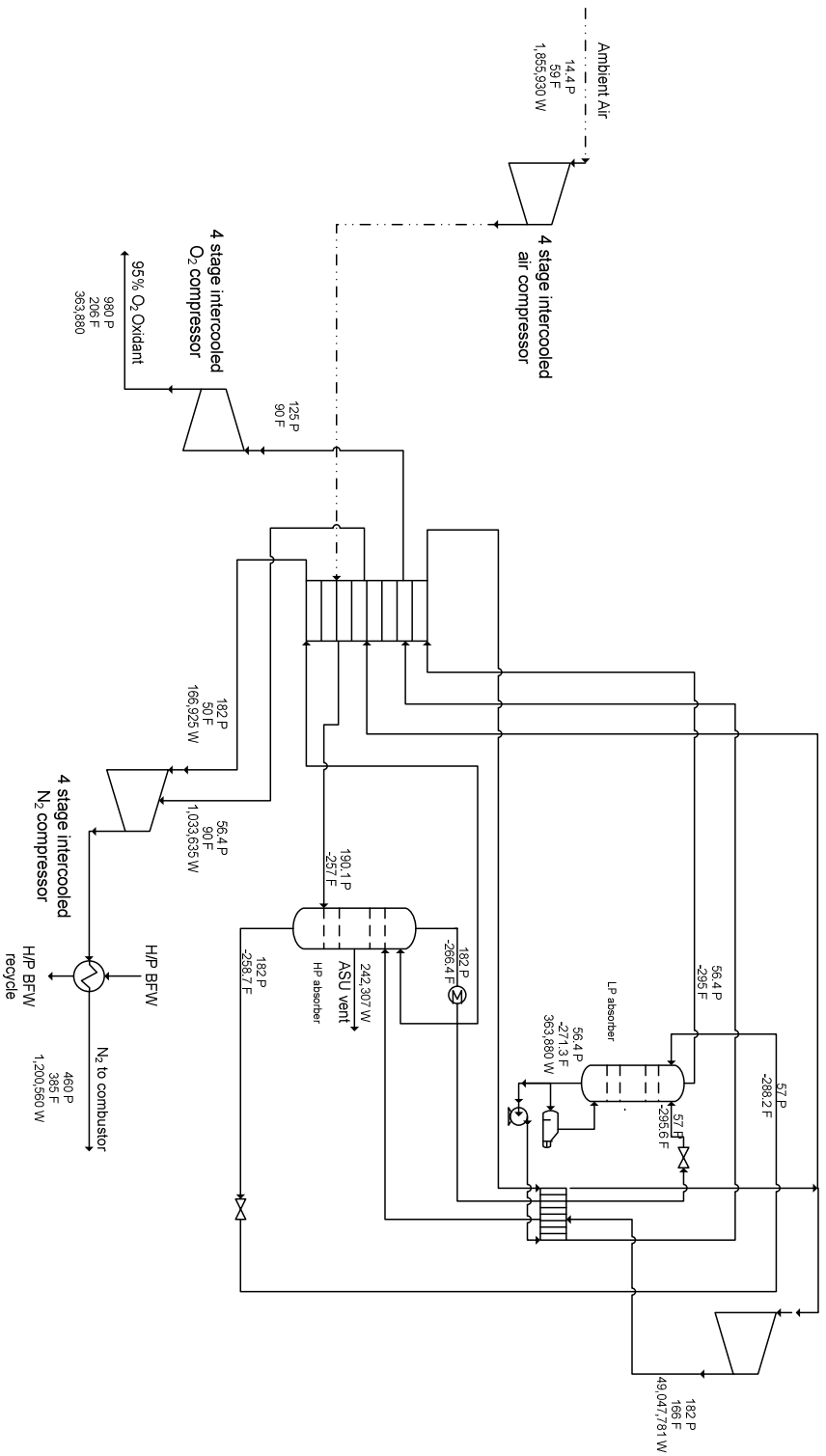

Figure 3-3: GEE IGCC EP ASU schematic in carbon capture mode

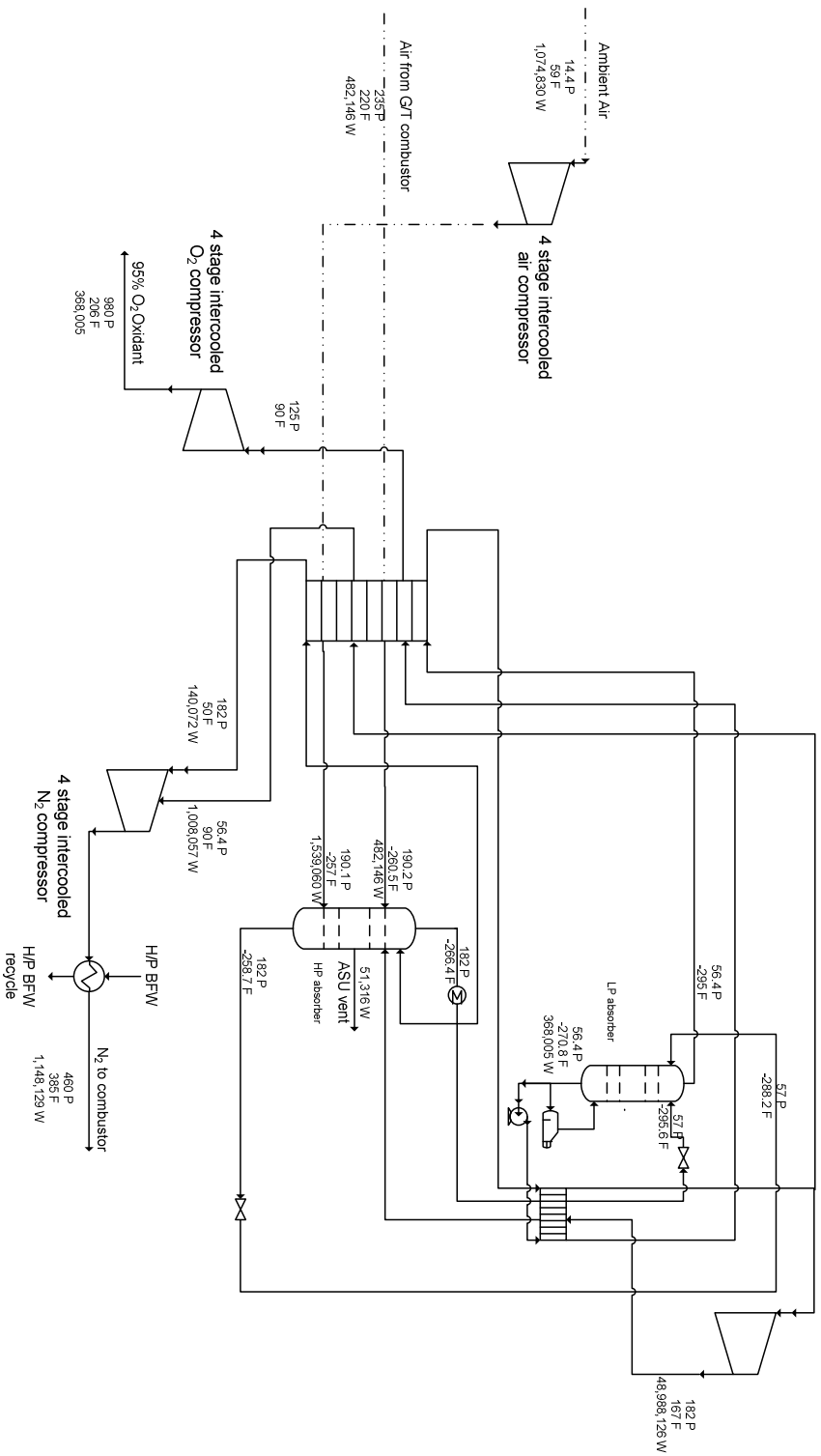

Figure 3-4: Shell IGCC EP ASU schematic in non-capture mode

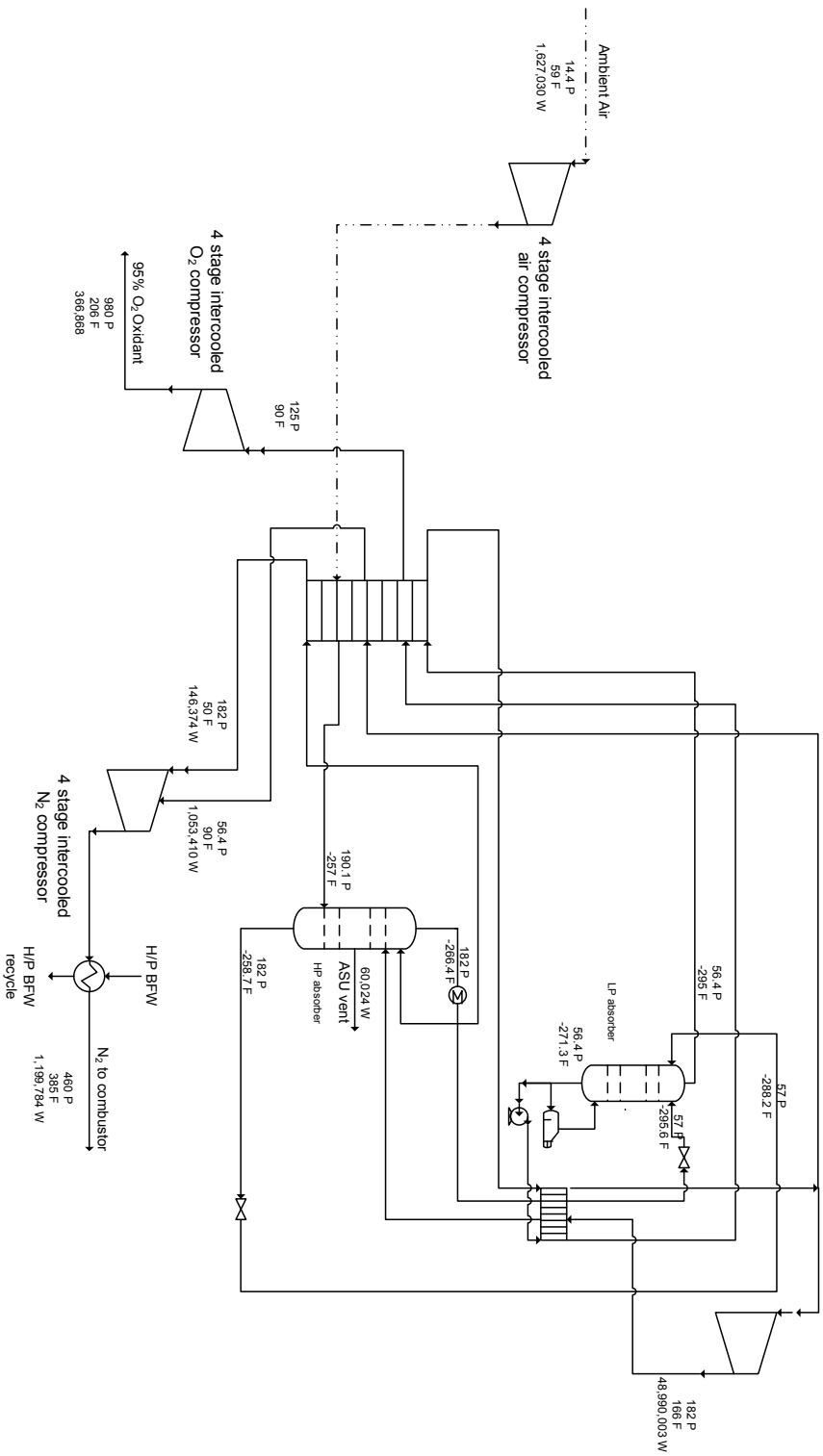

Figure 3-5: Shell IGCC EP ASU schematic in carbon capture mode

Table 3-3: Air feed of the EP ASU in all simulation cases

	GEE		Shell	
	Non capture	**Carbon capture**	**Non capture**	**Carbon capture**
Ar	0.0094	0.0094	0.0094	0.0094
H_2O	0.0104	0.0108	0.0104	0.0104
N_2	0.7722	0.7719	0.7722	0.7722
O_2	0.2077	0.2076	0.2077	0.2077
F, kg/s	193.93	233.85	135.42	204.37
(lb/h)	(1,539,150)	(1,855,930)	(1,074,830)	(1,622,030)
T, K	385	384	384	389
(°F)	(233)	(232)	(232)	(238)
P, 10^5Pa	13.11	13.14	13.14	13.10
(psia)	(190.1)	(190.6)	(190.6)	(190.0)

Note: Components with non-zero compositions only are presented. Other stream components' compositions not shown should be considered to be zero.

Table 3-4: Extracted air feed in the EP ASU for the non-capture simulation cases

	GEE	**Shell**
Ar	0.0094	0.0094
H_2O	0.0104	0.0108
N_2	0.7722	0.7719
O_2	0.2077	0.2076
F, kg/s (lb/h)	36.04 (286,060)	60.75 (482,146)
T, K (°F)	706 (811)	706 (811)
P, 10^5 Pa (psia)	16.2 (234.9)	16.2 (234.9)

Table 3-5: EP ASU oxygen product streams for non-capture and carbon capture GEE and Shell IGCCs

	GEE		Shell	
	Non capture	**Carbon capture**	**Non capture**	**Carbon capture**
Ar	0.0267	0.0298	0.0432	0.0369
N_2	0.0232	0.0201	0.0068	0.0128
O_2	0.9501	0.9501	0.9500	0.9503
F, kg/s	45.36	45.85	46.37	46.22
(lb/h)	(360,028)	(363,880)	(368,005)	(366,868)
T, K	308	308	305	305
(°F)	(95)	(95)	(90)	(90)
P, 10^5 Pa	3.89	3.89	8.62	8.62
(psia)	(56.4)	(56.4)	(125)	(125)

Table 3-6: EP ASU nitrogen product streams for non-capture and carbon capture GEE and Shell IGCCs

	GEE		Shell	
	Non capture	**Carbon capture**	**Non capture**	**Carbon capture**
Ar	0.0028	0.0021	0.0003	0.0003
N_2	0.9910	0.9976	0.9952	0.9951
O_2	0.0061	0.0003	0.0045	0.0046
F, kg/s	138.86	151.27	145.91	144.66
(lb/h)	(1,102,080)	(1,200,560)	(1,158,057)	(1,148,149)
T, K	469	469	469	469
(°F)	(385)	(385)	(385)	(385)
P (10^5Pa)	31.72	31.72	31.72	31.72
(psia)	(460)	(460)	(460)	(460)

3.3 Syngas clean up

The syngas exiting the gasifier, after cooling, passes through a syngas scrubber where a water wash is used to remove the remaining chlorides and particulate. The syngas exiting the scrubber is saturated with water, in temperatures ranging from 472 to 483K (199-210°C), depending on the gasification technology incorporated.

In non-capture cases, the gas stream resulting from the syngas scrubber is cooled down and sent to H_2S removal unit. In carbon capture cases, after the raw synthesis gas is enriched in CO_2 and H_2 at the WGSRs, the shifted gas produced is ready to be directed

to the H_2S/CO_2 co-removal unit. However, regardless of the gasification technology, the stream exiting the WGSRs is saturated with water, in temperatures that are in the range of 544-687 K (271-414°C). It is therefore essential that the stream is cooled down to temperatures that favour the physical absorption adopted in the H_2S/CO_2 co-removal unit downstream.

The gas clean up and cooling section consists of several heat exchangers and drums as shown in **Figure 3-6** to **Figure 3-9**.

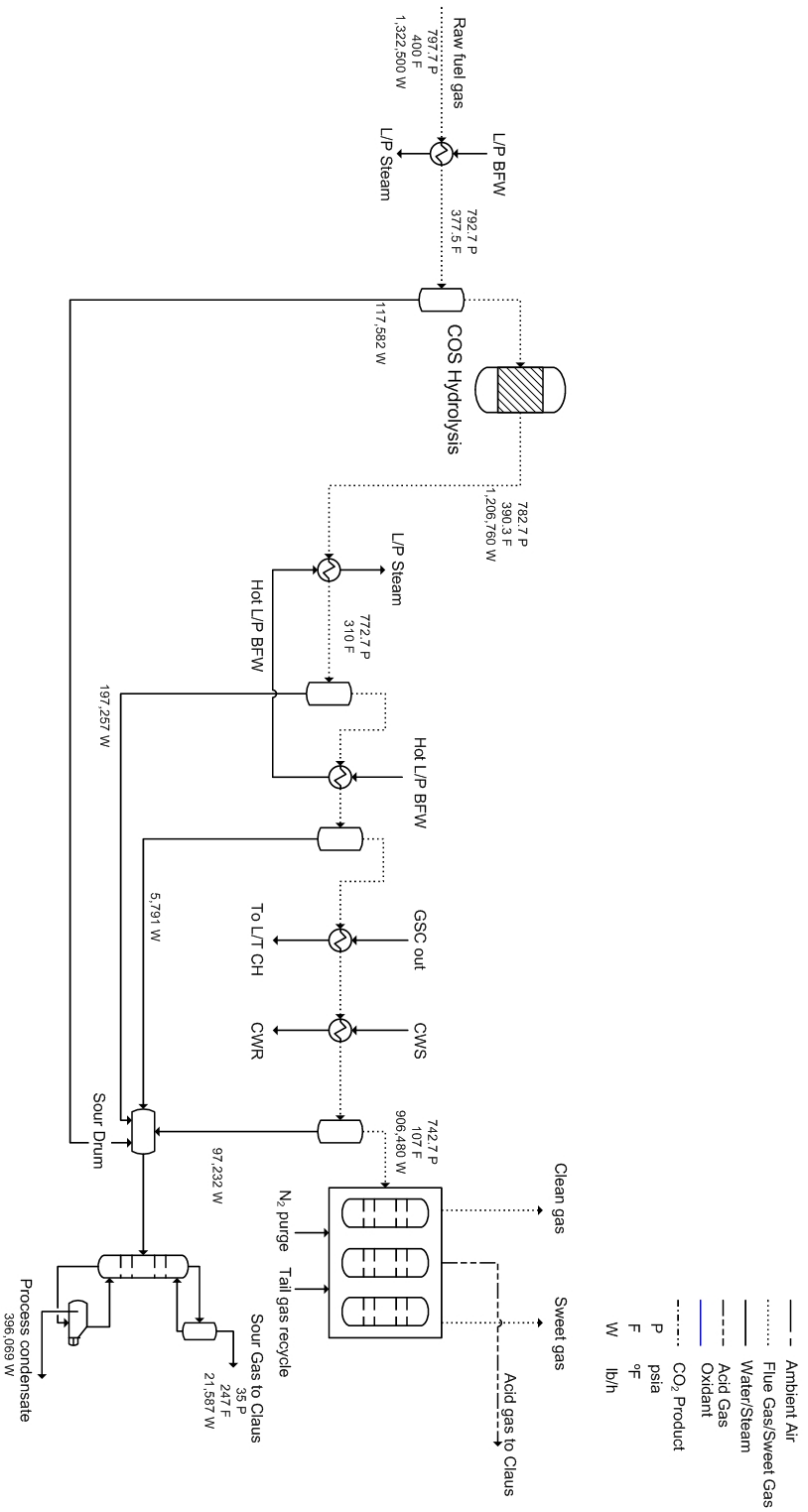

Figure 3-6: Non capture GEE IGCC syngas cleanup and sour stripper

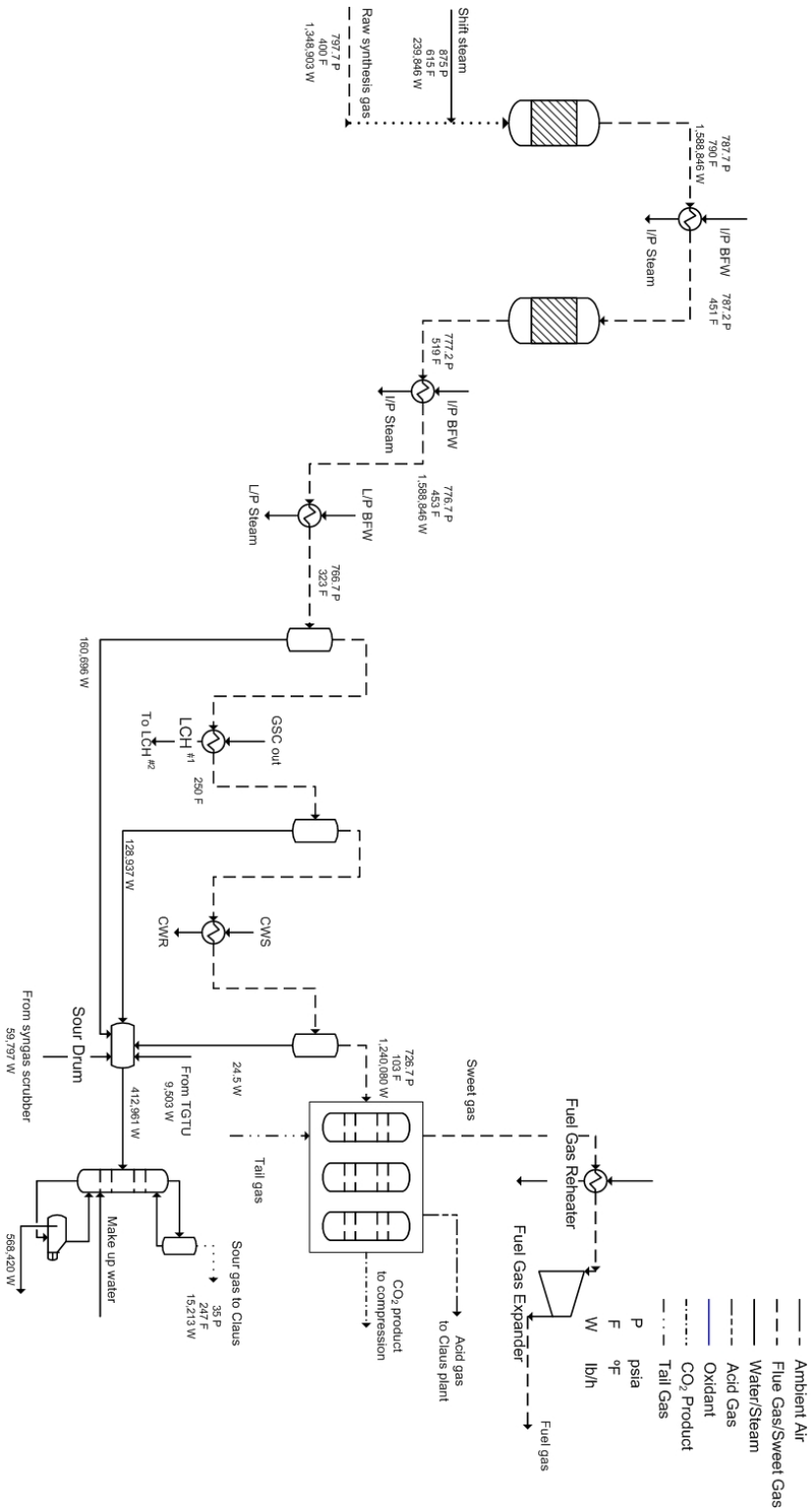

Figure 3-7: Carbon capture GEE IGCC WGSRs, syngas clean up and sour stripper

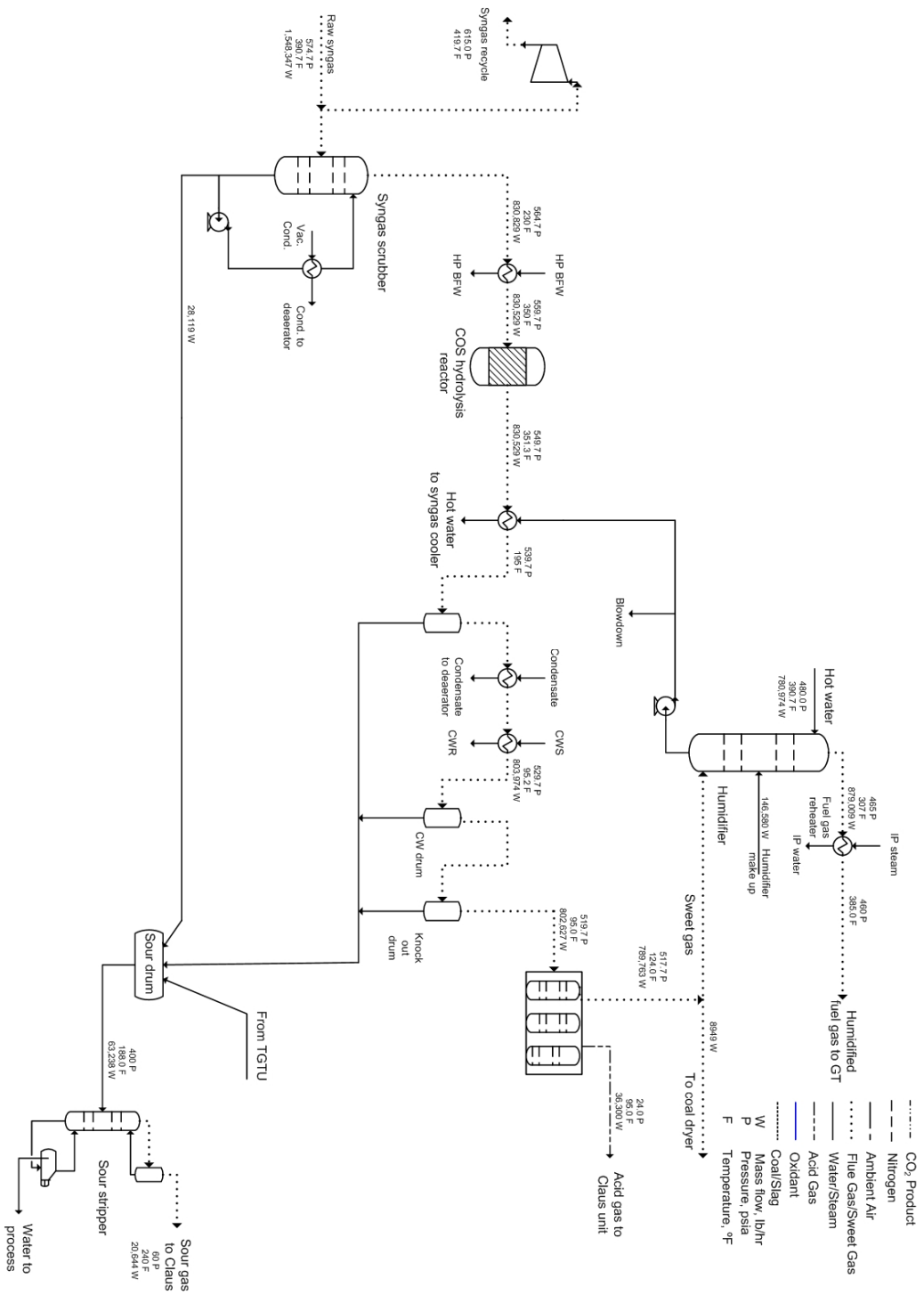

Figure 3-8: Non capture Shell IGCC syngas clean up and sour stripper

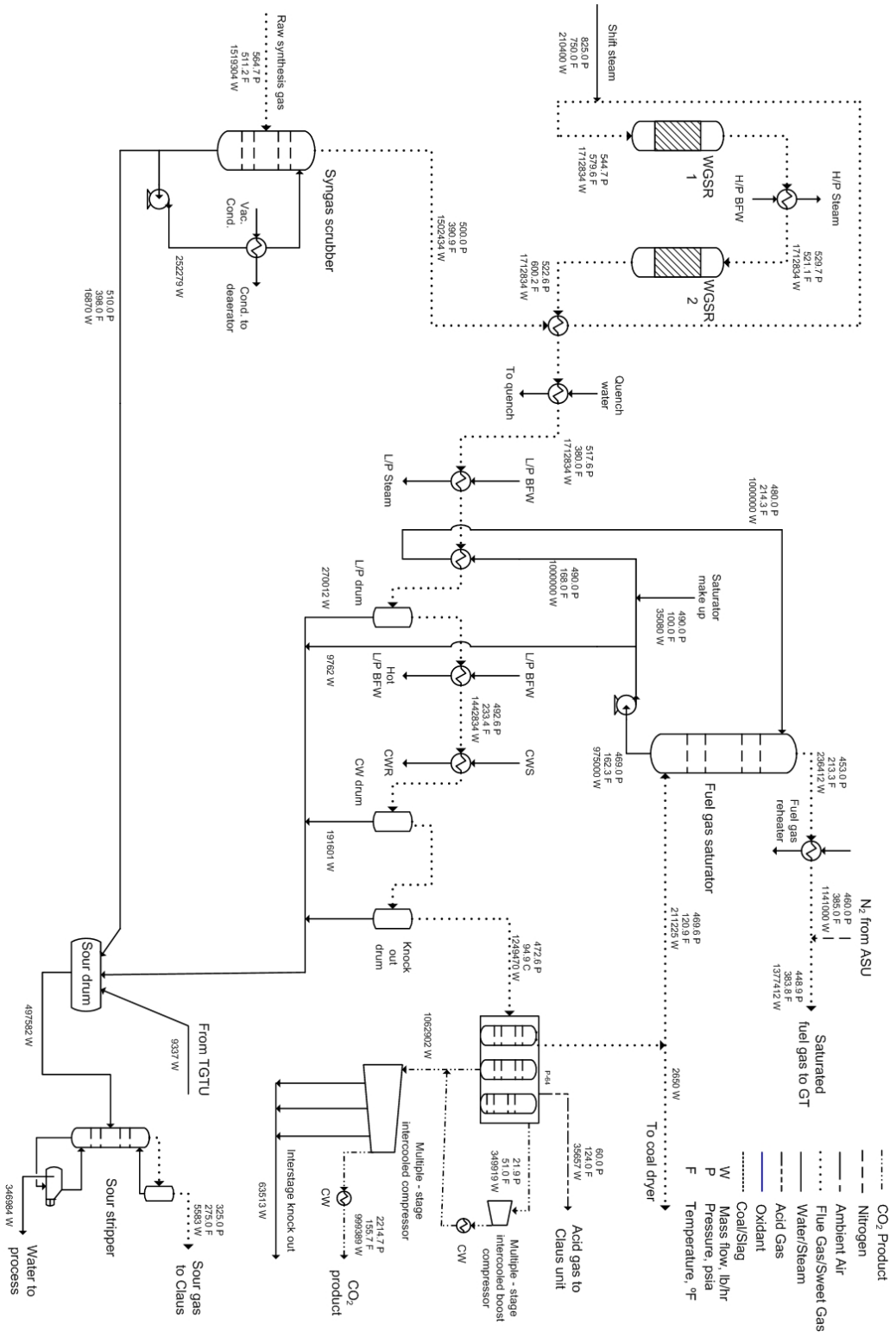

Figure 3-9: Carbon capture Shell IGCC WGSRs, syngas clean up and sour stripper

The sour water stripper removes NH_3, SO_2, and other impurities from the scrubber and other waste streams. The stripper consists of a sour drum that accumulates sour water from the gas scrubber and condensate from synthesis gas coolers. Sour water from the drum flows to the sour stripper. Sour gas is stripped off the liquid and sent to the sulphur recovery unit. It has been assumed that the remaining water can be sent to a wastewater treatment plant.

3.3.1 Syngas cooling simulation approach

For the sour water stripper section, the electrolyte non-random two liquid (NRTL) activity coefficient model has been used in the literature for liquid phase physical property calculation (Bhattacharyya et al. 2010). The Peng Robinson equation of state (EOS) is used for the vapour phase.

In commercial simulators, electrolytic models account for the dissociation of molecular species in water, and all components are treated as Henry's Law components[3]. The electrolytic packages are applicable to systems containing compounds which dissociate to form ions, such as ammonia, amines, acid gases, etc., therefore they are sufficient to represent realistically the cooling, knock down and sour processes.

Although Honeywell UniSim Design R400 is sufficient to simulate the majority of the units involved in an IGCC power plant, this is not the case when it comes to the syngas cooling section. First and foremost, there is no option of selecting an electrolyte package from the readily available fluid packages. The difficulty encountered with Honeywell UniSim Design R400 to predict accurately the performance of the syngas clean up unit with imposing the readily available fluid packages was confirmed by comparing the results produced from the two simulators against the data reported in the literature (NETL 2007). It is worth underlining that although Honeywell UniSim design represents accurately the absorption rate of most of the gases in water occurring

[3] Henry's law components are automatically assigned by the simulator for components that have a normal boiling point below that of propylene.

in the syngas clean up section, this is not the case for the absorption regime of ammonia in water, for the particular process.

It is the syngas cooling and clean up section of the power plant where the stream directed to the AGR/CO_2 capture unit is generated. Hence the accurate prediction of the overall operation is important.

The BR&E ProMax simulator was used for the simulation[4] of the syngas cooling sections and the simulation results obtained from ProMax were utilised to construct the downstream processes of the IGCC power plant at the UniSim simulation in order to develop a unified process flow diagram. The results obtained from ProMax were exported to a database sheet. This was then used to provide inputs to UniSim environment which was run manually. ProMax provides the option to opt for electrolytic packages including electrolyte NRTL that has been reported in the literature, while UniSim electrolytic packages are not available in the default package. The ability to opt for electrolytic environments as reported in the literature for this part of the IGCC plant by default provides a more fundamental approach increasing confidence in the results obtained by ProMax.

The electrolyte packages available in BR&E ProMax simulator have been investigated in detail before selecting the one that is most appropriate for the simulation of this section of the IGCC power plant. The main objective of this process is to remove NH_3 from the raw synthesis gas however sulphur components will be removed to a degree as well. Therefore, it is crucial to examine the ability of the packages to predict accurately the solubility of these components in water. The electrolyte packages available from the simulator were tested including electrolytic NRTL reported in the literature. The results produced were compared to the experimental data reported in the literature for H_2S (Burgess and Germann 1969) and NH_3 for several temperatures (Gillespie 1985).

[4] BR&E simulation case diagrams can be found in the Appendix C.

Figure 3-10 to **Figure 3-12** present this comparison using electrolyte NRTL and electrolyte Extended Long Range (ELR) fluid packages reported to represent better the phenomena occurring. The solubility of H_2S in water with pressure is shown in **Figure 3-10** which demonstrates that electrolyte NRTL fluid package can represent the phenomena occurring sufficiently accurately. In the case of NH_3 however, as it can be seen from **Figure 3-11**, the predicted solubilities are far from the values reported in literature. The corresponding values are nonetheless in very good agreement with the experimental values when electrolyte ELR is used as it is illustrated in **Figure 3-12**. Therefore, electrolyte ELR was chosen for the simulation of this section of the power plant.

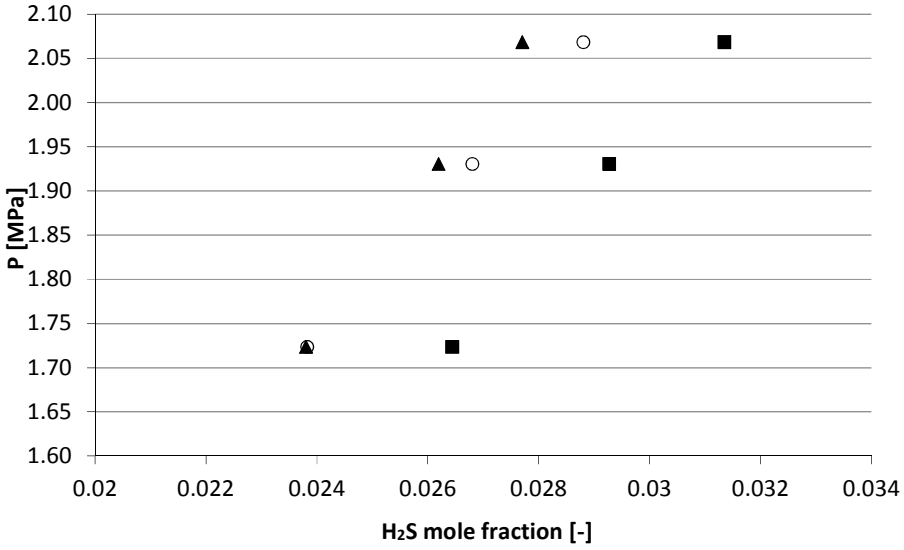

Figure 3-10: H_2S solubility in water as predicted for T=303.15 K by Electrolyte ELR (▲) and Electrolyte NRTL (■).Non solid markers for experimental data (Burgess 1966)

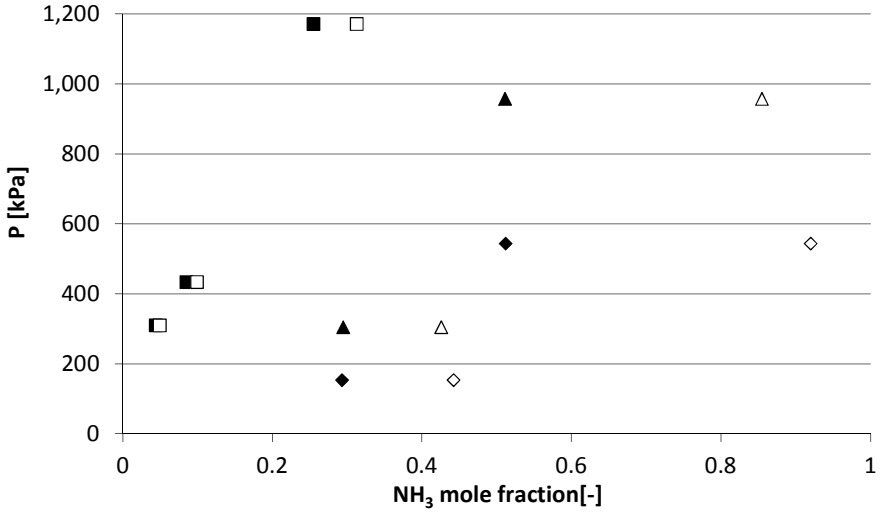

Figure 3-11: NH_3 solubility in water as predicted by Electrolyte NRTL for T=313.15 K (♦), T=333.15 K (▲), T= 394.25 K (■). Non solid markers for experimental data (Gillespie 1985) and solid marker for simulation

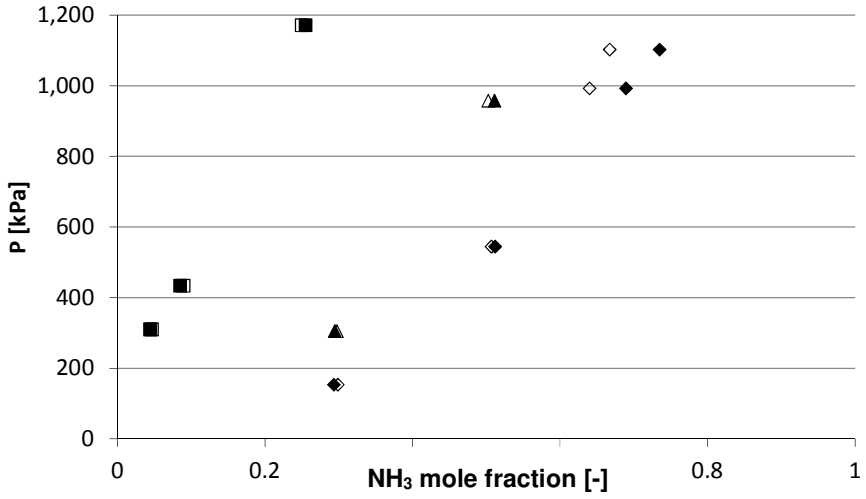

Figure 3-12: NH_3 solubility in water as predicted by Electrolyte ELR for T=313.15 K (♦), T=333.15 K (▲), T= 394.25 K (■). Non solid marker for experimental data (Gillespie 1985) and solid marker for simulation

Electrolytic NRTL (Non Random Two Liquid) is a predefined property package that may be specified from the available packages of the simulator. The Electrolytic NRTL

property package is a Gibbs Excess Energy/Activity Coefficient model which calculates liquid phase activity coefficients for predicting mul-ticomponent phase equilibria (Chen and Evans 1986). Electrolyte ELR is, as NRTL, a predefined property package that may be specified from the available packages in the simulation environment. The electrolyte ELR property package is a Gibbs Excess Energy/Activity Coefficient model which calculates liquid phase activity coefficients for predicting multicomponent phase equilibria. It is based on the Pitzer-Debye-Hückel model (Pitzer and Kim 1974). The molar excess Gibbs energy model accounts for molecular/ionic interactions between all liquid-phase species. An equation of state (Peng-Robinson herein), can be further selected to predict the vapour phase properties. BR&E recommends opting for Electrolytic ELR for sour processes, mentioning "significant improvements" on this model (BR&E ProMax, User Guide 2013)

The raw fuel/synthesis gas entering the syngas clean up and cooling section varies over the different gasification options. The stream properties for each case examined are based on the DOE/NETL (NETL 2007) reported values[5]. The cooling and saturation with water occurring in the syngas scrubber is performed by process water fed in the top of the scrubber.

The base for the comparison of the results obtained with different simulators is the final stream of the syngas clean-up process, i.e. the AGR/CO_2 capture unit inlets and is presented in **Table 3-7** to **Table 3-10**. The discrepancies as appear by comparing the results obtained by the different simulators against the reference report, while not significant, still highlight the effect of the different approaches taken. More specifically, the discrepancy that can be observed for H_2O between the reference report and the simulators can be speculated to be due to the choice of "ideal gas" thermodynamic environment in the reference report. This approach has been reported in the literature to lead underestimation of the water fraction on gas (Harvey 2008). It

[5] Streams entering the syngas scrubber of non-capture and carbon capture GEE and Shell IGCCs, as presented in DOE NETL 2007 are presented in Appendix A.

should also be noted that some NH_3 is expected to slip on the syngas cooling section outlet (AGR/CO_2 capture unit inlet) with ProMax confirming this expectation. The result obtained by ProMax for NH_3, as presented in **Table 3-8**, appears as zero due to rounding up.

Table 3-7: Comparison of results produced by BR&E and Honeywell UniSim Design R400 simulators for non-capture GEE IGCC syngas clean up section (AGR unit inlet)

	DOE/NETL	BR&E ProMax	Honeywell UniSim Design R400
Ar	0.0092	0.0092	0.0093
CH_4	0.0011	0.0011	0.0012
CO	0.3992	0.4025	0.4015
CO_2	0.1780	0.1740	0.1757
COS	0.0000	0.0000	0.0000
H_2	0.3935	0.3924	0.3906
H_2O	0.0012	0.0019	0.0022
H_2S	0.0069	0.0082	0.0085
N_2	0.0103	0.0104	0.0092
NH_3	0.0006	0.0000	0.0004
F, kg/s	113.95	114.21	115.07
(lb/h)	(904,411)	(906,480)	(913,249)
T, K	315	315	315
(°F)	(107)	(107)	(107)
P, 10^5 Pa	51.21	51.21	51.21
(psia)	(742.7)	(742.7)	(742.7)

Table 3-8: Comparison of results produced by BR&E and Honeywell UniSim Design R400 simulators for carbon capture GEE IGCC syngas clean up section (CO_2 capture unit inlet)

	DOE/NETL	BR&E ProMax	Honeywell UniSim Design R400
Ar	0.0057	0.0066	0.0066
CH_4	0.0008	0.0008	0.0008
CO	0.0117	0.0117	0.0122
CO_2	0.4057	0.4040	0.4040
COS	0.0000	0.0000	0.000
H_2	0.5609	0.5613	0.5594
H_2O	0.0009	0.0018	0.0020
H_2S	0.0054	0.0061	0.0062
N_2	0.0075	0.0075	0.0075
NH_3	0.0003	0.0000	0.0005
F, kg/s	156.62	156.25	156.96
(lb/h)	(1,243,070)	(1,240,080)	(1,245,711)
T, K	313	313	313
(°F)	(103)	(103)	(103)
P, 10^5 Pa	50.10	50.10	50.10
(psia)	(726.7)	(726.7)	(726.7)

Table 3-9: Comparison of results produced by BR&E and Honeywell UniSim Design R400 simulators for non-capture Shell IGCC syngas clean up section (AGR inlet)

	DOE	BR&E ProMax	Honeywell UniSim Design R400
Ar	0.0101	0.0101	0.0101
CH_4	0.0004	0.0004	0.0004
CO	0.5940	0.5926	0.5931
CO_2	0.0226	0.0226	0.0226
H_2	0.3015	0.3008	0.3006
H_2O	0.0015	0.0017	0.0019
H_2S	0.0091	0.0091	0.0091
N_2	0.0608	0.0608	0.0595
NH_3	0.0000	0.0000	0.0017
F, kg/s	100.93	101.13	101.09
(lb/h)	(801,076)	(802,627)	(802,289)
T, K	308	308	308
(°F)	(95)	(95)	(95)
P, 10^5 Pa	35.85	35.85	35.85
(psia)	(520)	(520)	(520)

Table 3-10: Comparison of results produced by BR&E and Honeywell UniSim Design R400 simulators for carbon capture Shell IGCC syngas clean up section (CO_2 capture unit inlet)

	DOE	BR&E ProMax	Honeywell UniSim Design R400
Ar	0.0064	0.0064	0.0064
CH_4	0.0002	0.0003	0.0003
CO	0.0166	0.0165	0.0161
CO_2	0.3771	0.3744	0.3759
COS	0.0000	0.0004	0.0005
H_2	0.5547	0.5558	0.5542
H_2O	0.0014	0.0020	0.0022
H_2S	0.0050	0.0052	0.0053
N_2	0.0385	0.0388	0.0380
NH_3	0.0000	0.0000	0.0005
F, kg/s	157.43	156.77	156.77
(lb/h)	(1,249,470)	(1,244,240)	(1,251,965)
T, K	308	308	308
(°F)	(95)	(95)	(95)
P, 10^5 Pa	32.58	32.58	32.58
(psia)	(472.6)	(472.6)	(472.6)

3.4 Summary and conclusions

The simulation approach adopted to represent parts for GEE and Shell IGCC power plants have been presented in this Chapter. The methodology followed to represent EP ASU, syngas cooling, sulphur recovery and combined cycle within the IGCC power plants was introduced in detail. For all the sections, attempts for validation were made by comparing results obtained by the ones presented in DOE NETL study (2007). Several inconsistencies have been identified and illustrated and suggestions for improvement have been introduced by detailed process flow diagrams.

In particular, the EP ASU was simulated using Honeywell UniSim Design R400. It was found that the DOE/NETL report (2007) failed to represent in detail the ASU process flow diagram. Contrary to the reference report, detailed process configurations were presented herein. Inconsistencies where discovered in terms of overall mass balances around the EP ASU unit. The oxygen balance for example is negative in both non capture and carbon capture GEE cases. In both Shell cases, there is negative balance for argon.

The syngas clean-up section was also presented. The main objective of this process is to remove NH_3 from the raw synthesis gas however sulphur components will be removed to a degree as well. The electrolyte packages available in BR&E ProMax simulator have been investigated in detail. The results produced were found to be in agreement with the experimental data reported in the literature for H_2S (Burgess and Germann 1969) and NH_3 for several temperatures (Gillespie 1985). Moreover, comparison has been conducted between ProMax and UniSim to evaluate their ability to represent this section. It was found that UniSim fails to represent the removal of NH_3 within this section with the default thermodynamic packages.

It should also be highlighted that DOE also predicts NH_3 to be slipping from the syngas clean-up section to the AGR/Selexol for GEE IGCCs. While it is expected that the syngas cooling outlet stream will contain some NH_3, it is very probable that DOE NETL reporting to have used Aspen Plus have overestimated this. In fact, it is very

probable that DOE used different thermodynamic environment within the different simulator for this section, hence the discrepancies as reported.

The Claus process simulation for sulphur recovery within non-capture and carbon capture for the GEE and Shell IGCC power plants was conducted using both Honeywell UniSim R400 and BR&E ProMax and their performance was presented. ProMax results proved to be in better agreement with DOE NETL presented data.

The air compressor, combustor and expander block for all IGCC cases was simulated using Honeywell UniSim design R400. The schematics of the processes for each IGCC case investigated were based on the configurations reported from DOE/NETL (NETL 2007)**.** It was found that while is very probable that DOE/NETL report has overestimated the nitrogen required for dilution in the combustor, and subsequently the overall electrical output, further examination of this section by simulations with specific software for power blocks, is essential to validate this observation. The combustor simulations developed in UniSim however, can predict the combustion product stream accurately in terms of flows and component mole fractions.

Finally, the simulation of the HRSG, steam and feedwater systems as part of the overall process flow diagram performed in Honeywell UniSim design R400, based on the data reported on the DOE/NETL report (NETL 2007) The Peng-Robinson equation of state was used for the flue gas properties and the ASME steam package, for the water properties calculation. Contrary to DOE NETL report detailed combined cycle process configurations have been presented in this study.

Chapter 4 Carbon capture processes in IGCC power plants

4.1 Selexol™ for carbon capture

Since the partial pressure of acid gas in the syngas is generally high in IGCC power plants, physical solvents appear to be a favourable CO_2 capture option. Dimethyl Ether of Polyethylene Glycol (DEPG) or Selexol™ can be used for the absorption of acid gases taking advantage of the high solubility into the solvent. DEPG is a mixture of dimethyl ethers of polyethylene glycol of the following chemical formula:

$CH_3O(C_2H_4O)_nCH_3$, with n being between 2 and 9.

Compared to other solvents, DEPG has a higher viscosity which reduces mass transfer rates and tray efficiencies and increases packing or tray requirements, especially at reduced temperatures (Burr 2008). .

The maximum operating temperature for DEPG in the Selexol process is usually 448K (175°C), while the minimum operating temperature is 255K (−18°C) (Burr and Lyddon 2008).

Typically the process consists of two stages, where H_2S is removed prior to CO_2 and the regeneration of the solvent is achieved in two sections:

1. In the stripper, by imposing a pressure drop along the column and using steam extracted from the Low Pressure (LP) section of the power plant's steam cycle.
2. By a series of pressure vessels downstream the CO_2 removal stage.

One of the first detailed schemes for the two stage Selexol process was presented by EPRI, as shown in **Figure 4-1**.

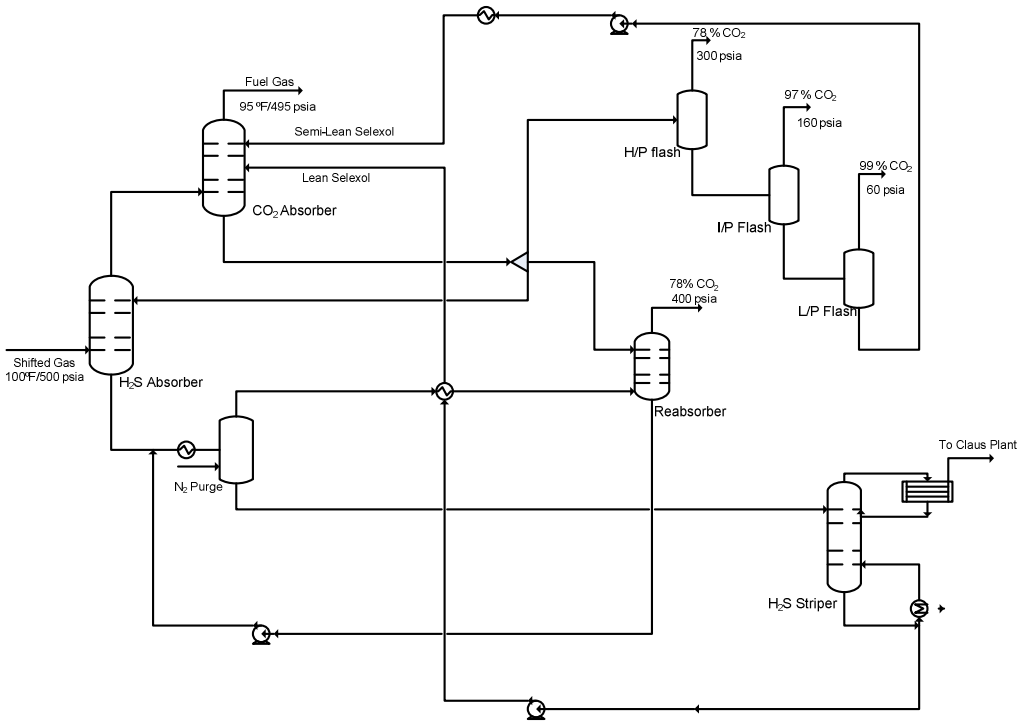

Figure 4-1: Configuration of the Selexol Unit (reproduced after Kubek 2009)

4.2 Thermodynamic approach

To evaluate the separation performance of the units in the Selexol process it is essential to describe correctly the vapour-liquid equilibrium (VLE) of the mixtures involved. VLE calculations for these systems can be based on advanced equations of state such as the approaches adopted by Field and Brasington (2011), Mansouri Majoumerd et al. (2012) and Nannan et al. (2013), or on the description of gas solubility based on Henry's law and the use of fugacity coefficients to correct for the non-ideality of the gas phase. Mansouri Majoumerd et al. (2012) incorporated H_2S removal (i.e. AGR) unit modelled in ASPEN Plus using Perturbed-Chain Statistical Associating Fluid Theory (PC-SAFT) equation of state, for cases without CO_2 capture. They did however use Henry's law for the two-stage Selexol process used in the CO_2 capture cases they investigated.

Given the commercial nature of the solvent, there is only a limited set of data available and often these are reported either as solubilities or as Henry law constants. At high

pressures, vapour-liquid equilibrium is often expressed in terms of K values (Kister, Henry Z. 1992; Perry and Green 1997).

The solubility behaviour of the solute gas in physical solvents for the IGCC case conditions will closely approach Henry's law, with the acid gas loading in the solvent being proportional to the acid gas partial pressure (Sciamanna and Lynn 1988; Xu et al. 1992; Henni, et al. 2005). Peng Robinson equation of state was used for the gas phase. Therefore, the mole fraction of the solute in the liquid phase, i.e. the solubility, can be expressed with the following equation:

$$x_i = \frac{y_i \cdot P}{K_i} = \frac{p_i}{K_i} \tag{4-1}$$

where y refers to the mole fraction of component i in the gas phase and x is the mole fraction in the liquid phase.

The temperature dependency of the Henry's law constant for H_2S and CO_2 in Selexol has been reported in the literature (Xu et al. 1992; Henni et al. 2005) and is illustrated in **Table 4-1.**

Table 4-1: Henry's law constants for H_2S and CO_2 in Selexol (Xu et al. 1992; Henni et al. 2005)

Temperature (K)	Henry's law constant (MPa)	
	H_2S	**CO_2**
298	0.440	3.570
313	0.506	3.950
323	0.641	4.670
343	0.787	5.620
353	1.010	6.550

The enthalpy change from vapour to dissolved solute represents the heat of solution (or heat of absorption) and can be indicated by the variation of the Henry's law constants with changes in temperature. The correlation between the Henry's law constants and the heat of solution can be represented with equation 4-2.

$$\frac{d\ln K}{d\left(\frac{1}{T}\right)} = \frac{\Delta H}{R} \tag{4-2}$$

The enthalpy of solution can be therefore calculated by the slope of a linear equation obtained by integrating equation 4-2 with an assumption of constant heat of solution, given the Henry constants at different temperatures. For H_2S and CO_2, the corresponding values are presented in **Table 4-2**.

Table 4-2: Standard state heats of solution for H_2S and CO_2 in Selexol (Xu et al. 1992)

Standard state heats of solution (kJ/mol)	
H_2S	**CO_2**
19.1	14.3

Equilibrium solubility data for H_2S and CO_2 in various representative solvents have been reported in the EPRI report as well as the DOE/NETL report (NETL 2007; Kubek 2009) as shown in **Figure 4-2**. This figure shows an order of magnitude higher solubility of H_2S over CO_2 at a given temperature, which enables the selective absorption of H_2S over CO_2 with physical solvents. It also illustrates that the acid gas solubility in physical solvents increases with lower solvent temperatures. Moreover, **Table 4-3** illustrates the gas solubilities of some physical solvents relative to CO_2. DEPG is therefore the best option between physical solvents for H_2S and CO_2 removal.

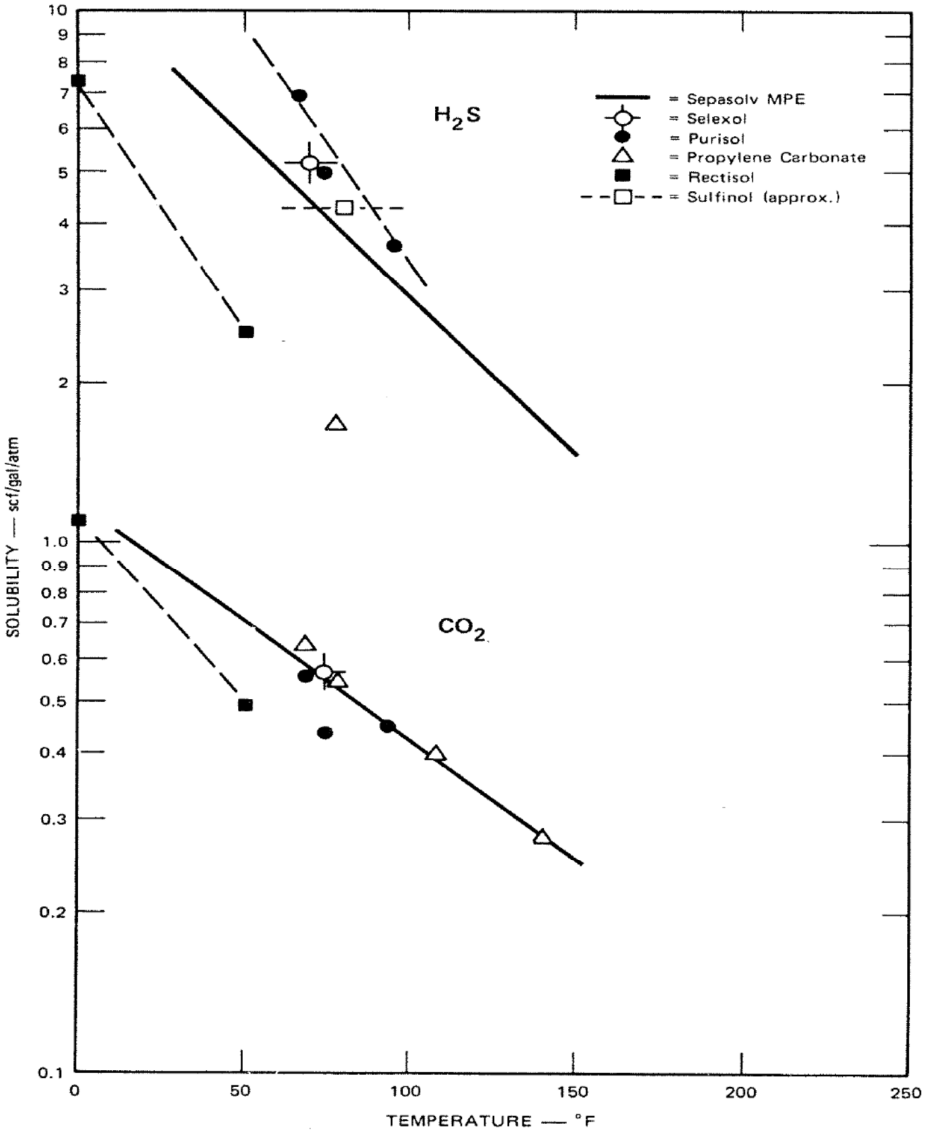

Figure 4-2: Gas solubilities of H_2S and CO_2 in physical solvents (NETL 2007)

Table 4-3: Gas solubilities of some physical solvents relative to CO2 (Epps and June 1992)

Component	DEPG at 25°C	PC at 25°C	NMP at 25°C	MeOH at –25°C
CO_2	1.000	1.000	1.000	1.000
H_2	0.013	0.008	0.006	0.005
N_2	0.020	0.0084	-	0.012
CO	0.028	0.021	0.021	0.020
CH_4	0.420	0.038	0.072	0.051
NH_3	4.800	-	-	23.200
H_2S	8.820	3.290	10.200	7.060
H_2O	730.000	300.000	4,000.000	-

Some additional advantages for the application of DEPG in the Selexol process to gasification plants are listed below (Chen 2005):

- A very low vapour pressure that limits its losses to the treated gas
- High chemical and thermal stability (no reclaiming or purge) because the solvent is true physical solvent and does not react chemically with the absorbed gases
- Nontoxic for environmental compatibility and worker safety
- Non-foaming for operational stability
- Compatibility with gasifier feed gas contaminants
- High solubility for NH_3 allows removal without solvent degradation

- Low heat requirements for regeneration because, for CO_2 capture, the solvent can be regenerated by a simple pressure let down

4.2.1 Simulation of vapour-liquid equilibrium

In the commercial software Honeywell UniSim Design R400, Selexol is present as a pre-defined component and the thermodynamic database includes default Henry law constants. Initial simulations revealed inconsistencies with respect to the performance of the separation units and this has incited the investigation of the calculation approach further.

UniSim uses the following equation for the VLE calculations:

$$\ln H = A + \frac{B}{T} + C \cdot \ln T + D \cdot T^{E} \qquad (4\text{-}3)$$

where T is the temperature in K.

Table 4-4 presents the parameters used in the calculation of the Henry law constant from the UniSim thermodynamic database available for the simulation of the Selexol absorption units.

Table 4-4: Original UniSim parameters

	A	B	C	D	E
CO_2	69.68	–3892	–8.408	$1.07 \cdot 10^{-03}$	1
H_2S	37.84	–2972	–3.395	$-3.15 \cdot 10^{-03}$	1

A comparison of the VLE curves calculated from the original parameters and the solubility data in the literature (Xu et al. 1992) is shown in **Figure 4-3** and **Figure 4-4**. The curvature of the calculated lines results from the non-ideality of the vapour phase. The selectivity of for H_2S the solvent is nearly 9.

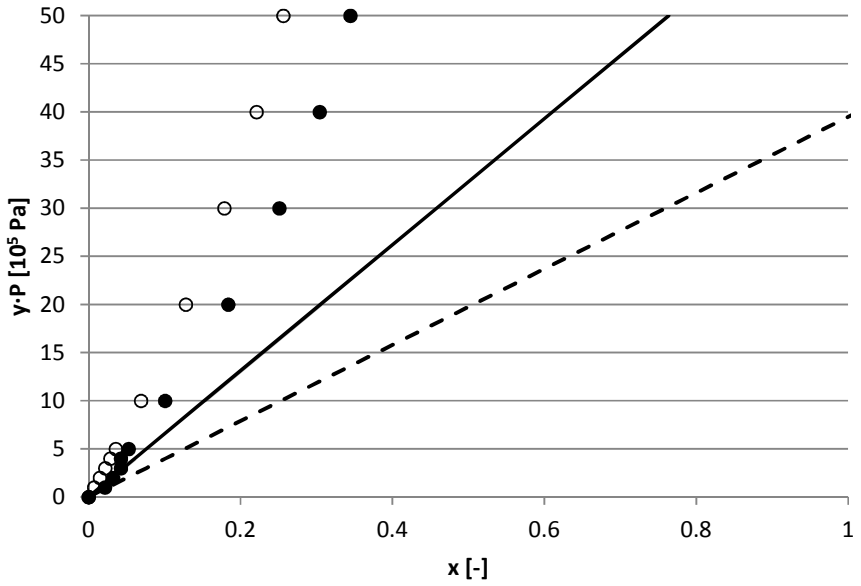

Figure 4-3: Solubility of CO_2 in Selexol at 333K (solid line) and 303K (dashed line). Marker points are UniSim calculations with default parameters (○) at 333K and (●) at 303 K

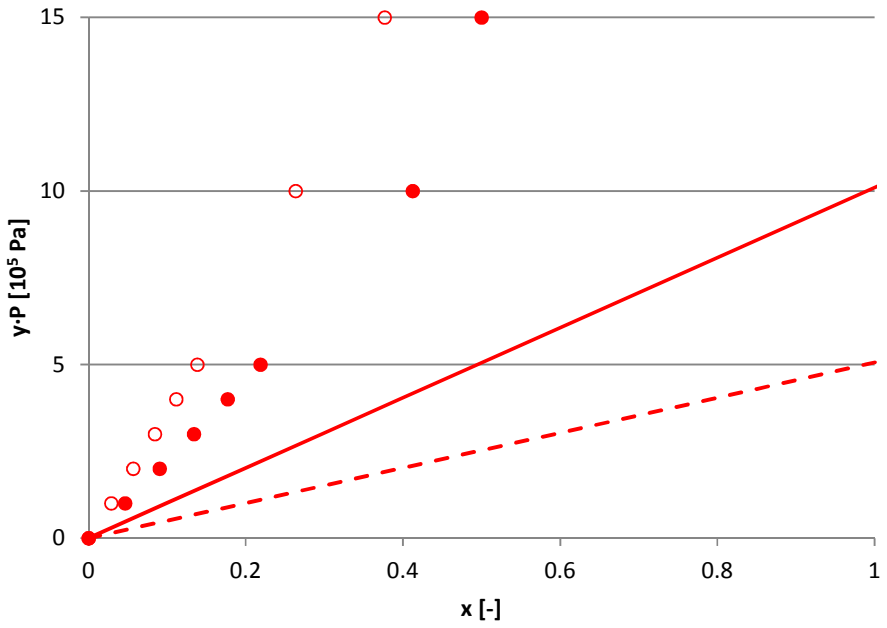

Figure 4-4: Solubility of H_2S in Selexol at 333 K (solid line) and 303K (dashed line). Marker points are UniSim estimations with default parameters (○) at 333K and (●) at 303K

What is clear from the comparison is that the default UniSim parameters predict a relatively low selectivity for H_2S and this will result in a higher absorbed amount of CO_2 in the first stage of the Selexol process. For the overall capture process this means that more CO_2 will then be sent to the Claus process complicating the task of finding suitable conditions to guarantee 90% or more capture rates.

The lower absolute solubility will also result in a much higher solvent flowrate requirement yielding an overall process performance that is not satisfactory with respect to both the purity/recovery requirements and the energy penalty.

To implement the correct solubility data in the software's database the Henry's law constants were described using equation 4-3:

Given the relatively limited temperature range of interest, it is clear that the two parameters, A and B, are required in order provide sufficient accuracy. C, D and E were therefore set to zero. Experimental solubility data for H_2S and CO_2 were regressed and the values obtained are summarised in **Table 4-5**. The Henry constants for CH_4, CO and N_2 are obtained based on their solubility relative to CO_2 reported in the literature (Bucklin and Schendel, 1984) assuming that the selectivity is constant regardless temperature (the same heat as CO_2, i.e. the B constant). However, the temperature dependency of the Henry constant for hydrogen in Selexol is neglected in contrast to those of the other components. It is assumed that the Henry constant estimated at 298K (25 °C) on a basis of solubility selectivity relative to CO_2 does not change in the range of operating temperatures in the Selexol process. Ar has been assumed to behave as an inert.

Table 4-5: Coefficients of Henry constant equation used in the Selexol process simulation

Component	A	B
CO_2	13.83	-1,719
H_2S	13.68	-2,297
H_2	12.40	0
CH_4	16.53	–1,719
CO	17.40	–1,719

Figure 4-5 and **Figure 4-6** illustrate results obtained using the default UniSim data, results after the implementation of the regressed parameters for the Henry's law equation and experimental data (Xu et al. 1992; Henni et al. 2005).

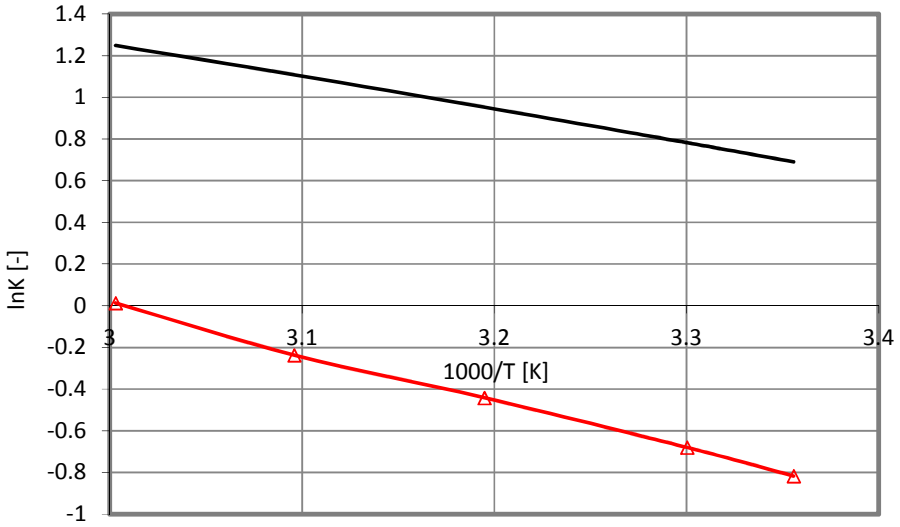

Figure 4-5: lnK against T for H_2S in Selexol. Marker for experimental data (Xu et al 1992), red line for simulation results and black line for UniSim results with default package

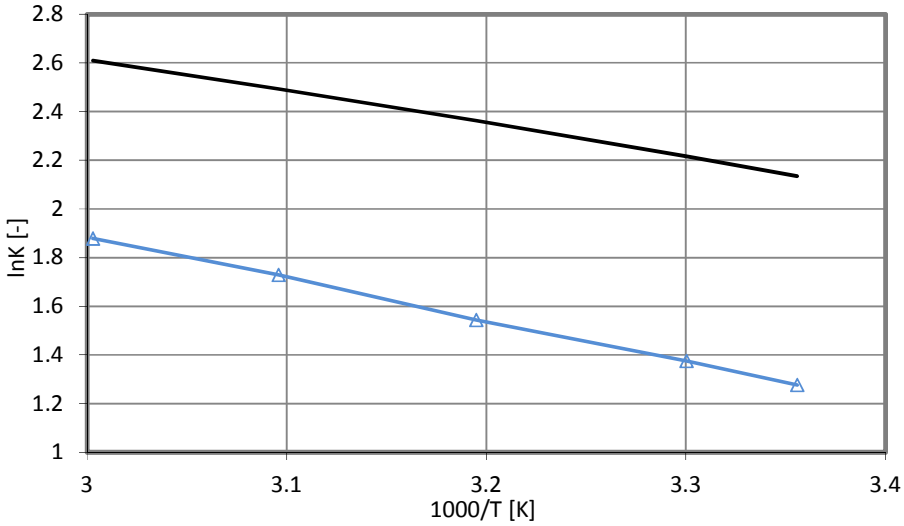

Figure 4-6: lnK against T for CO_2 in Selexol. Marker for experimental data (Xu et al 1992) blue line for simulation results and black line for UniSim results with default package

4.3 Proposed configurations and energy requirements

4.3.1 Process flow diagram

Several authors have discussed the two-stage Selexol processes (Kakaras et al.2006; Kubek 2009; Robinson and Luyben 2010; Battacharrya et al. 2011; Ferguson et al. 2013). One of the simplest and probably traditional configurations is the one presented in *Gas Purification* by Kohl (Kohl 1997) and is shown in **Figure 4-7**.

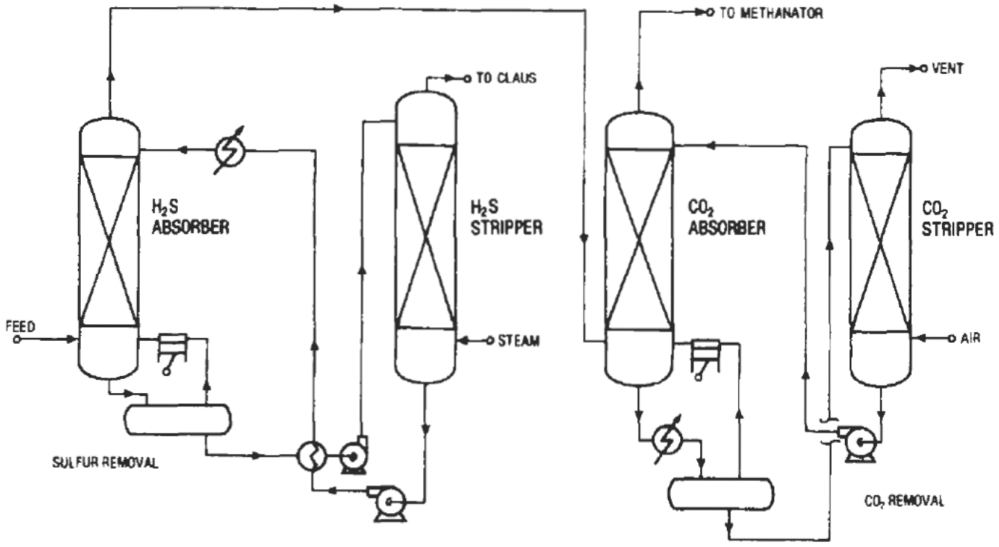

Figure 4-7: Flow diagram of Selexol process for selective H_2S and CO_2 removal (Kohl 1997)

The general concept of this scheme was followed by Robinson and Luyben (2010), with the difference that they imposed the H_2S removal unit prior to the WGSRs, while the CO_2 capture part is located downstream. Battacharaya et al. (2010), presented a significantly modified scheme compared to the scheme presented in **Figure 4-7** for the two-stage Selexol process, as they eliminated the CO_2 stripper.

Integrated scheme

The exact scheme adopted in the DOE/NETL study for the two stage Selexol process was not presented in a detailed process flow diagram. It was however mentioned that

the scheme operates in two solvent loops (integrated scheme) which perform both the H_2S removal and the CO_2 capture stages.

In the configuration described here (**Figure 4-8**), the gas product of the WGSRs enters the first absorber where H_2S is preferentially removed using solvent from the CO_2 absorber. The gas exiting the H_2S absorber passes through the second absorber where CO_2 is removed using regenerated solvent from the flash drums, combined with the thermally regenerated solvent from the bottoms of the stripping column.

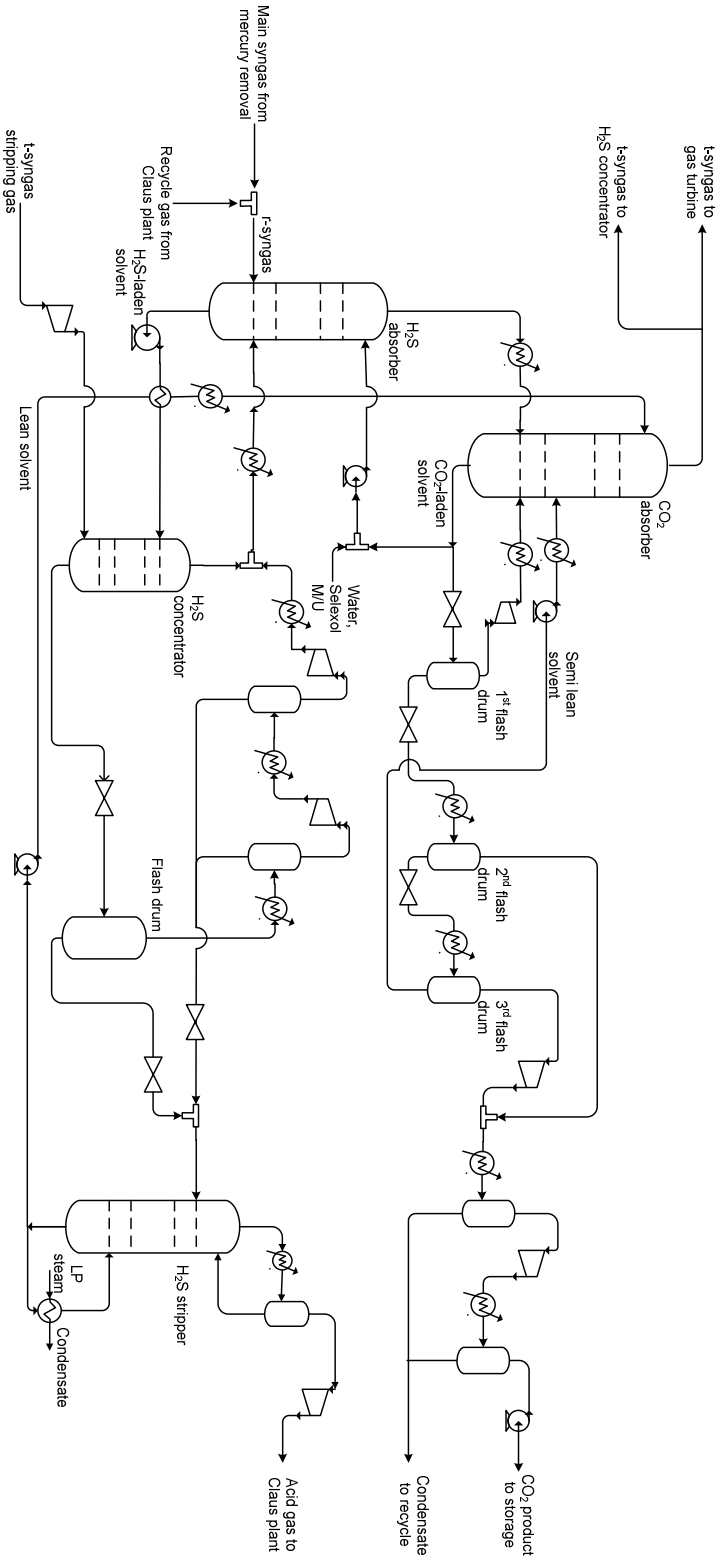

Figure 4-8: Simplified schematic of the integrated Selexol process

The clean gas exits the absorber and is sent either directly to the combustion turbine or is partially humidified prior to entering the combustion turbine depending on the gasification technology incorporated.

The CO_2 loaded solvent exits the CO_2 absorber and some of it is sent to the H_2S absorber, while the rest of the solvent is sent to a series of flash drums for regeneration. The CO_2 product stream is obtained from the second and third flash drums, and after flash regeneration the solvent is recycled to the CO_2 absorber.

The rich solvent exiting the H_2S absorber enters the H_2S concentrator and partially flashes. The solvent exiting the H_2S concentrator is sent to a flash drum and while the gas stream is recycled to the H_2S absorber, the liquid product is sent to the stripper. The acid gas from the stripper is sent to the Claus plant for further processing. The lean solvent exiting the stripper is then cooled and recycled to the top of the CO_2 absorber.

The scheme is capable of capturing 90% of the carbon contained in the coal feed of the power plant. The H_2S recovery target of this configuration is set to >99.9% and at the same time the CO_2 product should have less than 10 ppm H_2S in agreement with the current legislation (Directive 2009/31/EC). The amount of hydrogen recovered from the syngas stream is dependent on the Selexol process design conditions. Herein, the hydrogen recovery is set to 99.4 per cent.

The degree of solvent dilution is a parameter that has been investigated for the integrated two stage Selexol process. Apart from the effect of water in the properties of the solvent, primarily the viscosity, its effect on the energy requirements of the process was also examined. Focusing on the regenerated solvent pump energy requirement, as it is the most energy demanding component of the process, **Figure 4-9** was produced.

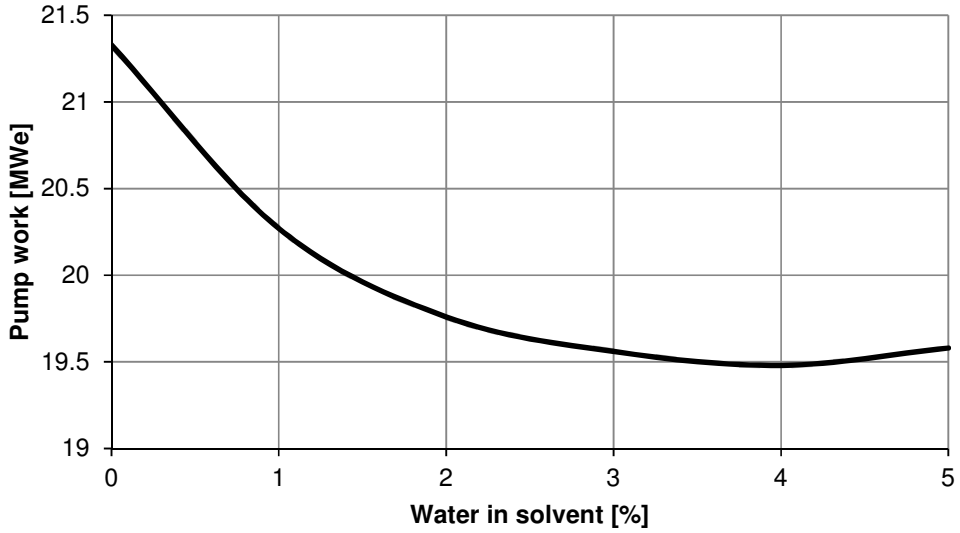

Figure 4-9: Optimal dilution for the solvent circulating in the integrated Selexol process

As illustrated in **Figure 4-9**, there is a point of solvent dilution which is optimal, for the solvent pump work to be at the minimum. Water is absorbing the heat generated by the solution of the gases in the solvent resulting in a temperature drop, therefore facilitating the absorption rate. After this point (4% of water), by increasing the water content there is an increase at the mass flowrate across the solvent pump, therefore increasing the pump work again.

Non-integrated scheme

The configuration presented in this section, contrary to the previously described scheme, is operated with two separate solvents loops. Again, the gas product of the WGSRs enters the first stage of the process, where H_2S is removed in the first absorber. In this scheme, however, the H_2S absorber uses regenerated solvent solely from the bottoms of the gas stripper. The gas exiting the H_2S absorber is then sent to the second absorber where CO_2 is removed using exclusively solvent regenerated from the flash drums. In this scheme, as there is no need for steam regenerated solvent for the CO_2 removal stage, the Selexol solvent circulating would contain just enough water, to maintain the viscosity of the solvent in low levels. The clean gas exits the absorber and

is sent either directly to the combustion turbine in the GEE IGCC or a humidifier in the Shell IGCC case.

The rich solvent exiting the H_2S absorber enters the H_2S concentrator and the solvent exiting the H_2S concentrator is sent to a flash drum as in the integrated configuration. The gas stream is again recycled to the H_2S absorber while the liquid product is sent to the stripper. The acid gas from the stripper is sent to the Claus plant.

The recovery specification for the syngas components of interest is the same as those in the integrated scheme so that a fair comparison between the two configurations can be conducted. The schematic of this process is presented in **Figure 4-10**.

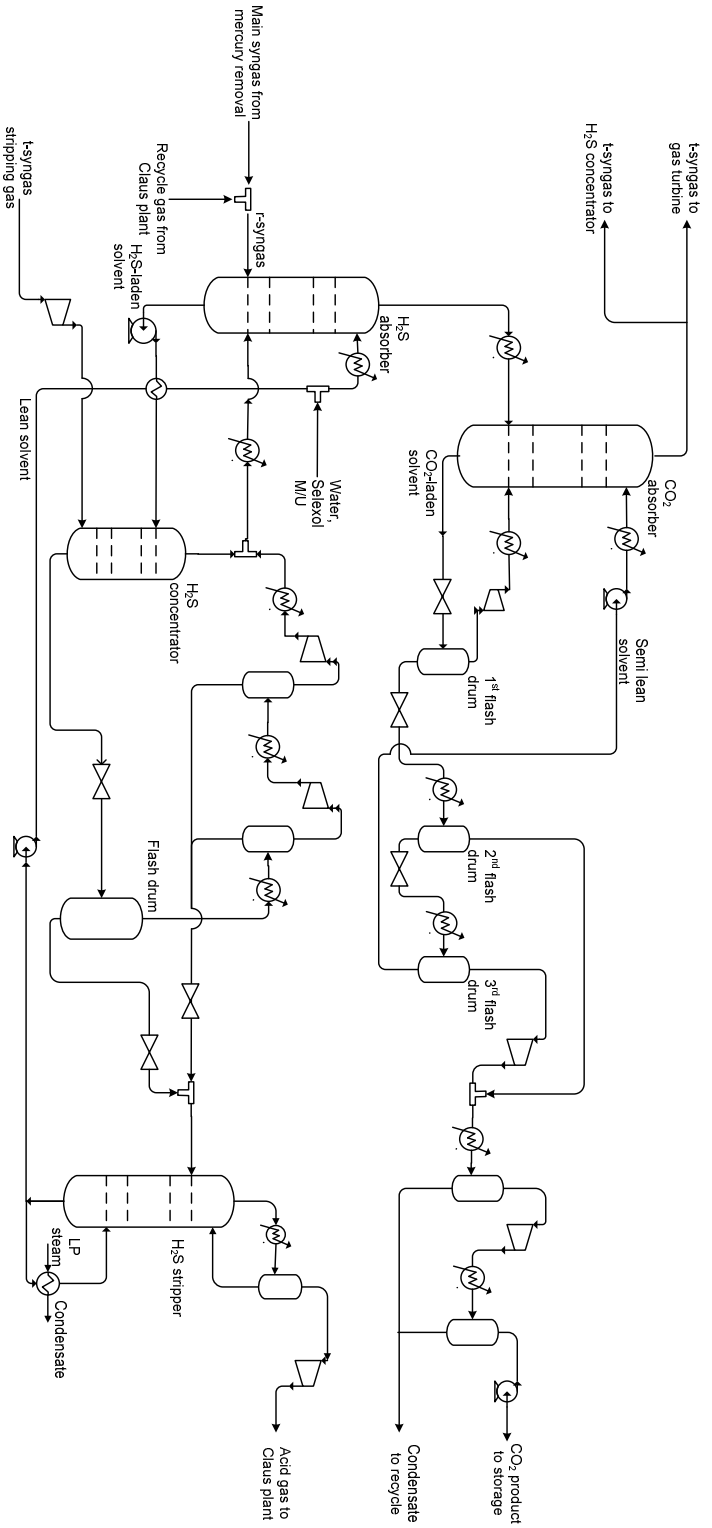

Figure 4-10: Simplified schematic of the non-integrated Selexol process

4.3.2 Energy requirements

The two configurations examined yield different energy requirements. The major components contributing to the energy consumption of the two-stage Selexol unit are shown in **Table 4-6**:

Table 4-6: Energy requirements for integrated and non-integrated two-stage Selexol configurations

	Integrated	Non-integrated
H_2S stripper duty [MW_{th}]	14.6	20.8
CO_2 compression power [MW_e]	32.09	30.64
Auxiliary power consumption in two-stage Selexol units [MW_e]		
Total auxiliary power consumption	20.01	27.99
H_2S concentrator stripping gas compressor	0.14	0.13
1st flashed gas compressor	0.68	2.01
2nd flashed gas compressor	0.32	0.71
Gas compressor for recycle gas from 1st flash drum	0.74	0.57
H_2S-laden solvent pump	0.10	0.15

Table 4-6 (Continued): Energy requirements for integrated and non-integrated two stage Selexol configurations

CO_2-laden solvent pump	0.04	0.0
Lean solvent pump	2.235	3.84
Semi-lean solvent pump	15.57	20.37
Sour gas compressor	0.20	0.22

4.4 Points of discussion

Similar to all physical solvents DEPG or Selexol^{TM} involves the absorption of the acid gas taking advantage of its high solubility into the solvent. Propylene Carbonate (PC) has a vapour pressure much higher than the high molecular weight solvents and the selectivity demonstrated is generally low compared to the rest physical solvents. The use of NMP is more energy demanding, making it therefore less beneficial compared to DEPG for acid gas removal and CO_2 capture (Bucklin and Schendel 1984).

Various schemes can be used in an IGCC power plant for acid gas removal and CO_2 capture. From the two schemes investigated for IGCC, focusing solely on the performance of the capture scheme, the integrated scheme presented in this chapter illustrated better results in terms of performance. Since the solvent diluted with water is only required for steam stripping, the idea of using near pure Selexol solvent for the CO_2 capture loop in a non-integrated scheme would lead to less solvent circulation therefore less energy requirement. However, it was observed that the absence of water in the solvent, apart from the fact that it affects the viscosity of the solvent, also causes an increase of the temperature along the column. This is due to the fact that when water is present in the solvent it absorbs the heat of solution maintaining the temperature of the column at lower levels. As the temperature is increasing in the CO_2 absorber of the non-integrated scheme, the physical absorption is not as favoured as in the integrated

scheme. Hence, more solvent is required to circulate in the absorber for the CO_2 removal rate that is desired to be achieved.

The operating lines of the CO_2 absorber of the non-integrated scheme were produced and examined in detail, in order to investigate the simulation stability. **Figure 4-11**, presents the operating and equilibrium lines of the CO_2 absorber at the non-integrated dual-stage Selexol unit at various solvent flowrates.

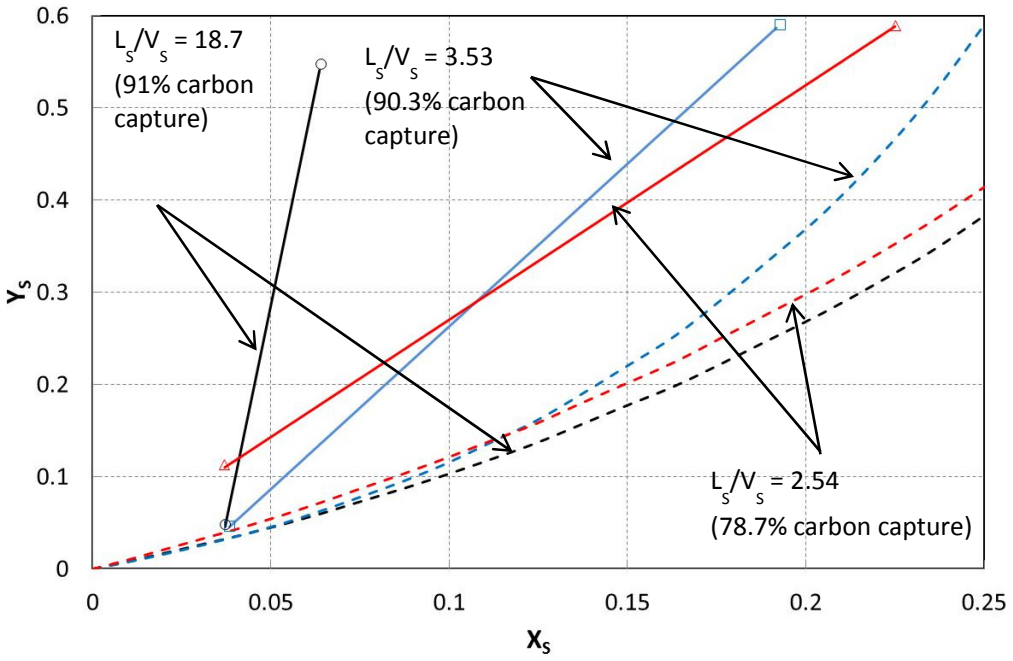

Figure 4-11: Operating and equilibrium lines around the CO_2 absorber at the non-integrated dual-stage Selexol simulation at various solvent flowrates. (Solid lines: operating lines, broken lines: equilibrium curves along the column, markers: simulation results)

The equilibrium lines are plotted assuming that the temperature along the column changes linearly. Since Selexol solvent has a negligible vapour pressure in the range of the operating temperatures, it is useful to plot the operating lines in terms of molar ratio instead of molar fraction with the equation below:

$$Y = \frac{L_{Sc}}{V_{Sc}} X + \frac{V_{Sc}Y_c - L_{Sc}X_c}{V_{Sc}} \quad (4\text{-}4)$$

Where X and Y are the molar ratio in liquid and gas phases, i.e. $x_{CO2}/(1-x_{CO2})$ and $y_{CO2}/(1-y_{CO2})$, L_S and V_S are total molar flowrates except CO_2 in liquid and gas phases, $L(1-x_{CO2})$ and $V(1-y_{CO2})$. Subscript c denotes an arbitrary position along the vertical direction of the column.

Since the other gas components such as CO, CH_4 and H_2 are not inert to solvent, the slope, L_S/V_S, cannot be kept constant along the absorber. Nevertheless the change of slope can be neglected as the compositions of CO and CH_4 are significantly small in the syngas compared to CO_2 and the solubilities of CO, CH_4 and H_2 are very low relative to CO_2.

Initially, the non-integrated dual-stage Selexol unit was simulated with an L_S/V_S of 2.54, as an initial value depicted from the original simulation of the integrated scheme, and the carbon capture rate achieved was only 78.7%. The capture rate was improved further by increasing the solvent flowrate. As expected, the carbon capture rate increased up to 90.3% by increasing L_S/V_S to 3.53 from 2.54.

However, it was discovered that it is particularly difficult to achieve further improvement of the carbon capture rate above 90% in this configuration. At L_S/V_S = 3.53, the operating line is already very close to the corresponding equilibrium line, which means that a pinch point is almost reached at the top of the CO_2 absorber. Therefore, even if a significant increase in the solvent flowrate is applied, it is expected that the carbon capture rate cannot be increased further. At L_S/V_S = 18.7 that is more than five times greater than that for the 90% carbon capture case, the carbon capture rate is only 91.8%. In other words, the increase of solvent flowrate cannot decrease the CO_2 molar fraction of the gas stream leaving the CO_2 absorber but decrease the CO_2 molar fraction of rich solvent at the bottom. Additionally, the increasing solvent flow absorbs more hydrogen from the syngas so the H_2 recovery would be reduced well below 99% if there is no reduction of the pressure in the 1st flash drum.

95% Carbon capture rate

As already discussed in the previous paragraph, it is very difficult to achieve stricter carbon capture rates with the non-integrated two-stage Selexol unit with reasonable solvent flowrates and auxiliaries consumption. In order to achieve carbon capture rates as high as 95%, the pinch point formed at the top end of the CO_2 absorber should be eliminated. One way of avoiding such a pinch point at the top end is to feed a lean solvent, i.e. CO_2-free solvent, to the top end and the existing semi-lean solvent to the middle of the column just as in the conventional integrated dual-stage Selexol unit. The CO_2-free lean solvent flow can move the operating line far from the equilibrium line by setting the CO_2 mole fraction in the liquid phase at the top to zero. Therefore, the integrated dual-stage Selexol unit can achieve a higher carbon capture rate that is not possible with the non-integrated process.

Improving the carbon capture rate by 5 % can be achieved by increasing the lean solvent flowrate. However, there is a maximum beyond which the lean solvent flowrate cannot increase. In order to increase the lean solvent flowrate to the CO_2 absorber, the CO_2 rich solvent flowrate flowing to the H_2S absorber has to be increased in order to generate more lean solvent at the H_2S stripper and subsequently feed the lean solvent to the CO_2 absorber. However, as more CO_2 rich solvent flows to the H_2S absorber, more CO_2 is conveyed with the CO_2 rich solvent to the H_2S absorber. As a consequence, the pressure of the flash drum for enriching the H_2S in the solvent would need to decrease, being however higher than the operating pressure of the H_2S stripper.

In the first place, the integrated dual-stage Selexol unit simulation at 90% carbon capture rate was modified to a new case with the higher lean solvent flowrate (Run1, **Figure 4-12**).

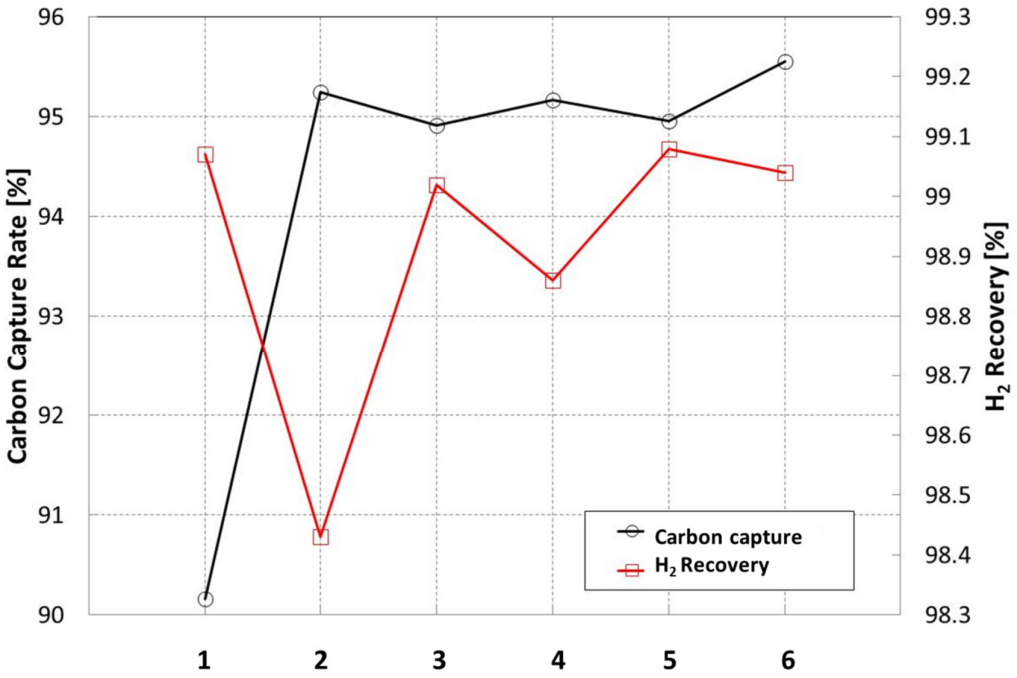

Figure 4-12: Carbon capture rate from 90% to 95% vs the H_2 recovery over the simulation runs of the integrated dual-stage Selexol unit

At Run 1, the semi-lean solvent flowrate can be lowered due to the increased lean solvent flowrate. However the L_S/V_S is still as high as 5.35 which is higher than the one calculated for the original 90% carbon capture case. This can be explained by more CO_2 being required to be captured in the CO_2 absorber of the new 90% capture case to achieve the overall target of 90% carbon capture rate because the portion of CO_2 being sent to the H_2S absorber out of the total CO_2 captured at the CO_2 absorber is larger in the new 90% case than in the original 90% case. Therefore, more CO_2 is actually captured at the CO_2 absorber in the new 90% case than in the old 90% case but the

amount of CO_2 recovered is the same in the two cases, i.e. 90% carbon capture, since more CO_2 captured is sent to the H_2S removal section with the increased CO_2-laden solvent flow to the H_2S absorber.

Given the fact that the lean solvent flowrate cannot be increased further, the carbon capture rate has been increased up to 95% by increasing the total solvent flowrate from 5.35 to 5.99 of L_S/V_S by increasing only the semi-lean flowrate (Run 2). However, the H_2 recovery starts to decrease from 99.0% to 98.5% due to more hydrogen being sent to the CO_2 product stream. In Run 3, the 1st flash drum pressure is reduced to 20.5 bar from 23.5 bar to recover more hydrogen and recycle it to the CO_2 absorber. As more gas stream is recycle to the CO_2 absorber, the carbon capture rate drops below 95% so the semi-lean solvent flowrate needs to be increased again (Run 4). At Run 5, the 1st flash drum pressure is reduced to 19.5 bar to maintain the H_2 recovery over 99%. Finally, Run 6 can meet both targets of 95% carbon capture rate and 99% H_2 recovery by increasing the circulating solvent flowrate slightly. The simulation parameters and results are presented in **Table 4-7**.

Table 4-7: Operating conditions, CO_2 compression requirement and auxiliary power consumption of Selexol units at 90 and 95% carbon capture

Case	Integrated dual-stage Selexol unit (90% carbon capture)	Integrated dual-stage Selexol unit (95% carbon capture)
Carbon capture rate [%]	90.0	95.0
CO_2 product purity [mol%]	97.22	97.55
H_2 recovery [%]	99.0	99.1
L_{S_lean}/V_S (CO_2 absorber)	0.71	1.82
L_S/V_S (CO_2 absorber)	5.20	6.01
1st flash drum P [bar]	18.5	19.5
H_2S stripper duty [MW_{th}]	14.6	39.1
CO_2 compression power [MW_e]	32.09	31.81
Total auxiliary power consumption [MW_e]	20.01	32.97

The total auxiliary power consumption also increases with increasing semi-lean solvent flowrate and decreasing pressure at the 1st flash drum as shown in **Figure 4-13**.

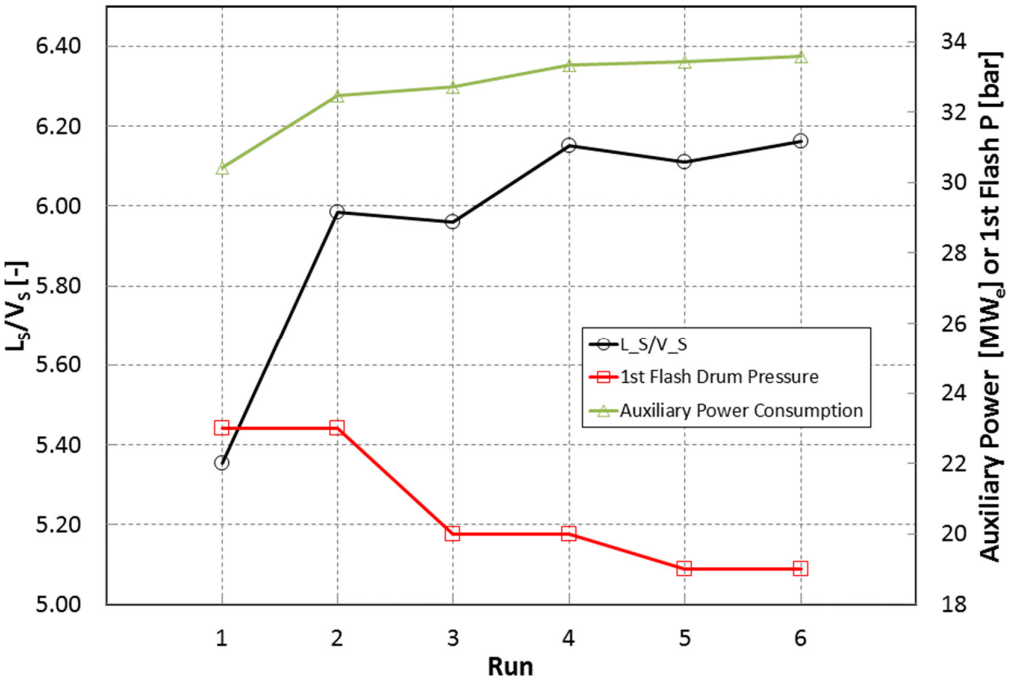

Figure 4-13: Ls/Vs, 1st flash drum pressure and auxiliary power consumption over the simulation runs of the integrated dual-stage Selexol unit

4.5 Summary and conclusions

Physical solvents have been a subject of research for several years, both in academia and in industry. There are advantages and disadvantages interconnected with the use of each of them however the use of Selexol is demonstrating better results both in terms of removal rate and energy requirements.

The absorption regime was successfully approached producing a predictive simulation tool developed to accurately describe the behaviour of the acid/shifted syngas in the solvent and therefore assess correctly the process configurations. In this study the targeted hydrogen recovery was set to 99.4 %. It is however recommended that thorough investigation of hydrogen solubility in Selexol is conducted as higher recovery rate targets might inevitably limit the carbon capture rate.

CO_2 capture processes using DEPG in a Selexol process have been examined in detail for IGCC power plants and were presented. In all the schemes examined, DEPG solvent in a two-stage Selexol process has been implemented, to achieve the acid gas

removal in the first stage and the CO_2 capture in the second stage. For the two-stage Selexol process, two different configurations were tested and compared in terms of acid gas and CO_2 capture removal as well as the energy required in each scheme to achieve the purity and recovery targets set. The two configurations demonstrate different energy requirements. It was illustrated that the first scheme presented (integrated scheme) is less energy demanding. In particular the integrated scheme auxiliary requirement is almost 20 MW_e while the corresponding requirement for the non-integrated scheme is approximately 28 MW_e. The integrated scheme is therefore beneficial.

The conventional, integrated dual-stage Selexol unit can achieve 90% and as high as 95% carbon capture rates easily without having to modify the process configuration. Capture rates as high as 95% would be challenging to achieve with post combustion capture processes due to intensive solvent regeneration energy, equipment size and high solvent losses (Abu-Zahra 2013). However, it is difficult to achieve 95% capture rate with the non-integrated dual-stage Selexol unit due to a pinch point at the top end of the CO_2 absorber. Finally, moving to stricter carbon capture rate it is expected that the auxiliaries consumption will increase significantly.

Chapter 5 Alternative processes for carbon capture in IGCC power plants

5.1 Introduction

This chapter discusses the IGCC power plant performance, focusing on the viability of different carbon capture options. The cases investigated incorporate physical solvents in combination with membranes and are compared to the two-stage Selexol process.

Different schemes can be incorporated to improve the power plant's efficiency. Krishnan et al. (2009) discussed the efficiency losses of the power plant using H_2 selective membranes but they assumed that H_2S can be sent for storage together with CO_2. Franz and Scherer (2010) examined CO_2 and H_2 selective membrane process designs, using however MDEA as a sulphur removal option. Merkel and co-investigators (2012) also focused on the membrane modules design of the carbon capture process in IGCC power plants. They examined both CO_2 selective and H_2 selective membranes. For sulphur compounds, they assumed a low temperature absorption process but no further details were provided. In this study, contrary to aforementioned, a detailed single stage Selexol scheme for AGR combined with a membrane module for carbon capture has been introduced, achieving very strict requirements for H_2S removal, i.e. >99% removal.

The IGCC power plant driven by the GEE coal slurry gasifier was chosen and three different cases were proposed with respect to carbon capture technology as listed below:

- Case 1: Two-stage Selexol (base case),
- Case 2:

  (a) Single stage Selexol for H_2S removal upstream WGSRs and polymeric H_2 selective membrane,

(b) Single stage Selexol for H_2S removal downstream WGSRs and polymeric H_2 selective membrane,

- Case 3:

(a) Single stage Selexol for H_2S removal upstream and metallic H_2 selective membrane.

(b) Single stage Selexol for H_2S removal downstream WGSRs and metallic H_2 selective membrane.

Schemes, alternative to the state-of-the-art that will lead to the least energy consumption for the carbon capture process are suggested. The results reported in this chapter are obtained after the full integration of the novel capture processes with the power plant simulation.

5.2 Methodology

The block flow diagram of the IGCC power plant is shown in **Figure 5-1** for Case 1, while the cases with hybrid processes are represented in **Figure 5-2** and **Figure 5-2**. The coloured blocks indicate additional units required for the IGCC power plant when carbon capture is incorporated.

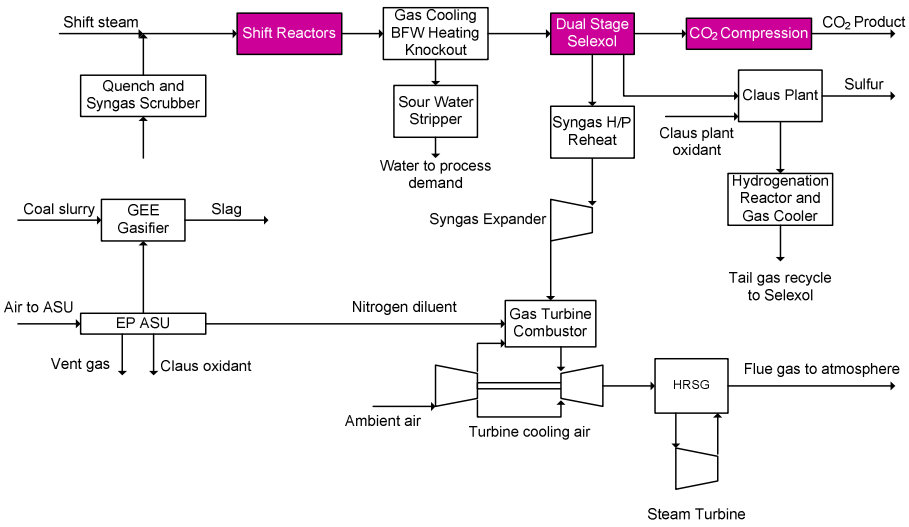

Figure 5-1: IGCC block flow diagram with dual stage Selexol

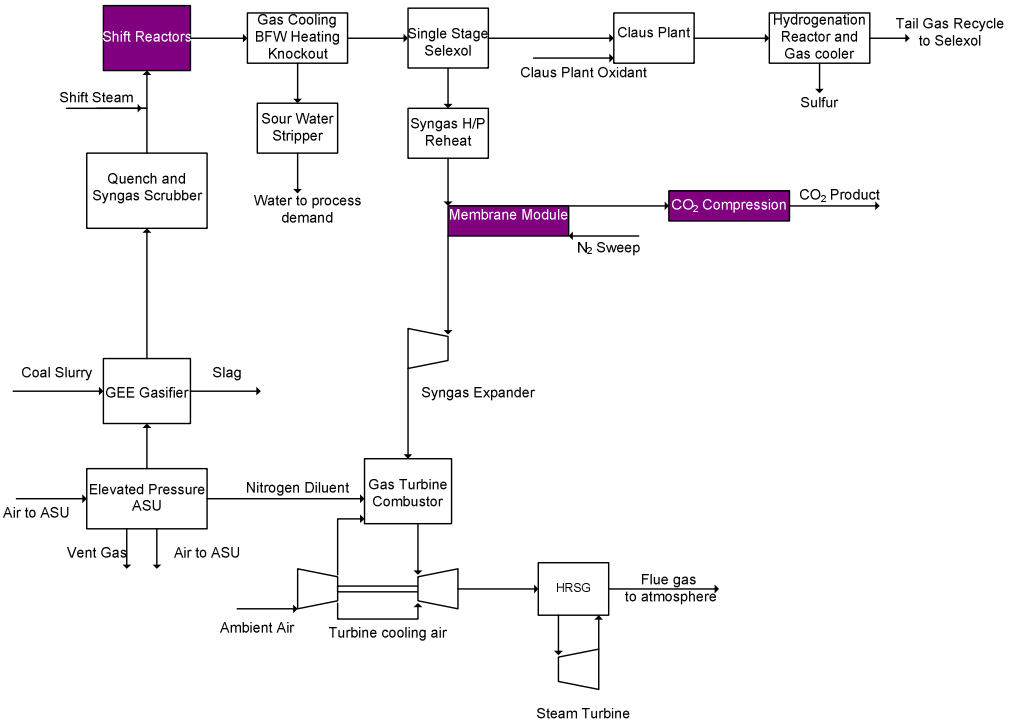

Figure 5-2: IGCC block flow diagram with single stage Selexol and metallic membrane module

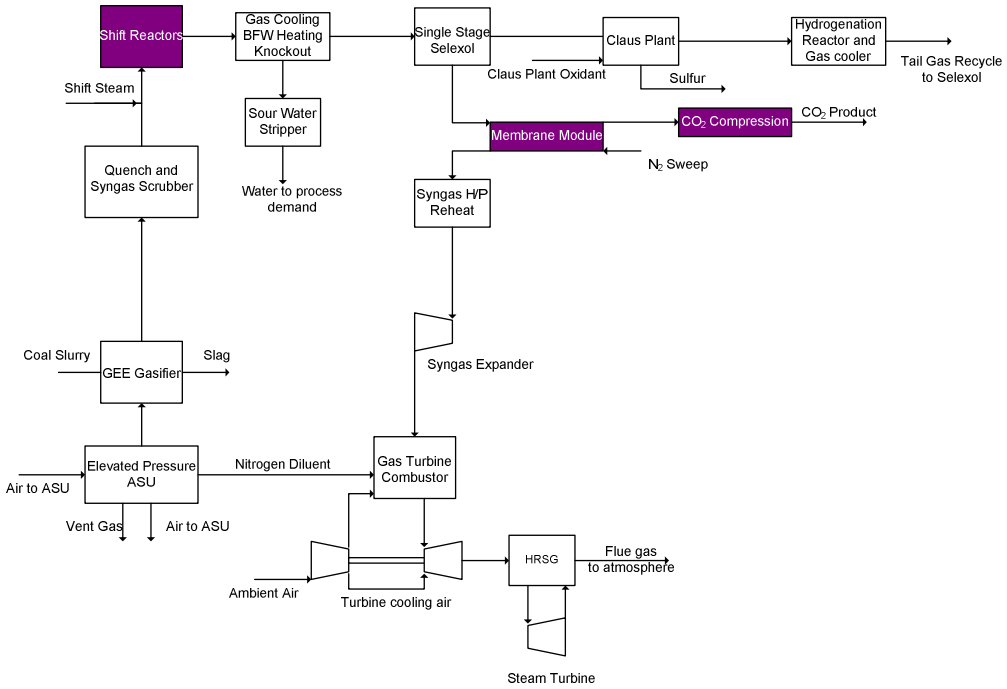

Figure 5-3: IGCC block flow diagram with single stage Selexol and polymeric membrane module

The vapour–liquid equilibrium of H_2S and CO_2 in Selexol, as discussed in Chapter 5 of this thesis, was implemented for the single stage Selexol process with the Peng-Robinson EOS to correct for vapour phase non-ideality and was used to represent the AGR removal section within the IGCC plant.

For the WGSRs a two stage catalytic fixed bed concept is adopted. The final product passes through a series of coolers where water is knocked out and sent to the membrane module for the removal of CO_2. Polymeric and metallic membranes were examined to find out that they are the best candidates for the membrane module.

In general, the transport of the gas in polymeric membranes can be expressed by equation 5-1 (Wijmans and Baker 1995):

$$J_i = P_i \cdot \frac{p_{io} - p_{il}}{l} \tag{5-1}$$

Where J_i is the molar flux (cm^3 (STP) of component i/cm^2s), l stands for the membrane thickness, P_i is the permeability of component i, while p_{io} and p_{il} are the partial pressures of component i in the feed and permeate side, respectively. Permeability P_i, is the measure of the membrane's ability to permeate the gas. The product of the diffusion and the solubility coefficients describes the permeability according to the solution–diffusion theory, and is represented by equation 5-2 (Baker 2004).

$$P_i = D_i K_i \tag{5-2}$$

D_i is the diffusion coefficient (cm^2/s), K_i represents the solubility coefficient which is the number of the dissolved molecules in the membrane (cm^3 (STP) of component i/ cm^3 of polymer cm Hg),

Metallic membranes, such as Palladium (Pd) membrane in particular, do not follow the solution–diffusion theory. In these cases, the flux should be described by the equation below (Yun and Oyama 2011):

$$J_i = P_i \cdot \frac{{p_{io}}^n - {p_{il}}^n}{1} \quad (5\text{-}3)$$

Where J_i is the flux of the permeating species, Pi is the permeability, p_{io} and p_{il}, are as in equation 5-1, the partial pressures of component i in the feed and permeate side, respectively, and n is the pressure exponent. According to the Sievert's law, when the controlling step is bulk diffusion through the Pd membrane, n=0.5 because the isotherm is proportional to the square root of the hydrogen pressure. However, the exponent ranges from 0.5 to 1 depending on which step is the rate determining step (Caravella et al. 2008; Yun and Oyama 2011). In this study, it has been assumed that permeation through the palladium membrane is very fast, as the palladium layer is thin therefore, the pressure exponent equals unity. Furthermore, to ensure that this assumption is reasonable and applicable, only materials where n=1 as presented by Yun and Oyama (2011) have been considered.

The membrane module used in this study was developed in the University of Edinburgh (Bocciardo et al. 2013). The governing equations for the mass balance across the system adopted in the membrane module incorporated for carbon capture are presented below (Baker 2004):

$$\frac{d(F_r x_i)}{dA} = -J_i \quad (5\text{-}4)$$

$$\frac{d(F_p y_i)}{dA} = J_i \quad (5\text{-}5)$$

Where F_r and F_p are the retentate and permeate molar flow, and x and y the retentate and permeate molar fraction, respectively. The main assumptions are constant permeability along the module, no pressure drops and ideal and isothermal behaviour. While reasonable as an initial approach, these assumptions should be further verified in more detailed simulations.

5.3 Hybrid Configurations

In IGCC power plants, the stream resulting from the single stage Selexol system contains 38 % CO_2 and approximately 58 % H_2. The objective therefore is to separate the two gases, i.e. highly selective membranes for either H_2 or CO_2 are required for the separation. Since the CO_2 compressor is one of the major contributors to the energy penalty, it is desired to produce the CO_2 product at high pressures so that this energy penalty can be reduced. For this reason, H_2 selective membranes in a module with sweep gas have been selected for the process. This configuration allows for CO_2 as the retentate product to maintain its high pressure (approximately 50 bars) while the permeated H_2 leaves the module at the combustor pressure.

While a membrane process in post-combustion capture is usually configured to produce CO_2 product as the permeate gas, in pre-combustion capture the objective is to keep CO_2 on the retentate side. This is due to the significant difference in operational pressures of the two techniques. In post-combustion capture the pressure is atmospheric while in pre-combustion capture the pressures are as high as 55 bars. It is therefore beneficial to maintain the CO_2 stream's high pressure so that the compression work needed for CO_2 to meet the storage conditions requirement is reduced. The permeate gas enriched in H_2 is mixed with a sweep gas at the H_2 selective membranes, which allows producing a pressurised feed for the gas turbine. The membrane modules use the N_2 (31.72 bar) already produced in the Air Separation Unit (ASU) of the plant as a sweep gas to create the partial pressure gradient. Additionally, the N_2 from the ASU provides the dilution required for the combustion in the turbine and balances the gas density which is important for the mechanical performance of the turbine.

5.3.1 Membrane module and materials

For the cases investigated, several H_2 selective membrane materials reported in the literature (Schiebahn et al. 2012; Basile 2008) have been examined using a membrane module simulator developed at the University of Edinburgh, to assess their performance for pre-combustion capture application. The membrane module considers

a one-dimensional, non-disperse plug-flow with a counter current configuration in which the sweep N_2 is used to improve the driving force through the module.

Krishnan et al (2009) examined Polybenzimidazole (PBI) polymer membrane, in an Aspen Plus based model achieving 90 % CO_2 capture. Their results show efficiency losses of 10–11.6% points, contrary to this study that actually suggest schemes that lead to increased efficiencies compared to the state-of-the art. Franz and Scherer (2010) used Pebax in an Aspen Plus membrane module in their study. They concluded that the results for H_2 and CO_2 selective membranes show that with membranes of state-of-the-art, the current requirements concerning CO_2 purity and CO_2 separation degree cannot be fulfilled. In fact, they reported to have achieved a CO_2 capture rate of 85 %. In their study, promising materials which are already developed, even if only at laboratory level, have been examined. Moreover, Franz and Scherer adopted sour shift in their investigation designs, without presenting a detailed study on the effect of the sour and sweet shifts on the performance of the designs. Two types of membranes were assumed in the approach adopted by Merkel et al. (2012). The first are polar rubbery membranes that selectively permeate CO_2. The second type of membrane used is a rigid glassy polymer that selectively permeates hydrogen. No acid gas removal was considered in this study. In fact it was assumed that the bulk of this hydrogen sulphide will end up with the liquid CO_2 product.

None of the studies above achieved a stream >95% pure in CO_2 and 90% carbon capture, while achieving H_2S removal rates of more than 90% as in this study. Moreover, none of the aforementioned publications examined the integration of membrane modules in such range of materials as discussed below.

To determine the best candidates for the membrane module material, a strategy was set to evaluate their potential for carbon capture within the IGCC process. Amongst the desired characteristics essential for their initial selection for examination was high permeability. The permeability of the best potential candidates is shown in **Table 5-1**.

Table 5-1: Candidate membrane module materials permeability and selectivity (Scholes et al. 2010; Yun and Oyama 2011)

	Material	**H_2 Permeability (Barrer)**
Polymeric	6 FDA-Durene modified by vapour-phase EDA cross linking	33
	6 FDA-Durene modified by liquid-phase EDA cross linking	120
	6 FDA-Durene modified by liquid-phase PDA cross linking	10
Metallic	Pd–Ni alloy/Cu/Ni powder	40,400
	$PdNi_{0.2–0.3}$/Ni powder	6,600
	Pd–Cu alloy/Silica/Ni	29,900

Permeability has been defined with equation 5-2. The ability of a membrane to separate gases is measured by its selectivity α_{ij}. The ideal selectivity of a membrane towards a species i or j, can be defined as the ratio of the permeabilities of the gases, as shown in equation 5-6:

$$a_{ij} = \frac{P_i}{P_j} \tag{5-6}$$

Among the materials examined as presented in the literature and references therein (Scholes et al. 2010; Yun and Oyama 2011; Ockwig and Nenoff 2007; Czyperek et al. 2010) polymeric and metallic membranes showed the best performance in terms of CO_2 purity and recovery, due to their higher permeability and selectivity. However, polymeric membranes demonstrate lower selectivity compared to metallic and as a consequence resulting lower CO_2 recovery. This means that contrary to metallic

membranes, polymeric membrane modules were expected to require more than one stage to provide a CO_2 product stream which satisfies the desired purity and recovery. Inorganic membranes which were the third class of materials examined, demonstrated the weakest performance.

Each class of materials has several advantages and drawbacks. For example, both materials can achieve the desired results, but the area required for the separation differs. Moreover, since metallic membranes working temperatures are high, the syngas stream leaving the single-stage Selexol that is at low temperature has to be heated. Additional heating duty is therefore required for the overall process which is affecting the steam cycle electrical output. Polymeric membranes should not operate above 373K (100 °C) to maintain their stability and metallic membranes should not operate below 573K (300 °C) due to phase change of the material below this temperature (Scholes et al. 2010). In this study each membrane module is assumed to operate within the range of temperature where it can work properly, as presented in the literature.

For the cases that refer to polymeric membrane module configurations, 6FDA Durene modified by vapour phase EDA cross linking is selected, while Pd-based membrane is chosen for the cases using metallic membranes. The properties of the materials finally chosen for the case studies are listed in **Table 5-2.**

Table 5-2: Membrane module simulation parameters

	Material	**Temperature (K)**	**H_2 Permeability (Barrer)**	**H_2/ CO_2**	**Area (m^2)**
Polymeric	6 FDA-Durene modified by vapour-phase EDA cross linking (Scholes et al. 2010)	308	33	102	100,000
Metallic	Pd alloy (Yun and Oyama 2011; Bientinesi 2011)	623	14,550	5,000	5,500

The choice of the specific materials among the wide range of other available was primarily based on their performance in terms of CO_2 purity as a function of membrane area as presented in **Figures 5-4** and **5-5.** As seen in **Figure 5-4**, 6FDA Durene modified by liquid phase EDA cross linking can provide the highest CO_2 purity with respect to the membrane module area due to its high permeability towards H_2 (120 barrers) (Scholes et al. 2010). 6FDA Durene modified by vapour phase EDA cross linking and 6FDA Durene modified by liquid phase PDA cross linking with permeabilities of 33 and 10 barrers respectively, require greater areas to produce gas streams with high CO_2 purity. However, since 6FDA Durene modified by vapour phase EDA cross linking has the highest selectivity of the three materials, it gives the best results in terms of CO_2 recovery. Therefore, 6FDA Durene modified by vapour phase EDA cross linking was finally chosen for the simulation cases as a trade-off to be achieved for both CO_2 purity and recovery. Moreover, from all the metallic materials examined, as presented in the literature (Scholes et al 2010; Yun and Oyama 2011), Pd alloys have given the best results for the CO_2 product purity due to their high selectivity towards Hydrogen. Pd Ni with Ni powder alloy requires the greatest area to

achieve the desired high CO_2 purity. Since there are no significant differences between Pd alloys with Ni and Cu respectively, in terms of CO_2 purity results with area, the criterion to choose the best between them was the CO_2 recovery, which is shown in **Figure 5-6.**

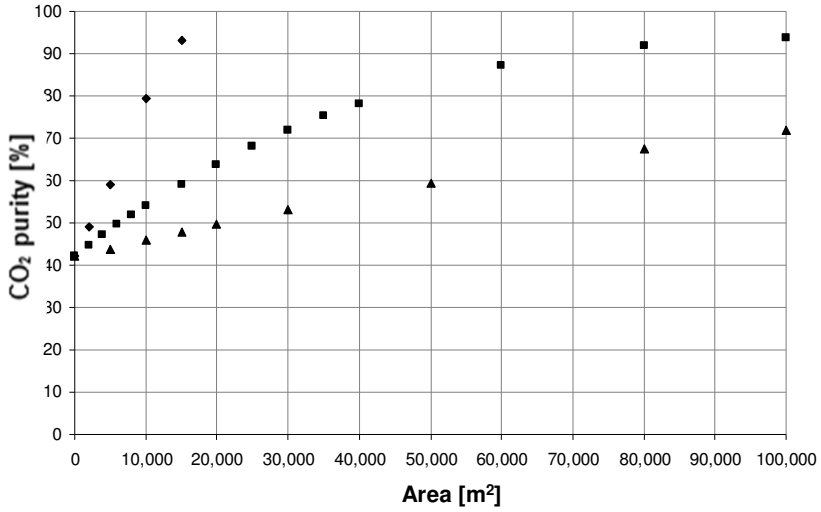

Figure 5-4: CO_2 purity as a function of polymeric membrane area, (▲) 6 FDA Durene with liquid phase PDA cross linking, (■) 6 FDA Durene with vapour phase EDA cross linking, (♦) 6 FDA Durene with liquid phase EDA cross linking

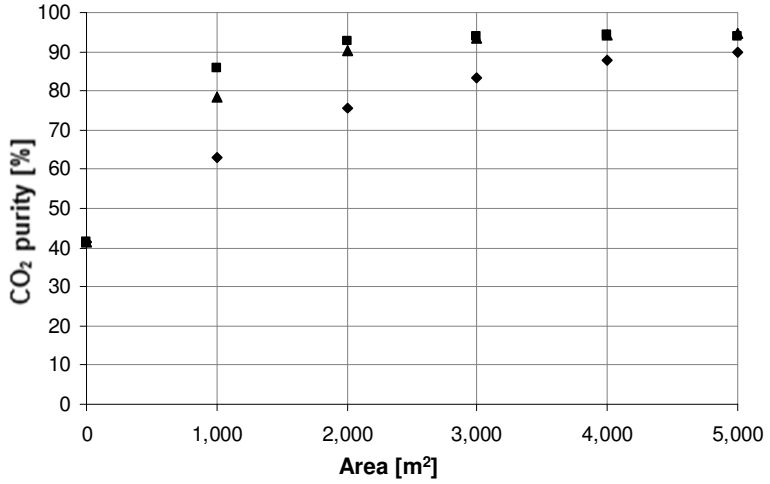

Figure 5-5: CO_2 purity as a function of metallic membrane area, (■) Pd-Cu/Silica Ni powder, (▲) Pd-Ni/Cu/Ni powder, (♦) Pd-Ni0.2-0.3/Ni powder

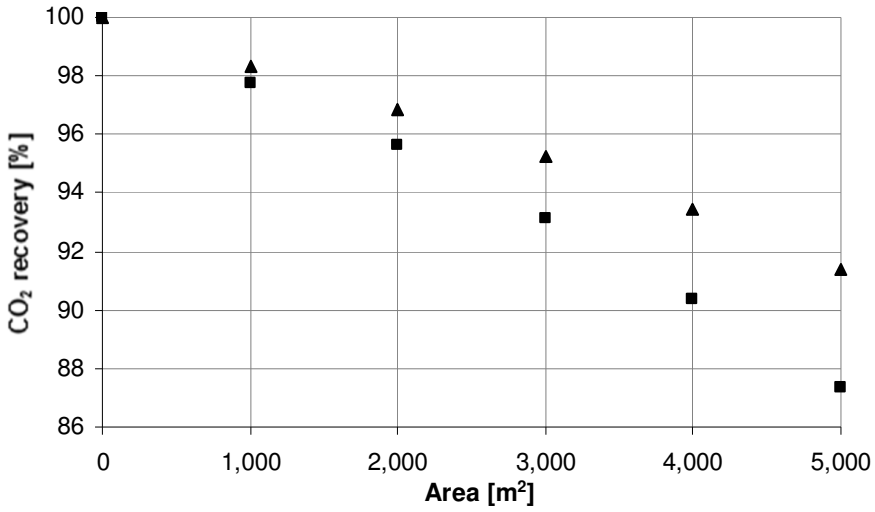

Figure 5-6: CO_2 recovery as a function of metallic membrane area, (■) Pd-Cu/Silica Ni powder, (▲) Pd-Ni/Cu/Ni powder

The materials chosen for the complete IGCC power plant simulation showed that they can result in high CO_2 purity product streams with the least area required among other materials of the same classes.

5.3.2 Upstream vs downstream location of the hybrid system

Amongst the challenges faced in the process integration decision making is also whether the H_2S removal unit should be located upstream or downstream of the WGSRs (**Figure 5-7** and **Figure 5-8**). Between the two options, there is a significant difference in the CO_2 concentration of the carbon capture feed stream. Upstream placement of the AGR unit of the hybrid system should lead to better CO_2 recovery as the raw gas composition in CO_2 is lower than the gas exiting from the WGSRs. However, there are additional cooling and heating requirements which should be satisfied by the steam cycle. For downstream located configurations, there is a smaller effect on the power plant's steam cycle energy output , but there is a significant reduction in CO_2 recovery due to the fact that the stream entering the system is rich in CO_2 and Selexol is highly selective not only to H_2S but also to CO_2. Both options have been thoroughly investigated and results of both incorporating the hybrid system (AGR and membrane module) are presented in the next paragraph.

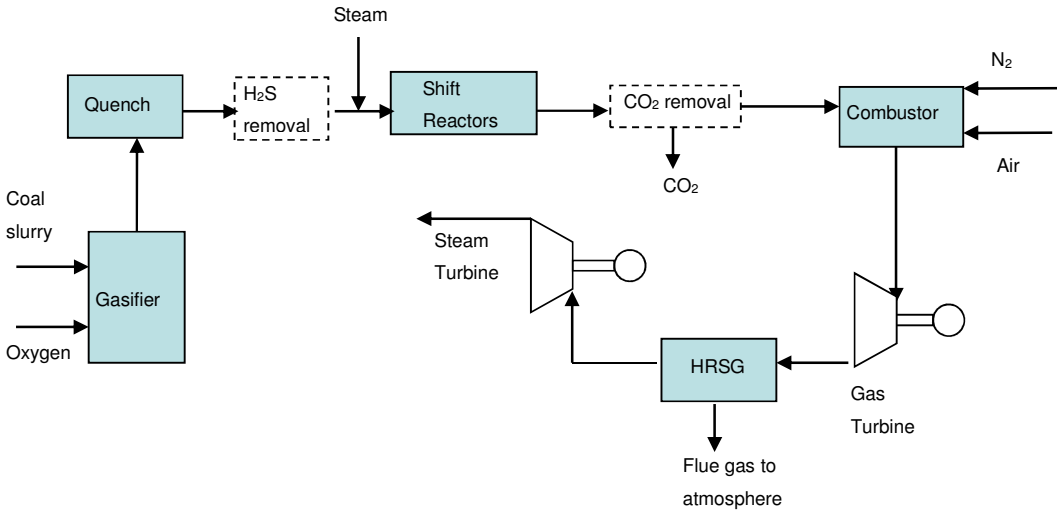

Figure 5-7: IGCC with H_2S removal upstream of WGSRs

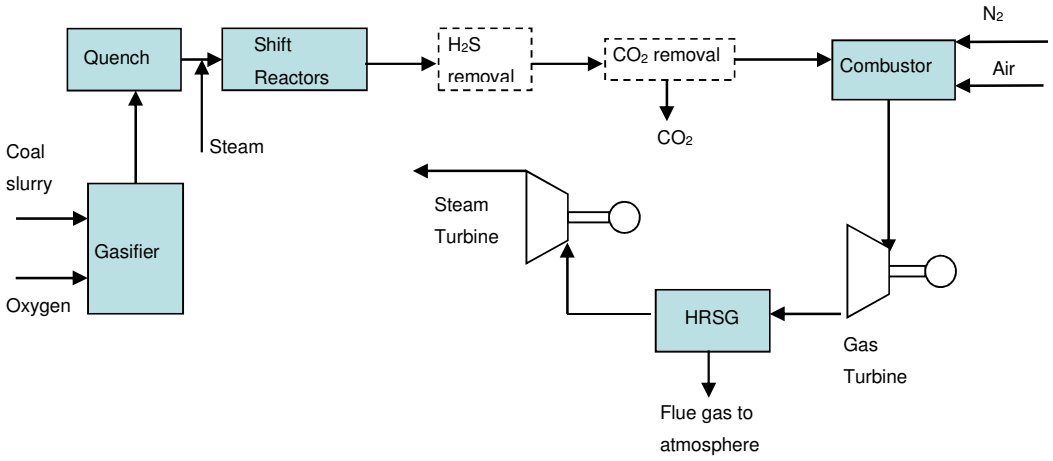

Figure 5-8: IGCC with H_2S removal downstream of WGSRs

5.4 Results and points of discussion

Additional cooling and heating requirements may arise when hybrid systems are incorporated in the IGCC power plant for AGR and CC. The generation of the grand composite curve is a useful tool to determine accurately these heating and cooling requirements. These requirements differ depending on the configuration used. As the additional cooling and heating needs of the process will most probably have to be

satisfied by extracting energy from the steam cycle, each configuration will have different effects on the steam cycle's electrical output. Therefore, the assumption of constant steam turbine electrical output is unrealistic and the production of the composite curve is essential to accurately predict this effect. The composite curves were produced by using well established methods available in the literature (Kemp 2007).

The cooling and heating requirements for the location of the H_2S removal single stage Selexol unit upstream of the WGSRs are shown in **Figure 5-10** and **5-11**. The Figures represent the Grand Composite Curve (GCC) of the base case. Cases 2a and 3a, respectively, with the AGR located upstream of the WGSRs. It can be seen that these configurations require additional cooling. In particular, for the polymeric membrane module case (Case 2a), the cooling duty can be read on the left side of **Figure 5-10** and is 10.5 MW. This comes mostly from the requirement for the gasification product stream to be cooled down before entering the single-stage Selexol unit.

The left side of **Figure 5-11**,, shows that in the case of the Pd alloy in the membrane module that is combined with a H_2S removal single-stage Selexol unit located upstream of the WGSRs configuration (Case 3a), the cooling duty is almost 3.9 MW. Since the membrane's working temperature is high, the stream after the knock out train has to be heated up before entering the membrane module. Therefore, this cold stream (knock out train outlet) can be partially exploited to cool down the hot stream entering the AGR after gasification, resulting in a reduced cooling duty. The heating duty shown on the right side of the curve in **Figure 5-11** is almost 9.91 MW due to the requirement of the metallic membrane for high working temperatures. The product stream of the AGR which is directed to the WGSRs has to be heated prior to entering the membrane module.

For the cases with the single-stage Selexol unit located downstream of the WGSRs, no additional heating/cooling requirements compared to the base case have been assumed. A steam cycle similar to the one of the base case was assumed to sufficiently accommodate the steam requirements of these cases, given that the heating and cooling

requirements of these cases up until the AGR and carbon capture processes would be similar.

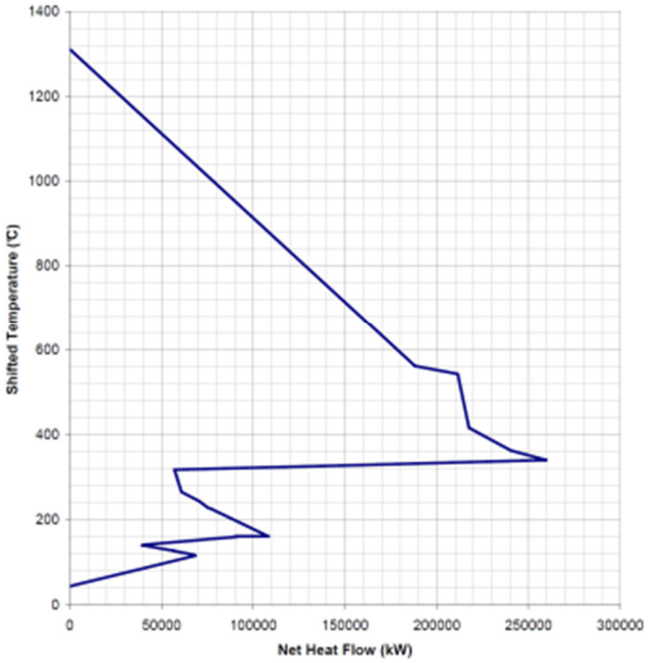

Figure 5-9: Grand composite curve for the base case

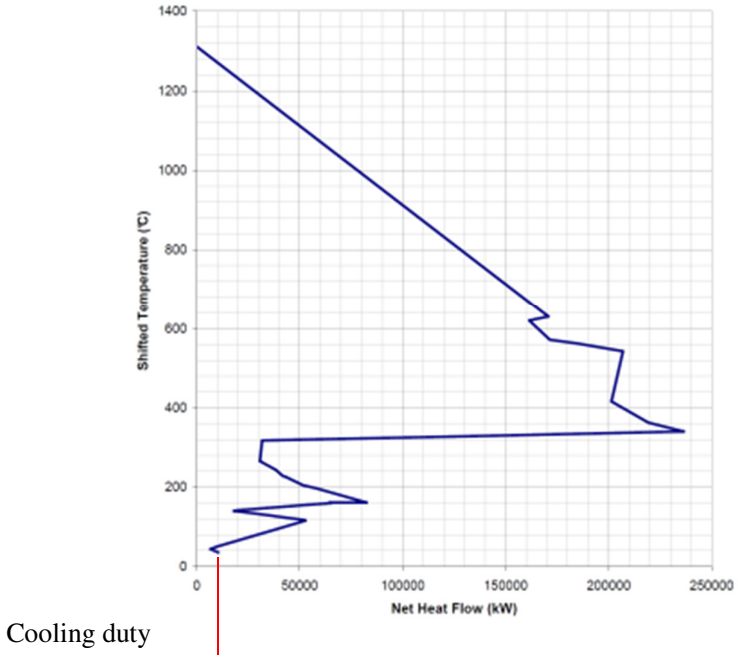

Figure 5-10: Grand composite curve for polymeric membrane that is combined with a H_2S removal single-stage Selexol unit located upstream of WGSRs (Case 2a)

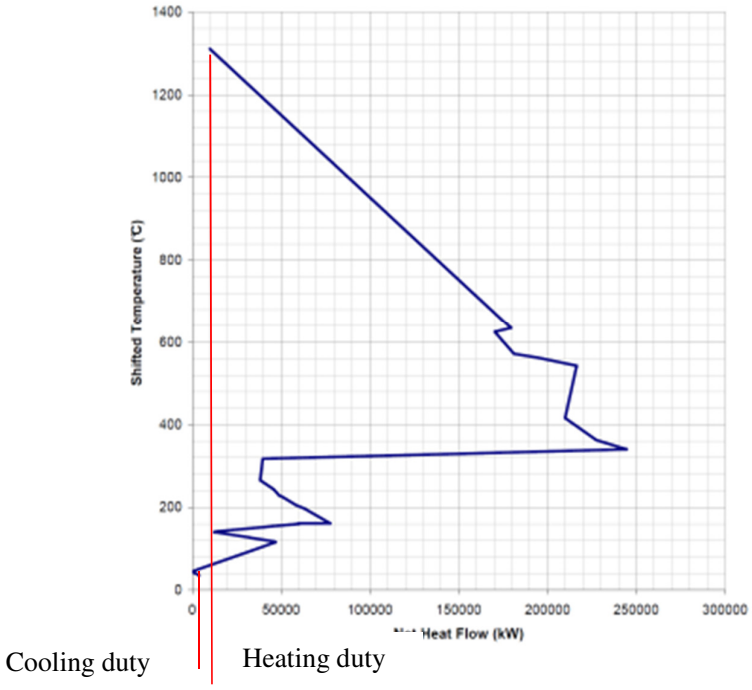

Figure 5-11: Grand composite curve for metallic membrane that is combined with a H_2S removal single-stage Selexol unit located upstream of WGSRs (Case 3a)

Table 5-3 and **Table 5-4** summarize the detailed results of the cases examined. All the cases are compared on the basis of 99.5 % H_2S removal and 90 % overall carbon capture. The reported results clearly illustrate that hybrid systems can be competitive with the base case in which a two stage Selexol process is used for the H_2S and CO_2 co-capture. Among the cases examined, the ones in which the H_2S removal unit is located downstream of the WGSRs ('sour shift') demonstrated the best performance due the lowest heating/cooling requirements within the processes prior to AGR, the lower AGR unit auxiliaries, as well as to the lower CO_2 compression requirement compared to the base case.

Table 5-3: Performance results of the different hybrid systems with AGR unit upstream the WGSRs

	Case 1	**Case 2a**	**Case 3a**
Gas Turbine, MW_e	464.00	464.00	464.00
Steam Turbine, MW_e	274.69	269.45	267.78
Reboiler duty, MW_{th}	34.95	29.89	30.24
Capture Unit Auxiliaries, MW_e	17.32	21.41	11.87
Overall C capture, %	90.00	90.00	90.00
CO_2 compression, MW_e	27.40	3.72	4.16
Thermal Input, MW_{th}	1,710.78	1,710.78	1,710.78
Plant Efficiency (HHV), %	32.50	31.75	32.81

Table 5-4: Performance results of the different hybrid systems with AGR unit downstream of the WGSRs

	Case 1	Case 2b	Case 3b
Gas Turbine, MW_e	464.00	464.00	464.00
Steam Turbine, MW_e	274.69	274.70	274.70
Reboiler duty, MW_{th}	34.95	35.76	35.19
Capture Unit Auxiliaries, MW_e	17.32	15.96	6.17
Overall C capture, %	90.00	90.00	90.00
CO_2 compression, MW_e	27.40	6.52	6.71
Thermal Input, MW_{th}	1,710.78	1,710.78	1,710.78
Plant Efficiency (HHV), %	32.50	33.27	33.94

As in Case 2a there is a change in the steam turbine electrical output, it shows lower efficiency compared to the base case. This results can also be justified by the higher total auxiliaries estimated for this case. Polymeric membranes have a lower selectivity and as a consequence low CO_2 recovery. The simulations of the polymeric membranes conducted confirmed that membrane modules required more than one stage to provide a CO_2 product stream which satisfies the purity/recovery specifications. **Figure 5-12** and **Figure 5-13** represent the configuration used when a polymeric membrane is incorporated in the membrane module, for sweet and sour shift respectively. The multistage compressor is the component that adds to the auxiliaries' consumption of these configurations.

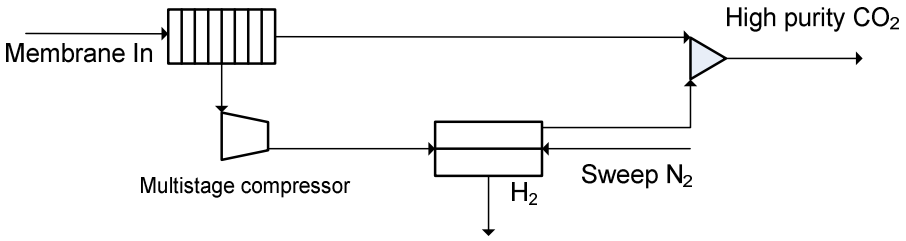

Figure 5-12: Dual stage membrane configuration for hybrid system incorporating polymeric membrane upstream WGSRs

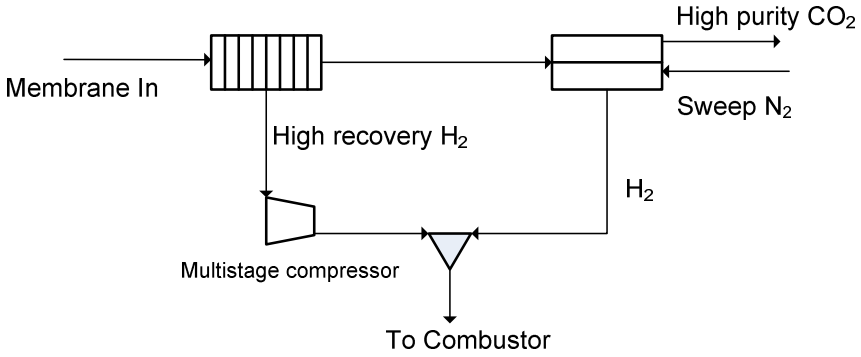

Figure 5-13: Dual stage membrane configuration for hybrid system incorporating polymeric membrane downstream WGSR

Case 3a demonstrates considerable loss in steam turbine output compared to Case 1 due to the metallic membrane's requirement for the feed stream to be sufficiently heated as explained above. This case however shows better performance in terms of net plant efficiency compared to Case 2a, and clear competitiveness towards the base case.

Both Cases 2b and 3b operating in sour shift mode demonstrate decreased auxiliaries consumption; therefore the net power plant efficiency is increased. It has to be pointed out that the CO_2 compressor duty for all the cases investigated is impressively decreased compared to the base case. The first and foremost reason for this decrease is that the regeneration of the solvent used in the AGR occurs only in the gas stripper, neglecting the pressure vessels required in the two-stage Selexol configuration used in the base case. This is a significant gain as in the base case the CO_2 stream has to be

compressed from around 3.4 bar leading to very high CO_2 compression energy demands. As shown in **Table 5-4**, for the cases incorporating hybrid configurations, the CO_2 compression duty shows an 86.4 % drop for Case 2b and almost 85 % for Case 3b compared to the base case. Cases incorporating metallic membranes demonstrate higher CO_2 compression duty compared to polymeric membrane cases due to the difference in the temperature of the product stream which has to be compressed, which could however, improve by further cooling. Additionally, for the cases in sour mode, the CO_2 compression duty is higher than the ones in sweet mode. This is due to the fact that the inlet pressure of the compression train for the cases in sweet mode is essentially the WGSRs' pressure (50.1 bar), while the corresponding pressure for the configurations in sour mode is the AGR unit pressure (35.2 bar).

5.5 Conclusions

This Chapter focuses on the viability of hybrid systems for IGCC power plants with carbon capture and their competitiveness with the state-of-the-art CC process for IGCC which is the two stage Selexol unit. The objective of the hybrid system is not only to obtain a CO_2 pure product stream but also to produce a hydrogen rich stream which will be directed to the combustor so that electricity is produced at the gas turbine. Hydrogen selective polymeric and metallic membranes are therefore selected for the membrane module of the hybrid systems. None of the studies reported in the literature achieved a product stream >95% pure in CO_2 and 90 % carbon capture, while keeping H_2S removal rates as high as >99% as in this study, and more importantly within continuous and overall IGCC plant process simulation.

Amongst the cases investigated, Case 3, which refers to an IGCC power plant with single stage Selexol and a metallic membrane module for H_2S and CO_2 capture respectively, demonstrated the best performance in terms of net power plant efficiency, in both 'sweet' (Case 3a) and 'sour' (Case 3b) AGR removal modes. Although in this case when operating in sweet mode there is loss in the steam turbine electrical output resulting from the heating/cooling requirements of the processes, there is a significant gain in the CO_2 compressor energy requirement. In particular, for Case 3b with the hybrid system downstream the WGSRs, the decrease in energy demand for the CO_2

compressor is as high as approximately 20.7 MW_e. This case appears to be the most competitive configuration of all towards the base case (Case 1) with a net power plant efficiency of 33.94 % (HHV). It can be therefore concluded that the alternative systems for carbon capture suggested in this Chapter can improve the overall efficiency of an IGCC power plant.

Further work is essential towards the optimised power plant configurations in which H_2S is preferentially removed. This can be done by investigating the use of physical solvents other than Selexol, or even mixed solvents such as Sulfinol-M and Sulfinol-D. The VLE of physical and mixed solvents should be investigated in detail so that useful and practical conclusions are deduced to evaluate the viability of these systems. Examining their potential to achieve more efficient H_2S removal and hence reduced auxiliaries of the AGR removal unit, might provide further improvement to the overall performance of the IGCC power plant.

Finally, optimised heat integration can provide improved results in terms of heating and cooling requirements which would subsequently improve the overall performance of the plant.

Chapter 6 IGCC major units approach and simulation downstream carbon capture processes

6.1 Introduction

Within the effort to provide complete and fully functional representation of the overall IGCC power plant operation, all the units involved have been investigated and simulated. The approach adopted for units downstream carbon capture i.e. sulphur recovery plant, combined cycle and steam and feed water parts of IGCC power plants are presented in this Chapter.

6.2 Sulphur recovery

The sulphur recovery plant selected in this study is a Claus process where H_2S is converted to elemental sulphur. The original Claus process was developed by C.F Claus in 1883. There are several process implementations which have been developed to increase the sulphur recovery. However, all these processes are based on the same principles, which are primarily the oxidation of hydrogen sulphide at high temperatures and the formation of sulphur at low temperatures (Wozny 2011).

The Claus process principal objective is the recovery of sulphur more commonly from acid gas streams containing hydrogen sulphide in high concentrations. These streams typically result from acid gases stripped off sour liquids, such as processes utilising physical solvents for the purification of sour gases, i.e. the Selexol process. Established regulations worldwide strictly prohibit sulphur compounds to be vented to the atmosphere. Therefore, the Claus process is of considerable significance within the general scope of IGCC power plant technology. Furthermore, the Claus process yields elementary sulphur products that are of extremely good quality (Kohl 1997).

Complete conversion of hydrogen sulphide to elemental sulphur under Claus plant operating conditions is precluded by the equilibrium relationships of the chemical reactions upon which the process is based. As a result of this limitation, the basic Claus

process is, in many instances, not adequate to reduce atmospheric emission of sulphur compounds to the level required by air pollution control regulations. In these cases, the basic Claus process has to be supplemented with another process specifically designed to remove residual sulphur compounds from the Claus plant tail gas (Kohl 1997). These processes are usually referred to as "tail gas clean-up" or "tail gas treating" processes.

Since the disclosure of the process by Claus in 1883, it has undergone several modifications. The most significant modification was that made by I.G. Farbenindustrie A.G. in 1936 which introduced the process concept currently in use, which consists of a thermal conversion step followed by a catalytic conversion step (Kohl 1997). The Claus processes that are currently in operation are similar to their original design with respect to their basic concept and differ only in the design and arrangement of the equipment.

6.2.1 Claus plant simulation approach

The sulphur recovery plant selected in this study is the Claus process, where H_2S is converted to elemental sulphur. Approximately one-third of the H_2S in the feed is burned in the furnace with oxygen and the SO_2 produced reacts with the remaining H_2S forming sulphur of mainly S_2, S_6 and S_8 species. A waste heat boiler is incorporated after the furnace to recover the heat from the exothermic reactions occurring in the furnace by producing high pressure steam. Sulphur is condensed in a series of condensers and the tail gas goes to several catalytic conversion stages, where the remaining sulphur is recovered. The reactions describing the typical Claus process are the following (Kohl 1997):

$$H_2S + \frac{3}{2}O_2 \Leftrightarrow H_2O + SO_2 \tag{6-1}$$

$$2H_2S + SO_2 \Leftrightarrow 2H_2O + 3S \tag{6-2}$$

The overall reaction is:

$$3H_2S + \frac{3}{2}O_2 \Leftrightarrow 3H_2O + 3S \quad (6\text{-}3)$$

The simulation of the Claus process was conducted for non-capture and carbon capture GEE and Shell IGCC power plants using both Honeywell UniSim R400 within the overall plant simulation and BR&E ProMax software.[6] The comparison between the software tools was primarily incited because there is no option of selection sulphur species as components in the default database of UniSim therefore robust control of sulphur conversion within the plant cannot be conducted with this software.

The simulation cases developed to represent the operation of the Claus process were based on the process flow diagram reported from DOE/NETL. Due to the inconsistencies in mass and energy balances identified in the processes as reported in DOE report, Case 2[7] was used as the main tool and validation guide for all the cases investigated. Regarding inconsistencies, first and foremost, DOE/NETL fails to clearly report the compositions of the sulphur plant inlet stream, in particular the sour gas composition from the syngas scrubber gas outlet. Moreover, very limited data are available within the processes of the Claus plant. More specifically, while flowrates and operating conditions are reported for some unit operations, there is no clarity regarding resulting compositions or key assumptions. Attempting to validate a proposed sulphur plant model with the DOE report data is therefore extremely challenging. The tool case developed was used as a guide to simulate the behaviour of the Claus process in the different IGCC power plant cases investigated, by modifying the process inlets in accordance with the power plant's upstream units outputs. For both GEE and Shell IGCC cases the acid gas from the gas stripper of the Selexol unit is routed to the Claus plant. The schematics of the Claus plants of the non-capture and carbon capture GEE IGCCs are presented in **Figure 6-1** and **6-2**.

---

[6] The Claus plant schematic process flow diagram as produced in ProMax can be found in the Appendix D.

[7] DOE/NETL Case 2 refers to a GEE IGCC power plant with carbon capture.

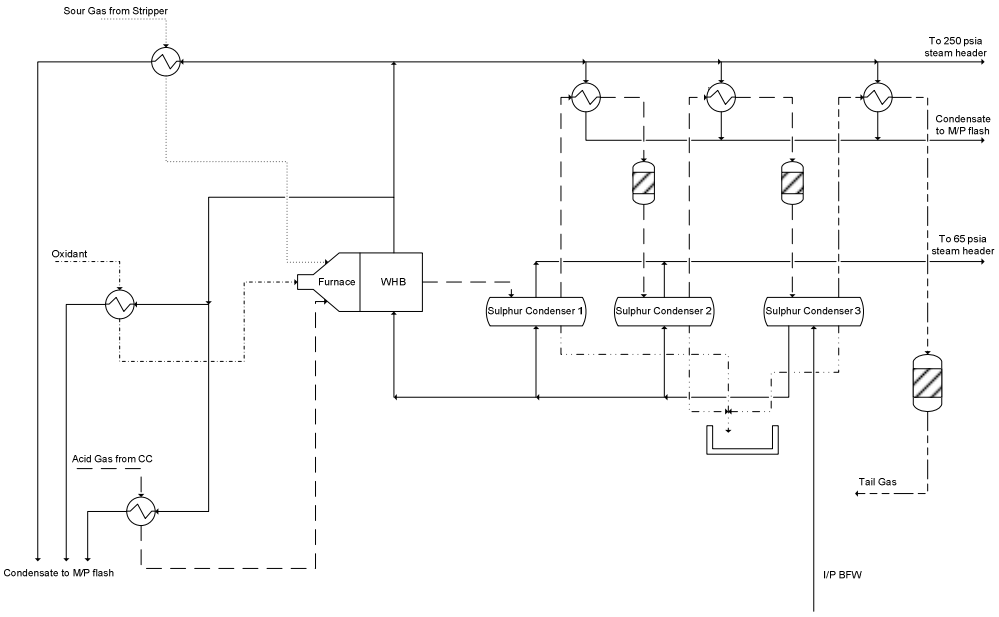

Figure 6-1: Non capture GEE IGCC sulphur recovery schematic

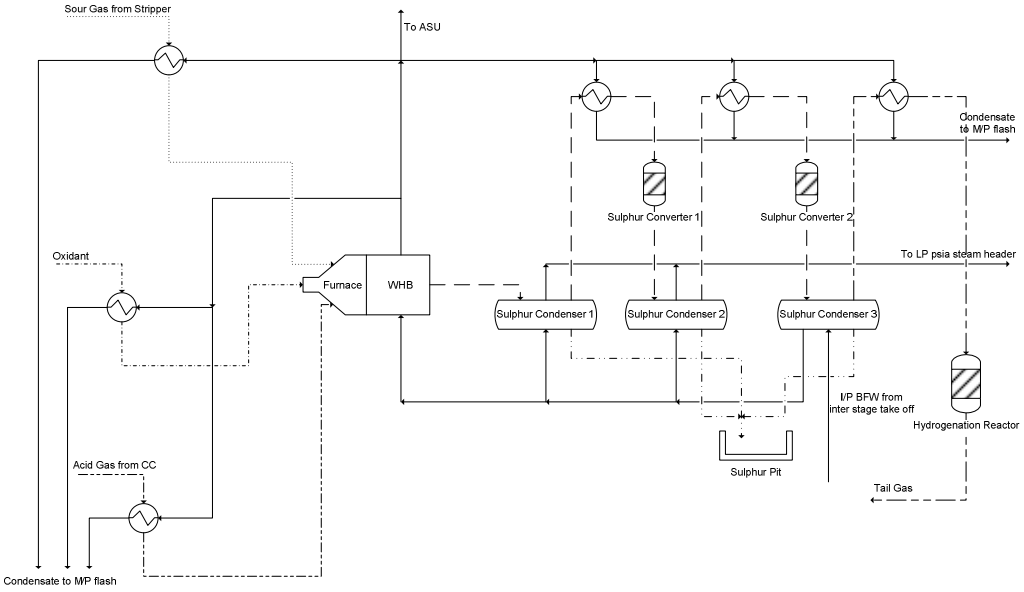

Figure 6-2: Carbon capture GEE IGCC sulphur recovery schematic

The acid gas along with all of the sour gas from the stripper and oxygen from the ASU are fed to the Claus furnace. In the furnace, H_2S is catalytically oxidized to SO_2.

Following the thermal stage and condensation of sulphur, two reheaters and two sulphur converters are used for the conversion of H_2S. The Claus Plant tail gas is hydrogenated and recycled back to the AGR/Selexol process. The steam produced in the furnace waste heat boiler (WHB) is used to satisfy the preheating and reheating requirements of the Claus process. Regarding the steam produced in the WHB, DOE NETL overestimated the IP BFW required. In particular, while DOE estimated that 3.77 kg/s of IP BFW are required in the WHB, in this study it was found that approximately 3.02 kg/s are enough to produce the steam required while cooling down the furnace outlet to611K (338°C).

The furnace temperatures range from 1,513-1,613K (1,240-1,340°C), values that lie within the typical Claus furnace temperatures as reported in DOE/NETL report (NETL 2007) and are sufficiently high to ensure that NH_3 contained in the sour gas stream is thermally decomposed. The simulation developed in BR&E ProMax to represent the H_2S conversion with the temperatures occurring in the operation of the Claus plant was validated with the thermodynamic data reported in the literature (Paskall 1979). As shown in **Figure 6-3**, the model is capable of representing the conversion of H_2S accurately in all the range of temperatures of the Claus plant.

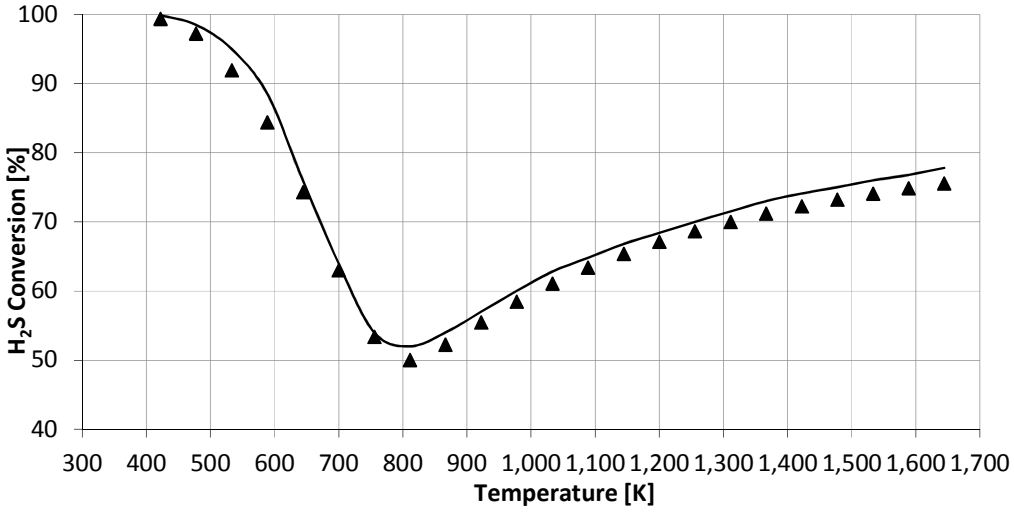

Figure 6-3: H_2S conversion % with temperature (solid line data from Paskall, 1979, ▲ simulation results)

The model utilised runs in the so-called "sulphur" environment in the simulator. The Sulphur Property Package is a Gibbs Excess Energy/Activity Coefficient model which is designed to model the liquid phase properties and compositions of liquid sulphur. For liquid compositions which are predominantly sulphur, the thermodynamic model treats pure sulphur species S_1 through S_8 as Lewis-Randall components and all other species as Henry's law components. The liquid phase properties are predicted by the sulphur model and vapour phase properties using an equation of state (ProMax User Guide 2013).

As shown in **Figure 6-4**, the model is capable of describing the fact that the average molecular weight of sulphur vapour increases with decreasing temperature. At temperatures below 644 K (371°C), sulphur vapour is predominately S_6 and S_8, while at the same partial pressure, but at temperatures above 811 K (538°C), the sulphur is mostly S_2 (Kohl 1997).

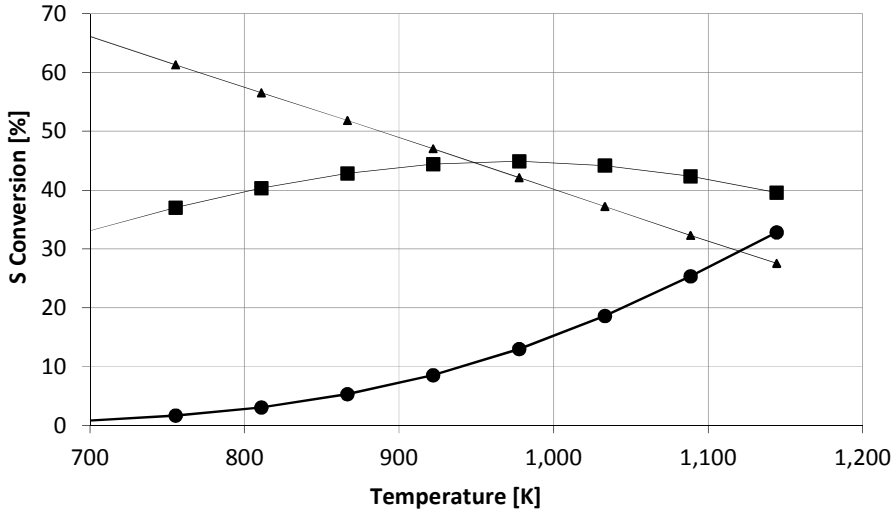

Figure 6-4: Sulphur conversion % to species with temperature (● S_2, ■ S_6, ▲ S_8)

No information is given in the reference report about the process streams within the Claus process to make the presentation of the simulation results for the corresponding streams meaningful. Therefore, only the stream entering the Claus furnace and the tail

gas stream resulting from the Claus process are shown in **Table 6-1** and **Table 6-2** respectively.

Table 6-1: Claus furnace inlet streams for carbon capture GEE IGCC

	GEE		
	DOE/NETL[8]	**BR&E ProMax**	**Honeywell UniSim R400**
Ar	0.0089	0.0060	0.0052
CH_4	0.0000	0.0000	0.0000
CO	0.0016	0.0027	0.0027
CO_2	0.2975	0.3066	0.3069
COS	0.0003	0.0003	0.0000
H_2	0.0173	0.0190	0.0189
H_2O	0.1135	0.0670	0.0670
H_2S	0.2830	0.3136	0.3138
N_2	0.0579	0.0585	0.0594
NH_3	0.0663	0.0694	0.06924
O_2	0.1536	0.1570	0.0000
F, kg/s (lb/h)	5.48 (43,513)	5.49 (43,565)	5.49 (43,660)
T, K (°F)	505 (450)	505 (450)	505 (450)
P, 10^5 Pa (psia)	2.07 (30)	2.07 (30)	2.07 (30)

[8] Inlet stream for DOE/NETL Case 2 is not directly reported but was calculated by the information given in the report

Table 6-2: Tail gas streams for carbon capture GEE IGCC

	GEE		
	DOE/NETL	**BR&E ProMax**	**Honeywell UniSim R400**
Ar	0.0182	0.0140	0.0097
CH_4	0.0577	0.0629	0.0004
CO	0.0003	0.0002	0.0000
CO_2	0.6784	0.6608	0.5787
H_2	0.0170	0.0193	0.0000
H_2O	0.0005	0.0016	0.0031
H_2S	0.0228	0.0228	0.0278
N_2	0.2051	0.2183	0.1773
NH_3	0.0000	0.0000	0.0000
F, kg/s	2.77	2.62	3.36
(lb/h)	(21,951)	(20,819)	(26,638)
T, K	308	308	308
(°F)	(95)	(95)	(95)
P, 10^5 Pa	53.50	53.50	53.50
(psia)	(776)	(776)	(776)

6.3 Combined cycle

The clean gas coming out of the AGR/CO_2 capture unit is directed to the combustor and the combustion product passes through the advanced F Class turbine to produce 464 MW of total electric energy in all IGCC cases. The oxygen required for the combustion is provided by compressed ambient air. In the carbon capture cases, there is no air integration between the air compressor and the ASU so that the typical fuel specifications and contaminant levels for normal F Class combustion turbine operation as presented in GEI-41040G (GEI-41040G 2002) are met.

The schematics of the processes for each IGCC case investigated were based on the configurations reported from DOE/NETL (NETL 2007) and are presented in **Figure 6-5** to **Figure 6-8**.

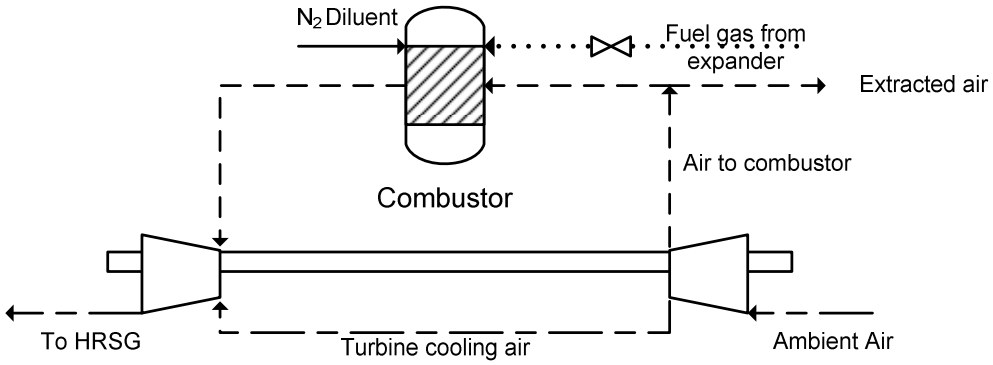

Figure 6-5: Non capture GEE IGCC power block schematic

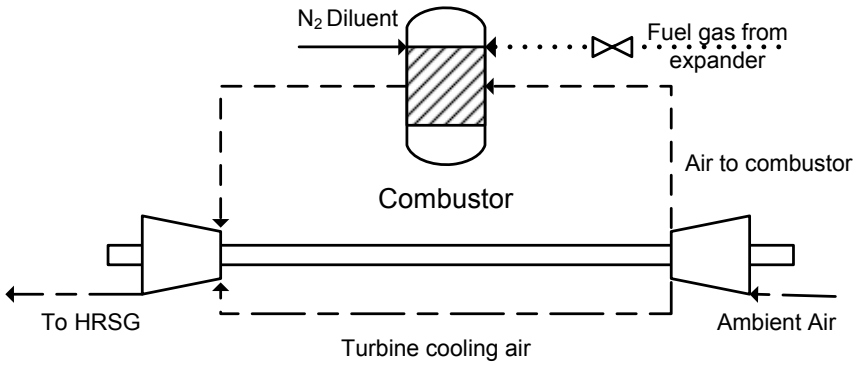

Figure 6-6: Carbon capture GEE IGCC power block schematic

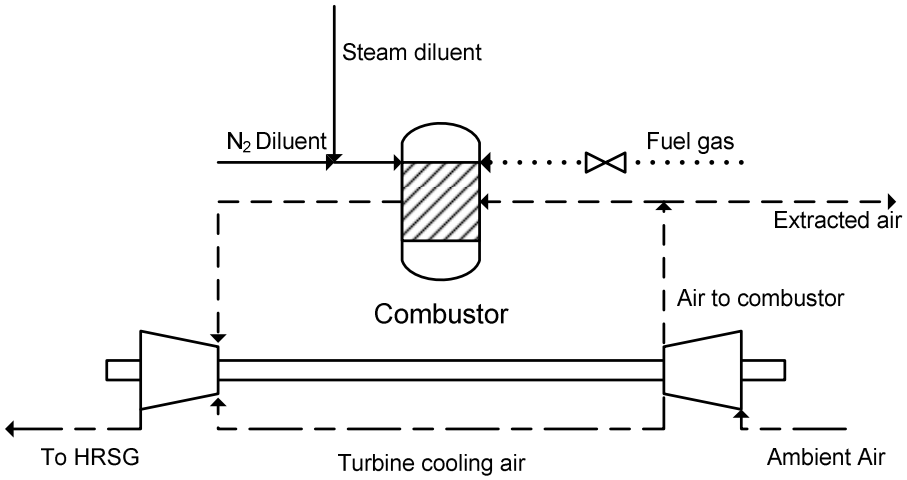

Figure 6-7: Non capture Shell IGCC power block schematic

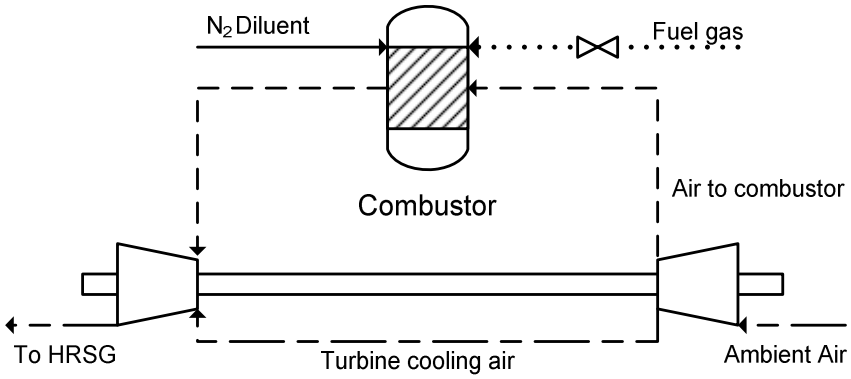

Figure 6-8: Carbon capture Shell IGCC power block schematic

It has been assumed that issues interconnected with high H_2 fuel combustion such as flame stability, flashback and NO_X formation would be overcome in the time frame needed to support deployment (NETL 2007). Certain flexibility has been therefore assumed selecting the gas turbine, allowing for incorporating more appropriate units if necessary.

A gas turbine when fired on low calorific value syngas has the potential to increase power output due to the increase in flow rate through the turbine. The higher turbine flow and moisture content of the combustion products can contribute to overheating of turbine components, affect rating criteria for the parts lives, and require a reduction in syngas firing temperatures (compared to the natural gas firing) to maintain design metal temperature (Brdar 2000).

The firing temperature in the non-capture IGCC cases is 1,616 to 1,627K (1,343-1,354°C) and in the CO_2 capture cases is 1,591 to 1,600K (1,318-1,327°C) (NETL 2007). Typical fuel specifications and contaminant levels for successful combustion turbine operation can be found elsewhere I-41040G January 2002).

The primary diluent used in the combustor is nitrogen produced in the ASU. The advantages of using nitrogen are (NETL 2007):

- Nitrogen from the ASU is already partially compressed and using it for dilution eliminates wasting the compression energy
- Limiting the water content reduces the need to de-rate firing temperature, particularly in the high-hydrogen (CO_2 capture) cases

However, there are some disadvantages when using nitrogen as the primary diluent, and these are (NETL 2007):

- There is a significant auxiliary power requirement to further compress the large nitrogen flow from the ASU pressures of 0.4 and 1.3 MPa (56 and 182 psia) to the Combustion Turbine (CT) pressure of 3.2 MPa (465 psia)
- Nitrogen is not as efficient as water in limiting NOx emissions

The combustion products are expanded in the three-stage turbine-expander. The CT exhaust temperature is nominally 872K (599°C) for non-capture cases and 839K (566°C/1,050°F) for capture cases, given the assumed ambient conditions, back-end loss, and HRSG pressure drop (NETL 2007).

6.3.1 Combustor and power generation block simulation approach

The air compressor, combustor and expander block for all IGCC cases was simulated using Honeywell UniSim design R400.

In all cases examined, the combustor was modelled as a "Gibbs reactor". With this model the phase and chemical equilibria of the outlet streams can be attained. The Gibbs reactor model does not use a specified reaction stoichiometry to compute the outlet stream composition. The product mixture composition is calculated under the condition that the Gibbs free energy of the reacting system at equilibrium is at its minimum. The simulation results were verified for all the cases examined, and are presented in **Table 6-3** to **Table 6-6**.

Table 6-3: Power block simulation data inputs and results for non-capture GEE IGCC case

	Fuel gas	**N_2 Diluent**	**Ambient Air**	**Extracted air**	**To HRSG**
Ar	0.0094	0.0023	0.0094	0.0094	0.0087
CH_4	0.0026	0.0000	0.0000	0.0000	0.0000
CO	0.3926	0.0000	0.0000	0.0000	0.0000
CO_2	0.1762	0.0000	0.0003	0.0003	0.0865
H_2	0.3823	0.0000	0.0000	0.0000	0.0669
H_2O	0.0017	0.0000	0.0104	0.0104	0.0000
N_2	0.0348	0.9924	0.7722	0.7722	0.7344
O_2	0.0004	0.0053	0.2077	0.2077	0.1035
F, kg/s	118.57	130.46	883.07	36.04	1,096.05
(lb/h)	(941,044)	(1,035,410)	(7,008,680)	(286,060)	(8,699,036)
T, K	453	469	288	706	875
(°F)	(355)	(385)	(59)	(811)	(1,115)
P,10^5Pa	31.72	31.72	1.01	16.20	31.72
(psia)	(460)	(460)	(14.7)	(235)	(460)

Table 6-4: Power block simulation data inputs and results for carbon capture GEE IGCC case

	Fuel gas	**N_2 Diluent**	**Ambient Air**	**To HRSG**
Ar	0.0112	0.0024	0.0094	0.0014
CH_4	0.0022	0.0000	0.0000	0.0000
CO	0.0198	0.0000	0.0000	0.0000
CO_2	0.0447	0.0000	0.0003	0.0084
H_2	0.9087	0.0000	0.0000	0.0000
H_2O	0.0000	0.0000	0.0108	0.1138
N_2	0.0134	0.9922	0.7719	0.7682
O_2	0.0000	0.0054	0.2076	0.1082
F, kg/s	25.15	151.27	886.83	1,063.24
(lb/h)	(199,613)	(1,200,560)	(7,038,470)	(8,438,609)
T, K	470	469	288	840
(°F)	(386)	(385)	(59)	(1,052)
P,10^5Pa	31.72	31.72	1.01	1.05
(psia)	(460)	(460)	(14.7)	(15.2)

Table 6-5: Power block simulation data inputs and results for non-capture Shell IGCC case

	Fuel gas	**N_2 Diluent**	**Steam Diluent**	**Ambient Air**	**Extracted Air**	**To HRSG**
Ar	0.0087	0.0024	0.0000	0.0094	0.0094	0.0079
CH_4	0.0003	0.0000	0.0000	0.0000	0.0000	0.0000
CO	0.5084	0.0000	0.0000	0.0000	0.0000	0.0000
CO_2	0.0005	0.0004	0.0000	0.0003	0.0003	0.0706
COS	0.0000	0.0000	0.0000	0.0000	0.0000	0.0000
H_2	0.2576	0.0000	0.0000	0.0000	0.0000	0.0000
H_2O	0.1754	0.0000	1.0000	0.0108	0.0108	0.2658
H_2S	0.0000	0.0000	0.0000	0.0000	0.0000	0.0000
N_2	0.0491	0.9918	0.0000	0.7719	0.7719	0.5599
NH_3	0.0000	0.0000	0.0000	0.0000	0.0000	0.0000
O_2	0.0000	0.0054	0.0000	0.2076	0.2076	0.0958
SO_2	0.0000	0.0000	0.0000	0.0000	0.0000	0.0000
F, kg/s	110.75	137.53	8.32	903.87	60.75	1,099.72
(lb/h)	(879,013)	(1,091,540)	(66,022)	(7,173,720)	(482,146)	(8,728,107)
T, K	469	469	519	288	706	869
(°F)	(385)	(385)	(475)	(59)	(811)	(1,105)
P, 10^5Pa	31.72	31.72	31.72	1.01	16.20	1.05
(psia)	(460)	(460)	(460)	(14.7)	(235)	(15.2)

Table 6-6: Power block simulation data inputs and results for carbon capture Shell IGCC case

	Fuel gas	**N_2 Diluent**	**Ambient Air**	**To HRSG**
Ar	0.0061	0.0024	0.0094	0.0091
CH_4	0.0002	0.0000	0.0000	0.0000
CO	0.0126	0.0000	0.0000	0.0000
CO_2	0.0101	0.0000	0.0003	0.0063
COS	0.0000	0.0000	0.0000	0.0000
H_2	0.4284	0.0000	0.0000	0.0000
H_2O	0.0176	0.0004	0.0108	0.1263
H_2S	0.0000	0.0000	0.0000	0.0000
N_2	0.5222	0.9918	0.7719	0.7509
NH_3	0.0000	0.0000	0.0000	0.0000
O_2	0.0028	0.0054	0.2076	0.1074
SO_2	0.0000	0.0000	0.0000	0.0000
F, kg/s	173.51	143.72	889.83	1,063.34
(lb/h)	(1,377,115)	(1,140,640)	(7,062,330)	(8,439,412)
T, K	469	469	288	839
(°F)	(385)	(385)	(59)	(1,051)
P, 10^5Pa	31.03	31.72	1.01	1.05
(psia)	(450)	(460)	(14.7)	(15.2)

In the non-capture IGCC cases, the air compressor allows for extraction of cooling air for which no information is available in the report regarding the flow ratio, conditions

etc. Although the turbine cooling air is a crucial issue and has been investigated in detail elsewhere (Kim 2009), in this study, the flow ratio was determined to match the combustor outlet temperature, as reported from DOE/NETL report.

In the DOE/NETL report it is clearly mentioned that the inlet air is compressed to a pressure ratio of approximately 16:1, which corresponds to a discharge pressure of approximately 1.63 MPa (235 psia).

Since the DOE/NETL report uses different reference conditions (32.02 °F and 0.089 psia) from the simulator it is not reasonable to compare the simulation results with the ones presented in terms of LHV of the combustion product. The combustor outlet product temperature is, however affected by the selection of the compressor/turbine efficiencies (i.e. compressor discharge and turbine inlet temperature) and with the conditions presented in the report, the combustor outlet temperature predicted from the simulation is lower than the ones to be met (1,616-1,628K for non-capture and 1,591 to 1,600K for CO_2 capture IGCC cases). It is therefore very probable that DOE/NETL report has overestimated the nitrogen required for dilution in the combustor, and subsequently the overall electrical output. The combustor simulations however, can predict the combustion product stream accurately in terms of flows and component mole fractions. For all cases investigated it was assumed a GT electrical output of 464 $MW_{e.}$

6.3.2 Steam and feed water

Heat Recovery Steam Generator (HRSG)

The heat recovery steam generator (HRSG) is a horizontal gas flow, drum-type, multi-pressure design that is matched to the characteristics of the gas turbine exhaust gas (NETL 2007). The flue gas exiting the combustor, after passing through the gas turbine is directed to the HRSG to recover the large quantity of thermal energy that it contains. The flue gas passes through the HRSG and exits at approximately 405K (132°C) for all IGCC cases. The schematics of this part of the IGCC power plant are presented in **Figure 6-9** to **Figure 6-12**.

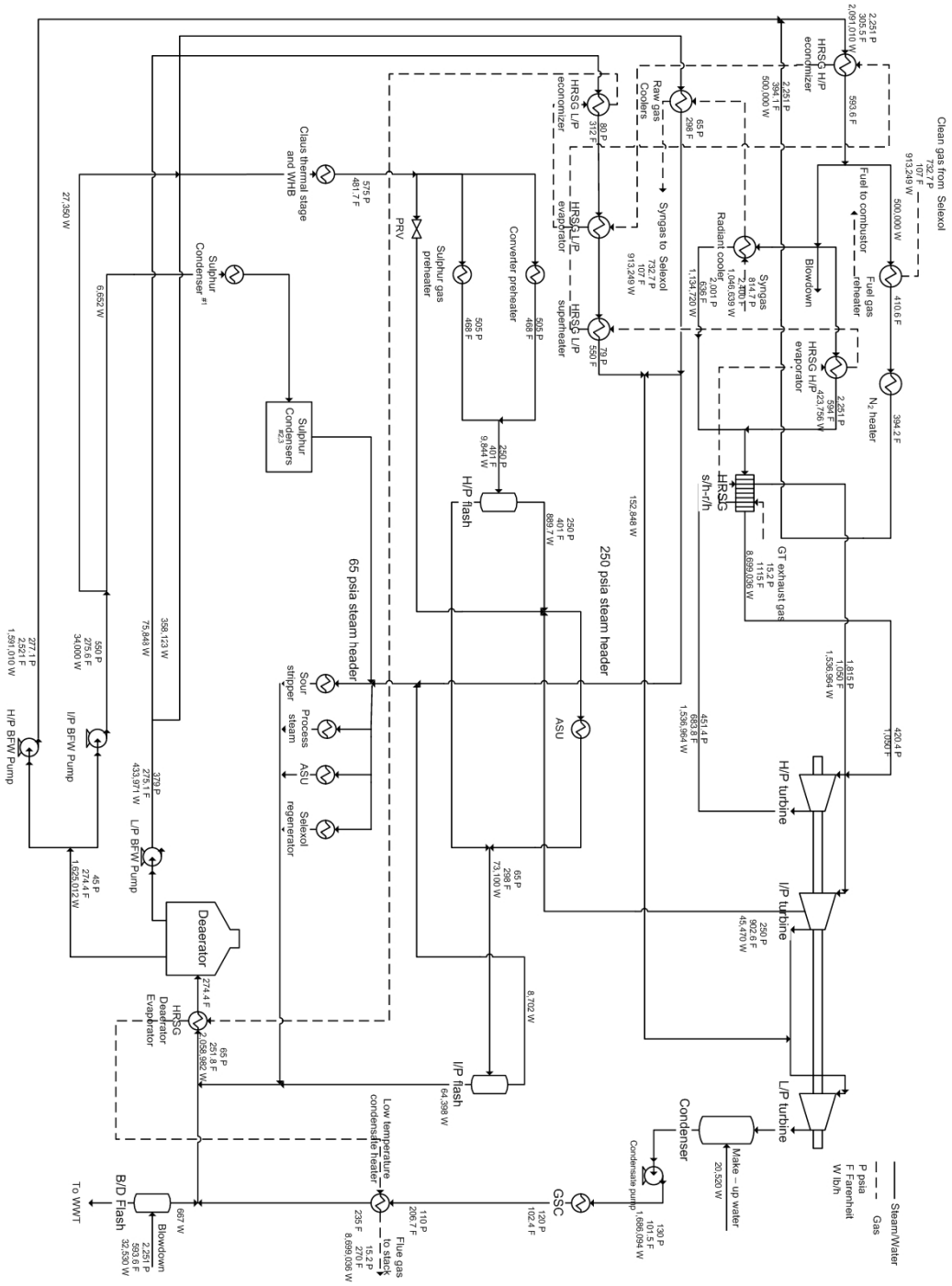

Figure 6-9: Non capture GEE IGCC steam and feedwater schematic

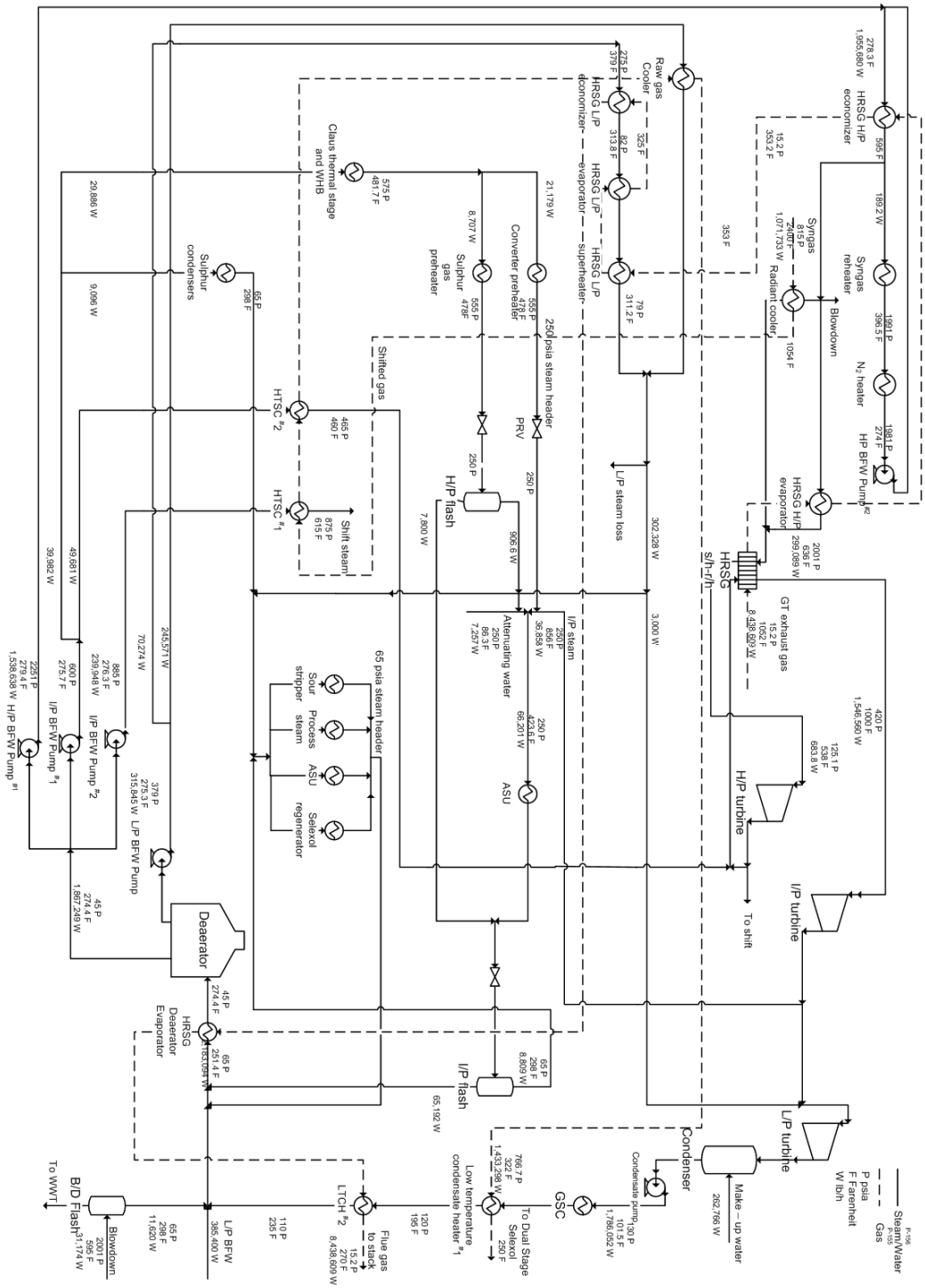

Figure 6-10: Carbon capture GEE IGCC steam and feedwater schematic

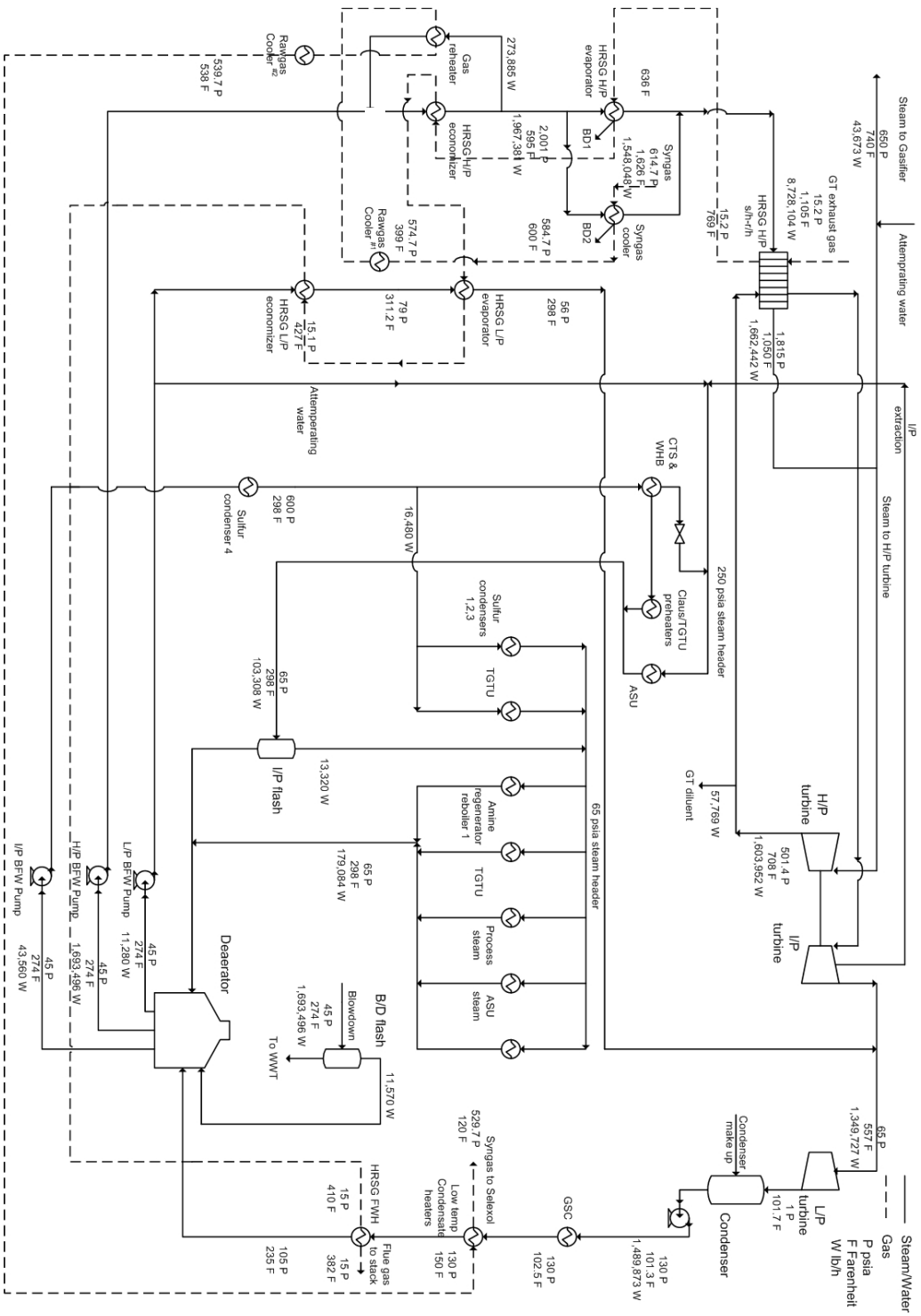

Figure 6-11: Non capture Shell IGCC steam and feedwater schematic

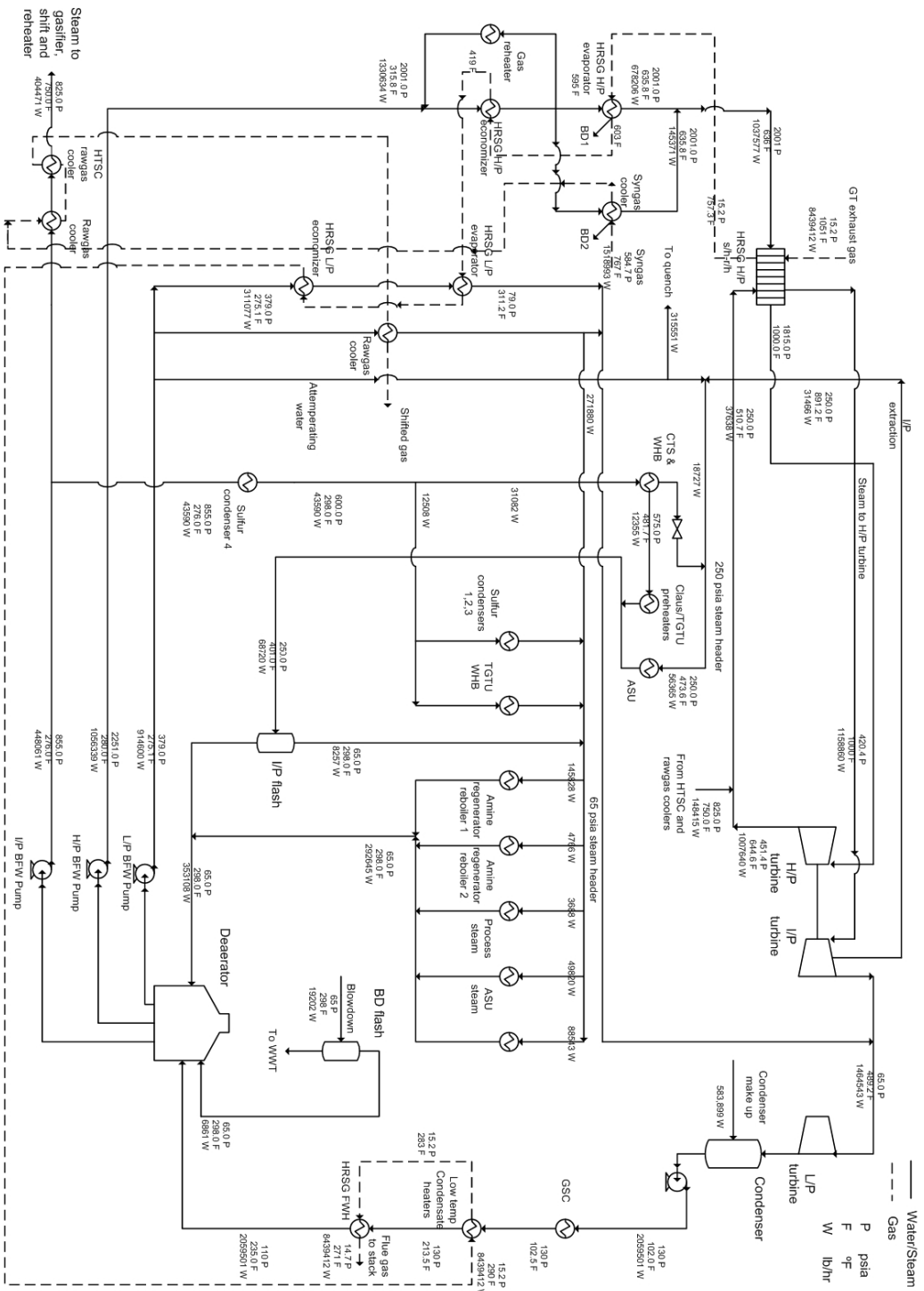

Figure 6-12: Carbon capture Shell IGCC steam and feedwater schematic

In addition to generating and superheating steam, the HRSG provides the heat duties for the cold/hot reheat steams for the steam turbine, condensate and feedwater heating and de-aeration of the condensate. Natural circulation of steam is accomplished in the HRSG by utilising differences in densities due to temperature differences of the steam. The natural circulation HRSG provides the most cost-effective and reliable design (NETL 2007).

Particular research effort has been devoted to the HRSG section of the IGCC power plants, as there is a significant potential of increasing its efficiency and as a consequence improving the overall performance of the power plant. Ganapathy has reported several aspects interconnected with HRSG operation (Ganapathy 1996; Ganapathy 1997). Franco and Casarosa (2002) examined different HRSG configurations such as parallel sections and limit subcritical conditions to achieve the goal of improved performance. Franco and Russo (2002) examined the effect of HRSG operating parameters such as temperature, pressure, mass flowrate and exchanger efficiencies in its performance and they conducted a thermodynamic and thermoeconomic optimisation procedure to achieve higher combined cycle efficiencies. Najafi performed a multi-objective optimisation of the HRSG to obtain optimum design parameters, such as pinch point and geometric variables, which yield the maximum efficiency and the minimum capital cost (Najafi 2009). Behbahani-nia et al. (2010) reported the optimisation of the design variables (pinch point and gas side velocity) and also applied thermodynamic and thermoeconomic optimisation to conclude to optimal values for the HRSG operation.

Steam Turbine

The steam turbine consists of a high pressure (HP) section, an intermediate pressure (IP) section, and a low pressure (LP) section, all connected to the generator by a common shaft. Steam from the HRSG is combined with steam from the gasifier island and enters the turbine at either 12.4 MPa/839K (566°C) for the non-carbon capture cases, or 12.4 MPa/811K (538°C) for the carbon capture cases. The T-S diagram for

the non-capture and carbon capture IGCC, as resulting from the GEE IGCC process simulations is shown in **Figure 6-13**.

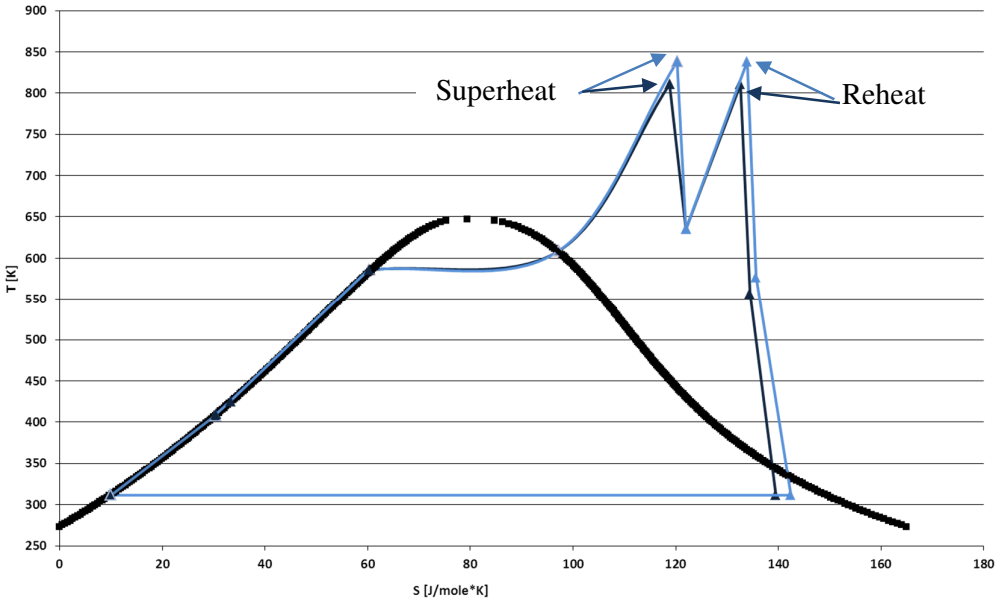

Figure 6-13: T-S diagram of IGCC steam cycle in non-capture (light blue path) and carbon capture (dark blue path)

The steam initially enters the turbine near the middle of the high-pressure span, flows through the turbine, and returns to the HRSG for reheating. The reheat steam enters the IP section at 2.6 to 2.9 MPa/839K (566°C) for the non-carbon capture cases or 2.6 to 2.9 MPa/811K (538°C) for the carbon capture cases. After passing through the IP section, the steam is transported to the LP section. The steam is then directed into the condenser and finally the condensate is sent to the deaerator. Feedwater from the deaerator is pumped to the various feedwater streams from in the HRSG. Feed pumps are provided for each of three pressure levels, HP, IP, and LP.

Main and Reheat Steam Systems

The function of the main steam system is to convey main steam generated in the synthesis gas cooler (SGC) and the HRSG to the HP turbine. The function of the reheat

system is to convey steam from the HP turbine exhaust to the HRSG reheater, and to the turbine reheat stop valves.

Main steam at approximately 12.4 MPa/839K (566°C) (non-carbon capture cases) or 12.4 MPa/811K (538°C) (carbon capture cases) exits the HRSG superheater and is routed to the HP turbine. Cold reheat steam at approximately 3.1 to 3.4 MPa/614K (341°C) exits the HP turbine and flows to the HRSG reheater. Hot reheat steam at approximately 2.9 to 3.2 MPa/839K (566°C) for non-carbon capture cases and 2.9 MPa/811K (538°C) for carbon capture cases exits the HRSG reheater and is routed to the IP turbines.

Circulating Water System

The circulating water system is a closed-cycle cooling water system that supplies cooling water to the condenser to condense the main turbine exhaust steam. The system also supplies cooling water to the AGR plant as required, and to the auxiliary cooling system. The auxiliary cooling system is a closed-loop process that utilizes a higher quality water to remove heat from compressor intercoolers, oil coolers and other ancillary equipment and transfers that heat to the main circulating cooling water system in plate and frame heat exchangers. The heat transferred to the circulating water in the condenser and other applications is removed by a mechanical draft cooling tower.

Raw Water and Cycle Makeup Water Systems

The raw water system supplies cooling tower makeup, cycle makeup, service water and potable water requirements. The water source was assumed to be groundwater (NETL 2007).

The makeup water system provides high quality demineralized water for makeup to the HRSG cycle and for steam injection ahead of the water gas shift reactors in CO_2 capture cases.

The simulation of the HRSG, steam and feedwater systems is part of the overall process flow diagram performed in Honeywell UniSim design R400, based on the data reported on the DOE/NETL report (NETL 2007) and briefly mentioned above. The schematics of this part of the IGCC power plant are presented in **Figure 6-9** to **Figure 6-12**. The Peng-Robinson equation of state was used for the flue gas properties and the ASME steam package, for the water properties calculation. Several assumptions and operating conditions had to be unveiled when information required to represent the full operation of the systems was not available from the report. In fact, neither the DOE report nor other published studies have presented in such detail the combined cycle as in this study.

The validation of the simulation results was examined for all the IGCC cases investigated. The simulation is capable of replicating the gas path of the combined cycle as presented in DOE/NETL report. The steam path results were compared with the reported data and the stream properties of the condenser outlet are presented in **Table 6-7** and **Table 6-8**.

Table 6-7: Condenser outlet streams validation for non-capture and carbon capture GEE IGCCs

	DOE		**Simulation**	
	Non capture	**Carbon capture**	**Non capture**	**Carbon capture**
Mole fraction H_2O	1.0	1.0	1.0	1.0
F, kg/s (lb/h)	213.13 (1,691,578)	224.92 (1,785,113)	213.07 (1,691,094)	225.04 (1,786,053)
T, K (°F)	312 (101.3)	312 (101.3)	312 (101.3)	312 (101.3)
P, 10^5 Pa (psia)	0.07 (1.0)	0.07 (1.0)	0.07 (1.0)	0.07 (1.0)

Table 6-8: Condenser outlet streams validation for non-capture and carbon capture Shell IGCCs

	DOE		Simulation	
	Non capture	Carbon capture	Non capture	Carbon capture
Mole fraction H_2O	1.0	1.0	1.0	1.0
F, kg/s	213.13	224.92	213.07	225.04
(lb/h)	(1,519,727)	(2,059,501)	(1,519,873)	(2,059,206)
T, K	312	312	312	312
(°F)	(101.1)	(101.1)	(101.1)	(101.1)
P, 10^5 Pa	0.07	0.07	0.07	0.07
(psia)	(1.0)	(1.0)	(1.0)	(1.0)

6.4 Summary and Conclusions

The simulation approach adopted to represent unit operations downstream carbon capture processes for GEE and Shell IGCC power plants have been presented in this Chapter. The methodology followed to represent the sulphur recovery plant and combined cycle within the IGCC power plants was introduced in detail. For all the sections, the simulation results have been validated by comparison with data presented in DOE NETL study (2007).

The Claus process simulation for sulphur recovery within non-capture and carbon capture for the GEE and Shell IGCC power plants was conducted using both Honeywell UniSim R400 and BR&E ProMax and their performance was presented. ProMax results proved to be in better agreement with DOE NETL presented data.

The air compressor, combustor and expander block for all IGCC cases was simulated using Honeywell UniSim design R400. The schematics of the processes for each IGCC case investigated were based on the configurations reported from DOE/NETL (NETL

2007). It was found that while is very probable that DOE/NETL report has overestimated the nitrogen required for dilution in the combustor, and subsequently the overall electrical output, further examination of this section by simulations with specific softwares for power blocks, is essential to validate this observation. The combustor simulations developed in UniSim however, can predict the combustion product stream accurately in terms of flows and component mole fractions.

Finally, the simulation of the HRSG, steam and feedwater systems as part of the overall process flow diagram performed in Honeywell UniSim design R400, based on the data reported on the DOE/NETL report (NETL 2007) The Peng-Robinson equation of state was used for the flue gas properties and the ASME steam package, for the water properties calculation. Contrary to DOE NETL report detailed combined cycle process configurations have been presented in this study.

Chapter 7 IGCC major modification for carbon capture and energy penalty

7.1 Introduction

Plants that have an initial design which takes into consideration the implementation of a CO_2 capture process can be defined to be "capture ready". The concept of capture-ready is not a specific plant design. On the contrary, when referring to a capture ready there is a combination of design parameters and decisions that should be taken during the design and construction of the plant. The definition of "capture ready" plants has been reported as follows (Bohn 2007):

"A plant can be considered "capture ready" if, at some point in the future, it can be retrofitted for carbon capture and sequestration and still be economical to operate."

The value and importance of capture ready power plant designs is recognised not only within the scientific community and the stakeholders but was also recognized by the members of the G8 nations back in 2005. In their plan of action, released at the conclusion of the conference, the members identified that the ''acceleration of the development and commercialization of carbon capture and storage technology should be pursued by 'investigating the definition, costs and scope for 'capture ready' plants and the consideration of economic incentives'' (G8 2005).

It is obvious that capture ready plants are a priority due to the long lifetime of power plants, along with the fact that plants that are not designed to be capture-ready could prove to be prohibitively expensive to retrofit in the future, resulting in either delayed reductions in CO_2 emissions, or stranded generation assets (Bohn 2007).

Some of the issues that are specific to IGCC plants withCO_2 capture include:

- The water-gas shift reaction of the syngas and CO_2 removal reduces the heating value of the syngas by approximately 15%, which would cause a derating of the combustion turbine.

- The convective and radiative gas coolers may no longer be required, as a water quench system can cool the syngas and generate the steam for the water-gas shift reaction.
- The acid gas removal system would require an additional unit to remove CO_2 in addition to H_2S. The methyldiethanolamine (MDEA) system (if present) may need to be removed and replaced with two-stage Selexol-type acid gas removal system.
- In order to operate on hydrogen gas, the turbine combustors may need replacement and the turbine blades may require modification.
- Compressed air for the air separation unit may no longer be available from the turbine, necessitating the addition of a parallel air compressor.
- Re-arrangement of existing equipment may be required to accommodate the addition of the water-gas shift reactors, a second acid gas removal unit and CO_2 compression and drying equipment.

In this Chapter, notable differences and additional components between non-capture and carbon capture IGCC power plants are presented and discussed. IGCC power plants will inevitably be subject to an energy penalty, i.e. a drop in the overall plant efficiency when in carbon mode. This energy penalty related to carbon capture mode is also presented.

7.2 Elevated Pressure Air Separation Unit (EP ASU)

The process configuration used to simulate the EP ASU is the same for all IGCC cases investigated. For the non-capture cases, air is extracted from the Gas Turbine (GT) compressor and is fed to the EP ASU together with ambient air. In carbon capture IGCCs, however, since the GT electrical output is assumed to be constant for all cases, it is required to make use of all the available combustion air without extracting it for the EP ASU.

Many studies have reported the challenges interconnected with air integration and investigated the optimal conditions for integrating the gas turbine air compressor and the ASU of IGCC power plants (Chan, Hyung-Taek et al. 1997; Geosits 2005). Jiang

et al. (2002), have pointed out that integration can be a key parameter in order to increase the efficiency of an IGCC plant (Jiang, Lin et al. 2002)(Jiang, Lin et al. 2002)(Jiang, Lin et al. 2002)(Jiang, Lin et al. 2002)(Jiang, Lin et al. 2002). Air integration can be beneficial as less ambient air would be required for the ASU Main Air Compressor (MAC). It is therefore expected that for non-capture IGCCs the ASU MAC energy consumption will be significantly lower compared to the carbon capture IGCCs.

7.3 Gasifier section in carbon capture IGCC

In carbon capture mode it can be expected that additional fuel would be fed to the gasifier of the IGCC power plant, in order to operate the same gas turbine. **Table 7-1** reports the coal feed in GEE and Shell gasifiers for carbon capture modes. The fuel increment is required because the heating value of the fuel gas will be reduced due to the exothermic shift reaction so more coal should be fed to the gasifier to compensate the heat loss. However, the increments of fuel in the different cases of gasification systems are also different. As seen in **Figure 7-1** and **Figure 7-2**, since the syngas generated from the Shell gasifiers contain less CO_2 and more CO than those from GEE gasifiers, the absolute amount of CO to be converted to CO_2 in shift reactors of the Shell IGCC case must be greater, given the overall CO conversion rate of 95.7% which is assumed to be the same for both gasifiers. Therefore, more fuel should be added to the coal feed and the difference of heat input between the two cases is almost equivalent to the difference of heat generated in the shift reaction (|41.1| kJ/mol). In addition, the different H_2 and CO recovery in the AGR units between the non-capture and capture cases would also affect the coal input increment.

In terms of configuration, the GEE gasifier is not subject to any conceptual changes when operated for carbon capture mode as can be seen from **Figure 7-3** and **Figure 7-4**. Both non capture and carbon capture modes flow diagrams are provided to facilitate direct comparisons.

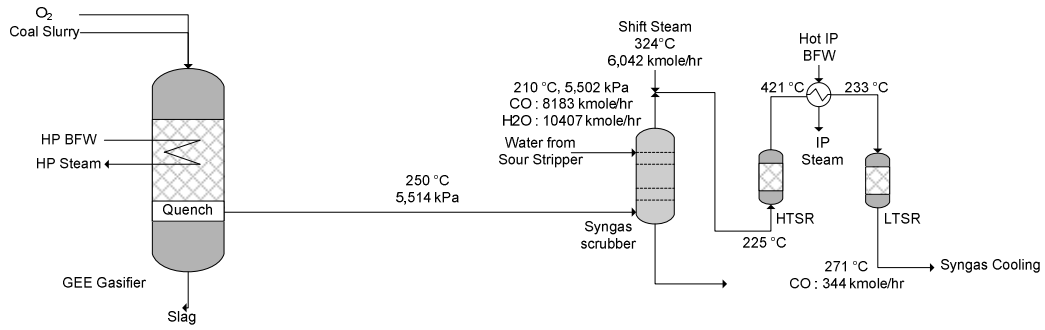

Figure 7-1: GEE Gasifier, syngas scrubber and WGS reactors for carbon capture mode (Kapetaki et al. 2013)

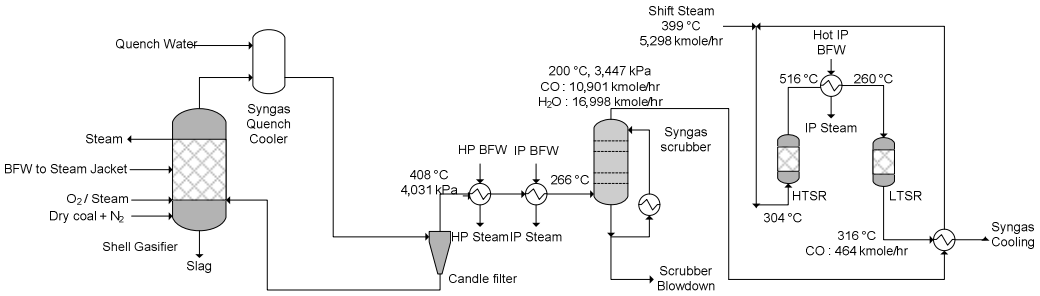

Figure 7-2: Shell Gasifier, syngas scrubber and WGS reactors for carbon capture mode (Kapetaki et al. 2013)

Table 7-1: Coal feed in GEE and Shell gasifiers for carbon capture modes

	GEE	**Shell**
H_2O	261,198	21,935
C	318,990	301,650
H	22,561	21,293
N	7,872	5,914
Cl	1,468	1,372
S	12,559	11,877
Ash	46,642	45,898
O	34,645	32,555
Mass density, kg/m^3	8.615	6.058
Total solids, kg/s (lb/h)	56.04 (444,737)	52.99 (420,559)
Thermal input, kW_t HHV	1,710,780	1,617,772
Oxygen feed, kg/s (lb/h)	52.77 (418,847)	46.12 (366,070)

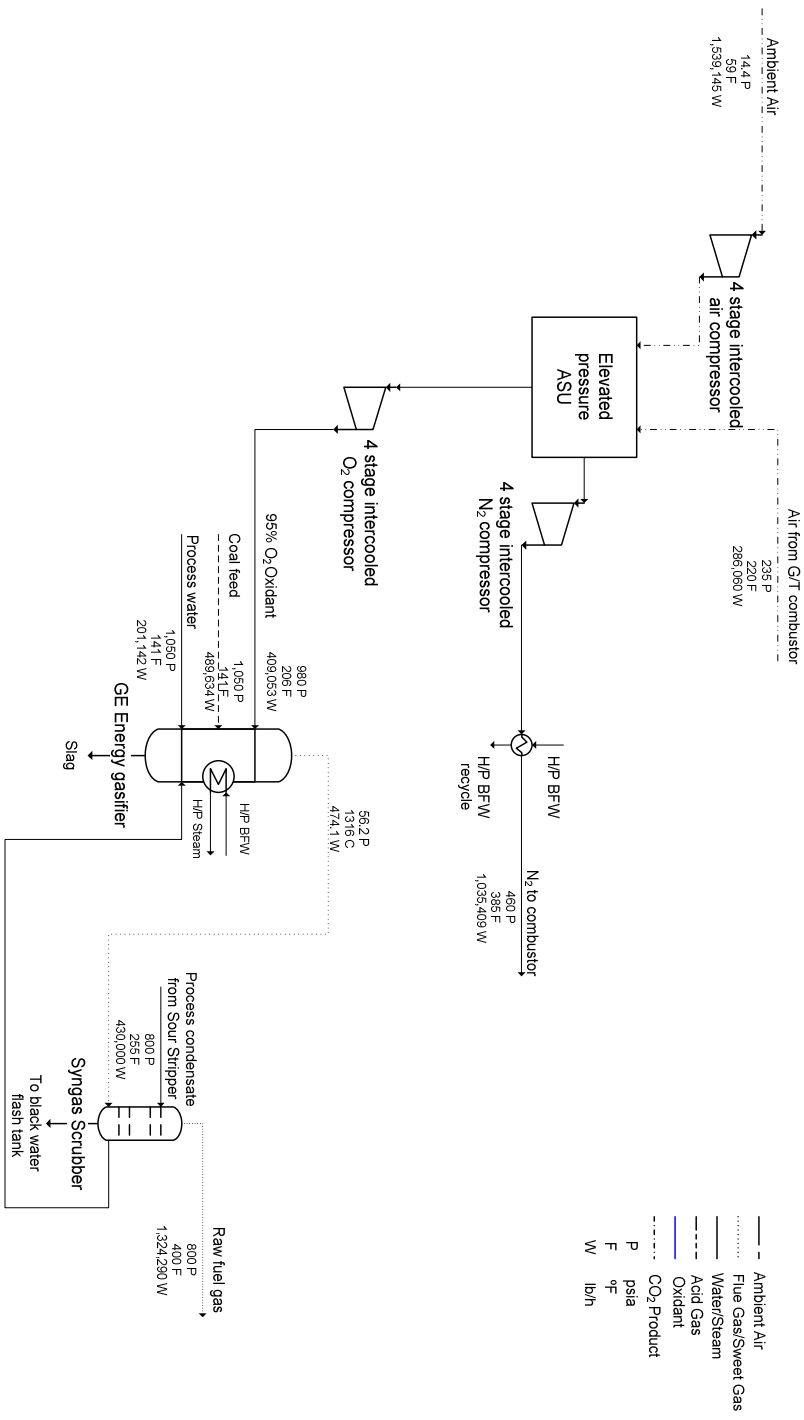

Figure 7-3: Coal Gasification and Air Separation Units (ASU) for non-capture GEE IGCC

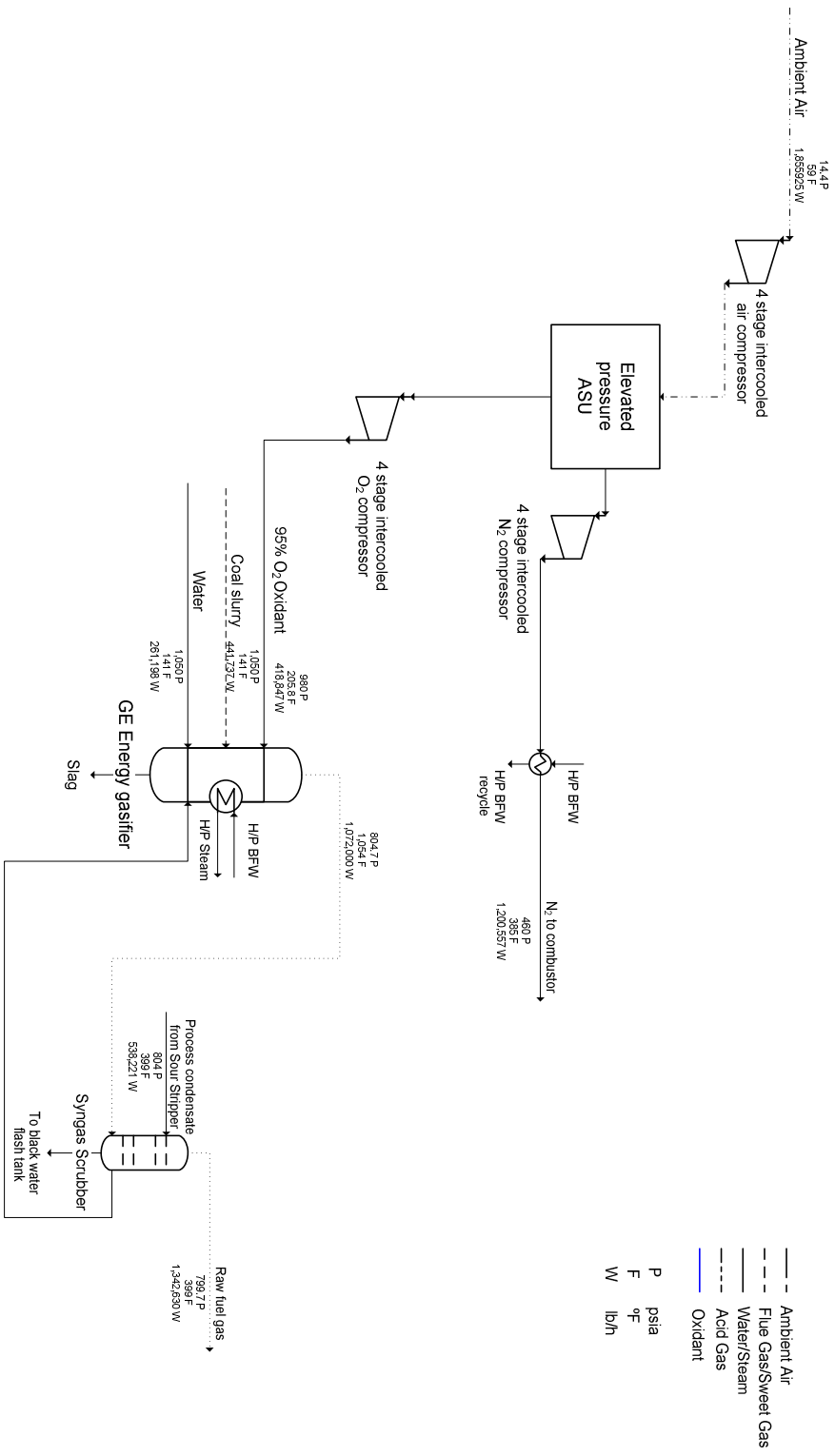

Figure 7-4: Coal Gasification and Air Separation Units (ASU) for carbon capture GEE IGCC

On the other hand, modifications are essential for the carbon capture Shell IGCC (**Figure 7-5** and **Figure 7-6**). One obvious change in the Shell IGCC with carbon capture is the requirement to cool down the raw syngas, making use of quench water instead of using the syngas recycle in the non-capture Shell IGCC. In the non-capture Shell IGCC, the syngas recycle reduces the syngas temperature to 1,158K (885 °C), which facilitates the operation of the syngas cooler at a lower temperature. In the carbon capture Shell IGCC, however, the syngas is cooled by water quench, which sacrifices most HP steam generation but enriches the syngas with water for subsequent shift reaction. This change is beneficial in that the amount of shift steam injection can be drastically reduced to a level similar to the steam usage in the GEE IGCC. The amount of water quench and its temperature are determined so that the syngas at the syngas scrubber outlet is saturated with water. It should be noted that the water molar flowrate carried by the syngas flowing to shift reactors is significantly higher in the Shell IGCC, since the total pressure of syngas is very different[9].

[9] Shell and GEE gasifier operating pressures are 4,171 kPa and 5,515 kPa, respectively.

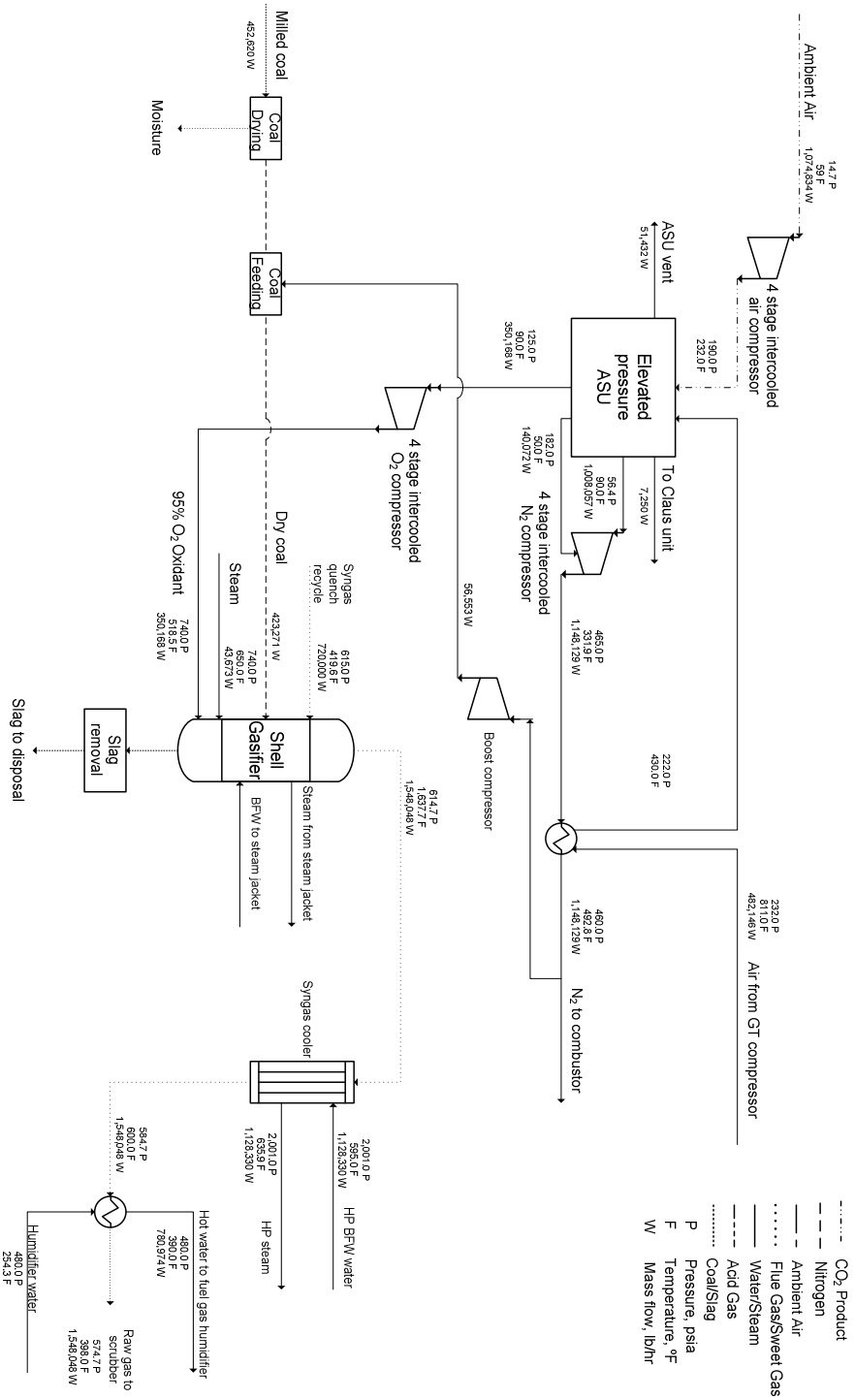

Figure 7-5: Coal Gasification and Air Separation Units (ASU) for non-capture Shell IGCC

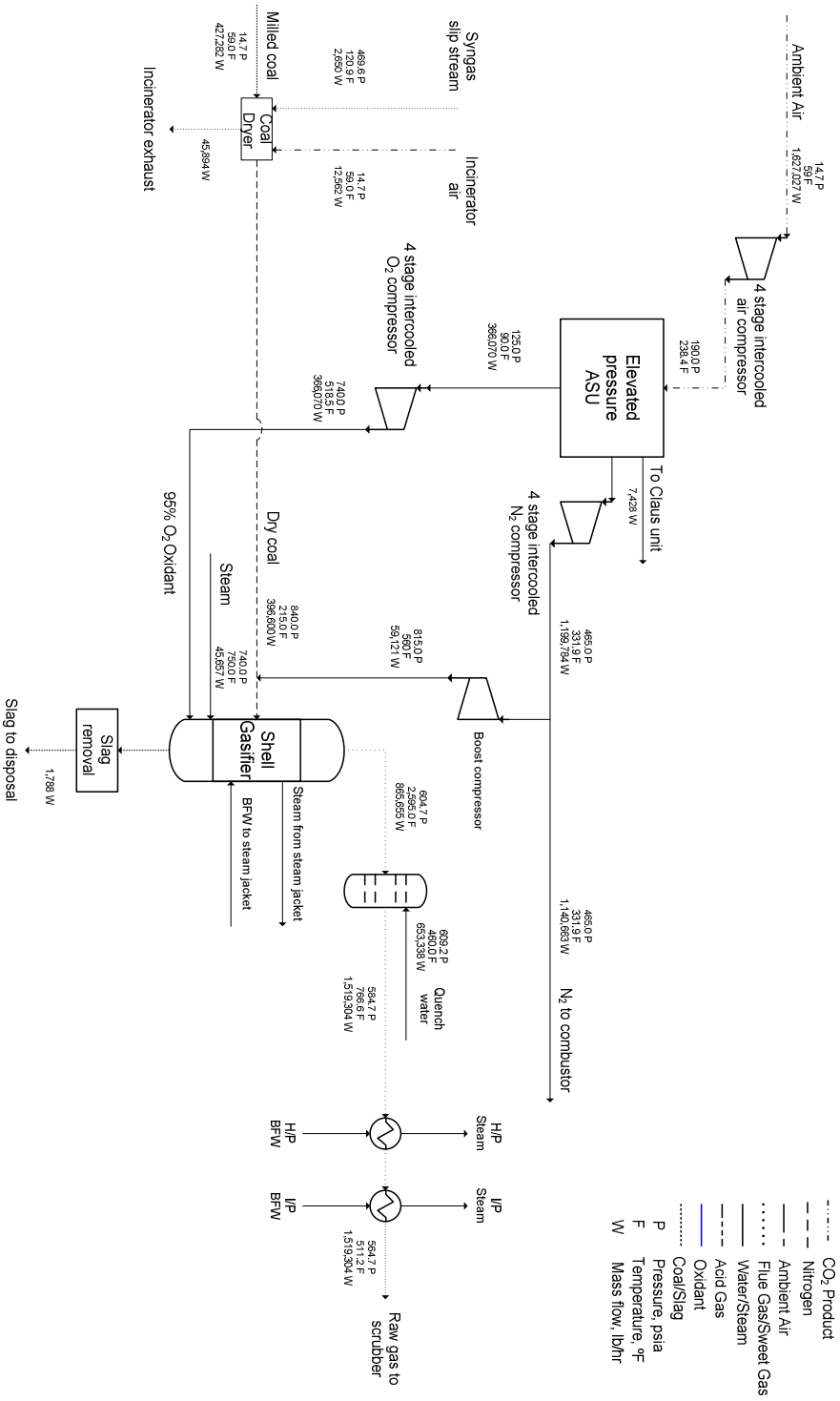

Figure 7-6: Coal Gasification and Air Separation Units (ASU) for carbon capture Shell IGCC

7.4 Water gas shift reactors (WGSRs)

While in the conventional IGCC power plants without CO_2 capture WGSRs are not required, this is not the case when the IGCC power plants operate in a carbon capture mode. The objective is to convert the CO of the syngas to H_2 and CO_2 by reacting it with water over a bed of catalyst, as described with equation 7-1.

$$CO + H_2O \leftrightarrow CO_2 + H_2 \qquad (7\text{-}1)$$

$$\Delta H_{298K} = -41.1 \frac{kJ}{mole}$$

Several types of shift catalysts are commercially available and widely applied in practice, the three most important being (Twigg 1996):

• High-temperature shift catalyst

Active component: Fe_3O_4 with Cr_2O_3 as stabiliser

Operating conditions: 350 – 500 ºC; sulphur content syngas < 100 ppm

• Low-temperature shift catalysts

Active component: Cu supported by ZnO and Al_2O_3

Operating conditions: 185 – 275 ºC; sulphur content syngas < 0.1 ppm

• Sour shift catalysts

Active component: Sulphided Co and Mo (CoMoS)

Operating conditions: 250 – 500 ºC; sulphur content syngas > 300 ppm

The molar ratio of H_2O to CO was set approximately 2 to 1 (NETL 2007). This adjustment is achieved by utilising IP steam extracted from the steam cycle of the power plant.

The position in which the WGSRs are located within the power plant is an important parameter. In the case that the WGSRs are located before the H_2S removal unit then the shift reaction is considered as a "sour shift". When the WGSRs are placed immediately downstream the H_2S removal unit, the shift reaction is called "sweet". Each mode has advantages and disadvantages and the selection of the mode is also dependent on the catalyst used in terms of poisoning occurring by the presence of sulphur components in the WGSRs feed stream. At the moment, there are two main classes of materials being used in industry as CO-shift catalysts: Fe-based and Cu-based. However, further developments of the catalysts are introduced and materials such as Co, Au and Pt can be also used, along with Pd-based membrane reactors (Mendes et al. 2010).

In sweet shift, where the AGR unit is located before the WGSRs, the gas stream has to be cooled down to the operating temperature of the AGR unit. Most water contained in the syngas is condensed out of the syngas at the stage of the AGR unit usually operating at very low close to ambient temperature, indicating that further amounts of steam will be required to meet the desired H_2O:CO molar ratio for the water gas shift reaction. The excessive steam requirement makes the sweet shift unfavourable for the IGCC with carbon capture. Therefore, sour shift was considered as more reasonable choice for the WGSRs to be adopted herein. It should be noted that in this study the coal feed (Illinois No.6) contains high sulphur content. Sulphur content might however have a significant effect on the choice of sour versus sweet shift. This aspect should therefore examined in detail in the perspective of coal use other than Illinois No.6.

For the WGS reaction, there is a high steam demand to favour the reaction towards its products. Therefore, WGSRs contribute significantly to the overall energy penalty as the steam required is extracted from the steam cycle, resulting in a lower steam turbine electrical output compared to those in the conventional IGCC power plant. Many studies have investigated WGS Membrane Reactors (WGS-MR) for IGCC power plants. Lima et al. (2012) published a study incorporating a WGS-MR with a H_2 selective molecular sieve. Higher conversions, compact modules, and absence of solvent disposal requirement, compared to conventional processes, are reported as the

advantages of this approach. Schiebahn et al. (2012) examined a WGS-MR concept for IGCC power plants focusing on the energy penalty caused by the WGSR unit demand in steam. They have reported an increased CO conversion compared to the WGSRs previously reported for IGCC and also a decrease in the power plant's energy penalty when the WGS-MR is used in the IGCC power plant. Basile (2008) has also revised several studies published about WGS-MR in several applications concluding that the rationalization of industrial production obtained using the MRs technologies permits low environmental impacts, low energy consumption as well as higher quality final products. In this work, however, a two-stage catalytic WGSRs process has been adopted.

The CO-shift sections consist of two fixed bed reactors arranged in series: High Temperature Shift Reactor (HTSR) and Low Temperature Shift Reactor (LTSR). It should be noted that the same overall CO conversion rate was assumed in both cases (95.7%) even though the syngas composition is very different. For example, the syngas at the Shell gasifier contains a lower H_2/CO ratio and a lower CO_2 content than at the corresponding values in the GEE gasifier. However, this is a reasonable assumption since, in the Shell gasifier, the lower H_2 to CO ratio and lower CO_2 mole fractions which favour CO conversion are offset by the higher operating temperature that is unfavourable for the exothermic reaction. In the simulations, equilibrium reactors were used in UniSim Design R400, to allow for the simulator to calculate the conversion rates at the given conditions. The conversion rates obtained were 80% and 79% for the HTSR and LTSR, respectively, which correspond to 95.7% overall conversion.

The HTSR product is cooled before entering the LTSR to recover the exothermic heat by generating steam. For both the GEE and Shell IGCCs, the heat exchanger is located after the HTSR to produce Intermediate Pressure (IP) steam from the Boiler Feed Water (BFW). The IP steam is subsequently injected into the syngas for the shift reaction. The final product passes through a series of coolers where water is knocked out and is sent to the AGR/Selexol unit.

7.5 Acid Gas Removal (AGR) and CO_2 capture unit

In 2000 there were over thirty AGR processes in commercial use throughout the oil, chemical and natural gas industries. In 2002 SFA Pacific produced a report in which 42 operating and planned gasifiers are presented (Korens 2002). The most commonly used method for AGR is physical absorption where acid gases in the gas stream are selectively removed by the solvent in the absorbing column.

For the conventional non-capture IGCC power plants, a single-stage Selexol unit was used herein for the H_2S removal. A dual-stage Selexol unit has been modelled for H_2S and CO_2 co-removal in carbon capture IGCC cases. In the conventional scheme, the syngas exiting the H_2S absorber is routed to another absorber for CO_2 removal. While the rich solvent leaving the H_2S column is sent to steam stripper for its regeneration, the solvent leaving the CO_2 absorber is sent to several flash drum stages to recover CO_2 from the solvent at higher pressures than ambient pressure. The clean syngas leaving the CO_2 absorber is sent to either a humidifier in the Shell IGCC or a fuel gas reheater in the GEE IGCC. The recovered H_2S-rich acid gas is sent to the Claus process to produce sulphur from H_2S. The CO_2 product is finally sent to the compression train where it is pressured up to a pressure suitable for CO_2 transport and its subsequent CO_2 storage. This section of the integrated power plant it is discussed further in detail in Chapter 5.

7.6 CO_2 compression

The CO_2–laden solvent leaving the CO_2 absorber is depressurised in stages at three flash drums in series operating at three pressure levels. Since the CO_2-laden solvent contains a significant amount of hydrogen as well as CO_2, the vapour stream at the first High Pressure (HP) flash drum is recycled to the CO_2 absorber to minimise the H_2 losses to the CO_2 product pipeline. The HP CO_2 stream is flashed at 1.2 MPa (174 psia), compressed, and recycled back to the CO_2 absorber. The MP CO_2 stream is flashed at 0.35 MPa (50 psia). The LP CO_2 stream is flashed at 0.12 MPa (18 psia), compressed to 0.35 MPa (50 psia), and combined with the MP CO_2 stream. The combined stream is compressed from 0.35 MPa (50 psia) to a supercritical condition

at 15.0 MPa (2,180 psia) using a multiple-stage, intercooled compressor. The pressures reported above where selected to achieve 90% carbon capture, >99 H_2S removal and >99% hydrogen recovery, but no optimisation was conducted. During compression, the CO_2 stream is cooled to 298K (25 ºC). The final CO_2 product when compressed reaches over 99% CO_2 purity. The simplified schematic of the CO_2 compression process is shown in **Figure 7-7**.

It should be highlighted that in IGCC power plants with pre combustion CO_2 capture, the CO_2 resulting after absorption product is in pressures higher than the corresponding stream with post combustion. Therefore, the energy requirement to compress the CO_2 product adequately for storage or EOR is lower, compared to the corresponding requirement for CO_2 compression in post combustion cases. This difference can be as high as more than 50% in favour of IGCC power plants when compared with PC Rankine plants, according to estimations that can be conducted from reported data (NETL 2007). This gives a clear advantage of this configuration over post combustion and is further discussed in Chapter 6.

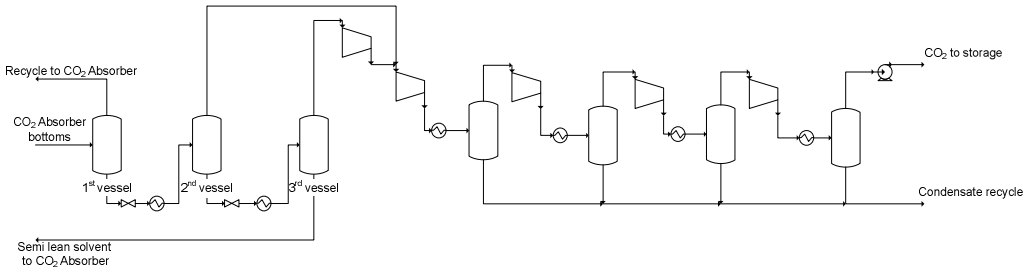

Figure 7-7: CO_2 compression simplified schematic

7.7 HRSG, steam turbine and power block

In the combined cycle a heat recovery steam generator extracts heat from the combustion turbine exhaust to power a steam turbine. However, the carbon capture cases consume more extraction steam than the non-capture cases, thus reducing the steam turbine output.

One obvious change in the steam and feed water schematic between the non-capture and capture cases is the embodiment of heat exchangers producing the steam required in the shift reactors and providing partly the required cooling to the syngas before entering the AGR/carbon capture unit. Particularly, in the Shell IGCC with carbon capture the required cooling down of the raw syngas is provided by quench water instead of syngas recycle as in the non-capture case. Therefore, in the carbon capture Shell IGCC, most of the HP steam generation occurring in the syngas cooler is sacrificed. This change is not required in the GEE IGCC.

For the High Pressure (HP), Intermediate Pressure (IP) and Low Pressure (LP) the enthalpy difference between the outlet and inlet of the turbine section was used to estimate the electrical output utilising enthalpy values as given in the reference report. The electrical outputs calculated for the HP, IP and LP sections of the turbine are demonstrated in **Table 7-2**.

Table 7-2: HP, IP and LP electrical outputs of IGCC steam turbine

	GEE IGCC non-capture	GEE IGCC carbon capture	Shell IGCC non-capture	Shell IGCC carbon capture
HP	71,780	56,070	69,950	44,530
IP	101,271	97,384	104,960	73,529
LP	121,700	121,236	105,600	111,400
Total loss, kW_e		20,061		51,051

In the power block, the fuel gas coming out of the syngas expander is directed to the combustor and the combustion product passes through the two advanced F Class turbines to produce 464 MW of total electric energy in all IGCC cases. The oxygen required for the combustion is provided by compressed ambient air. In the carbon

capture cases, there is no air integration between the air compressor and the ASU so that the typical fuel specifications and contaminant levels for normal F Class combustion turbine operation as presented in GEI-41040G (GEI-41040G January 2002) are met.

The firing temperature is subjected to a decrease from 1,616-1,647K (1,343-1,354°C /2,450-2,470°F) in the non-capture IGCC cases, to 1,591-1,620K (1,318-1,327°C /2,405-2,420°F) in the CO_2 capture cases (NETL 2007). This reduction is done to maintain parts life as the water content of the combustion products increases from 8-10 volume percent (vol%) in the non-capture cases to 14-16 vol% in the capture cases. This firing temperature decrease is also the reason for the lower temperature steam cycle in the carbon capture cases.

7.8 Energy penalty related to carbon capture

IGCC power plants will inevitably be subject to a drop in the overall plant efficiency when in carbon capture mode. This drop in the overall plant efficiency is often reported as the energy penalty interconnected with CCS. For some types of facilities, like IGCC plants, the addition of CO_2 capture technology changes both the net plant output and the fuel input. Thus, a more general definition of the energy penalty is based on the change in net plant heat rate or efficiency (η) as given by the following equation:

$$EP = 1 - (\eta_{ccs} / \eta_{ref}) \quad (7\text{-}2)$$

where EP is the energy penalty (fractional reduction in output), and η_{ccs} and η_{ref} refer to the net efficiencies of the plant in carbon capture mode and reference plant, respectively (Rubin et al. 2005).

In non-capture Shell IGCC, the syngas temperature is allowed to decrease below the COS hydrolysis temperature as long as the water content is more than what is required in the reaction. But, in carbon capture Shell IGCC, the syngas temperature should be kept higher than 200 °C until it enters the shift reactor since the amount of water quench was determined as the amount of water needed to saturate the syngas with water at this temperature.

The quench water should be heated to achieve the correct water content but maintain the syngas temperature at a sufficiently high temperature. Part of the quench water should be heated by the hot flue gas in the HRSG. This process change is not needed in the GEE IGCC since the raw syngas is already saturated with water by the water quench taking place inside the gasifier. This leads to a reduced drop in power generation in the steam cycle for GEE IGCC cases. **Table 7-3** shows the preliminary results of this work (Kapetaki, et al. 2013), and demonstrate efficiency drops which are 0.5 to 0.8% larger than those reported by the DOE (NETL 2007).

Table 7-3: Comparison of DOE NETL (NETL 2007) data and simulation

Plant Performance (MW_e)	GEE IGCC non-capture		GEE IGCC with capture		Shell IGCC non-capture		Shell IGCC with capture	
	NETL	This work	NETL	This work	NETL	This work	NETL	This work
Power summary								
Gas turbine power	464.3	464.0	464.0	464.0	464.0	464.0	463.6	464.0
Steam turbine power	298.9	299.0	274.7	274.7	284.0	284.0	230.0	230.0
Syngas Expander	7.1	7.3	6.3	6.3	–	–	–	–
Total power generation	770.4	770.3	745.0	745.0	748.0	748.0	693.6	694.0
Total Auxiliaries	130.1	130.8	189.3	197.7	112.2	111.4	176.4	189.2
Net Power	640.3	639.5	545.9	547.4	635.9	636.6	517.1	504,.8
Net power plant efficiency (HHV), %	38.2	38.2	32.5	32.0	41.1	41.1	32.0	31.2

In the DOE report, it was assumed that 100% H_2 can be recovered at the dual-stage Selexol unit, but it is more likely that a small amount of H_2 would be lost in both the steam stripper sour gas and the CO_2 product. In this study, the H_2 solubility in the Selexol solvent was taken into account and the dual-stage Selexol processes were designed such that they can recover 99.4% H_2 from the AGR feed H_2. At the same time, the operating conditions have been selected to meet 99.5% H_2S removal, 90%

overall carbon capture and around 10ppm sulphur in CO_2 product. The overall net plant efficiency is reduced mainly because of the higher power consumption in the AGR unit predicted in this study.

The energy penalty relating to carbon capture in both gasifier cases is summarised in **Table 7-4** while all the auxiliaries consumption occurring in each case is presented in **Table 7-5**.

Table 7-4: Energy penalty in simulation cases

Source of energy penalty	GEE IGCC		Shell IGCC	
	Energy change	Energy penalty	Energy change	Energy penalty
Heat input increase, kW_{th}	36,736	-	70,279	-
Gas turbine, kW_e	0	0.60 %	0	1.30 %
Sweet Gas Expander, kW_e	–943	0.06 %	-	-
Steam Turbine, kW_e	–24,276	1.80 %	–54,046	4.14 %
Gross Power Generation, kW_e	–25,219	2.46 %	–54,046	5.44 %
Auxiliary Total, kW_e	66,898	3.74 %	77,783	4.50 %
Total , kW_e	–92,117	6.20 %	–131,829	9.94 %

The Shell IGCC would experience higher energy penalty than the GEE IGCC since more fuel should be fed to the gasifier to overcome the loss of the heat flow in the shift reaction. Also the higher loss of power generation at the steam turbine can be explained by the use of water quench instead of syngas recycle in cooling down the syngas temperature and the greater steam consumption at WGSR.

Table 7-5: Auxiliaries consumption comparison between non-capture and carbon capture IGCCs (DOE 2007)

	GEE IGCC without capture	GEE IGCC with capture	Shell IGCC without capture	Shell IGCC with capture
Coal Handling	450	460	430	440
Coal Milling	2,280	2,330	2,110	2,210
Coal Slurry Pumps	740	760	–	–
Slag Handling (and Dewatering)	1,170	1,200	540	570
Air Separation Unit Auxiliaries	1,000	1,000	1,000	1,000
Air Separation Unit Main Air Compressor	60,070	72,480	41,630	62,970
Oxygen Compressor	11,270	11,520	10,080	10,540
Nitrogen Compressor	30,560	35,870	37,010	38,670

Table 7-5 (Continued): Auxiliaries consumption comparison between non-capture and carbon capture IGCCs

	GEE IGCC without capture	GEE IGCC with capture	Shell IGCC without capture	Shell IGCC with capture
Syngas Recycle Compressor	–	–	1,650	0
Incinerator Air Blower	–	–	160	160
Claus Plant Tail Gas Recycle Compressor	1,230	990	–	–
CO_2 Compressor	–	27,400	–	28,050
Boiler Feedwater Pumps	4,590	4,580	4,670	3,290
Condensate Pump	250	265	230	310
Flash Bottom Pump	200	200	200	200
Circulating Water Pumps	3,710	3,580	3,150	3,440
Cooling Tower Fans	1,910	1,850	1,630	1,780
Scrubber Pumps	300	420	120	390

Table 7-5 (Continued): Auxiliaries consumption comparison between non-capture and carbon capture IGCCs

	GEE IGCC without capture	GEE IGCC with capture	Shell IGCC without capture	Shell IGCC with capture
Selexol/ Sulfinol Unit Auxiliaries	3,420	17,320	660	15,500
Gas Turbine Auxiliaries	1,000	1,000	1,000	1,000
Steam Turbine Auxiliaries	100	100	100	100
Claus Plant Auxiliaries	200	200	250	250
Miscellaneous Balance of Plant	3,000	3,000	3,000	3,000
Transformer Loss	2,650	2,760	2,550	2,550
Total, kW_e	130,100	189,285	112,170	176,420

7.9 Summary and conclusions

When it comes to IGCC power plants with CO_2 capture, parts of the conventional non-capture plant are inevitably affected. Modifications of the conventional plant in terms

of configuration are strongly dependent on the type of the gasifier incorporated in the power plant. When the IGCC power plant operates with a GEE gasifier, there are no conceptual process unit modifications necessary to apply apart from the obvious difference in scale and stream flowrates associated with the energy penalty of carbon capture. However, this is not the case for the Shell gasifier case. Essential alterations for the Shell IGCC to operate in carbon capture mode with the most obvious one being the addition of quench.

In both gasification options, for a carbon capture IGCC, it is expected that there will be increments in the fuel that are fed to the gasifiers to operate the same gas turbine. The extent of this increment depends on the type of the gasifier, with Shell IGCC requiring higher amounts of fuels on the carbon capture case.

It was found that the energy penalty varies over different gasification technologies, being almost 6 % for GEE IGCC and reaching approximately 10 % for the Shell IGCC cases. This still confirms though the lower energy penalty of IGCC power plants as par PC Rankine cycle plants which demonstrate an energy penalty of nearly 12%.

Water gas shift reactors are another essential addition to the IGCC power plant when it is to be operated in carbon capture mode. In order to promote the conversion of CO to CO_2, IP steam extracted from the steam cycle has to be added. The conversion occurring is around 95.7 % for both gasification options.

For the conventional non-capture IGCC power plants, a single-stage Selexol unit can be used for the H_2S removal. In carbon capture IGCC cases, however, the state of the art process is the dual-stage Selexol configuration as the objective is not only to remove H_2S, but also to capture CO_2. The CO_2 compression train downstream of the CO_2 capture process is another additional component to the carbon capture IGCCs where the CO_2 product is compressed up to a pressure suitable for CO_2 transport and storage.

One obvious, yet significant change in the carbon capture IGCC cases, regarding the EP ASU, is the fact that there is no potential for air integration between the GT compressor and the EP ASU.

In summary, the discussed modifications necessary for the carbon capture operation of the IGCC power plant are interlinked with an effect on the performance of the plant and an energy penalty which is interpreted as the loss in the plant's efficiency. For the GEE IGCC most of the energy penalty occurring arises from the increase in auxiliaries (3.74%) for carbon capture operation, notably occurring by the CO_2 compressor energy demand. The same applies to Shell IGCC, where moreover energy penalty occurs in the steam turbine due to the addition of quench (4.14%).

Chapter 8 Conclusions and directions for future work

The research project presented in this thesis focuses on the development of robust simulation tools that can represent realistically and accurately the operation and performance of IGCC power plants through detailed process flow diagrams. Despite the fact that IGCC is a well-established industrial process for power generation, there is significant potential in improving its performance. Benchmarking of the conventional cases has been achieved giving the opportunity to investigate areas that could improve further the IGCC power plants performance and establish the full details of the main assumptions needed to establish an integrated process flow sheet. It became rapidly obvious that a realistic and reliable representation of the IGCC operation is neither trivial nor simple to accomplish. This is due to the challenges posed by the complexity of the plant itself. More than three hundred unit operations are involved in the complete and continuous process flow diagrams developed, depending on the case examined. The examination of the overall performance of the plant, rather than focusing only on specific parts like most approaches in the literature, was very challenging.

The automated tools developed are therefore beneficial for the deployment of the technology by evaluating different engineering options with respect to the plant's performance. IGCC power plant operation and performance has received significant research interest, but no previous studies have presented detailed continuous designs for IGCC power plants with carbon capture targets as high as 90%, as in the work presented in this thesis.

Fully functional process flow diagrams have been developed to describe the overall operation and performance of the IGCC power plants for GEE and Shell gasification technologies.

EP ASU

For IGCC power plants the elevated pressure ASU process was selected as it minimizes power consumption and decreases the size of some of the equipment, therefore being advantageous towards the traditional schemes. Air integration was considered for the non-carbon capture cases only. EP ASU was simulated using Honeywell UniSim Design R400. It was found that the DOE/NETL report (2007) failed to represent in detail the ASU process flow diagram. Contrary to the reference report, detailed process configurations were presented herein. Inconsistencies where discovered in terms of overall mass balances around the EP ASU unit. The oxygen balance for example is negative in both non capture and carbon capture GEE cases. In both Shell cases, there is negative balance for argon.

The simulation cases developed for the EP ASU and the configurations suggested are a conservative yet realistic representation of the actual operation. Oxygen and nitrogen are produced in sufficient amounts to accommodate the requirements of the gasifier for oxygen for both GEE and Shell gasification technologies, and the combustor injection with nitrogen.

Gasifier

Particular simulation effort has been made to develop the process flow diagrams of the different IGCC power plant cases of interest. The effect of different gasification options for IGCC power plant has been discussed in Chapter 7. Four simulation cases for GEE IGCC and Shell IGCC without and with carbon capture have been constructed based on data reported in the literature. It should be highlighted that discrepancies have been found within the reference report in the non-carbon capture GEE and Shell IGCCs for the composition of the gasification product stream in nitrogen and oxygen. Particularly for nitrogen, the discrepancy is nearly 13% between the simulation result and the reference for the GEE IGCC. The same applies to non-capture Shell IGCC, even if to a lesser extent. Particularly for nitrogen, the discrepancy is nearly 2% between the simulation result and the reference. Moreover, results in the reference report present remaining oxygen in the gasification product of the non-capture GEE

IGCC case (0.3%). It is therefore probable that there are inaccuracies in the estimations of the reaction stoichiometry in this gasifier. No discrepancies have been found regarding oxygen in Shell cases.

Syngas cooling and knock out

Particular effort has been devoted to examine the syngas cooling and clean up section in detail. Two simulators have been used to represent this section of the IGCC plant. The results produced from the two simulators were compared against the data reported in the literature (NETL 2007). The ability to opt for electrolytic environments as reported in the literature for this part of the IGCC plant by default provides a more fundamental approach increasing confidence in the results obtained by ProMax.

For the sour water stripper section, electrolytic activity coefficient model has been used for the liquid phase physical property calculation with an equation of state for the vapour phase. The model developed can provide an accurate prediction of the VLE for both H_2S and NH_3 in water, along with robust estimations of water/steam requirements throughout the process.

Carbon capture processes

For IGCC power plants, the state-of-the-art is the use of physical solvents for carbon capture. There are advantages and disadvantages interconnected with the use of each, as discussed in Chapter 4. The use of Selexol was found to be the one demonstrating better results both in terms of removal rate and energy requirements.

- For the two stage Selexol process, two different configurations were tested and compared in terms of acid gas and CO2 capture removal as well as the energy required in each scheme to achieve the purity and recovery targets set.

- While both configurations can achieve 90% carbon capture, they demonstrate significant differences in energy requirements. It was found that the first scheme presented (integrated scheme) is less energy demanding than the second scheme investigated (non-integrated) being therefore advantageous.

- The integrated dual-stage Selexol unit can achieve carbon capture rates as high as 95%, without having to modify the process configuration. This is particularly important especially keeping in mind the ambitious targets that many countries have already set to reduce GHG emissions. It should be however noted that moving to stricter carbon capture rate it is expected the auxiliaries' consumption will increase significantly.

The absorption regime occurring with DEPG solvent in the Selexol process was successfully modelled by calibrating existing models in UniSim against literature data. This was used to describe the behaviour of the acid/shifted syngas in the solvent in order to assess correctly the process configurations. It is however recommended that more detailed investigation of hydrogen solubility in Selexol is conducted, especially with reference to the new configurations proposed in this study aimed at achieving higher carbon capture rates. Moreover, it would be useful to carry out a comparison of the different configurations with more advanced VLE models (i.e. SAFT), continuing work as referenced in Chapter 4 (Field and Brasington 2011; Mansouri Majoumerd et al. 2012; and Nannan et al. 2013).

CO_2 capture schemes using DEPG in a Selexol process have been examined in detail for IGCC power plants and were presented. In all the schemes examined, DEPG solvent in a two stage Selexol process has been implemented, to achieve the acid gas removal in the first stage and the CO_2 capture in the second stage. For the two stage Selexol process, two different configurations were tested and compared in terms of acid gas and CO_2 capture removal as well as the energy required in each scheme to achieve the purity and recovery targets set. While both configurations can achieve the purity recovery targets set, they demonstrate significant differences in energy requirements. It was found that the first scheme presented (integrated scheme) is less energy demanding being therefore advantageous.

The integrated two-stage Selexol unit can moreover achieve carbon capture rates as high as 95%, without having to modify the process configuration. This is particularly important especially keeping in mind the ambitious targets that many countries have

already set to reduce GHG emissions. Moreover, in the United Nations Conference of Parties in 2015, countries are expected to agree on emission reduction targets. 95% carbon capture rate might be the only way of effective action to achieve environmental targets, given the time that has been wasted in addressing climate change but essentially continuing with near to "business as usual" so far. It should be however noted that moving to stricter carbon capture rate it is expected that the auxiliaries' consumption will increase significantly. The simulation tools developed in this thesis can be used to guide the selection of reasonable cut-off in terms of maximum recovery with acceptable energy penalties.

Finally, dynamic models of the entire system and its sub-systems are significant tools for process and control design. As a result of the development of dynamic models, a realistic representation of the actual plant operation can be achieved. Simulations of the dynamic operation of the process can be used to test the effect of different process configurations and compare equipment options. Dynamic simulations are also indispensable to test different control strategies and for tuning of control parameters, but were beyond the scope of the current study.

Alternative processes for carbon capture

The viability of hybrid systems for IGCC power plants with carbon capture and their competiveness with the state-of-the-art CC process for IGCC which is the dual stage Selexol unit has been presented and discussed in Chapter5. The objective of the hybrid system is not only to obtain a CO_2 pure product stream, but also to produce a hydrogen rich stream which will be directed to the combustor so that electricity is produced at the Gas Turbine. Hydrogen selective polymeric and metallic membranes are therefore selected for the membrane module of the hybrid systems. Amongst the cases investigated, the IGCC power plant with single stage Selexol and a metallic membrane module for H_2S and CO_2 capture respectively, demonstrated the best performance in terms of net power plant efficiency, in both "sweet" and "sour" AGR removal. For the hybrid cases investigated, it was found that there is a significant gain in the CO_2

compressor energy requirement, even as high as to reflect a decrease in energy demand for the CO_2 compressor of approximately 20.7 MW_e compared to the base case.

None of the studies presented in the literature examining a combination of AGR and membranes for carbon capture reported such strict targets as aiming for product stream >95% pure in CO_2 and 90 % carbon capture, while keeping H_2S removal rates as high as >99% as in this study, within an continuous and overall IGCC plant process simulation. However, some of the main assumptions such as no pressure drops and nonideal/nonisothermal behaviour have to be verified by more detailed simulations. In particular, due to the high pressures in the membrane module, nonidealities should be expected. Moreover, taking into account pressure drops along the retentate side membrane module would result in a CO_2 product of a lower pressure. Therefore, the potential gain in CO_2 compressor energy requirement would be lower than the ones estimated in this thesis. The cases investigated therefore can be considered as starting point for more detailed future analysis.

In summary:

- The viability of hybrid systems for IGCC power plants with carbon capture was examined, and confirmed.

- It was found that and their performance can not only be competitive with the state-of-the-art two stage Selexol process, but they can improve the overall performance of IGCC power plants.

- It was found that there is a significant gain in the CO_2 compressor energy requirement, achieved with the proposed configurations.

- However, some of the main assumptions such as no pressure drops and nonideal/nonisothermal behaviour have to be verified by more detailed simulations. In particular, due to the high pressures in the membrane module, nonidealities should be expected.

Claus plant for sulphur recovery

The simulation of the sulphur process was conducted for all IGCC cases. The simulation model developed can represent accurately both the process configuration and the H_2S conversion within the range of the Claus plant temperatures contrary to the reference study. Additionally, the dominance of each species in the Claus process temperature range was represented successfully in ProMax. This is particularly important given that UniSim does not allow for instant access to control the different sulphur species with the default functions.

Combined Cycle

The air compressor, combustor and expander block for all IGCC simulation cases has also been presented in Chapter6. The combustor simulations can predict the combustion product stream accurately in terms of flows and component mole fractions. However, particular effort has to be put for simulating accurately the power block. It is recommended that specific software is used to develop a simulation tool capable of representing realistically the operation of the combustor, air compressor and gas turbine block.

The simulation of the HRSG developed as presented in the final part of Chapter6, is capable of replicating the reference gas path of the combined cycle for the all the cases examined. The steam path results were also compared with the reported data. The increased feedwater requirements appearing in carbon capture cases can be justified with the inevitable increase of steam requirements in the WGSRs for these cases. Additionally, Shell cases feedwater requirement is higher than GEE, to accommodate the quench configuration.

IGCC modifications for carbon capture

CO_2 capture processes in power plants can be a viable and efficient option to overcome the challenge of capturing CO_2 and comply with the targets set to reduce the greenhouse gas emissions. For IGCC power plants with CO_2 capture processes, however, parts of the conventional, non-capture plant are affected. Chapter 7 of this

thesis identified and discussed the modifications of the conventional plant necessary for carbon capture. Especially in terms of configuration, modifications in carbon capture mode are strongly dependent on the type of the gasifier incorporated in the power plant. In both GEE and Shell gasification options, for an IGCC with integrated carbon capture, it is expected that there will be increments in the fuel feed for the gasifiers to operate the same gas turbine. The extent of this increment depends on the type of the gasifier, with Shell IGCC requiring higher amounts of fuel on the carbon capture case, when integrating a carbon capture unit.

Water gas shift reactors are an essential addition to the IGCC power plant when it is to be operated in carbon capture mode. In order to promote the conversion of CO to CO_2, steam extracted from the Intermediate Pressure section of the steam cycle has to be added. Significant work has been reported in the research community regarding the WGSRs, as by now, its effect to the overall power plant performance and its potential for improved operation has been well established. The use of membrane reactors has been reported to affect moderately the overall performance of the plant compared to catalytic WGSRs. It could therefore be beneficial to integrate these in future IGCC designs.

For the conventional non capture IGCC power plants, a single-stage Selexol unit can be used for the H_2S removal. In carbon capture IGCC cases however, the state of the art process is the two-stage Selexol configuration, as the objective is not only to remove H_2S, but also to capture CO_2.

The CO_2 compression train downstream the CO_2 capture process is another additional component to the carbon capture IGCCs' necessary to compress the CO_2 product in the conditions required for storage.

Most of the modifications necessary for the carbon capture operation of the IGCC power plant discussed in Chapter 7 are directly connected with an effect to the performance of the plant and an energy penalty which is interpreted as a loss in the plant's efficiency. The effect of the CO_2 capture process to the power plant's performance is of significant importance. It is unrealistic however, to assume that it

will be only the CO_2 capture process that will cause energy loses. The power plant operation is a continuous process all plant units are connected and will therefore be affected by the implementation of the CO_2 capture process. It was found that the discussed modifications necessary for the GEE IGCC impose an energy penalty, the majority of which arises from the increase in auxiliaries (3.74%) for carbon capture operation, notably occurring by the CO_2 compressor energy demand. The same applies to Shell IGCC, where moreover energy penalty occurs in the steam turbine due to the addition of quench (4.14%).

In overall, while there is one study reporting simulation efforts to represent the operation in various sections of a GEE IGCC power plant, no unified approach, i.e. units continuously operating within a single IGCC simulation process flow diagram, can be found in the literature. In this thesis, contrary to other studies, EP ASU, gasifiers, syngas scrubber, sour water stripper, WGSRs and syngas cooling, Selexol unit and CO_2 compression, HRSG and GT are all simulated in a unified simulation flow diagram. Moreover, no such unified approach has ever been presented respectively for a Shell IGCC power plant, as in this thesis. Particular focus has been given to syngas cooling sections and Claus units, using ProMax for simulating these sections.

The results presented in this thesis illustrate a detailed, overall investigation of IGCC power plants and it is hoped that can be a helpful tool for engineers and stakeholders in their relevant decision making process

References

Abu-Zahra, M., Abbas, Z., Singh, P., Feron, P., 2013. Carbon Dioxide Post-Combustion Capture: Solvent Technologies: Overview, Status and Future Directions. Materials and processes for energy: communicating current research and technological developments. Mendez-Vilas, A. Formatex Research Center.

Ahn, H. and S. Brandani, 2005. Dynamics of Carbon Dioxide Breakthrough in a Carbon Monolith Over a Wide Concentration Range. Adsorption 11 (1): 473-477.

Ahn, H., Luberti, M., Liu, Z., Brandani, S., 2013. Process configuration studies of the amine capture process for coal-fired power plants. International Journal of Greenhouse Gas Control 16, 29–40.

Ahn, H., Luberti, M., Zhengyi L., Brandani, S., 2013. Process Simulation of Aqueous MEA Plants for Post- combustion Capture from Coal-fired Power Plants. Energy Procedia 37(0): 1523-1531.

Ansolabehere, S., Beer, J., Deutch, J., Ellerman, AD., Friedman, S., Herzog, H. Jacoby, H., Joskow, P., McRae, G., Lester, R., Moniz, E., Steinfeld, E., 2007. The future of coal. An interdisciplinary study. See also: http://web.mit.edu/coal/ [accessed 10.09.13].

Baker, R. W., 2004. Membrane Technology and Applications, 2nd edition, John Wiley & Sons Ltd., Chichester, England.

Basile, A., 2008. Hydrogen Production Using Pd-based Membrane Reactors for Fuel Cells. Topics in Catalysis 51(1): 107-122.

Behbahani-nia, A., Sayadi, S., Soleymani, M., 2010. Thermoeconomic optimization of the pinch point and gas-side velocity in heat recovery steam generators. Proceedings of the Institution of Mechanical Engineers, Part A: Journal of Power and Energy 224(6): 761-771.

Bhattacharyya, D., R. Turton, Zitney, S., 2010. Steady-State Simulation and Optimization of an Integrated Gasification Combined Cycle Power Plant with CO_2 Capture. Industrial & Engineering Chemistry Research 50 (3): 1674-1690.

Bientinesi, M., Petarca, L., 2011. H_2 separation from gas mixtures through Palladium membranes on metallic porous supports. Chemical Engineering Transactions (24), 763 - 768.

Bocciardo, D., Ferrari, M., Brandani S., 2013. Modelling and Multi-stage Design of Membrane Processes Applied to Carbon Capture in Coal-fired Power Plants. Energy Procedia, Volume 37, Pages 932–940.

Bohm, M. C., H. J. Herzog, Parsons J. Sekar, R., 2007. Capture-ready coal plants—Options, technologies and economics. International Journal of Greenhouse Gas Control 1 (1): 113-120.

BP, 2011. Energy outlook 2030. London, BP.

Brdar, R. D., Jones, R.M., 2000. GE IGCC Technology and Experience with Advanced Gas Turbines. Schenectady, NY, GE Power Systems.

Bucklin, R. W. and R. L. Schendel, 1984. Comparison of Fluor Solvent and Selexol processes. Journal Name: Energy Prog; (United States); Journal Volume: 4:3: Medium: X; Size: Pages: 137-142.

Burgess, M. P. and R. P. Germann, 1969. Physical properties of hydrogen sulfide-water mixtures. AIChE Journal 15(2): 272-275.

Burr, B., Lyddon, L., 2008. A Comparison of Physical Solvents for Acid Gas Removal. 87th Annual GPA Convention. Grapevine, Texas.

Caravella, A., Scura, F., Barbieri, G., Drioli, E. Sieverts Law Empirical Exponent for Pd-Based Membranes: Critical Analysis in Pure H_2 Permeation. The Journal of Physical Chemistry B 114 (18): 6033-6047.

Alessio Caravella †, Francesco Scura †, Giuseppe *† and Enrico †‡

Chen, C., 2005. A Technical and Economic Assessment of CO_2 Capture Technology for IGCC Power Plants. Pittsburgh, Pennsylvania, Carnegie Mellon University. Doctor of Philosophy.

Chen, C. and E. S. Rubin, 2009. CO_2 control technology effects on IGCC plant performance and cost. Energy Policy 37(3): 915-924.

Chiesa, P. and S. Consonni, 1999. Shift reactors and physical absorption for low-CO_2 emission IGCCs. Journal of Engineering for Gas Turbines and Power-transactions of The Asme 121(2): 295-305.

Coates, J. F., 2002. Energy Needs, Choices, and Possibilities, Scenarios to 2050: The Global Business Environment, Shell International 2001, 60 pp. Technological Forecasting and Social Change 69(5): 527-531.

Collot, A. G., 2002. Matching gasifiers to coals. IEA Clean Coal Centre, IEA.

Cormos, C. C., Agachi, P.S., 2012. Integrated assessment of carbon capture and storage technologies in coal-based power generation using CAPE tools. 22 EUROPEAN SYMPOSIUM ON COMPUTER AIDED PROCESS ENGINEERING. UCL, London, ENGLAND. 30: 56-60.

Czyperek, M., Zapp, P., Bouwmeester, H., Modigell, M., Ebert, K., Voigt, I., Meulenberg, W.A., Singheiser, L., Stöver D., 2010. Gas separation membranes for

zero-emission fossil power plants: MEM-BRAIN. Journal of Membrane Science, Volume 359, Issues 1–2, 149–159.

Doctor, R. D., Molburg, J.C., Thimmapuram, P.R., 1996. KRW oxygen-blown gasification combined cycle carbon dioxide recovery, transport, and disposal. ANL/ESD-34.

Encyclopedia of Energy. Volumes 1-6, 2004.

Epps, R., Union Carbide Chemicals & Plastics Technology Corporation, 1992. Processing of Landfill Gas for Commercial Applications: the SELEXOL Solvent Process. ECO WORLD '92, Washington D. C.

EPRI, 1987. Process Screening Study of Alternative Gas Treating and Sulfur Removal Systems for IGCC Power Plant Applications. Mountain View, California, SFA Pacific, Inc.

Erickson, D. M., Day, S.A., Doyle, R., 2003. Design Considerations for Heated Gas Fuel." GE Power Systems Greenville, GEK-4189.

European CCS Demonstration Project Network Situation Report 2012. See also: http://ccsnetwork.eu/publications/situation-report-2012-public-report-outlining-progress-lessons-learnt-and-details-european-ccs [accessed 10.01.13]

European Technology Platform for Zero Emission Fossil Fuel Power Plants, 2011. The Costs of CO_2 Capture Post-demonstration CCS in the EU. Brussels, Belgium.

Ferguson, S., Skinner, G., Schieke, J., Lee, K., Van Dorst E., 2013. High Efficiency Integrated Gasification Combined Cycle with Carbon Capture via technology advancements and improved heat integration. Energy Procedia 37, 2245– 2255.

Field, R., Brasington, R., 2011. Baseline Flowsheet Model for IGCC with Carbon Capture. Ind. Eng. Chem. Res., 50 (19), pp 11306–11312.

Figueroa, J., Fout, T., Plasynski, S., McIlvried, H., Srivastava, R., 2008. Advances in CO_2 capture technology—The U.S. Department of Energy's Carbon Sequestration Program. International Journal of Greenhouse Gas Control. Volume 2, Issue 1, Pages 9–20.

Field. R. and Brasington, R., 2011. Baseline Flowsheet Model for IGCC with Carbon Capture. Ind. Eng. Chem. Res., 50 (19), pp 11306–11312.

Foster Wheeler, 2003. Potential for improvement in gasification combined cycle power generation with CO_2 capture. Report # PH4/19.

Franco, A. and C. Casarosa, 2002. On some perspectives for increasing the efficiency of combined cycle power plants. Applied Thermal Engineering 22 (13): 1501-1518.

Franco, A. and A. Russo, 2002. Combined cycle plant efficiency increase based on the optimization of the heat recovery steam generator operating parameters. International Journal of Thermal Sciences 41 (9): 843-859.

Franz, J. and V. Scherer, 2010. An evaluation of CO_2 and H_2 selective polymeric membranes for CO2 separation in IGCC processes. Journal of Membrane Science 359, 173-183.

G8, 2005. Gleneagles Plan of Action on Energy and Sustainable Development.

Ganapathy, V., 1996. Heat-Recovery Steam Generators: Understand the Basics. Chemical Engineering Progress.

Ganapathy, V., 1997. Efficiently generate steam from cogeneration plants. Chemical Engineering, 104 (5).

Gasification Technologies Council, 2008. Gasification: redefining clean energy, GTC See also: http://www.gasification.org/Docs/Final_whitepaper.pdf [accessed 18.08.13].

GEI-41040G, 2002. Process Specification for Fuel Gases for Combustion in Heavy-Duty Turbines.

Geosits, R. F., Schmoe, L.A., 2005. IGCC-The challenges of integration. GT2005-ASME Turbo Expo 2005: Power for Land, Sea and Air. Reno-Tahoe, Nevada, USA.

Gillespie, P. C., Wilding, W.V., Wilson, G.M., 1985. Vapor-Liquid Equilibrium Measurements on the Ammonia-Water System from 313K to 589K. Provo, Utah, Joint research report for GPA and AIChE-DIPPR, Wiltec Research Co.

Harvey, A., 2008. Application of Molecular Modelling to Vapour-Liquid Equilibrium of Water with Synthesis Gas. Berlin, NIST.

Haslbeck, J. L., 2002. Advanced fossil power systems comparisons study. NETL, Parsons Infrastructure & Technology Group Inc.

Haslbeck, J. L., 2002. "Evaluation of Fossil Power Plants with CO_2 Recovery." Parsons Infrastructure & Technology Group Inc.

Hendriks, C. A., K. Blok, and W.C. Turkenburg, 1989. The recovery of carbon dioxide from power plants. Symposium on Climate and Energy, Utrecht, The Netherlands.

Henni, A., P. Tontiwachwuthikul, Chakma, A., 2005. "Solubilities of Carbon Dioxide in Polyethylene Glycol Ethers." The Canadian Journal of Chemical Engineering 83(2): 358-361.

Henni, A., P. Tontiwachwuthikul, Chakma, A., 2005. Solubility of carbon dioxide, methane and ethane in fourteen promising physical solvents for gas sweetening.

Greenhouse Gas Control Technologies 7. E. S. Rubin, D. W. Keith, C. F. Gilboyet al. Oxford, Elsevier Science Ltd: 1887-1889.

Higman, C., van der Burgt, M., 2003. Gasification, Elsevier.

Hoffmann, B. S. and A. Szklo, 2011. Integrated gasification combined cycle and carbon capture: A risky option to mitigate CO_2 emissions of coal-fired power plants. Applied Energy 88 (11): 3917-3929.

Honeywell UniSim Design User Guide, 2010. Canada.

Horn, F. L. and M. Steinberg, 1982. Control of carbon dioxide emissions from a power plant (and use in enhanced oil recovery). Fuel 61 (5): 415-422.

Huang, Y., Rezvani, S., McIlveen-Wright, D., Minchener, A., Hewitt, N., 2008. Techno-economic study of CO2 capture and storage in coal fired oxygen fed entrained flow IGCC power plants. Fuel Processing Technology, 89, 916–925.

IPCC, 2005. Special report for Carbon Dioxide Capture and Storage, Summary for Policy Makers.

Jiang, L., R. Lin, Jin, H., Cai, R., Liu, Z., 2002. Study on thermodynamic characteristic and optimization of steam cycle system in IGCC. Energy Conversion and Management 43 (9–12): 1339-1348.

Jones, D., D. Bhattacharyya, Turton, R., Zitney, S., 2011. Optimal design and integration of an air separation unit (ASU) for an integrated gasification combined cycle (IGCC) power plant with CO_2 capture. Fuel Processing Technology 92 (9): 1685-1695.

Jou, F. Y., A. E. Mather, Otto, F., 1982. Solubility of hydrogen sulfide and carbon dioxide in aqueous methyldiethanolamine solutions. Industrial & Engineering Chemistry Process Design and Development 21 (4): 539-544.

Ju, J., Kocaoglu, D., 2013. Assessment on Carbon Capture Technology: A Literature Review. 2014 Proceedings of PICMET '14: Infrastructure and Service Integration.

Kakaras E., Doukelis A., Giannakopoulos D., Koumanakos A., 2006. Novel concepts for near-zero emissions IGCC power plants. Thermal Science, Volume 10, Issue 3, 81-92.

Kanniche M, Gros-Bonnivard R, Jaud P, Valle-Marcos J, Amann JM, Bouallou C., 2010. Pre-combustion, post-combustion and oxy-combustion in thermal power plant for CO_2 capture. Appl Therm Eng; 30:53–62.

Kapetaki, Z., Brandani, P. Brandani S., Ahn, H., 2013. Detailed Process Simulation of Pre-combustion IGCC Plants Using Coal-slurry and Dry Coal Gasifiers. Energy Procedia, Volume 37, 2196–2203.

Karg, J., Hannemann, F., 2004. IGCC - Fuel-Flexible Technology for the Future. Sixth European Gasification Conference. Brighton, UK.

Katzer, J. R., 2008. The future of coal-based power generation. American Institute of Chemical Engineers (AIChE). See also: http://www.aiche.org/cep [accessed 10.09.13]).

Kehlhofer, R., Hannemann, F., Stirnimann, F., Rukes, B., 2009. Combined-Cycle Gas and Steam Turbine Power Plants. 3rd Edition. Pennwell Corporation, Tulsa, Oklahoma, USA.

Kemp, I. C., 2007. Pinch Analysis and Process Integration. Amsterdam, Boston Butterworth-Heinemann.

Kim, Y. S., Lee, J.J., Cha, K.S., Kim, T.S., Sohn, J.L., Joo, Y.J., 2009. GT2009-59860 Analysis of Gas Turbine Performance in IGCC Plants Considering Compressor Operating Condition and Turbine Metal Temperature. ASME TURBO EXPO. New York, ASME

Kister, Henry Z., 1992. Distillation Design. 1st Edition edition. McGraw-hill.

Knoef, H., 2005. Biomass Gasification. Biomass Technology Group (BTG), The Netherlands.

Kohl A., L., Nielsen R., B., 1997. Gas Purification. 5th edition. Gulf Professional Publishing.

Korens, N., Simbeck, D.R., Wilhelm, D.J., 2002. Process Screening Analysis of Alternative Gas Treating and Sulfur Removal for Gasification, SFA Pacific for NETL.

Kreutz T, Martelli E, Carbo M, Consonni S, Jansen D., 2010. Shell gasifier-based coal IGCC with CO_2 capture: partial water quench vs. novel water-gas shift. In: ASME paper, GT2010-22859. ASME Turbo Expo, Glasgow, UK.

Krishnan, G., D. Steele, O'Brien, K., Callahan, R., Berchtold, K., Figueroa, J., 2009. Simulation of a Process to Capture CO_2 From IGCC Syngas Using a High Temperature PBI Membrane. Energy Procedia 1 (1): 4079-4088.

Kubek, D., 2009. CO_2 Sources & Capture Systems. EPRI/DOE/NIST, Gas processing solutions LLC.

Kumar, G. S., Viswandham, M., Gupta, A.V.S.S.K.S, Kumar, S.G., 2013. A review of pre-combustion CO_2 capture in IGCC. International Journal of Research in Engineering and Technology 2 (8): 847-853.

Lee, C. Hyung-Taek, K., Yun, Y., 1997. Optimal integration condition between the gas turbine air compressor and the air separation unit of IGCC power plant. Energy

Conversion Engineering Conference, 1997. IECEC-97., Proceedings of the 32nd Intersociety.

Leunga, D., Caramannab, G., Maroto-Valerb, M., 2014. An overview of current status of carbon dioxide capture and storage technologies**.** Renewable and Sustainable Energy Reviews. Volume 39, 426–443

Lima, F., Daoutidis, P., Tsapatsis, M., 2012. Modeling and Optimization of Membrane Reactors for Carbon Capture in Integrated Gasification Combined Cycle Units. Industrial & Engineering Chemistry Research 51 (15): 5480-5489.

Mansouri Majoumerd, M., Raas, H., De, S., Assadi, M., 2014. Estimation of performance variation of future generation IGCC with coal quality and gasification process – Simulation results of EU H2-IGCC project. Applied Energy 113, 452–462.

Maurstad, O., 2005. An Overview of Coal based Integrated Gasification Combined Cycle (IGCC) Technology. Massachussets Institute of Technology (MIT).

Maurstad, O., Herzog, H., Bolland, O., Beer, J., 2006. Impact of coal quality and gasifier technology on IGCC performance. Presented at GHGT-8, Trondheim, Norway.

Mendes, D., Chibante, V., Zheng, J., Tosti, S., Borgognoni F., Mendesa, A., Madeira, L., 2010. Enhancing the production of hydrogen via water–gas shift reaction using Pd-based membrane reactors. International Journal of Hydrogen Energy 35 (22): 12596-12608.

Merkel, T. C., M. Zhou, Baker, R., 2012. Carbon dioxide capture with membranes at an IGCC power plant. Journal of Membrane Science 389 (0): 441-450.

Minchener, A. J., 2005. Coal gasification for advanced power generation. Fuel 84 (17): 2222-2235.

Najafi, H. and B. Najafi, 2009. Multi-objective optimization of a fire-tube heat recovery steam generator system. Electrical Power & Energy Conference (EPEC), 2009 IEEE.

Nasir, P., 1990, A Mixed Solvent to Achieve Low Sulfur Content, AICHE National Meeting, San Diego, California.

Nannan, N., De Servi, C., Van der Stelt, T., Colonna, P. and Bardow, A.**,** 2013. An Equation of State Based on PC-SAFT for Physical Solvents Composed of Polyethylene Glycol Dimethylethers. Ind. Eng. Chem. Res., 52 (51), pp 18401–18412

NETL. Gasification in detail. Retrieved 08/08, 2013, from http://netldev.netl.doe.gov/research/coal/energysystems/gasification/gasifipedia/gasification-in-detail.

NETL, 2007. Cost and Performance Baseline for Fossil Energy Plants Volume 1: Bituminous Coal and Natural Gas to Electricity Rev.1. 2007/1281.

NETL, 2007. Advanced Amine Solvent Formulations and Process Integration for Near-Term CO2 Capture Success. DE-FG02-06ER84625.

Newman, S., Houston, A., 1985. Acid and sour gas treating processes: latest data and methods for designing and operating today's gas treating facilities. London, Gulf Pub. Co.

Ockwig, N., Nenoff, T., 2007. Membranes for hydrogen separation. Chem. Rev. 107 (10), pp 4078–4110.

O'Keefe, L. F., Griffiths, J., Weissman, R.C., De Puy, R.A., and Wainwright, J.M., 2002. A Single IGCC Design for Variable CO_2 Capture. Fifth European Gasification Conference.

Padurean, A., Cormos, C., Agachi, P., 2012. Pre-combustion carbon dioxide capture by gas–liquid absorption for Integrated Gasification Combined Cycle power plants. International Journal of Greenhouse Gas Control 7 (0): 1-11.

Paskall, H. G., 1979. Capability of the Modified Claus Process. Alberta, Canada, Alberta/Canada Energy Resources Research Fund.

Pérez-Fortes, M., A. D. Bojarski, Velo, E., Nougués, J., Puigjaner, L., 2009. Conceptual model and evaluation of generated power and emissions in an IGCC plant. Energy 34 (10): 1721-1732.

Perry, R.H. and Green, D.W., 1997. Perry's Chemical Engineers' Handbook.7th Edition. McGraw-hill.

Pitzer, K. S. and J. J. Kim, 1974. Thermodynamics of electrolytes. IV. Activity and osmotic coefficients for mixed electrolytes. Journal of the American Chemical Society 96 (18): 5701-5707.

Poling, B. E., Prausnitz, J.M., O'Connel, J.P., 2001. The properties of gases and liquids. New York, Chicago, San Francisco, Lisbon, London, Madrid, Mexico City, Milan, New Delhi, San Juan, Seoul, Singapore, Sydney, Toronto, McGraw-Hill.

Puigjaner, L., 2011. Syngas from Waste: Emerging Technologies, Springer.

Reinelt, P. S., Keith, D.W., 2007. Carbon Capture Retrofits and the Cost of Regulatory Uncertainty. The Energy Journal 28 (4): 101-128.

Rigdon, R., Schmoe, L., 2005. The IGCC Reference Plant. Gasification Technologies Conference 2005. San Francisco, CA.

Robinson, P. J. and W. L. Luyben, 2010. Integrated Gasification Combined Cycle Dynamic Model: H_2S Absorption/Stripping, Water–Gas Shift Reactors, and CO_2

Absorption/Stripping. Industrial & Engineering Chemistry Research 49(10): 4766-4781.

Roh K., and Lee J. H., 2014. Control Structure Selection for the Elevated-Pressure Air Separation Unit in an IGCC Power Plant: Self-Optimizing Control Structure for Economical Operation. Ind. Eng. Chem. Res., 53 (18), pp 7479–7488

Rubin, E., Chen, C., Rao, A., 2007. Cost and performance of fossil fuel power plants with CO2 capture and storage. Energy Policy 35 (9): 4444-4454.

Rubin, E., Keith D. and Gilboy C. 2005. Comparative Assessments of Fossil Fuel Power Plants with CO_2 Capture and Storage. Proceedings of 7th International Conference on Greenhouse Gas Control Technologies (GHGT-7), Vancouver, Canada, September 5-9, 2004, Volume 1: Peer-Reviewed Papers and Overviews.

Samadi, A., Kemmerlin, R. Husson, S., 2010. Polymerized Ionic Liquid Sorbents for CO_2 Separation. Energy Fuels, 24, 5797–5804.

Schiebahn, S., Riensche, E., Weber, M., Stolten, D. Integration of H_2-Selective Membrane Reactors in the Integrated Gasification Combined Cycle for CO2 Separation. Chemical Engineering & Technology 35 (3): 555-560.

Schiffer, H.W., 2008. WEC energy policy scenarios to 2050. Energy Policy 36 (7): 2464-2470.

Scholes, C. A., K. H. Smith, Kentish, S., Stevens, G., 2010. CO_2 capture from pre-combustion processes: Strategies for membrane gas separation. International Journal of Greenhouse Gas Control 4 (5): 739-755.

Sciamanna, S. F. and S. Lynn, 1988. Solubility of hydrogen sulfide, sulfur dioxide, carbon dioxide, propane, and n-butane in poly(glycol ethers). Industrial & Engineering Chemistry Research 27 (3): 492-499.

Sekar, R. C., 2005. Carbon Dioxide Capture from Coal-Fired Power Plants: A Real Options Analysis, Massachusetts Institute of Technology. Master of Science Dissertation.

Simbeck, D. R., Korens, D. R., Biasca, F. E., Vejtasa, S., and Dickenson, R. L., 1993. Coal Gasification Guidebook: Status, Applications, and Technologies. Palo Alto, Calif.: Electric Power Research Institute (EPRI).

Smith, A. R. and J. Klosek, 2001. A review of air separation technologies and their integration with energy conversion processes. Fuel Processing Technology 70 (2): 115-134.

Songolzadeh, M., Soleimani, M., Takht Ravanchi M., and Songolzadeh R., 2014. Carbon Dioxide Separation from Flue Gases: A Technological Review Emphasizing

Reduction in Greenhouse Gas Emissions. The Scientific World Journal, Article ID 828131, 34 pages.

Takami, K. M., J. Mahmoudi, et al., 2009. A simulated H_2O/CO_2 condenser design for oxy-fuel CO_2 capture process. Energy Procedia 1 (1): 1443-1450.

Twigg, M. V., 1996. Catalyst Handbook, Second Edition, Manson Publishing Ltd., London.

Wall, T. F. (2007). Combustion processes for carbon capture. Proceedings of the Combustion Institute 31 (1): 31-47.

Wijmans, J. G. and R. W. Baker, 1995. The solution-diffusion model: a review. Journal of Membrane Science 107: 1-21.

World Coal Institute, 2009. The Coal Resource, A comprehensive overview of Coal. See also:http://www.worldcoal.org/bin/pdf/original_pdf_file/coal_resource_overview_of_coal_report(03_06_2009).pdf [accessed 10.09.13].

World Energy Outlook. International Energy Agency, 2004.

World Energy Outlook. International Energy Agency, 2012.

Wozny, G., Hady, L., 2011. Process Engineering and Chemical Plant Design. Berlin, Universitatsverlag der TU Berlin.

Xu, Y., R. P. Schutte, Hepler, L., 1992. Solubilities of carbon dioxide, hydrogen sulfide and sulfur dioxide in physical solvents. The Canadian Journal of Chemical Engineering 70 (3): 569-573.

Yun, S. and S. Ted Oyama, 2011. Correlations in palladium membranes for hydrogen separation: A review. Journal of Membrane Science 375: 28-45.

Zhao, M., Minett, A., Harris, A., 2013. A review of techno-economic models for the retrofitting of conventional pulverised-coal power plants for post-combustion capture (PCC) of CO_2. Energy Environ. Sci., **6**, 25-40.

Zheng, L. and E. Furinsky, 2005. Comparison of Shell, Texaco, BGL and KRW gasifiers as part of IGCC plant computer simulations. Energy Conversion and Management 46 (11–12): 1767-1779.

Appendices

A. Main IGCC unit simulation models and assumptions

Unit	Simulator Model		Simulation Environment	
	Honeywell UniSim	**BRE ProMax**	**Honeywell UniSim**	**BRE ProMax**
EP ASU				
HP absorber	Absorber		Peng-Robinson	
LP absorber	Absorber		Peng-Robinson	
MAC	Compressor		Peng-Robinson	
Gasifier	Conversion Reactor		Peng-Robinson	
Quench and Syngas Scrubber	Absorber		Sour-PR	
COS Hydrolysis	Conversion Reactor		Peng-Robinson	
Shift Reactors	Equilibrium Reactor		Peng-Robinson	
Gas Cooling, BFW heating and Knockout	Separator		Sour-PR	Electrolytic-PR
Sour Water Stripper	Distillation Column		Sour-PR	Electrolytic-PR
Selexol Unit				
H_2S absorber	Absorber		Uniquac-PR	
CO_2 absorber	Absorber		Uniquac-PR	
H_2S concentrator	Absorber		Uniquac-PR	
Sour Stripper	Distillation Column		Uniquac-PR	
Syngas Humidification	Absorber		Peng-Robinson	
Syngas Reheat	Heat Exchanger		Peng-Robinson	
Syngas Expander	Expander		Peng-Robinson	
Gas Turbine Combustor	Gibbs Reactor		Peng-Robinson	
Ambient Air Compressor	Compressor		Peng-Robinson	
Gas Turbine	Expander		Peng-Robinson	
HRSG	Heat Exchanger			
Gas			Peng-Robinson	
Water/Steam			ASME	

Unit	Simulator Model		Simulation Environment	
	Honeywell UniSim	**BRE ProMax**	**Honeywell UniSim**	**BRE ProMax**
Steam Turbine	Expander		ASME	
CO_2 Compressor	Compressor		Peng-Robinson	
Claus Plant				
Furnace	Gibbs Reactor-Specify equilibrium reactions	Gibbs Minimization-Acid Gas Burner	Sour-PR	Sulphur-PR
Thermal Reaction Zone	Gibbs Reactor-Specify equilibrium reactions	Gibbs Minimization-Sulphur Thermal Reaction Zone	Sour-PR	Sulphur-PR
Sulphur redistribution	Heat Exchanger & Separator	Gibbs Minimization-Sulphur Redistribution	Sour-PR	Sulphur-PR
Sulphur condensers	Heat Exchanger & Separator	Gibbs Minimization-Sulphur Condenser	Sour-PR	Sulphur-PR
Converters	Gibbs Reactor	Gibbs Minimization-Claus Bed	Sour-PR	Sulphur-PR
Hydrogenation Reactor	Gibbs Reactor	Gibbs Minimization-General	Sour-PR	Sulphur-PR

B. NETL cases data and schematics

B.1 NETL case 1 block flow diagram and data

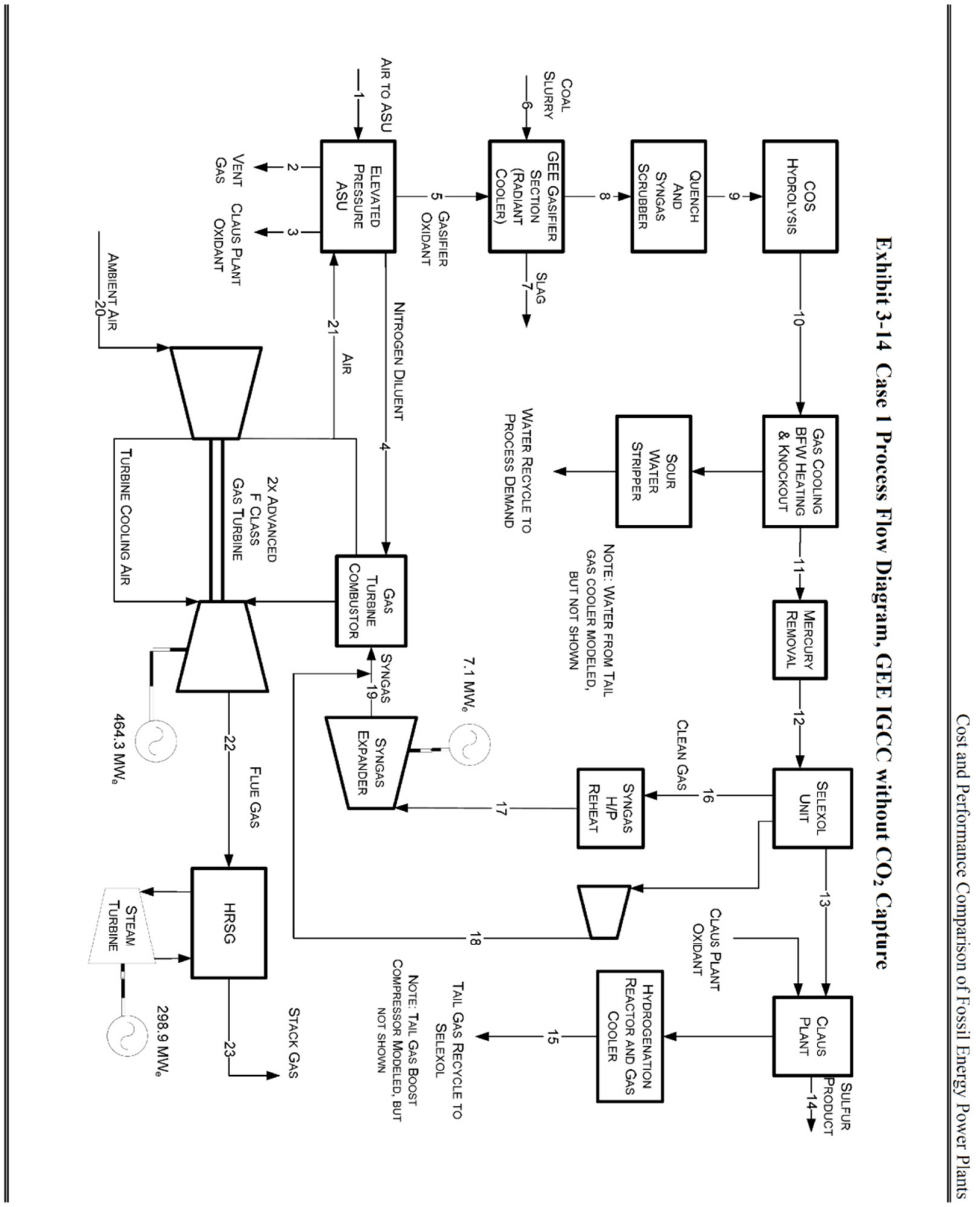

V-L Mole Fraction	1	2	3	4	5	6
Ar	0.0094	0.0065	0.0360	0.0023	0.032	0.0000
CH_4	0.0000	0.0000	0.0000	0.0000	0.0000	0.0000
CO	0.0000	0.0000	0.0000	0.0000	0.0000	0.0000
CO_2	0.0003	0.0015	0.0000	0.0000	0.0000	0.0000
COS	0.0000	0.0000	0.0000	0.0000	0.0000	0.0000
H_2	0.0000	0.0000	0.0000	0.0000	0.0000	0.0000
H_2O	0.0014	0.0496	0.0000	0.0000	0.0000	1.0000
H_2S	0.0000	0.0000	0.0000	0.0000	0.0000	0.0000
N_2	0.7722	0.8978	0.0140	0.9924	0.0180	0.0000
NH_3	0.0000	0.0000	0.0000	0.0000	0.0000	0.0000
O_2	0.2077	0.0445	0.9500	0.0053	0.9500	0.0000
SO_2	0.0000	0.0000	0.0000	0.0000	0.0000	0.0000
Total	1.0000	1.0000	1.0000	1.0000	1.0000	1.0000

Temperature (F)	233	58	90	385	206	141
Pressure (psia)	190.1	16.4	125.0	460.0	980.0	1,050.0
Enthalpy (Btu/lb)	55.6	16.6	12.5	87.8	37.7	-
Density (lb/ft^3)	0.738	0.085	0.683	1.424	4.416	-
V-L FIowrate (Ibmol/hr)	53,342	13,347	277	36,897	12,736	14,199
V-L Flowrate (Ib/hr)	1,539,150	371,000	8,942	1,035,410	409,853	255,589
Solids Flowrate (Ib/hr)	0	0	0	0	0	0

V-L Mole Flows	7	8	9	10	11	12
Ar	0.0000	0.0079	0.0067	0.0067	0.0092	0.0092
CH_4	0.0000	0.0010	0.0008	0.0008	0.0011	0.0011
CO	0.0000	0.3442	0.2922	0.2922	0.3992	0.3992
CO_2	0.0000	0.1511	0.1276	0.1276	0.1780	0.1780
COS	0.0000	0.0002	0.0002	0.0002	0.0000	0.0000
H_2	0.0000	0.3349	0.2849	0.2849	0.3935	0.3935
H_2O	0.0000	0.1429	0.2726	0.2726	0.0012	0.0012
H_2S	0.0000	0.0073	0.0061	0.0061	0.0069	0.0069
N_2	0.0000	0.0089	0.0076	0.0076	0.0103	0.0103
NH_3	0.0000	0.0017	0.0014	0.0014	0.0006	0.0006
O_2	0.0000	0.0000	0.0000	0.0000	0.0000	0.0000
SO_2	0.0000	0.0000	0.0000	0.0000	0.0000	0.0000
Total	0.0000	1.0000	1.0000	1.0000	1.0000	1.0000

Temperature (F)	410	1,100	390	390	107	107
Pressure (psia)	797.7	799.7	792.7	782.7	742.7	732.7
Enthalpy (Btu/lb)	1,710	535.5	400.3	400.3	27.4	27.4
Density (lb/ft^3)	-	0.975	1.718	1.718	2.534	2.534
V-L FIowrate (Ibmol/hr)	0	51,249	60,278	60,278	43,585	43,585
V-L Flowrate (Ib/hr)	0	1,046,880	1,206,760	1,206,760	904,410	904,410
Solids Flowrate (Ib/hr)	53,746	0	0	0	0	0

V-L Mole Flows	**13**	**14**	**15**	**16**	**17**	**18**	**19**
Ar	0.0000	0.0000	0.0188	0.0097	0.0097	0.0059	0.0097
CH_4	0.0000	0.0000	0.0764	0.0012	0.0012	0.0169	0.0012
CO	0.0000	0.0000	0.0003	0.4195	0.4195	0.0814	0.4195
CO_2	0.3802	0.0000	0.6066	0.1414	0.1414	0.5518	0.1414
COS	0.0002	0.0000	0.0000	0.0000	0.0000	0.0000	0.0000
H_2	0.0000	0.0000	0.0126	0.4164	0.4164	0.0532	0.4164
H_2O	0.0200	0.0000	0.0020	0.0009	0.0009	0.0000	0.0009
H_2S	0.3576	0.0000	0.0103	0.0000	0.0000	0.0001	0.0000
N_2	0.2106	0.0000	0.2728	0.0110	0.0110	0.2908	0.0110
NH_3	0.0313	0.0000	0.0000	0.0000	0.0000	0.0000	0.0000
O_2	0.0000	0.0000	0.0000	0.0000	0.0000	0.0000	0.0000
SO_2	0.0000	0.0000	0.0000	0.0000	0.0000	0.0000	0.0000
Total	1.0000	0.0000	1.0000	1.0000	1.0000	1.0000	1.0000

Temperature (°F)	120	358	100	112	460	151	380
Pressure (psia)	30.0	24.9	368.0	719.0	714.0	460.0	460.0
Enthalpy (Btu/Ib)	31.1	-99.5	16.1	162.2	162.2	27.1	131.2
Density (lb/ft^3)	0.172	329.192	2.252	1.414	1.414	2.481	0.998
V-L FIowrate (Ibmol/hr)	863	0	860	40,704	40,704	3,978	40,704
V-L Flowrate (lb/hr)	30,839	0	31,584	795,498	795,498	140,512	795,498
Solids Flowrate (lb/hr)	0	12,235	0	0	0	0	0

V-L Mole Flows	**20**	**21**	**22**	**23**
Ar	0.0094	0.0094	0.0091	0.0091
CH_4	0.0000	0.0000	0.0000	0.0000
CO	0.0000	0.0000	0.0000	0.0000
CO_2	0.0003	0.0003	0.0859	0.0859
COS	0.0000	0.0000	0.0000	0.0000
H_2	0.0000	0.0000	0.0000	0.0000
H_2O	0.0104	0.0104	0.0668	0.0668
H_2S	0.0000	0.0000	0.0000	0.0000
N_2	0.7722	0.7722	0.7337	0.7337
NH_3	0.0000	0.0000	0.0000	0.0000
O_2	0.2077	0.2077	0.1045	0.1045
SO_2	0.0000	0.0000	0.0000	0.0000
Total	1.0000	1.0000	1.0000	1.0000

Temperature (°F)	59	811	1,155	270
Pressure (psia)	14.7	234.9	15.2	15.2
Enthalpy (Btu/Ib)	13.5	200.0	327.2	103.2
Density (lb/ft^3)	0.076	0.497	0.026	0.057
V-L FIowrate (Ibmol/hr)	242,899	9,914	297,284	297,284
V-L Flowrate (lb/hr)	7,008,680	286,060	8,694,060	8,694,060
Solids Flowrate (lb/hr)	0	0	0	0

B.2 NETL case 2 block flow diagram and data

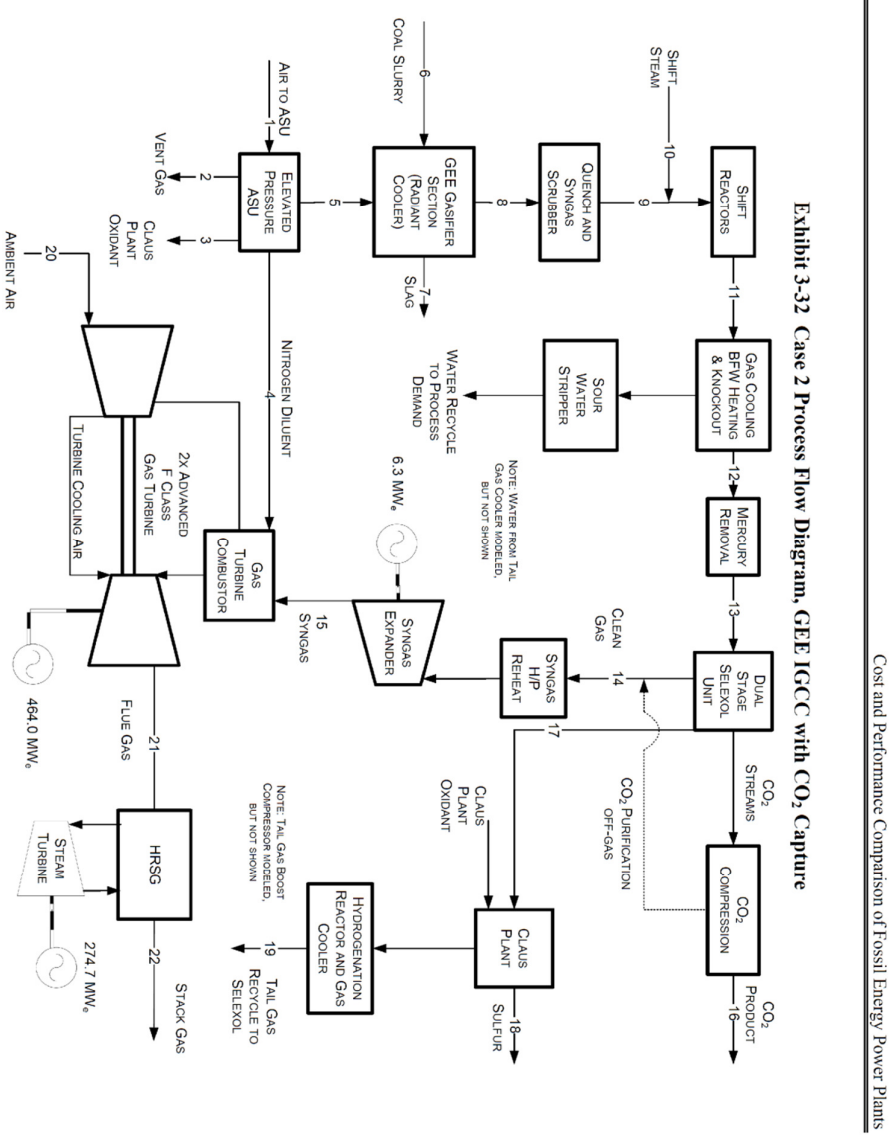

V-L Mole Fraction	1	2	3	4	5	6
Ar	0.0094	0.0089	0.0360	0.0024	0.0320	0.0000
CH_4	0.0000	0.0000	0.0000	0.0000	0.0000	0.0000
CO	0.0000	0.0000	0.0000	0.0000	0.0000	0.0000
CO_2	0.0003	0.0023	0.0000	0.0000	0.0000	0.0000
COS	0.0000	0.0000	0.0000	0.0000	0.0000	0.0000
H_2	0.0000	0.0000	0.0000	0.0000	0.0000	0.0000
H_2O	0.0014	0.0836	0.0000	0.0000	0.0000	1.0000
H_2S	0.0000	0.0000	0.0000	0.0000	0.0000	0.0000
N_2	0.7722	0.8367	0.0140	0.9922	0.0180	0.0000
NH_3	0.0000	0.0000	0.0000	0.0000	0.0000	0.0000
O_2	0.2077	0.0685	0.9500	0.0054	0.9500	0.0000
SO_2	0.0000	0.0000	0.0000	0.0000	0.0000	0.0000
Total	1.0000	1.0000	1.0000	1.0000	1.0000	1.0000

Temperature (F)	232	60	90	385	206	141
Pressure (psia)	190.6	16.4	145.0	460.0	980.0	1,050.0
Enthalpy (Btu/lb)	55.6	18.0	12.5	87.8	37.7	-
Density (lb/ft^3)	0.741	0.087	0.792	1.424	4.416	-
V-L FIowrate (Ibmol/hr)	64,331	8,321	214	42,780	13,015	14,811
V-L Flowrate (Ib/hr)	1,855,930	229,617	6,904	1,200,560	418,847	261,198
Solids Flowrate (Ib/hr)	0	0	0	0	0	0

V-L Mole Flows	7	8	9	10	11	12
Ar	0.0000	0.0079	0.0062	0.0000	0.0051	0.0057
CH_4	0.0000	0.0010	0.0008	0.0000	0.0006	0.0008
CO	0.0000	0.3442	0.2666	0.0000	0.0090	0.0117
CO_2	0.0000	0.1511	0.1166	0.0000	0.3113	0.4057
COS	0.0000	0.0002	0.0001	0.0000	0.0000	0.0000
H_2	0.0000	0.3349	0.2594	0.0000	0.4305	0.5609
H_2O	0.0000	0.1429	0.3365	1.0000	0.2317	0.0009
H_2S	0.0000	0.0073	0.0056	0.0000	0.0058	0.0054
N_2	0.0000	0.0089	0.0069	0.0000	0.0011	0.0075
NH_3	0.0000	0.0017	0.0013	0.0000	0.0000	0.0003
O_2	0.0000	0.0000	0.0000	0.0000	0.0000	0.0000
SO_2	0.0000	0.0000	0.0000	0.0000	0.0000	0.0000
Total	0.0000	1.0000	1.0000	1.0000	1.0000	1.0000
Temperature (F)	410	1,100	410	615	519	103
Pressure (psia)	797.7	799.7	797.7	875.0	777.2	736.7
Enthalpy (Btu/lb)	1,710	535.5	474.7	1,275.0	433.3	28.0
Density (lb/ft^3)	-	0.975	1.697	1.367	1.447	2.443
V-L FIowrate (Ibmol/hr)	0	52,422	67,674	13,313	80,987	62,118
V-L Flowrate (Ib/hr)	0	1,069,860	1,343,900	239,836	1,587,740	1,243,070
Solids Flowrate (Ib/hr)	54,925	0	0	0	0	0

V-L Mole Flows	**13**	**14**	**15**	**16**	**17**	**18**
Ar	0.0057	0.0111	0.0111	0.0000	0.0000	0.0000
CH_4	0.0008	0.0022	0.0022	0.0000	0.0000	0.0000
CO	0.0117	0.0190	0.0190	0.0000	0.0000	0.0000
CO_2	0.4057	0.0448	0.0448	1.0000	0.4488	0.0000
COS	0.0000	0.0000	0.0000	0.0000	0.0005	0.0000
H_2	0.5609	0.9095	0.9095	0.0000	0.0000	0.0000
H_2O	0.0009	0.0000	0.0000	0.0000	0.0394	0.0000
H_2S	0.0054	0.0000	0.0000	0.0000	0.4102	0.0000
N_2	0.0075	0.0134	0.0134	0.0000	0.0807	0.0000
NH_3	0.0003	0.0000	0.0000	0.0000	0.0203	0.0000
O_2	0.0000	0.0000	0.0000	0.0000	0.0000	0.0000
SO_2	0.0000	0.0000	0.0000	0.0000	0.0000	0.0000
Total	1.0000	1.0000	1.0000	1.0000	1.0000	0.0000

Temperature (°F)	103	100	386	155	120	373
Pressure (psia)	736.7	696.2	460.0	2,214.0	30.5	25.4
Enthalpy (Btu/Ib)	28.0	91.4	480.6	-46.5	39.7	-96.5
Density (lb/ft^3)	2.443	0.602	0.263	30.975	0.184	-
V-L FIowrate (Ibmol/hr)	62,118	38,323	38,323	23,493	855	0
V-L Flowrate (lb/hr)	1,243,070	198,981	198,981	1,033,930	31,703	0
Solids Flowrate (lb/hr)	0	0	0	0	0	12,514

V-L Mole Flows	**19**	**20**	**21**	**22**
Ar	0.0182	0.0094	0.0092	0.0092
CH_4	0.0577	0.0000	0.0000	0.0000
CO	0.0003	0.0000	0.0000	0.0000
CO_2	0.6784	0.0003	0.0085	0.0085
COS	0.0000	0.0000	0.0000	0.0000
H_2	0.0000	0.0000	0.0000	0.0000
H_2O	0.0170	0.0108	0.1226	0.1226
H_2S	0.0005	0.0000	0.0000	0.0000
N_2	0.0228	0.7719	0.7527	0.7527
NH_3	0.2051	0.0000	0.0000	0.0000
O_2	0.0000	0.2076	0.1071	0.1071
SO_2	0.0000	0.0000	0.0000	0.0000
Total	1.0000	1.0000	1.0000	1.0000

Temperature (°F)	95	59	1,052	270
Pressure (psia)	776.1	14.7	15.2	15.2
Enthalpy (Btu/Ib)	14.0	13.8	361.5	361.5
Density (lb/ft^3)	4.966	0.076	0.026	0.026
V-L FIowrate (Ibmol/hr)	576	243,972	307,385	307,385
V-L Flowrate (lb/hr)	21,951	7,038,470	8,438,010	8,438,010
Solids Flowrate (lb/hr)	0	0	0	0

B.3 NETL case 5 block flow diagram and data

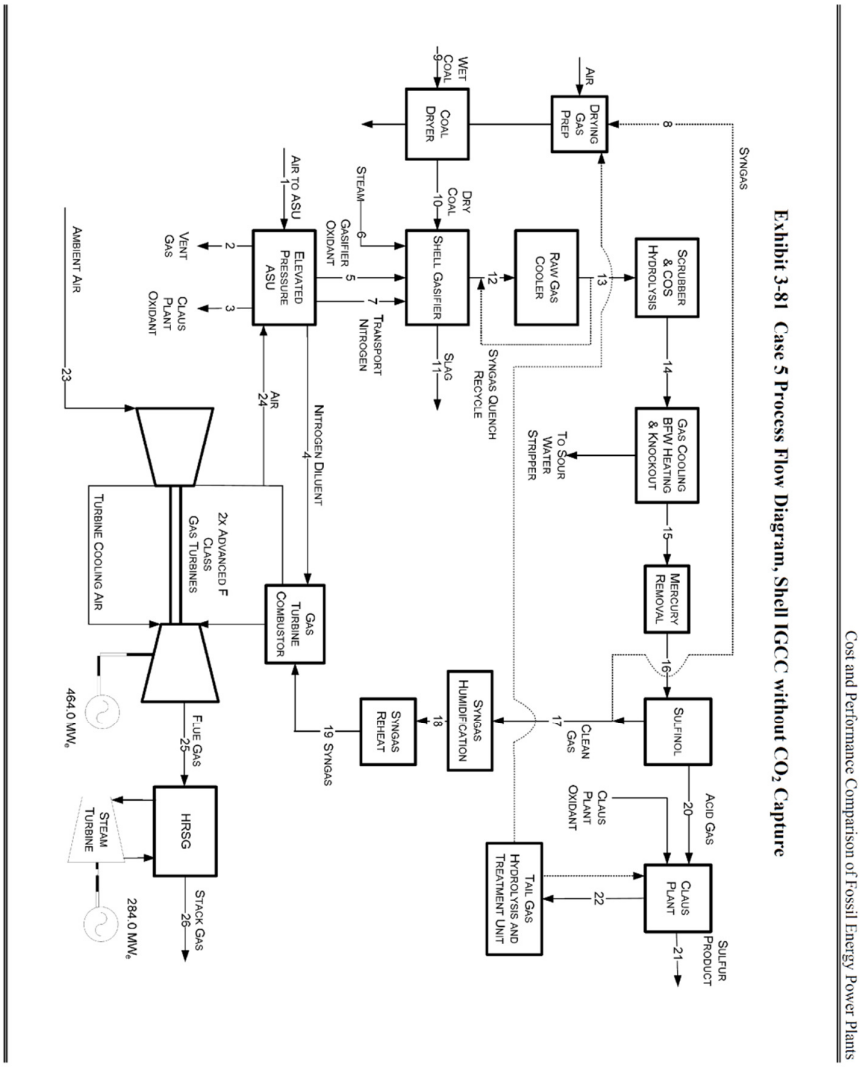

V-L Mole Fraction	1	2	3	4	5	6
Ar	0.0094	0.0263	0.0360	0.0024	0.0360	0.0000
CH_4	0.0000	0.0000	0.0000	0.0000	0.0000	0.0000
CO	0.0000	0.0000	0.0000	0.0000	0.0000	0.0000
CO_2	0.0003	0.0091	0.0000	0.0000	0.0000	0.0000
COS	0.0000	0.0000	0.0000	0.0000	0.0000	0.0000
H_2	0.0000	0.0000	0.0000	0.0000	0.0000	0.0000
H_2O	0.0104	0.2820	0.0000	0.0004	0.0000	1.0000
H_2S	0.0000	0.000	0.0000	0.0000	0.0000	0.0000
N_2	0.7722	0.4591	0.0140	0.9918	0.0140	0.0000
NH_3	0.0000	0.0000	0.0000	0.000	0.0000	0.0000
O_2	0.2077	0.2235	0.9500	0.0054	0.9500	0.0000
SO_2	0.0000	0.000	0.0000	0.0000	0.0000	0.0000
Total	1.0000	1.0000	1.0000	1.0000	1.0000	1.0000

Temperature (F)	232	70	90	385	518	650
Pressure (psia)	190.6	16.4	125.0	460.0	740.0	740
Enthalpy (Btu/lb)k	55.3	26.8	12.5	88.0	107.7	1,311.5
Density (lb/ft^3)	0.741	0.104	0.683	1.424	2.272	1.119
V-L FIowrate (Ibmol/hr)	37,250	1,938	225	38,900	10,865	2,424
V-L Flowrate (Ib/hr)	1,074,830	51,432	7,250	1,091,540	350,168	43,673
Solids Flowrate (Ib/hr)	0	0	0	0	0	0

V-L Mole Flows	**7**	**8**	**9**	**10**	**11**	**12**
Ar	0.0000	0.0105	0.0000	0.0000	0.0000	0.0097
CH_4	0.0000	0.0004	0.0000	0.0000	0.0000	0.0004
CO	0.0000	0.6151	0.0000	0.0000	0.0000	0.5716
CO_2	0.0000	0.0006	0.0000	0.0000	0.0000	0.0211
COS	0.0000	0.0000	0.0000	0.0000	0.0000	0.0007
H_2	0.0000	0.3122	0.0000	0.0000	0.0000	0.2901
H_2O	0.0000	0.0014	1.0000	1.0000	0.0000	0.0364
H_2S	0.0000	0.0000	0.0000	0.0000	0.0000	0.0081
N_2	1.0000	0.0599	0.0000	0.0000	0.0000	0.0585
NH_3	0.0000	0.0000	0.0000	0.0000	0.0000	0.0033
O_2	0.0000	0.0000	0.0000	0.0000	0.0000	0.0000
SO_2	0.0000	0.0000	0.0000	0.0000	0.0000	0.0000
Total	1.0000	1.0000	1.0000	1.0000	0.0000	1.0000

Temperature (F)	560	124	59	215	2,600	1,635
Pressure (psia)	815	516	14.7	14.7	614.7	614.7
Enthalpy (Btu/lb)k	132.2	33.1	11,676.0	-	1.167	619.8
Density (lb/ft^3)	2.086	1.651	-	-	-	0.563
V-L FIowrate (Ibmol/hr)	2,019	447	2,796	1,165	0	40,232
V-L Flowrate (Ib/hr)	56,553	8,949	50,331	20,982	0	828,347
Solids Flowrate (Ib/hr)	0	0	402,289	402,289	45,315	0

V-L Mole Flows	**13**	**14**	**15**	**16**	**17**
Ar	0.0097	0.0097	0.0101	0.0101	0.0105
CH_4	0.0004	0.0004	0.0004	0.0004	0.0004
CO	0.5716	0.5716	0.5940	0.5940	0.6151
CO_2	0.0211	0.0211	0.0226	0.0226	0.0006
COS	0.0007	0.0007	0.000	0.0000	0.0000
H_2	0.2901	0.2901	0.3015	0.3015	0.3122
H_2O	0.0364	0.0364	0.0015	0.0015	0.0014
H_2S	0.0081	0.0081	0.0091	0.0091	0.0000
N_2	0.0585	0.0585	0.0608	0.0608	0.0599
NH_3	0.0033	0.0033	0.0000	0.0000	0.0000
O_2	0.0000	0.0000	0.0000	0.0000	0.0000
SO_2	0.0000	0.0000	0.0000	0.0000	0.0000
Total	1.0000	1.0000	1.0000	1.0000	1.0000

Temperature (F)	398	351	95	95	124
Pressure (psia)	574.4	549.7	529.7	519.7	516.7
Enthalpy (Btu/lb)k	160.2	146.2	22.6	22.6	33.1
Density (lb/ft^3)	1.286	1.300	1.841	1.807	1.651
V-L FIowrate (Ibmol/hr)	40,232	40,353	38,715	38,715	44,695
V-L Flowrate (Ib/hr)	828,347	830,529	801,076	801,076	878,868
Solids Flowrate (Ib/hr)	0	0	0	0	0

V-L Mole Flows	**18**	**19**	**20**	**21**	**22**
Ar	0.0086	0.0086	0.0003	0.0000	0.0041
CH_4	0.0003	0.0003	0.0000	0.0000	0.0000
CO	0.5080	0.5080	0.0112	0.0000	0.0674
CO_2	0.0005	0.0005	0.6315	0.0000	0.4947
COS	0.0000	0.0000	0.0000	0.0000	0.0002
H_2	0.2579	0.2579	0.0000	0.0000	0.0179
H_2O	0.1752	0.1752	0.0062	0.0000	0.3199
H_2S	0.0000	0.0000	0.0042	0.0000	0.0015
N_2	0.0494	0.0494	0.2596	0.0000	0.0898
NH_3	0.0000	0.0000	0.0870	0.0000	0.0000
O_2	0.0000	0.0000	0.0000	0.0000	0.0000
SO_2	0.0000	0.0000	0.0000	0.0000	0.0000
Total	1.0000	1.0000	1.0000	0.0000	1.0000
Temperature (°F)	312	312	124	344	280
Pressure (psia)	465.0	465.0	60.0	23.6	23.6
Enthalpy (Btu/Ib)	269.4	269.4	21.9	-102.1	255.2
Density (lb/ft^3)	1.111	1.111	0.378	-	0.097
V-L FIowrate (Ibmol/hr)	44,695	44,695	1,353	0	2,088
V-L Flowrate (lb/hr)	878,868	878,868	53,431	0	67,836
Solids Flowrate (lb/hr)	0	0	0	11,307	0

V-L Mole Flows	**23**	**24**	**25**	**26**
Ar	0.0094	0.0094	0.0088	0.0088
CH_4	0.0000	0.0000	0.0000	0.0000
CO	0.0000	0.0000	0.0000	0.0000
CO_2	0.0003	0.0003	0.0755	0.0755
COS	0.0000	0.0000	0.0000	0.0000
H_2	0.0000	0.0000	0.0000	0.0000
H_2O	0.0108	0.0108	0.0847	0.0847
H_2S	0.0000	0.0000	0.0000	0.0000
N_2	0.7719	0.7719	0.7277	0.7277
NH_3	0.0000	0.0000	0.0000	0.0000
O_2	0.2076	0.2076	0.1033	0.1033
SO_2	0.0000	0.0000	0.0000	0.0000
Total	1.0000	1.0000	1.0000	1.0000
Temperature (°F)	59	811	1,105	270
Pressure (psia)	14.7	234.9	15.2	15.2
Enthalpy (Btu/Ib)	13.8	200.3	340.0	116.4
Density (lb/ft^3)	0.076	0.497	0.026	0.056
V-L FIowrate (Ibmol/hr)	248,660	16,712	302,092	302,092
V-L Flowrate (lb/hr)	7,173,720	482,146	8,728,000	8,728,000
Solids Flowrate (lb/hr)	0	0	0	0

B.4 NETL case 6 block flow diagram and data

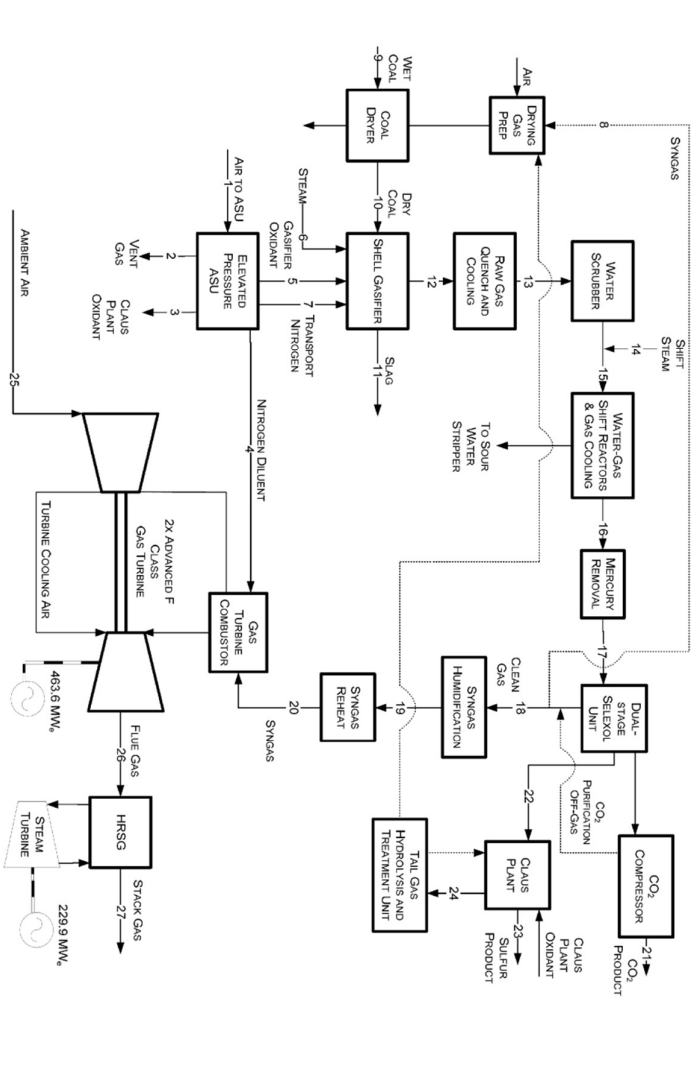

V-L Mole Fraction	1	2	3	4	5	6
Ar	0.0094	0.0263	0.0360	0.0024	0.0360	0.0000
CH_4	0.0000	0.0000	0.0000	0.0000	0.0000	0.0000
CO	0.0000	0.0000	0.0000	0.0000	0.0000	0.0000
CO_2	0.0003	0.0091	0.0000	0.0000	0.0000	0.0000
COS	0.0000	0.0000	0.0000	0.0000	0.0000	0.0000
H_2	0.0000	0.0000	0.0000	0.0000	0.0000	0.0000
H_2O	0.0104	0.2820	0.0000	0.0004	0.0000	1.0000
H_2S	0.0000	0.000	0.0000	0.0000	0.0000	0.0000
N_2	0.7722	0.4591	0.0140	0.9918	0.0140	0.0000
NH_3	0.0000	0.0000	0.0000	0.000	0.0000	0.0000
O_2	0.2077	0.2235	0.9500	0.0054	0.9500	0.0000
SO_2	0.0000	0.000	0.0000	0.0000	0.0000	0.0000
Total	1.0000	1.0000	1.0000	1.0000	1.0000	1.0000

Temperature (F)	238	70	90	385	518	750
Pressure (psia)	190.0	16.4	125.0	460.0	740.0	740
Enthalpy (Btu/lb)k	56.9	26.8	11.4	88.0	107.7	1,409.5
Density (lb/ft^3)	0.732	0.104	0.688	1.424	2.272	1.027
V-L FIowrate (Ibmol/hr)	56,388	2,025	230	40,650	11,358	2,534
V-L Flowrate (Ib/hr)	1,627,030	53,746	7,428	1,140,640	366,070	46,657
Solids Flowrate (Ib/hr)	0	0	0	0	0	0

V-L Mole Flows	**7**	**8**	**9**	**10**	**11**	**12**
Ar	0.0000	0.0102	0.0000	0.0000	0.0000	0.0097
CH_4	0.0000	0.0004	0.0000	0.0000	0.0000	0.0004
CO	0.0000	0.0265	0.0000	0.0000	0.0000	0.5716
CO_2	0.0000	0.0211	0.0000	0.0000	0.0000	0.0211
COS	0.0000	0.0000	0.0000	0.0000	0.0000	0.0007
H_2	0.0000	0.8874	0.0000	0.0000	0.0000	0.2901
H_2O	0.0000	0.0001	1.0000	1.0000	0.0000	0.0364
H_2S	0.0000	0.0000	0.0000	0.0000	0.0000	0.0081
N_2	1.0000	0.0543	0.0000	0.0000	0.0000	0.0585
NH_3	0.0000	0.0000	0.0000	0.0000	0.0000	0.0033
O_2	0.0000	0.0000	0.0000	0.0000	0.0000	0.0000
SO_2	0.0000	0.0000	0.0000	0.0000	0.0000	0.0000
Total	1.0000	1.0000	1.0000	1.0000	0.0000	1.0000

Temperature (F)	560	121	59	215	2,595	2,595
Pressure (psia)	815.0	469.6	14.7	14.7	614.7	604.7
Enthalpy (Btu/lb)k	132.2	113.8	11,676.0	-	-	1,012.8
Density (lb/ft^3)	2.086	0.407	-	-	-	0.563
V-L FIowrate (Ibmol/hr)	2,110	491	2,923	1,218	0	42,059
V-L Flowrate (Ib/hr)	59,121	2,651	52,617	21,935	0	865,967
Solids Flowrate (Ib/hr)	0	0	420,559	420,559	47,374	0

V-L Mole Flows	**13**	**14**	**15**	**16**	**17**	**18**
Ar	0.0052	0.0000	0.0064	0.0064	0.0064	0.0102
CH_4	0.0002	0.0000	0.0002	0.0002	0.0002	0.0004
CO	0.3070	0.0000	0.0166	0.0166	0.0166	0.0265
CO_2	0.0113	0.0000	0.3771	0.3771	0.3771	0.0211
COS	0.0004	0.0000	0.0000	0.0000	0.0000	0.0000
H_2	0.1559	0.0000	0.5547	0.5547	0.5547	0.8874
H_2O	0.4826	1.0000	0.0014	0.0014	0.0014	0.0001
H_2S	0.0043	0.0000	0.0050	0.0050	0.0050	0.0000
N_2	0.0314	0.0000	0.0385	0.0385	0.0385	0.0543
NH_3	0.0018	0.0000	0.0000	0.0000	0.0000	0.0000
O_2	0.0000	0.0000	0.0000	0.0000	0.0000	0.0000
SO_2	0.0000	0.0000	0.0000	0.0000	0.0000	0.0000
Total	1.0000	1.0000	1.0000	1.0000	1.0000	1.0000

Temperature (F)	500	750	574	95	95	121
Pressure (psia)	564.4	825.0	544.7	482.6	472.6	469.6
Enthalpy (Btu/lb)k	665.9	1,368.0	767.7	25.6	25.6	113.8
Density (lb/ft^3)	1.064	1.145	0.944	1.598	1.565	0.407
V-L FIowrate (Ibmol/hr)	78, 325	11,679	89,158	63,376	63,376	39,127
V-L Flowrate (Ib/hr)	1,519,300	210,400	1,714,460	1,246,470	1,246,470	211,226
Solids Flowrate (Ib/hr)	0	0	0	0	0	0

V-L Mole Flows	**19**	**20**	**21**	**22**	**23**
0.0000	0.0099	0.0099	0.0000	0.0000	0.0000
0.0000	0.0004	0.0004	0.0000	0.0000	0.0000
0.0000	0.0256	0.0256	0.0000	0.0000	0.0000
CO_2	0.0204	0.0204	1.0000	0.3526	1.0000
COS	0.0000	0.0000	0.0000	0.0006	0.0000
H_2	0.8584	0.8584	0.0000	0.0000	0.0000
H_2O	0.0327	0.0327	0.0000	0.0502	0.0000
H_2S	0.0000	0.0000	0.0000	0.3122	0.0000
N_2	0.0526	0.0526	0.0000	0.2845	0.0000
NH_3	0.0000	0.0000	0.0000	0.0000	0.0000
O_2	0.0000	0.0000	0.0000	0.0000	0.0000
SO_2	0.0000	0.0000	0.0000	0.0000	0.0000
Total	1.0000	1.0000	1.0000	1.0000	0.0000
Temperature (°F)	213	385	156	124	352
Pressure (psia)	453.9	448.9	2,214.7	60.0	23.6
Enthalpy (Btu/Ib)	327.0	535.7	-46.4	37.9	362.5
Density (lb/ft^3)	0.365	0.288	30.929	0.343	0.080
V-L FIowrate (Ibmol/hr)	40,448	40,448	22,707	1,017	0
V-L Flowrate (lb/hr)	235,031	235,031	999,309	35,657	0
Solids Flowrate (lb/hr)	0	0	11,307	0	11,825

V-L Mole Flows	**24**	**25**	**26**	**27**
Ar	0.0074	0.0094	0.0091	0.0091
CH_4	0.0000	0.0000	0.0000	0.0000
CO	0.0792	0.0000	0.0000	0.0000
CO_2	0.2293	0.0003	0.0063	0.0063
COS	0.0003	0.0000	0.0000	0.0000
H_2	0.0417	0.0000	0.0000	0.0000
H_2O	0.4003	0.0108	0.1258	0.1258
H_2S	0.0013	0.0000	0.0000	0.0000
N_2	0.2379	0.7719	0.7513	0.7513
NH_3	0.0000	0.0000	0.0000	0.0000
O_2	0.0000	0.2076	0.1075	0.1075
SO_2	0.0026	0.0000	0.0000	0.0000
Total	1.0000	1.0000	1.0000	1.0000
Temperature (°F)	280	59	1,051	270
Pressure (psia)	23.6	14.7	15.2	15.2
Enthalpy (Btu/Ib)	362.5	13.8	364.1	150.8
Density (lb/ft^3)	0.080	0.076	0.026	0.053
V-L FIowrate (Ibmol/hr)	1,603	244,799	308,019	308,019
V-L Flowrate (lb/hr)	42,962	7,062,330	8,438,000	8,438,000
Solids Flowrate (lb/hr)	0	0	0	0

C. Syngas cooling ProMax simulations

C.1 NETL case 1

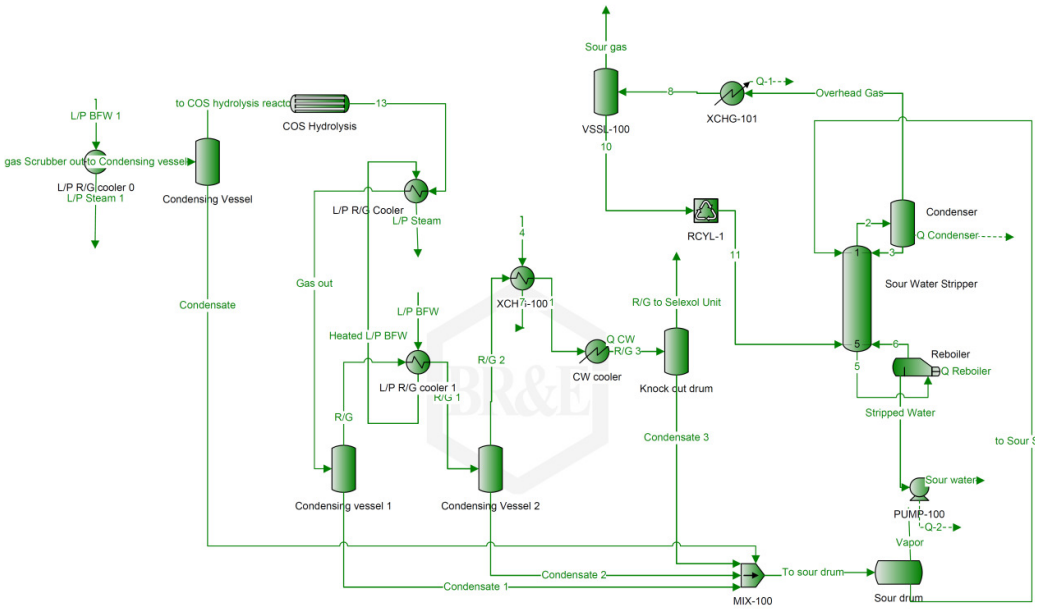

C.2 NETL case 2

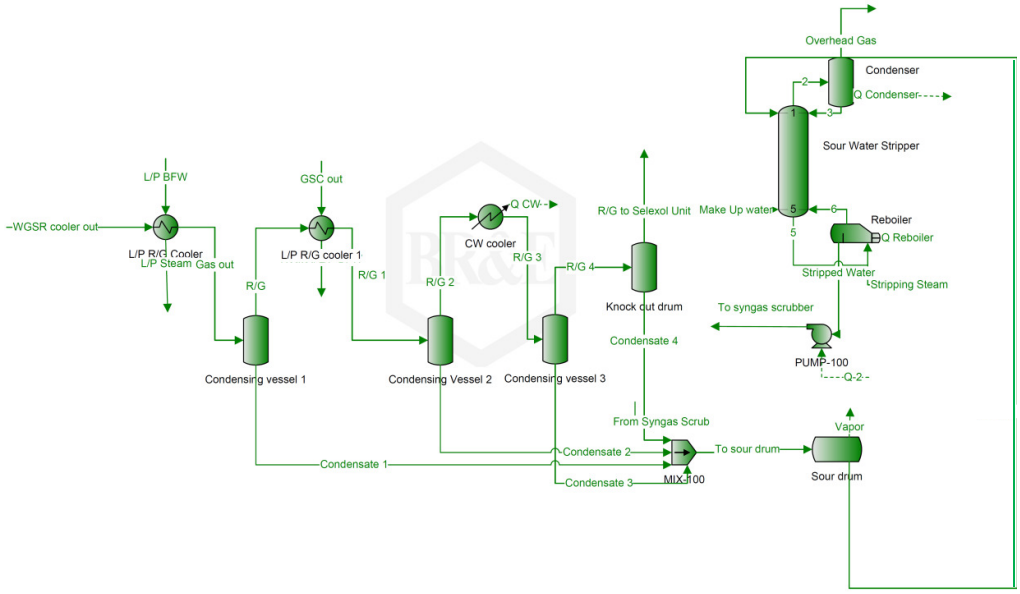

C.3 NETL case 5

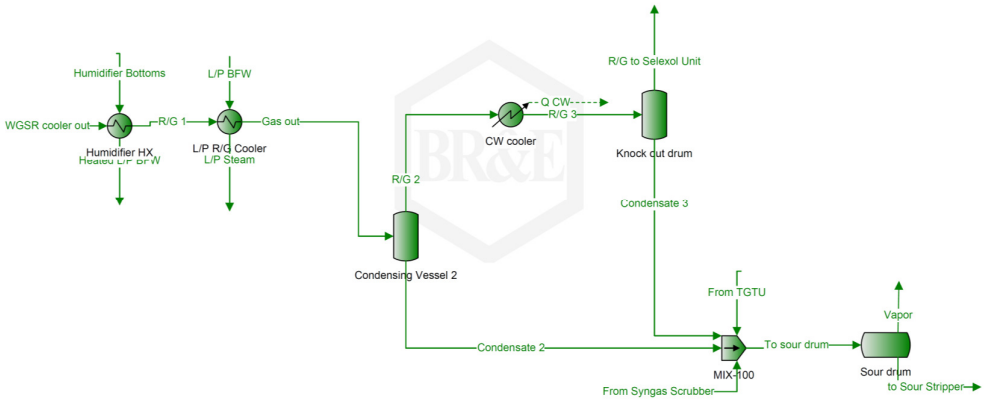

C.4 NETL case 6

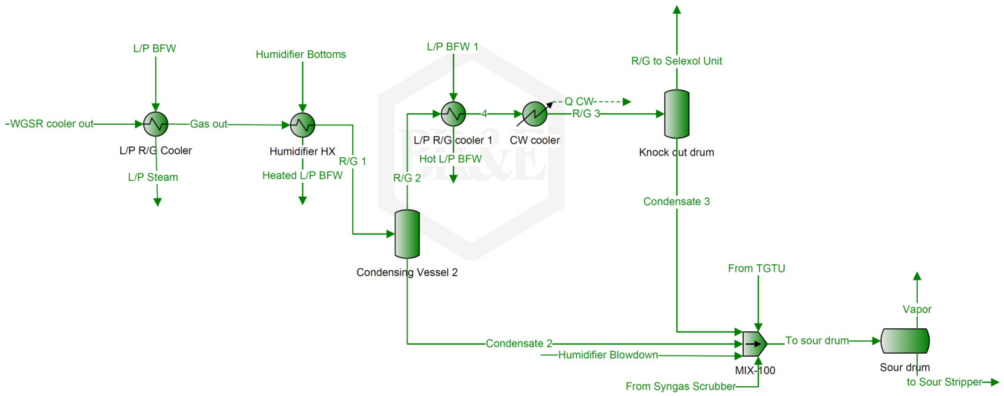

D. Claus ProMax simulations

D.1 NETL case 1

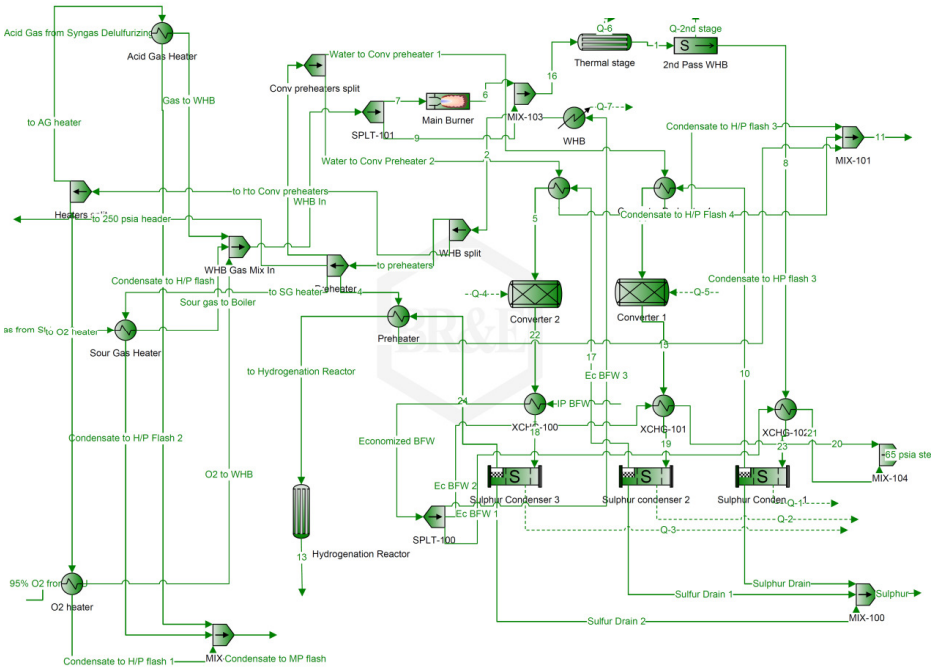

D.2 NETL case 2

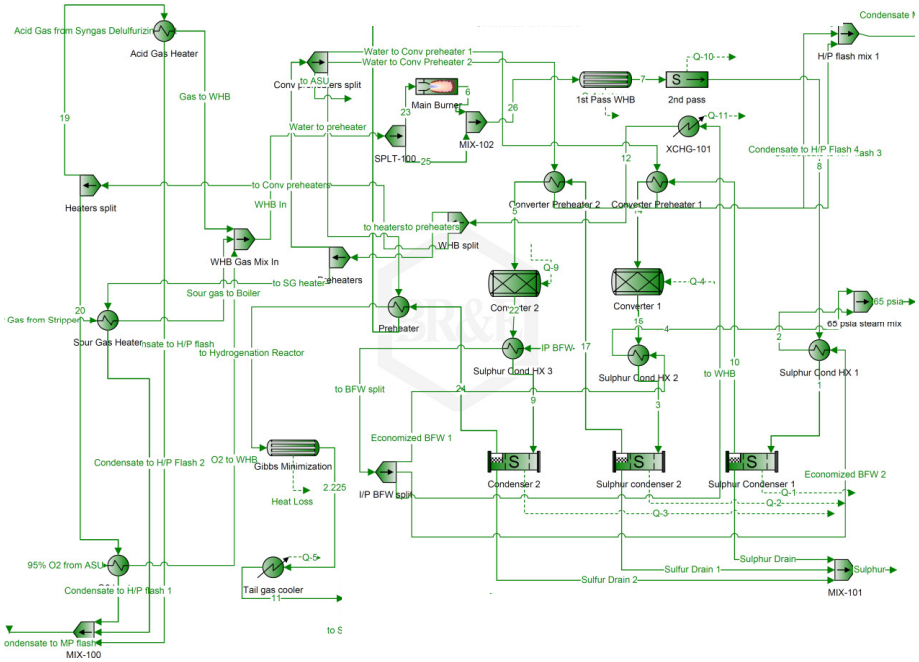

D.3 NETL case 5

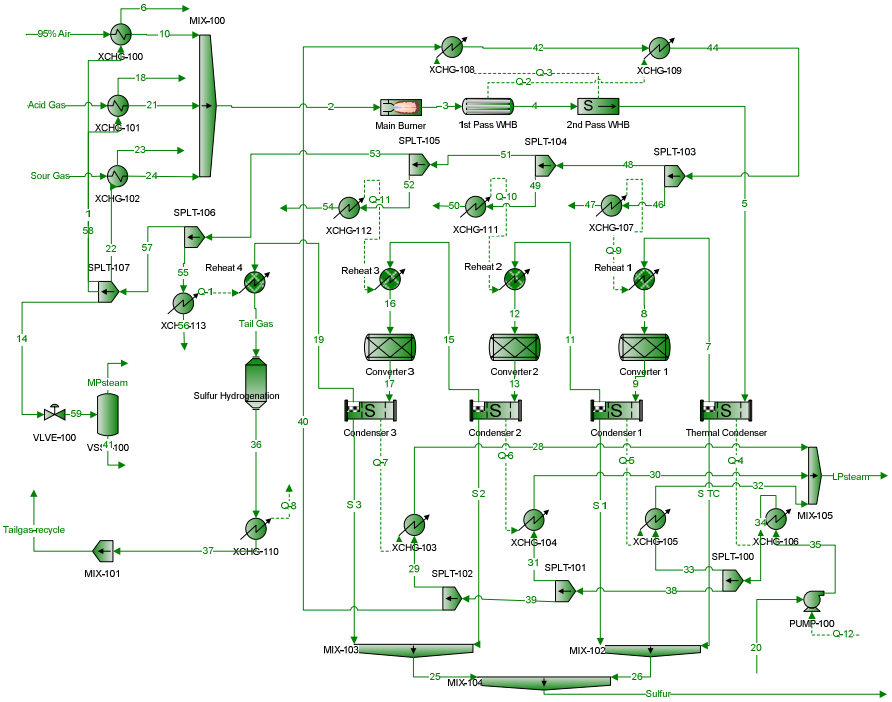

D.4 NETL case 6